# CONSTRUCTION OF A PORCINE SKELETAL MUSCLE cDNA MICROARRAY AND ITS APPLICATION ON THE IDENTIFICATION OF DIFFERENTIALLY EXPRESSED GENES IN DIFFERENT BIOLOGICAL CONTEXTS

**Qianfan Bai**

**A thesis presented for the degree of Doctor of Philosophy**

**In the Faculty of Veterinary Medicine**

**University of Glasgow**

# DEDICATION

This thesis is dedicated to my parents.

# DECLARATION

This thesis is the original work of the author:

Qianfan Bai

# ACKNOWLEDGEMENTS

I am very grateful to Dr. Kin-Chow Chang, Faculty of Veterinary Medicine, University of Glasgow, for accepting me as a student and finding funds for this study. I am grateful for his excellent supervision, invaluable cooperation, great support, kind help and patience which enabled me to complete this study. I am appreciative of his careful reading of the manuscript of this thesis, and his valuable comments and advice.

I owe a debt of gratitude to Professor David J. Taylor, Faculty of Veterinary Medicine, University of Glasgow, for his supervision, encouragement, invaluable patience and support during the course of this study. I am very appreciative of his careful reading of the manuscript of this thesis, and his valuable comments and advice.

It was indeed a pleasure to have collaborated with Dr. Gary Evans and Dr. Saffron Dornan, Department of Pathology, University of Cambridge. The facilities, materials and ideas which they provided added to the success of this study.

I am thankful to Mr Nuno Da Costa and Mrs. Christine McGillivray, University of Glasgow Veterinary School, for their constructive suggestions and technical support.

I wish to express my gratitude to my family and friends whose good wishes and constant support enabled me to complete this study.

# PUBLICATIONS

**Qianfan Bai, Christine McGillivray, Nuno da Costa, Saffron Dornan, Gary Evans, Michael James Stear and Kin-Chow Chang (2003).** Development of a porcine skeletal muscle cDNA microarray: analysis of differential transcript expression in phenotypically distinct muscles. BMC Genomics 2003 4:8.

**Nuno da Costa, Christine McGillivray, Qianfan Bai, Jeffrey D. Wood, Gary Evans, Kin-Chow Chang (2004).** Restriction of dietary energy and protein induces molecular changes in young porcine skeletal muscles. Journal of Nutrition 2004 Sep; 134(9):2191-2199.

# CONTENTS

1. INTRODUCTION

INTRODUCTION

1.1. SKELETA MUSCLE STRUCTURE AND FIBRE TYPES

1.1.1. GENERAL DESCRIPTION OF SKELETAL MUSCLE STRUCTURE

1.1.2. MYOFILAMENT SUBSTRUCTURE

1.1.2.1. Thin filaments

1.1.2.2. Thick filaments

1.1.3. SKELETAL MUSCLE FIBRE TYPES

1.1.3.1. Slow muscle and fast muscle

1.1.3.2. Myosin heavy chain isoforms and skeletal muscle fibre types

1.2. MOLECULAR PATHWAYS IN SKELETAL MUSCLE

1.2.1. MYOGENIC REGULATORY FACTORS AND SKELETAL MUSCLE

1.2.2. SKELETAL MUSCLE ATROPHY AND HYPERTROPHY

1.2.2.1. Skeletal muscle atrophy via induction of ubiquitin ligase pathway

1.2.2.2. The IGF-1/PI3K/AKT1/mTOR/p70S6K pathway and skeletal muscle hypertrophy

1.2.2.3. The IGF-1/PI3K/AKT/GSK3β pathway and skeletal muscle hypertrophy

1.2.3. CALCINEURIN SIGNALLING PATHWAY AND SKELETAL MUSCLE

1.2.3.1. Calcineurin and calcineurin inhibitors

1.2.3.2. Nuclear Factor of Activated T cells (NFATs)

1.2.3.3. $Ca^{2+}$/calmodulin/calcineurin/NFAT pathway

1.2.3.4. Calcineurin and Myocyte Enhancer Factor-2 (MEF2)

1.2.3.5. Calcineurin expression in skeletal muscle

*1.2.3.5.1. Calcineurin expression in skeletal muscle differentiation*

*1.2.3.5.2. Calcineurin expression and skeletal muscle size*

*1.2.3.5.3. Calcineurin expression determines slow muscle fibre type gene expression*

1.3. MICROARRAY TECHNOLOGY

1.3.1. GENERAL DESCRIPTION OF DNA MICROARRAYS

1.3.2. TYPES OF DNA MICROARRAYS

1.3.2.1. cDNA microarrays

1.3.2.2. Oligonucleotide microarrays

1.3.3. JUSTIFICATION OF USE OF MICROARRAYS IN COMPARISON WITH mRNA DIFFERENTIAL DISPLAY AND REPRESENTATIONAL DIFFERENCE ANALYSIS

1.4. JUSTIFICATION OF WORK

2. CONSTRUCTION OF A PORCINE SKELETAL MUSCLE cDNA MICROARRAY

2.1. INTRODUCTION

2.2. MATERIALS AND METHODS

2.2.1. MATERIALS

2.2.1.1. cDNA libraries

2.2.1.2. Bacteria and culture media

*2.2.1.2.1. Bacteria*

*2.2.1.2.2. Culture media*

2.2.1.3. Phage strains

2.2.1.4. Restriction endonucleases

2.2.1.5. Commercial kits

2.2.2. METHODS

2.2.2.1. *In vivo* mass excision of pBK-CMV phagemid vector from ZAP Express® vector

2.2.2.2. Colony blot hybridisations

*2.2.2.2.1. Membrane preparation for colony blot hybridisations*

*2.2.2.2.2. Probe preparation for colony blot hybridisations*

*2.2.2.2.2.1. mRNA extraction*

*2.2.2.2.2.2. Single-stranded cDNA syntheses*

*2.2.2.2.2.3. Labelling single-stranded cDNAs with [$\alpha$-$^{32}$P]*

*2.2.2.2.3. Colony blot hybridisations*

2.2.2.3. Clone selection

2.2.2.4. Bacterial culture of selected clones in 96-well flat-bottom blocks
2.2.2.5. Plasmid DNA extraction in 96-well plate format
*2.2.2.5.1. Preparation and clearing of bacterial lysates*
*2.2.2.5.2. Adsorption of DNA onto silica-gel membrane of QIAprep 96 plate*
*2.2.2.5.3. Washing and elution of plasmid DNAs*
2.2.2.6. Storage and accounting of plasmid DNAs
2.2.2.7. PCR in 96-well plate format
2.2.2.8. Purification of PCR product in 96-well plate format
2.2.2.9. Storage and accounting of purified PCR products
2.2.2.10. Printing microarray slides
2.2.2.11. Storage of microarray slides
2.2.2.12. Quality controls
*2.2.2.12.1. Individual bacterial culture of unselected clones*
*2.2.2.12.2. Individual plasmid DNA extraction*
*2.2.2.12.3. Southern blot hybridisation*
*2.2.2.12.4. Detection of cDNA inserts during microarray construction*
*2.2.2.12.5. Sequencing of plasmid DNAs derived from selected clones*
*2.2.2.12.6. Dot blot hybridisation*
*2.2.2.12.7. Microarray hybridisation using Cy3 labelled T7 primer target*
*2.2.2.12.8. Dual-colour microarray hybridisation*
2.3. RESULTS
2.3.1. RESULTS OF MICROARRAY CONSTRUCTION PROCESS
2.3.1.1. *in vivo* mass excision of pBK-CMV phagemid vector from ZAP Express® vector
2.3.1.2. Colony blot hybridisations
2.3.1.3. Clone selection
2.3.1.4. Plasmid DNA extraction
2.3.1.5. PCR and purification of PCR products in 96-well plate format
2.3.1.6. Printing microarray slides

2.3.1.7. Clone accounting

*2.3.1.7.1. Clone identification system for microarray slides*

*2.3.1.7.2. Clone identification system for stock plates*

2.3.2. QUALITY CONTROLS

2.3.2.1. Southern blot hybridisation

2.3.2.2. Sequencing of plasmid DNAs derived from selected clones

2.3.2.3. Dot blot hybridisation

2.3.2.4. Microarray hybridisation using Cy3 labelled T7 primer target

2.3.2.5. Dual-colour microarray hybridisation

2.4. DISCUSSION

2.4.1. CONSTRUCTION OF THE PORCINE SKELETAL MUSCLE cDNA MICROARRAY

2.4.2. DIVERSITY AND REDUNDANCY OF CLONES INCORPORATED IN THE PORCINE SKELETAL MUSCLE cDNA MICROARRAY

2.4.3. IMPORTANCE AND NECESSITY OF THE QUALITY ASSURANCE PROCESS

2.4.4. ADVANTAGES AND WEAKNESSES OF THE MICROARRAY CONSTRUCTED IN THIS STUDY

2.4.5. POTENTIAL IMPROVEMENTS TO THE MICROARRAY CONSTRUCTED IN THIS STUDY

2.4.6. POTENTIAL APPLICATIONS OF THE MICROARRAY AND ITS ASSOCIATED CLONE STOCKS

3. DIFFERENTIAL GENE EXPRESSION IN RED AND WHITE PORCINE SKELETAL MUSCLES

3.1. INTRODUCTION

3.2. MATERIALS AND METHODS

3.2.1. MATERIALS

3.2.1.1. Porcine tissues

3.2.1.2. Commercial kits, reagents and software

3.2.2. METHODS

3.2.2.1. Preparation of target cDNA samples for microarray hybridisation

*3.2.2.1.1. First strand cDNA synthesis and fluorescent*

*dye labelling*

*3.2.2.1.2. Target cDNA Purification*

*3.2.2.1.3. Dye-swap pairing*

3.2.2.2. Microarray hybridisations

3.2.2.3. Microarray image capture and quantification

3.2.2.4. Microarray data analysis

3.2.2.5. Sequence analysis to clone identification

3.2.2.6. Validation of gene expression by real-time quantitative RT-PCR

*3.2.2.6.1. Designing primes and probes for real-time quantitative RT-PCR*

*3.2.2.6.2. Selected genes, target templates and endogenous housekeeping gene for normalisation*

*3.2.2.6.3. Real-time quantitative RT-PCR*

3.3. RESULTS

3.3.1. RED AND WHITE MUSCLE MICROARRAY ANALYSIS

3.3.1.1. Genes more highly expressed in *psoas* red muscle

3.3.1.2. Genes more highly expressed in *longissimus dorsi* white muscle

3.3.2. VALIDATION OF GENE EXPRESSION BY REAL-TIME RT-PCR

3.4. DISCUSSION

4. MICROARRAY PROFILING OF IONOMYCIN REGULATED GENES

4.1. INTRODUCTION

4.2. MATERIALS AND METHODS

4.2.1. TARGET PREPARATION FOR MICROARRAY HYBRIDISATION

4.2.1.1. Primary cell culture and ionomycin treatment

4.2.1.2. Detection of desmin expression in the cultured cells

*4.2.1.2.1. Cell culture on glass slides and methanol/acetone fixation for adherent cells*

*4.2.1.2.2. Immunohistochemical staining of the cultured cells*

4.2.1.3. Calcinuerin cellular phosphatase activity assay

*4.2.1.3.1. Harvesting skeletal muscle myocytes*

*4.2.1.3.2. Preparation of skeletal muscle myocyte extracts*

*4.2.1.3.3. Removal of free phosphate from cell extracts*

*4.2.1.3.4. Protein quantification*

*4.2.1.3.5. GREEN™ phosphatase assay*

4.2.1.4. Preparation of cyanine dye labelled cDNA targets for microarray hybridisations

4.2.2. MICROARRAY HYBRIDISATION AND SEQUENCING ANALYSIS

4.3. RESULTS

4.3.1. DESMIN EXPRESSION IN THE CULTURED CELLS

4.3.2. CALCINEURIN TOTAL PHOSPHATASE ACTIVITY IN SKELETAL MUSCLE MYOCYTES

4.3.3. MICROARRAY IMAGE PROCESSING AND DATA ANALYSIS

4.3.4. DIFFERENTIALLY EXPRESSED GENES

4.3.4.1. Genes more highly expressed in the myocytes treated with ionomycin

4.3.4.2. Genes more highly expressed in the myocytes treated with vehicle (DMSO)

4.4. DISCUSSION

5. GENERAL DISCUSSION

5.1. IMPORTANCE OF THE PORCINE SKELETAL MUSCLE cDNA MICROARRAY FOR PROFILING DIFFERENTIAL GENE EXPRESSION

5.2. IMPORTANCE OF THE IDENTIFIED CLONES IN SKELETAL MUSCLE RESEARCH

5.3. FUTURE DIRECTION IN THE UTILISATION OF THE PORCINE SKELETAL MUSCLE cDNA MICROARRAY

APPENDIX (Further Details of Materials and Methods)

REFERENCES

# LIST OF FIGURES


| Figure No. | Title | Page |
|---|---|---|
| **Figure 2:1** | Expression cassette in ZAP Express® and pBK-CMV vectors | 35 |
| **Figure 2:2** | The entire process of microarray construction in this study | 39 |
| **Figure 2:3** | ZAP Express® vector excision | 41 |
| **Figure 2:4** | A paper-grid, which has 440 sub-squares labelled with numbers from 1 to 440, was attached to the underside of the 243×243×25 mm Bio-Assay dish | 44 |
| **Figure 2:5** | QIAGEN 96-well flat-bottom block and 96-well format filter plate | 50 |
| **Figure 2:6** | QIAGEN QIAvac 96 Vacuum Manifold | 52 |
| **Figure 2:7** | DNA clone stock plates for microarray construction and clone tracking | 58 |
| **Figure 2:8** | Scotlab 96-well format vacuum manifold and Hybaid™ blot processing pump used for the dot blot hybridisation | 65 |
| **Figure 2:9** | Estimation of porcine *Longissimus dorsi* muscle mRNAs extracted for [$\alpha$-$^{32}$P] labelling in colony hybridisations using agarose gel containing ethidium bromide | 71 |
| **Figure 2:10** | Colony hybridisations | 72 |
| **Figure 2:11** | Insert detection of selected clones by restriction enzyme digestion with *Eco*R I and *Xho* I and agarose gel electrophoresis | 75 |
| **Figure 2:12** | Detection of purified PCR-amplified cDNA inserts | 76 |
| **Figure 2:13** | Three types of stock plates kept at -20°C for the construction of porcine skeletal muscle cDNA microarray and clone tracking | 78 |
| **Figure 2:14** | The 48 printed squares of a hybridised microarray slide | 79 |
| **Figure 2:15** | Printing format for each square (16 spots × 16 spots) on the microarray slide | 80 |
| **Figure 2:16** | An example of gene naming and plate identity system of cDNA clones | 82 |
| **Figure 2:17** | An example of the Excel file established for tracking each gene name back to the location of a plasmid clone or a cDNA insert in the stock plates | 83 |
| **Figure 2:18** | Microarray clone tracking system | 84 |
| **Figure 2:19** | Restriction enzyme digestion of unselected clones with both *Eco*R I and *Xho* I prior to Southern blot hybridisation | 87 |
| **Figure 2:20** | Southern blot hybridisation using [$\alpha$-$^{32}$P] labelled cDNA probe derived from 3-day-old neonatal porcine skeletal muscle for unselected clones | 88 |

| Figure No. | Title | Page |
|---|---|---|
| **Figure 2:21** | Southern blot hybridisation using [$\alpha$-$^{32}$P] labelled cDNA probe derived from 3-day-old neonatal porcine skeletal muscle for unselected clones | 89 |
| **Figure 2:22** | Dot blot hybridisation of both selected and unselected plasmid clones with 3-dayold neonatal porcine skeletal muscle total cDNA probe | 100 |
| **Figure 2:23** | Dual-colour microarray hybridisation for monitoring microarray printing process | 101 |
| **Figure 3:1** | Steps taken for the red and white muscle microarray hybridisation | 113 |
| **Figure 3:2** | Procedures for microarray image processing, data mining and validation | 114 |
| **Figure 3:3** | Estimation of mRNAs extracted respectively from *psoas* red muscle and *longissimus dorsi* white muscle of 22-week-old pig 130 for red-white muscle microarray hybridisations using agarose gel containing ethidium bromide | 115 |
| **Figure 3:4** | Imagene™ processed image of red-white muscle microarray hybridisation | 126 |
| **Figure 3:5** | Imagene™ scatterplot demonstrating differential gene expression in red and white muscles | 127 |
| **Figure 3:6** | GeneSpring™ Scatterplot of normalised red-white muscle microarray hybridisation data | 128 |
| **Figure 3:7** | Bin 1 relative gene expression levels in *longissimus dorsi* and *psoas* muscles of four pigs | 135 |
| **Figure 3:8** | Bin 1 relative gene expression levels in eight different porcine tissues derived from the pig 4 | 136 |
| **Figure 3:9** | kc2725 relative gene expression levels in *longissimus dorsi* and *psoas* muscles of four pigs | 137 |
| **Figure 3:10** | kc2725 relative gene expression levels in eight different porcine tissues derived from the pig 4 | 138 |
| **Figure 3:11** | GAPDH and MyHC IIb relative mRNA levels in porcine *psoas* red muscle and *longissimus dorsi* white muscle | 139 |
| **Figure 4:1** | Flow diagram showing methods used for microarray gene expression analysis in this study | 147 |
| **Figure 4:2** | Estimation of mRNAs extracted respectively from ionomycin-treated and vector (DMSO)-treated porcine skeletal muscle myocyte groups using agarose gel containing ethidium bromide | 156 |

| Figure No. | Title | Page |
|---|---|---|
| **Figure 4:3** | Immunohistochemical staining of porcine skeletal muscle cells with monoclonal mouse anti-desmin antibody | 157 |
| **Figure 4:4** | Effects of ionomycin on skeletal muscle myocytes — calcineurin total phosphatase activity in skeletal muscle myocytes | 158 |
| **Figure 4:5** | Microarray image processing | 160 |
| **Figure 4:6** | Expression profiling of ionomycin-regulated genes using GeneSpring™ software | 161 |
| **Figure 4:7** | Expression profiling of total genes using GeneSpring™ software | 162 |

# LIST OF TABLES


| Table No. | Title | Page |
|---|---|---|
| **Table 2:1** | Summary of the main features of XL1-Blue MRF' cells and XLOLR cells | 34 |
| **Table 2:2** | Summary of main features of ZAP Express® vector and ExAssist® interference-resistant helper phage | 36 |
| **Table 2:3** | The commercial kits used in this study and their uses | 38 |
| **Table 2:4** | Reverse transcription reaction for single-stranded cDNA synthesis | 47 |
| **Table 2:5** | Materials used in plasmid DNA extraction in 96-well plate format | 54 |
| **Table 2:6** | T7 and T3 primers used for insert amplification by PCR | 56 |
| **Table 2:7** | Reaction mixture for each PCR in 96-well plate format | 56 |
| **Table 2:8** | Reaction of restriction enzyme digestion | 62 |
| **Table 2:9** | The T7-Cy3 primer target mixture prepared for the microarray hybridisation | 67 |
| **Table 2:10** | Cyanine dye labelling reaction for preparation of microarray hybridisation target | 68 |
| **Table 2:11** | The link between 384-well plates, 96-well plates and the two porcine cDNA libraries | 77 |
| **Table 2:12** | Results of the Southern blot hybridisation | 86 |
| **Table 2:13** | Sequencing of plasmid DNAs derived from the selected colonies | 91-98 |
| **Table 3:1** | Commercial kits and reagents | 111 |
| **Table 3:2** | Software used in microarray expression analysis and real-time quantitative RT-PCR | 111 |
| **Table 3:3** | Primers and TaqMan probes for real-time quantitative RT-PCR | 122 |
| **Table 3:4** | Reaction mixture prepared for real-time quantitative RT-PCR | 124 |
| **Table 3:5** | Genes more highly expressed in *psoas* red muscle than in *longissimus dorsi* white muscle | 129-130 |
| **Table 3:6** | Genes more highly expressed in *longissimus dorsi* white muscle than in *psoas* red muscle | 132 |
| **Table 4:1** | Genes that were at least two-fold ($P<0.05$) more highly expressed in the ionomycin-treated myocytes than in the vehicle-treated myocytes | 163 |
| **Table 4:2** | Genes that were at least two-fold ($P<0.05$) more highly expressed in the vehicle-treated myocytes than in the ionomycin-treated myocytes | 165 |

# ABBREVIATIONS

| | |
|---|---|
| **A** | Adenine |
| **AP-1** | Activator protein-1 |
| **APS** | Ammonium persulphate |
| **ATP** | Adenosine triphosphate |
| **bp** | Base pair(s) |
| **bHLH** | Basic helix-loop-helix |
| **Bin -1** | Box-dependent MYC-interacting protein-1 |
| **BLAST** | Basic local alignment search tool |
| **BMPs** | Bone morphogenic proteins |
| **C** | Cytosine |
| **$Ca^{2+}$** | Calcium ion |
| **$[Ca^{2+}]$** | Calcium concentration |
| **CALD1** | Caldesmon 1 |
| **CaMK** | $Ca^{2+}$-calmodulin-dependent protein kinase |
| **CDK2** | Cyclin-dependent kinase 2 |
| **cDNA** | Complementary DNA |
| **CK2** | Casein kinase 2 |
| **CKMT2** | Creatine kinase mitochondrial 2 |
| **CnA** | Calcineurin A |
| **CnB** | Calcineurin B |
| **$CO_2$** | Carbon dioxide |
| **$C_0t$** | Initial concentration of DNA × time |
| **cpm** | Count per minutes |
| **CsA** | Cyclosporin A |
| **$C_T$** | Cycle threshold |
| **CyDye** | Cyanine dye |
| **Cy3** | Cyanine 3 |
| **Cy5** | Cyanine 5 |
| **$ddH_2O$** | Double distilled water |
| **DEMED** | Dulbecco's modified Eagle's medium |
| **DMPK** | Myotonic dystrophy protein kinase |

| | |
|---|---|
| **DMSO** | Dimethyl sulfoxide |
| **DNA** | Deoxyribonucleic acid |
| **dNTP** | Deoxynucleotide triphosphate |
| **DSCR1** | Down syndrome critical region 1 |
| **DTT** | Dithiothreitol |
| **EB** | Ethidium bromide |
| ***E. coli*** | *Escherichia coli* |
| **EDTA** | Ethylenediaminetetra-acetic acid |
| **ELISA** | Enzyme linked immunosorbent assay |
| **ERK** | Extracellular signal-regulated kinase |
| **EST** | Expressed sequence tag |
| **FAM** | 6-carboxyfluorescein |
| **FIRE** | Fast intronic regulatory element |
| **FKBP12** | FK506-binding protein |
| **FMOD** | Fibromodulin |
| **FSCN** | Fascin |
| **G** | Guanine |
| **GAPDH** | Glyceraldehyde-3-phosphate-dehydrogenase |
| **GM-CSF** | Granulocyte/macrophage colony-stimulating factor |
| **GPS2** | G protein pathway suppressor 2 |
| **GSK-3** | Glycogen synthase kinase-3 |
| **GSK3β** | Glycogen synthase kinase 3β |
| **HEPES** | 4-2-hydroxyethyl-1-piperazineethanesulfonic acid |
| **$H_2O$** | Water |
| **HPRT** | Hypoxanthine guanine phosphoribosyl tranferase |
| **HSPA8** | Heat shock cognate protein |
| **HSS** | High speed supernatant |
| **IGF-1** | Insulin-like growth factor-1 |
| **IGF-1R** | IGF-1 receptor |
| **IGF-2** | Insulin-like growth factor-2 |
| **IL-1** | Interleukin-1 |
| **IL-2** | Interleukin-2 |
| **JNK** | *Jun*-amino-terminal kinase |

| | |
|---|---|
| **Kb** | Kilobase(s) |
| **lb.** | Pound |
| **LD** | *Longissimus dorsi* |
| **LOWESS** | Localised weighted regression |
| **LB** | *Luria-Bertani* |
| **MAFbx** | Muscle atrophy F-box |
| **MAPK** | Mitogen-activated protein kinase |
| **MAP3K7** | Mitogen-activated protein kinase kinase kinase 7 |
| **MCIP1** | Myocyte-enriched calcineurin-interacting protein 1 |
| **MCIP2** | Myocyte-enriched calcineurin-interacting protein 2 |
| **MEF2** | Myocyte enhancer factor-2 |
| **MEKK1** | MEK kinase 1 |
| **mbar** | Millibar |
| **mg** | Milligram |
| **ml** | Millilitre(s) |
| **µg** | Microgram |
| **µl** | Microlitre |
| **MOI** | Multiplicity of infection |
| **MRFs** | Myogenic regulatory factors |
| **mRNA** | Messenger RNA |
| **mTOR** | Mammalian target of rapamycin |
| **MyHCs** | Myosin heavy chains |
| **MuRF** | Muscle ring finger |
| **NaCl** | Sodium chloride |
| **NFATs** | Nuclear factor of activated T-cells |
| **ng** | Nanogram |
| **NHR** | NFAT-homology region |
| **NREs** | NFAT response elements |
| **°C** | Degrees Celsius |
| **OD** | Optical density |
| **$^{32}$P** | Phosphorous 32 isotope |
| **PBS** | Phosphate-buffered saline |
| **PCR** | Polymerase chain reaction |

| | |
|---|---|
| **PDK1** | 3'-phosphoinositide-dependent protein kinase 1 |
| **PGC-1α** | Peroxisome proliferator-activated receptor gamma coactivator-1 |
| **pH** | Negative logarithm of hydrogen ion concentration |
| **PI3K** | Phosphatidylinositol 3-kinase |
| **PKB** | Protein kinase B |
| **PP2B** | Protein phosphatase 2B |
| **p70S6K** | P70 S6 kinase |
| **PtdIns(3,4,5)$P_3$** | Phosphatidylinositol-3,4,5-trisphosphate |
| **PTEN** | Phosphatase and tensin homologous on chromosome 10 |
| **PTK9L** | Protein tyrosine kinase-9 like |
| **rRNA** | Ribosomal RNA |
| **RNA** | Ribonucleic acid |
| **RNase** | Ribonuclease |
| **RSD** | *Rel*-similarity domain |
| **RT-PCR** | Reverse transcription-polymerase chain reaction |
| **RyR1** | Ryanodine receptor 1 |
| **SERCA1** | Sarcoplasmic/endoplasmic reticulum calcium ATPase 1 |
| **SDS** | Sodium dodecyl sulfate |
| **Shh** | Sonic hedgehog |
| **SHIP** | SH2-domain-containing inositol 5'-phosphatase |
| **smpx** | Small muscle protein |
| **SNPs** | Single nucleotide polymorphisms |
| **sq.** | Square |
| **SR** | Sarcoplamic reticulum |
| **SURE** | Slow upstream regulatory element |
| **T** | Thymine |
| **TADs** | Transcriptional-activation domains |
| **TAE** | Tris-acetate |
| **TAMRA** | 6-carboxy-tetramethyl-rhodamin |
| **TBE** | Tris-boric acid |
| **TcR** | T-cell receptor |
| **TE buffer** | Tris, EDTA buffer |
| **TEMED** | N, N, N', N'-tetramethylethylenediamine |

| | |
|---|---|
| **TGF-β** | Transforming growth factor β |
| **Tm** | Melting temperature |
| **TnC** | Troponin C |
| **TNF** | Tumor necrosis factor |
| **TnIf** | Fast muscle fibre-specific troponin I |
| **TnIs** | Slow isoform of troponin I |
| **Tris** | Tris(hydroxymethyl)aminomethane |
| **tRNA** | Transfer RNA |
| **Tsc** | Tuberous sclerosis complex |
| **T-tubules** | Transverse tubular membrane |
| **UV** | Ultraviolet |
| **v/v** | volume/volume |
| **w/o** | Without |
| **w/v** | weight/volume |

# SUMMARY

Gene expression profiling using DNA microarrays has the potential to illuminate the molecular processes that govern the phenotypic characteristics of porcine skeletal muscles, such as hypertrophy or atrophy, and the expression of specific fibre types. This information is not only important for understanding basic muscle biology but also provides underpinning knowledge for enhancing the efficiency of livestock production. This thesis describes the *de novo* development of a composite skeletal muscle cDNA microarray, comprising 5,500 clones from two developmentally distinct cDNA libraries (*longissimus dorsi* of a 50-day porcine foetus and the *gastrocnemius* of a 3-day-old pig). The cDNA clones selected for the microarray assembly were of low to moderate abundance, as indicated by colony blot hybridisation. Once constructed, the porcine cDNA microarray was used to profile the differential expression of genes between the *psoas* (red muscle) and the *longissimus dorsi* (white muscle) of a pig, by co-hybridisation of Cy3 and Cy5 labelled cDNA derived from these two muscles. Clones that were preferentially more highly expressed in one muscle type were chosen for identification by sequencing. A number of novel candidate regulatory genes and candidate genes that could be involved in muscle phenotype determination were identified. Gene expression results from seven microarray slides (replicates) correctly identified genes (e.g., genes of mitochondrial origin, genes for myosin heavy chain fast isoforms) that were expected to be differentially expressed, as well as a number of candidate regulatory genes (e.g., genes for bin 1, heat shock cognate protein, casein kinase 2 α1 subunit). A novel gene kc2725 was also identified as being differentially expressed. These candidate genes could be involved in muscle phenotype determination, and include several members of the casein kinase 2 signalling pathways (e.g., casein kinase 2 α1 subunit, small muscle protein, tyrosine kinase 9-like A6-related protein). Quantitative real-time RT-PCR performed on the selected genes (e.g., bin 1, novel gene kc2725, myosin heavy chain IIb) was used to confirm the results from the microarray. The red-white muscle microarray expression analysis demonstrated the effectiveness of the porcine cDNA microarray for high throughput differential gene expression. Differential gene expression using the porcine skeletal muscle cDNA microarray was also studied in the ionomycin-treated and the control vehicle-treated porcine skeletal muscle myocytes by co-hybridisation of Cy3 and Cy5 labelled cDNA targets derived from both cell groups. Results from eight replicated microarray hybridisations profiled high throughput gene expression and identified a number

of ionomycin-regulated genes (e.g., genes for protein tyrosine phosphatase non-receptor type 13, dystrophia myotonica-protein kinase) in porcine skeletal muscle. This study further confirmed effectiveness of the porcine cDNA microarray for profiling differential gene expression.

# CHAPTER ONE

# INTRODUCTION

# INTRODUCTION

Complementary DNA (cDNA) microarrays are technological approaches that have the potential to accurately measure changes in global mRNA expression levels in various biological contexts (DeRisi and Iyer, 1999;Epstein and Butow, 2000). This project was designed to develop a porcine skeletal muscle cDNA microarray, and utilise the microarray in different biological contexts for investigating the molecular basis of skeletal muscle physiological processes.

To date, rapid progress has been made in delineating signalling pathways that influence skeletal muscle remodelling in response to environmental or pathological stresses (Chin et al., 1998;Dunn et al., 1999;Wu et al., 2000). While the causes and consequences of myocyte differentiation, proliferation, hypertrophy, atrophy and fibre phenotype switch are well known, the underlying transcriptional mediators of these processes and the molecular details of complex interactions among different signalling pathways which evoke these processes are less clear (Olson and Williams, 2000a;Olson and Williams, 2000b). To investigate molecular pathways involved in skeletal muscle, significant and pressing progress has been anticipated in obtaining vast amount of information on gene expression patterns in skeletal muscle in various biological contexts. With the advent of microarray technology, skeletal muscle research has seen increasing application of DNA microarray to simultaneous evaluation of expression levels of thousands of mRNA species (Stewart, 2000;Hughes and Shoemaker, 2001). Such studies have previously been limited to human and rodent systems. The pig is both an invaluable large animal experimental model for human health, and an important target farm animal species that serves as one of the major sources of protein for human consumption. For many decades, commercial swine industries have been pursuing higher growth rate and better meat quality in pigs as two of their highest priority goals for profitability. The study of complex genomic interactions has been the focus of research in recent years to identify pigs with better genetic potential for the improvement of pig production. In addition to its applicability to agriculture, the pig's role in biomedical research makes the study of the porcine genome important for the investigation of human skeletal muscle development, regeneration, function and diseases. To better understand the physiological complexity of the pig skeletal muscle transcriptomes for both agricultural purpose and for its importance to human biomedical concerns, high throughput gene expression profiling needs to be undertaken. Request and desire have, therefore, arisen for the development of a porcine skeletal muscle cDNA microarray, which has previously not been reported.

# 1.1. SKELETAL MUSCLE STRUCTURE AND FIBRE TYPES

## 1.1.1. GENERAL DESCRIPTION OF SKELETAL MUSCLE STRUCTURE

Skeletal muscles consist of bundles of multinucleated, differentiated and cylindrical cells, called muscle fibres, which lie side by side and run roughly parallel to the line of muscle action. Along the centre of each muscle fibre, occupying most of the intracellular space, are protein filaments called myofibrils. Consequently, nuclei and mitochondria are forced to peripheral locations in the cytoplasm (or sarcoplasm). Each myofibril comprises a continuous chain of contractile elements called sarcomeres. These are the basic units of muscle function, each capable of generating a vectoral force when activated. Sarcomeres are composed mostly of actin thin filaments and myosin thick filaments. Sarcomeres are directionally aligned and work co-operatively, so that when muscle contracts, tension develops along the axis of the myofibrils and, hence, along the muscle fibre itself. When it is observed with a light microscope, the skeletal muscle cells are characterised by a series of light and dark bands perpendicular to the long axis of the muscle fibre. This striated banding pattern in skeletal muscle results from the precise arrangement of numerous thick and thin filaments in the cytoplasm into myofibrils. Because the striations on adjacent myofibrils are usually aligned, the entire muscle fibre appears uniformly striated (McGavin et al., 2001;Russell et al., 2000).

## 1.1.2. MYOFILAMENT SUBSTRUCTURE

### 1.1.2.1. Thin filaments

The thin filaments consist largely of the contractile protein actin, as well as two other proteins - tropomyosin and troponin. Actin is a globular protein. An actin molecule is composed of a single polypeptide that polymerises with other actins to form two intertwined helical chains that make up the primary structure of a thin filament. Each actin molecule contains a binding site for myosin heavy chain. Tropomyosin molecules, which stretch along each strand of the thin filament, exist as homodimers or heterodimers of two identical or similar $\alpha$-helical polypeptide chains arranged in parallel. Tropomyosin is wedged into the grooves formed by the actin helix, and attached, at intervals, complexes of globular protein molecules, collectively called troponin.

Troponin is a complex of three subunits: troponin C, troponin I, and troponin T. In skeletal muscles, tropomyosin, together with the troponin complex, comprises the $Ca^{2+}$-dependent regulatory machinery by which the interaction of F-actin and myosin are controlled by the level of calcium ions (Vander et al., 2001;Randall et al., 2002;Pollard et al., 1999;Squire and Morris, 1998).

#### 1.1.2.2. Thick filaments

The thick filaments are composed almost entirely of a large contractile protein myosin. The skeletal muscle myosin molecule consists of two heavy chains (MyHCs), two essential light chains and two regulatory light chains. The N-terminal region of each heavy chain, along with the regulatory light chains and the essential light chains, forms the globular head region of the skeletal muscle myosin. The C-terminal portions of the two heavy chains coil together to form a rod of 150 nm long. Thus, each skeletal muscle myosin has two globular heads and a long coiled-coil α-helical rod. The head portions of the skeletal myosin reach out from the thick filament and interact with adjacent actin filaments, forming the cross bridges. Each cross-bridge consists of two identical globular myosin heads. Cross-bridges extend outward from myosin thick filaments and contact actin in the thin filaments during muscle contraction. Muscles contract when the cross-bridges on myosin molecules bind transiently to sites on actin molecules, causing molecules to change their physical conformation. These changes in the shape of the myosin molecules generate force, which drags the actin filaments past the myosin filaments and causes the sarcomere to shorten. The bond between actin and myosin is then broken. The cross-bridges bind and unbind over and over again, generating force each time they bind. Therefore, the principal determinant of skeletal muscle movement and performance is controlled by actin-myosin interaction in the sarcomere (Vander et al., 2001;Randall et al., 2002;Pollard et al., 1999).

### 1.1.3. SKELETAL MUSCLE FIBRE TYPES

#### 1.1.3.1. Slow muscle and fast muscle

Based on speeds of shortening, whole skeletal muscle can be classified as being slow muscle or fast muscle. Slow muscle fibres, also termed slow-twitch oxidative fibres, have long twitch

times, slow contraction velocity and high resistance to fatigue. Slow muscle fibres fatigue very slowly for two reasons. First, slow muscle fibres have a large number of mitochondria and oxidative enzymes, a rich blood supply supporting sustained oxidative phosphorylation, and a high capacity to generate ATP by oxidative metabolic processes. Slow muscle fibres contain very little glycogen and creatine phosphate. Second, slow muscle fibres use/split ATP at a relatively slow rate (Brooke and Kaiser, 1970; Chang et al., 1993). Skeletal muscles that contain a high proportion of slow muscle fibres are often called red muscles. The dark, reddish colour of slow muscles is caused by the high concentration of the oxygen-storage protein myoglobin in the sarcoplasm (cytoplasm) of slow muscle fibres. Hemoglobin, the pigment of red blood cells, brings oxygen from lungs to capillaries on the muscle fibre surface. From here, the transport of oxygen to the interior of the skeletal muscle fibre is facilitated by myoglobin. Slow muscle fibres contain an abundance of compounds that make them efficient at aerobic (complete oxidation of substrates with need for blood-borne oxygen) respiration. These compounds are high in both fat and sugar, which act as fuel for aerobic metabolism. Slow muscles produce less power for longer periods and are better suited for sustaining prolonged, low intensity contractile activity (e.g. postural maintenance; marathon running) (Brooke and Kaiser, 1970; Chang et al., 1993). Slow muscles are found in large numbers in the postural muscles of the neck and in the *soleus* muscle in the leg.

Fibres of fast muscles can be categorised into two subtypes: fast-twitch glycolytic fibres and fast-twitch oxidative-glycolytic fibres. Fast-twitch glycolytic fibres, also called white muscles, usually appear white in colour. The white colour of fast-twitch glycolytic fibres is due to anaerobic (incomplete oxidation of carbohydrates without need for oxygen) energy metabolism. The majority of mammalian muscles contain a mixture of both red and white muscle fibres, with white muscle fibres normally larger than red muscle fibres. Fast-twitch glycolytic fibres display a fast contraction velocity but fatigue quickly/easily. Fast-twitch glycolytic fibres fatigue very quickly for two reasons. First, fast-twitch glycolytic fibres generate most of their ATP by anaerobic metabolic processes, and produce high levels of power for short periods. These properties correlate with high glycolytic activities, high ATPase activity and low oxidative capacity of fast-twitch glycolytic fibres. Fast-twitch glycolytic fibres store high levels of glycogen and creatine phosphate, but contain relatively few mitochondria, relatively few blood capillaries, and a low content of myoglobin. Second, fast-twitch glycolytic muscle fibres use/split ATP at a fast rate. Fast-twitch glycolytic muscle fibres are suited to high power output and are usually recruited only where very rapid or very intense effort is required. Fast-twitch

oxidative-glycolytic fibres appear to occupy an intermediate position between slow-twitch oxidative fibres and fast-twitch glycolytic fibres (Brooke and Kaiser, 1970;Chang and Fernandes, 1997;Pierobon et al.,1981;Schiaffino and Reggiani, 1996). Fast-twitch oxidative-glycolytic fibres, which are high in oxidative enzymes, glycolytic enzymes, and ATPase activity, have both aerobic and anaerobic energy metabolism capabilities. Fast-twitch oxidative-glycolytic fibres have faster contraction speed when compared with slow muscle fibres, and are resistant to fatigue (Brooke and Kaiser, 1970;Chang and Fernandes, 1997;Pierobon et al.,1981;Schiaffino and Reggiani, 1996).

### 1.1.3.2. Myosin heavy chain isoforms and skeletal muscle fibre types

The MyHC of skeletal muscle is both a structural protein and an enzyme that hydrolyses ATP (Pollard et al., 1999;Sun et al., 2001). Currently, the definitive classification of skeletal muscle fibre types is based on the MyHC isoform identification. In mammalian skeletal muscle, nine MyHC isoforms have been identified. They are I/β, α, extra-ocular, neonatal, embryonic, IIa, IIb, IIx, and IIm (Sciote and Morris, 2000;Weiss and Leinwand, 1996). Each of these proteins is encoded by a distinct gene and each has its own ATPase activity located in the head region of the molecule (Schiaffino and Reggiani, 1994;Schiaffino and Reggiani, 1996). MyHC is the major structural protein of the myofibrillar thick filaments that are associated with power generation necessary for muscle contraction. Skeletal muscle fibres can be classified into types, since typically in any given muscle cell, the majority of the sarcomeric thick filaments contain the same isoform of MyHC, although co-expression of MyHCs within a single fibre is possible. MyHC α is a fast contracting MyHC isoform expressed in cardiac muscle. MyHC α also has rare tissue-specific expression in skeletal muscle and has been identified in both human and rabbit jaw-closing muscle. Extraocular MyHC is the main MyHC isoform in the posterior cricoarytenoid muscle. Embryonic and neonatal MyHC isoforms are typically expressed during muscle development. MyHC IIm has tissue-specific expression in the jaw-closing muscles of carnivores and primates (Sciote and Morris, 2000).

In mammals, the main MyHC isoforms in adult skeletal muscle are I/β, IIa, IIb and IIx. The expression of these four MyHC isoforms has been identified in postnatal porcine skeletal muscles (Chang et al., 1993;Chang et al., 1995;Chang, 2000;Chang and Fernandes, 1997;da Costa et al., 2002;da Costa et al., 2003). MyHC IIb fibres are absent in human, horse and cow

skeletal muscles (Smerdu et al., 1994; Eizema et al., 2003; Chikuni et al., 2004). MyHC I/β is the same slow contracting MyHC with β designating its presence in heart muscle and I in skeletal muscle (Sciote and Morris, 2000). MyHC I fibres are slow-twitch oxidative fibres. MyHC IIa, IIb and IIx are fast contracting isoforms with average fibre diameter and shortening speed relative to each other as IIb>IIx>IIa. Of the three fast fibres, MyHC IIx fibres appear to occupy an intermediate position between MyHC IIa and MyHC IIb fibres, with respect to oxidative capacity, fatigue resistance and velocity of contraction, resulting in the description of MyHC IIa and MyHC IIx fibres as fast-twitch oxidative-glycolytic fibres and MyHC IIb fibres as fast-twitch glycolytic fibres (Schiaffino and Reggiani, 1994). Metabolically, MyHC IIx fibres are more similar to MyHC IIb fibres, whilst MyHC IIa fibres are more closely related to MyHC I fibres. If only a weak contraction is needed to perform a task, only MyHC I fibres are activated by their motor units. If a stronger contraction is needed, the motor units of MyHC IIa fibres are activated. If a maximal contraction is required, motor units of MyHC IIb fibres are activated as well. Activation of various motor units is determined in the brain and spinal cord. Although fibre composition is strongly determined by genetic factors, these differences may also be strongly influenced by the type, intensity and duration of training, as well as the pre-training status of an individual. Remarkably, myofibres have the ability to transform between the different fibre types in response to environmental stimuli, changing the physiological properties of the skeletal muscle and facilitating adaptation of the skeletal muscle to environmental needs.

# 1.2. MOLECULAR PATHWAYS IN SKELETAL MUSCLE

## 1.2.1. MYOGENIC REGULATORY FACTORS AND SKELETAL MUSCLE

Embryonic skeletal myogenic cells arise from somitic progenitors in response to signalling molecules from surrounding tissues that specify myogenic cell fate. Adult myogenic cells, which are active during the post-natal growth and regeneration of skeletal muscle, are derived mainly from skeletal muscle satellite cells (Parker et al., 2003). Bone-marrow cells has been shown to participate in regenerative myogenesis (Ferrari et al., 1998;LaBarge and Blau, 2002). The signalling pathways and regulatory genes, which activate myogenesis in embryonic cells and adult stem cells, are largely unknown at this time (Buckingham, 2001). The myogenic regulatory

factors (MRFs) subfamily consists of MyoD (also termed Myf-3), Myf-5, myogenin (also termed Myf-1), and MRF4 (also termed Myf-6/Herculin) (Arnold and Braun, 1996). In all cases, overexpression of these factors converts non-muscle cells to the myogenic lineage, demonstrating their role in myogenic lineage determination and differentiation. Furthermore, the ability of each factor to initiate the expression of one or more of the other three suggests they form a cross-regulatory loop. The MRFs belong to the basic helix-loop-helix (bHLH) superfamily of transcription factors. The MRF proteins contain a conserved basic DNA-binding domain essential for sequence-specific DNA-binding and a helix-loop-helix domain that is responsible for heterodimerisation of the MRFs with the ubiquitously expressed E-protein family of transcription factors. Each of the MRFs has been shown to heterodimerise with E proteins. The heterodimers bind in a sequence-specific manner to E-box DNA sequences (CANNTG), which is present in the promoters of many skeletal muscle-specific genes and mediates gene activation in an MRF-dependent manner. Although the MRFs share a highly homologous bHLH domain, they have limited functional redundancy, owing to sequence divergence in their amino and carboxyl terminals.

During development, the MRFs are expressed in a highly regulated spatial and temporal fashion. Either directly or indirectly, the signalling pathways that influence the onset of myogenesis lead to activation of the myogenic determination genes Myf5 and MyoD. At least one of the two factors (MyoD and Myf5) is required for determining the myogenic/myoblast lineage during embryonic development (Rudnicki et al., 1993). Once myogenic cells have been specified, skeletal-muscle development requires the differentiation and fusion of progenitors to form multinucleated myotubes and myofibres. Expression of myogenin and MRF4 is dependent on both the Myocyte Enhancer Factor-2 (MEF2) family and the MRFs (Naidu et al., 1995;Ridgeway et al., 2000). Myogenin has an important role in differentiation rather than specification (Hasty et al., 1993;Nabeshima et al., 1993). MRF4 is important for terminal differentiation, fusion and myofibre maintenance (Braun and Arnold, 1995;Patapoutian et al., 1995;Zhang et al., 1995). Activation of myogenin and MRF4, is dependent upon the preceding expression of MyoD and/or Myf5, which are expressed prior to muscle cell differentiation. The paired-domain transcription factors Pax3 and Pax7, which are expressed by myogenic precursors, act upstream of MyoD and Myf5 (Parker et al., 2003). The temporal expression of Sonic hedgehog (Shh), Wnts that encode protein growth factors, bone morphogenic proteins (BMPs) and homeobox gene Msx1 (Bendall et al., 1999;Houzelstein et al., 1999;Odelberg et al., 2000;Woloshin et al., 1995) in embryonic skeletal myogenic cells ensures the appropriate

proliferation of myogenic precursors before myogenic differentiation. For example, Shh activates Myf5 (Borycki et al., 1999), Wnt1 activates expression of Myf5 indirectly (Cossu et al., 1996), Wnt7a activates expression of MyoD indirectly, and Wnt3a activates expression of MyoD either directly or indirectly (Tajbakhsh et al., 1998). BMPs, which inhibit expression of MyoD, might function to establish a sufficient number of myogenic progenitors before terminal differentiation (Amthor et al., 1998;Dietrich et al., 1998). BMP inhibitor noggin induces premature differentiation and prevents myogenic proliferation (Hirsinger et al., 1997;McMahon et al., 1998;Reshef et al., 1998). Wnt-mediated activation of β-catenin signalling might activate the paired-domain transcription factor Pax3, leading to the expression of myogenin and, ultimately, myogenic differentiation. Notch ligand DELTA-1 (Delfini et al., 2000;Hirsinger et al., 2001) might negatively regulate differentiation of myogenic cells. Therefore, the competing action of Msx1, Shh, Wnts, BMPs, noggin, DELTA-1, and β-catenin could function to regulate expression of the MRFs.

Satellite cells arise during the late stages of embryogenesis and are highly active during the postnatal growth and regeneration of skeletal muscle tissue, so they provide most of the myonuclei to adult muscles (Zammit and Beauchamp, 2001). In adult muscles, satellite cells, which lie between the basal lamina and the muscle fibre, constitute a reservoir of undifferentiated, quiescent muscle precursor cells that are activated in response to muscle damage or weight bearing, leading to regeneration of adult skeletal muscle (Seale and Rudnicki, 2000). Recently, multipotent capacity of satellite cells to differentiate into osteogenic or adipogenic cell types has also been reported (Seale et al., 2001;Goldring et al., 2002;Hawke and Garry., 2001;Asakura et al, 2003). Some studies indicated that satellite cells are derived from the somite, whilst other studies showed that satellite cells are derived from cells that are associated with the embryonic vasculature (Armand et al., 1983;De Angelis et al, 1999). The heterogeneity in satellite-cell populations described by recent studies might reflect several developmental origins for this lineage. Satellite cells were traditionally thought to give rise to all postnatal myogenic progenitors. Recently, bone-marrow derived stem cells have been shown to be able to first differentiate as satellite cells in injured or diseased skeletal muscle, thereby providing a renewable source of myogenic progenitors (Ferrari et al., 1998;Bittner et al., 1999;Gussoni et al., 1999). Independent adult stem-cell populations that are resident in skeletal muscle have also been defined and considered to function as satellite-cell myogenic progenitors (Seale et al., 2001). Quiescent satellite cells do not express detectable levels of MRF protein or transcripts.

However, in response to muscle damage, activated satellite cells commit to the myogenic lineage and express either MyoD or Myf5 prior to differentiation and fusion onto the existing damaged fibre. The co-expression of MyoD and Myf5 in satellite-cell-derived progenitors defines the myogenic precursor cells that proliferate in response to several growth factors and cytokines. Activation of myogenin and Mrf4 is associated with terminal differentiation and fusion of myogenic precursor cells to new or existing fibres. The MRF expression profile in the satellite-cell lineage indicates that satellite cells might share a common developmental programme for the acquisition of myogenic identity and subsequent muscle regeneration with embryonic muscle lineages. Although it is clear that similar transcriptional pathways control myogenic differentiation in embryonic and adult progenitors, there are notable differences. During regenerative responses, activated satellite cells, committed myoblasts or adult stem cells must give rise to new satellite cells. Such a mechanism involves a specific transcriptional programme that is probably not active in embryonic or foetal myoblasts. The development of the satellite-cell lineage is dependent on the activity of the paired-box transcription factor, Pax7, which might function in the specification of satellite cells upstream of the MRFs. However, the downstream genetic pathways that are regulated by the Pax proteins (Pax7 and Pax3) in both embryonic and adult muscle development remain largely unknown. At present, little is known about the signalling pathways and transcriptional factors that regulate the myogenic differentiation, or activation and specification of adult stem cells. In vertebrates, it is considered that the fundamental transcriptional programme which regulates embryonic myogenesis and builds foetal muscles, is reactivated in adult stem cells to produce myogenic progenitors for tissue repair. However, it remains to be determined whether myogenic induction in somitic and adult stem cells is under the influence of the same signalling molecules. It is not yet clear which environmental signalling molecules elicit their expression (Seale and Rudnicki, 2000), nor to what extent the myogenic strategy is strictly equivalent. As in the embryo, the important regulatory question of proliferative versus myogenic responses remains open, both at the stem cell and the satellite cell level (Goldring et al., 2002).

## 1.2.2. SKELETAL MUSCLE ATROPHY AND HYPERTROPHY

In the adult mammal, skeletal muscle hypertrophy is characterised by an increase in size (as opposed to the number) of individual myofibres, with or without the addition of new myonuclei.

Skeletal muscle myofibre size can be regulated by two distinct mechanisms. First, the cytoplasmic volume associated with individual myonuclei is regulated. This pathway appears to involve regulation of protein synthesis, through insulin-like growth factor-1 (IGF-1) mediated phosphatidylinositol 3-kinase (PI3K) signalling, and of protein degradation, through muscle-specific ubiquitin ligases (Glass, 2003a;Glass, 2003b). Second, the number of myonuclei within a myofibre also determines myofibre size. For example, the myonucleis are lost during atrophy whereas during postnatal growth and hypertrophy, the myonucleated muscle cells - myoblasts proliferate and fuse to existing myofibres (Schiaffino and Serrano, 2002). However, the mechanisms controlling myoblast fusion have remained elusive. Skeletal muscle hypertrophy results primarily from the growth of each muscle cell, rather than an increase in the number of cells. Hypertrophy occurs as an adaptive response to load-bearing exercise, and as a result of an enhanced rate of protein synthesis. This increase in protein synthesis enables new contractile filaments to be incorporated into the pre-existing muscle fibre, which in turn enables the muscle to generate greater force. Skeletal muscle hypertrophy can be induced by a number of stimuli, the most familiar of which is exercise. Whereas an increase in protein synthesis has been shown to occur during hypertrophy, atrophy has been associated with increases in protein breakdown. However, skeletal muscle atrophy is not necessarily the converse of skeletal muscle hypertrophy (Haddad et al., 2003a;Haddad et al., 2003b). Cancer and AIDS are disease conditions that cause skeletal muscle atrophy (Jagoe and Goldberg, 2001). A variety of circulating proteins have been shown to induce atrophy, including the cachexic cytokine interleukin-1 (IL-1), tumor necrosis factor (TNF) (Jagoe and Goldberg, 2001), and transforming growth factor β (TGF-β) family member myostatin (Kocamis and Killefer, 2002;Zimmers et al., 2002). Conditions that lead to skeletal muscle atrophy cause a decrease in the size of pre-existing muscle fibres, resulting from increases in the rate of ATP-dependent ubiquitin-mediated proteolysis (Mitch and Goldberg, 1996).

### 1.2.2.1. Skeletal muscle atrophy via induction of ubiquitin ligase pathway

During skeletal muscle atrophy, a dramatic increase in protein degradation and turnover is stimulated. This stimulation of proteolysis is shown to occur at least in part because of an activation of the ubiquitin ligase pathways (Jagoe et al., 2002). Ubiquitin is a short peptide that can be conjugated to specific protein substrates. A chain of polyubiquitin, built onto the substrate through ligation, targets the substrate, which is then proteolysed into small peptides. This process

requires three distinct enzymatic components, an E1 ubiquitin-activating enzyme, an E2 ubiquitin-conjugating enzyme, and E3 ubiquitin-ligating enzyme. The ubiquitin ligase pathways, which regulate ubiquitination, might be activated by the enhanced proteolysis of a key inhibitor protein, or be inactivated via the degradation of an activating enzyme. The involvement of the ubiquitin ligase pathways in skeletal muscle atrophy, during which rates of protein breakdown increase, has been well-established (Lecker et al., 1999;Lecker, 2003;Tawa, Jr. et al., 1997). Expression of two muscle-specific ubiquitin ligases - MuRF1 (muscle ring finger) and MAFbx (muscle atrophy F-box; also known as Atrogin-1) - is significantly increased in multiple settings of skeletal muscle atrophy (Bodine et al., 2001a;Gomes et al., 2001). MuRF1 and MAFbx do not seem to be required for normal muscle growth or function. Both of MuRF1 and MAFbx encode E3 ubiquitin ligases. Expression of MuRF1 and MAFbx is stimulated when the nerve innervating a muscle is cut, during sepsis, by treatment with a glucocorticoid that causes muscle cachexia, or by immobilisation of muscle (Bodine et al., 2001b;Wray et al., 2003).

### 1.2.2.2. The IGF-1/PI3K/AKT1/mTOR/p70S6K pathway and skeletal muscle hypertrophy

The downstream signalling mechanisms induced by insulin-like growth factor-1 (IGF-1) that are required for skeletal muscle hypertrophy has been a matter of some controversy. It was initially reported that calcineurin was critical for IGF-1-mediated hypertrophy and also required for load-induced hypertrophy (Dunn et al., 1999;Olson and Williams, 2000a; Olson and Williams, 2000b;Semsarian et al., 1999). However, recent work has shown that calcineurin signalling is not required for muscle fibre growth (Bodine et al., 2001a;Bodine et al., 2001b) and activated calcineurin shows no evidence for skeletal muscle hypertrophy (Naya et al., 2000;Serrano et al., 2001). Moreover, recent work has demonstrated that IGF-1 induces hypertrophy by stimulating the phosphatidylinositol 3-kinase (PI3K) and the subsequent direct target protein kinase, Akt, resulting in the downstream activation of proteins that are required for protein synthesis. IGF-1, as one of the major downstream targets of growth hormone, is essential for regulating growth and body size at both prenatal and postnatal stages. Increases in muscle load stimulate the expression of IGF-1 (DeVol et al., 1990). Overexpression of IGF-1 *in vitro* using a muscle-specific promoter have resulted in significant increase in muscle mass (Coleman et al., 1995;Musaro et al., 2001). IGF-1 stimulation is sufficient to induce hypertrophy of skeletal muscle in adult mammals (Vandenburgh et al., 1991). The IGF-1 receptor (IGF-1R) is a receptor tyrosine kinase that becomes activated upon IGF-1 binding. The binding of IGF-1 to IGF-1R on the outside surface of muscle cells induces IGF-1R to phosphorylate itself at several tyrosine

residues located inside the cell. This results in the recruitment of a lipid kinase termed phosphatidylinositol 3-kinase (PI3K) to the plasma membrane of cells. Therefore, PI3K activity is necessary for IGF-1 to induce skeletal muscle hypertrophy, and its activation is sufficient to induce hypertrophy (Murgia et al., 2000). Furthermore, skeletal myotube hypertrophy induced by IGF-1 could be inhibited by a pharmacological inhibitor of PI3K (Rommel et al., 1999).

Activated PI3K phosphorylates phosphatidylinositol-4,5-biphosphate, producing phosphatidylinositol-3,4,5-trisphosphate [PtdIns(3,4,5)$P_3$] (Matsui et al., 2003;Vivanco and Sawyers, 2002). PtdIns(3,4,5)$P_3$ is a membrane-binding site for two kinases: PDK1 (for 3'-phosphoinositide-dependent protein kinase 1) and Akt, which is also known as protein kinase B (PKB). Akt is a serine/threonine kinase and a major participant in growth factor-mediated cell survival (Kandel and Hay, 1999). Three major isoforms of Akt (Akt1, Akt2 and Akt3) encoded by three distinct genes have been found in mammalian cells (Altomare et al., 1995;Jones et al., 1991;Nakatani et al., 1999). All three Akt isoforms are ubiquitously expressed in mammals; and Akt1 is the predominant isoform in most tissues (Vivanco and Sawyers, 2002). Akt1 activity is required for IGF-1-mediated hypertrophy (Pallafacchina et al., 2002), and expression of a constitutively active form of Akt1 in skeletal muscle cells, either *in vitro* or *in vivo*, is sufficient to induce muscle hypertrophy (Bodine et al., 2001a;Bodine et al., 2001b;Chen et al., 2001;Rommel et al., 2001;Shioi et al., 2002;Takahashi et al., 2002). A pleckstrin homology domain of Akt binds to PtdIns(3,4,5)$P_3$, resulting in translocation of Akt from the cytosol to the plasma membrane where PtdIns(3,4,5)$P_3$ is located. Akt is phosphorylated and activated by PDK1 after translocation to the plasma membrane. Once activated, Akt dissociates from the plasma membrane and phosphorylates numerous substrates in both the cytoplasm and the nucleus, including proteins that mediate protein synthesis, gene transcription, cell proliferation and survival (Matsui et al., 2003;Vivanco and Sawyers, 2002). Akt1 activity can be regulated either by directly controlling its phosphorylation state or by altering the levels of PtdIns(3,4,5)$P_3$ that it binds at the cell membrane (Alessi et al., 1997). The Akt1 lipid-binding site PtdIns(3,4,5)$P_3$ is dephosphorylated by two lipid phosphatases — PTEN (for phosphatase and tensin homologous on chromosome 10) and SHIP (for SH2-domain-containing inositol 5'-phosphatase), which has two forms (SHIP1 and SHIP2) (Damen et al., 1996). Overexpression of PTEN (Bodine et al., 2001a;Bodine et al., 2001b;Rommel et al., 2001) or SHIP2 inhibits Akt1, causes subsequent decrease in cell size, and therefore blocks hypertrophy in muscle (Goberdhan et al., 1999;Huang et al., 1999;Stambolic et al., 1998;Xu et al., 2002). Akt1 phosphorylates and

activates mTOR (for mammalian target of rapamycin), which is also known as FRAP or RAFT-1, resulting in skeletal muscle hypertrophy. During muscle hypertrophy, phosphorylation of both Akt1 and mTOR are increased. Rapamycin, which is an inhibitor of mTOR, initially binds FK506-binding protein (FKBP12), and the complex of rapamycin and FKBP12 inhibits mTOR function. Tuberous sclerosis complex 1 (Tsc1) and Tsc2 proteins can also inhibit mTOR-mediated signalling (McManus and Alessi, 2002).

Activation of mTOR results in an increase in protein translation by two mechanisms. The first mechanism is that mTOR activates p70 S6 kinase (p70S6K), a positive regulator of protein translation. The second mechanism is that mTOR inhibits the activity of a eIF-4E binding protein, PHAS-1 (also known as 4E-BP1), which is a repressor of translation and a negative regulator of the protein elongation/initiation factor eIF-4E (Gingras et al., 1999a;Gingras et al., 1999b;Gingras et al., 2004;Hara et al., 1997;Sonenberg and Gingras, 1998). In unstimulated cells, eIF-4E and PHAS-1 exist as an inactive heterodimer. Upon growth factor stimulation, PHAS-1 is directly phosphorylated and inactivated by mTOR and dissociates from eIF4E. Therefore, eIF4E is free to bind eIF4G and activate mRNA translation (Brunn et al., 1997;Gingras et al., 1999a;Gingras et al., 1999b;Scott et al., 1998).

### 1.2.2.3. The IGF-I/PI3K/AKT/GSK3β pathway and skeletal muscle hypertrophy

Glycogen synthase kinase 3β (GSK3β) is a physiological substrate of activated Akt1 that has been shown to mediate muscle hypertrophy (Cross et al., 1995). Akt1 phosphorylates and inactivates GSK3β (Cross et al., 1995). Expression of a dominant-negative, kinase-inactive form of GSK3β induces dramatic hypertrophy in both skeletal myotubes (Rommel et al., 2001) and cardiac muscle (Hardt and Sadoshima, 2002) via the IGF-1-mediated, PI3K-dependent signalling process, linking GSK3β to the IGF-1/PI3K/Akt pathway. In hypertrophic muscles, GSK3β phosphorylation/inactivation is also evident. Glycogen synthase, which is a key substrate of GSK3β, catalyses the final step in glycogen synthesis. GSK3β is a serine/threonine kinase and an inhibitor of glycogen synthase. Activated GSK3β phosphorylates and inactivates glycogen synthase; and thereafter blocked the downstream glycogen synthesis. In contrast, inactivation of GSK3β by Akt1 results in dephosphorylation of glycogen synthase, and hence the activation of glycogen synthesis. GSK3β also phosphorylates and inhibits a guanine nucleotide exchange factor, eIF2B, which is required for initiation of protein translation. Therefore, inactivation of

GSK3β by Akt1 results in dephosphorylation of eIF2B. Dephosphorylated eIF2B stimulates the synthesis of protein from amino acids. Thus, IGF-1-dependent inactivation of GSK3β by Akt increases mRNA translation through activation of eIF2B (Welsh et al., 1998), and results in muscle hypertrophy by stimulating protein synthesis independent of the IGF-1/PI3K/Akt1/mTOR/p70S6K signalling pathway.

## 1.2.3. CALCINEURIN SIGNALLING PATHWAY AND SKELETAL MUSCLE

In skeletal muscle, the input received by motor neurons via acetylcholine receptors generates a motor neuron surface membrane depolarisation, which reaches the sarcolemma transverse tubular membrane (T-tubules). The skeletal muscle-specific isoform of the voltage-operated calcium channel or L-type calcium channel in the T-tubules interacts with, and thereafter, activates a skeletal muscle-specific sarcoplasmic reticulum calcium release channel, ryanodine receptor 1 (RyR1). This physical interaction causes the RyR1 to open and release calcium from the sarcoplasmic reticulum (SR). Thus cytosolic $Ca^{2+}$ is elevated locally to higher levels. After its release from the SR, $Ca^{2+}$ binds to troponin C (TnC) on the thin filament. Upon $Ca^{2+}$ binding to TnC, skeletal muscle contraction is activated. The energy-dependent $Ca^{2+}$ uptake into the SR is mediated by the SR ATPase, an enzyme that itself is regulated by both $Ca^{2+}$- and calmodulin-dependent phosphorylation (Berchtold et al., 2000). Elevations in intracellular calcium concentration serve as a second messenger to activate calcineurin, resulting in activation of gene transcription and muscle remodelling (Berridge et al., 2000;Berridge et al., 2003;Tomida et al., 2003). Activated calcineurin dephosphorylates molecules of the Nuclear Factor of Activated T-cells (NFAT). Calcineurin also activates Myocyte Enhancer Factor-2 (MEF2) and in combination with other signalling pathways activates gene transcription (Bassel-Duby and Olson, 2003).

### 1.2.3.1. Calcineurin and calcineurin inhibitors

Calcineurin, also called protein phosphatase 2B (PP2B), is a serine-threonine, calcium-dependent protein phosphatase localised to the cytoplasm. Calcineurin is a critical transducer of calcium signals that influence development, adaptation, and disease of cardiac and skeletal muscle. Calcineurin is ubiquitous, but is particularly abundant in both nerve and muscle cells.

Calcineurin exists as a heterodimer, composed of calcineurin A (CnA) and calcineurin B (CnB). CnA is a catalytic subunit containing a calmodulin-binding domain and an auto-inhibitory region. CnB is a $Ca^{2+}$-binding regulatory subunit (Olson and Williams, 2000a;Olson and Williams, 2000b;Ryder et al., 2003). Both CnA and CnB are essential for catalytic activity of the holoenzyme. Calcineurin, which is activated upon binding of calcium/calmodulin in response to low-amplitude, sustained elevation in intracellular $Ca^{2+}$, is tightly regulated by intracellular $Ca^{2+}$ concentration. Activated calcineurin affects gene expression by dephosphorylating specific substrates. The most potent, specific, and well-known inhibitors of calcineurin are the immuno-suppressant drugs, cyclosporin A (CsA) and tacrolimus (also called FK506). They inhibit calcineurin when complexed with their respective cytoplasmic receptors, cyclophilin A and FKBP12 (for FK506 binding protein 12). The complexes bind to inhibit calcineurin, and thereby prevent activation of calcineurin-dependent genes. Pimecrolimus (also called ASM981) is an ascomycin macrolactone derivative, closely related in structure to tacrolimus, and blocks calcineurin activity. Responsiveness to calcineurin activity can also be inhibited by cytoplasmic calcineurin-binding proteins, such as AKAP79, Cabin-1 (also called Cain), and MCIP1 (for Myocyte-enriched modulatory Calcineurin-Interacting Protein 1), which is also known as DSCR1 (for Down Syndrome Critical Region 1). The AKAP79 protein, which is a scaffolding protein, was the first calcineurin inhibitor to be found. AKAP79 binds calcineurin in conjunction with protein kinase A and C (Lai et al., 1998; Sun et al., 1998; Kashishian et al., 1998). Cabin-1/Cain binds both calcineurin and the transcription factor, MEF2 (for Myocyte Enhancer Factor-2). Overexpression of Cabin-1/Cain leads to calcineurin and MEF2 inhibition. The A238L protein encoded by African swine fever virus can bind tightly to calcineurin and blocks NFAT translocation and function (Miskin et al., 1998). MCIP2 (for Myocyte-enriched modulatory Calcineurin-Interacting Protein 2), also known as ZAKI-4 (assigned as DSCR1L1 by Human Nomenclature Committee), is a thyroid hormone-responsive protein, which bind to CnA and inhibit calcineurin activity (Rothermel et al., 2003).

### 1.2.3.2. Nuclear Factor of Activated T cells (NFATs)

NFAT was first identified in T cells as a rapidly inducible nuclear factor binding to the distal antigen receptor response element, ARRE-2, of the human interleukin-2 (IL-2) promoter. The induction of NFAT in T cells required calcium-activated signalling pathways and was blocked by CsA and FK506. The NFAT complex that formed on this site contained a cytoplasmic component and a nuclear component. The nuclear component was identified as the ubiquitous

transcription factor AP-1 (for Activator Protein-1), and consists of dimers of *Fos*- and *Jun*-family proteins. The cytoplasmic component was purified based on its ability to bind independently, in the absence of AP-1 proteins, to the distal NFAT site of the murine IL-2 promoter and as an NFAT:AP-1 complex to the human granulocyte/macrophage colony-stimulating factor (GM-CSF) promoter. The cytoplasmic component appears in the nucleus as a result of calcium mobilisation and calcineurin activation (Masuda et al., 1998). At present, five members of the NFAT family have been described in vertebrates. They are referred to as NFATc1 (NFATc/NFAT2), NFATc2 (NFATp/NFAT1), NFATc3 (NFATx/NFAT4), NFATc4 (NFAT3), and NFAT5 (Rao et al., 1997). All members of the NFAT family except NFAT5 are activated by calcineurin. Although NFAT proteins are expressed in many cell types, NFATc1 and NFATc3 isoforms are especially abundant in skeletal muscle. Members of the NFAT family have in common the following characteristics: (1) they are related by sequence similarity; (2) all five members cooperate with AP-1 polypeptides and bind the distal NFAT site of the IL-2 promoter *in vitro*; and (3) when over-expressed in appropriate cell lines, all can induce transcription from NFAT reporter constructs upon stimulation. There are three functional domains in NFAT proteins: the *Rel*-similarity domain (RSD), which is responsible for the DNA-binding activity and interaction with AP-1 polypeptides; the NFAT-homology region (NHR), which regulates the intracellular localisation; and the transcriptional-activation domains (TADs) (Rao et al., 1997). NFAT transcription factors are subject to a dynamic and reversible cycle of phosphorylation/dephosphorylation that controls their localisation to the nucleus and activation of NFAT-dependent genes. In unstimulated cells, NFAT proteins are maintained in the cytoplasm by phosphorylation of a serine-rich region near their amino-termini. Dephosphorylation of these serines by calcineurin unmasks two nuclear localisation sequences, resulting in rapid nuclear translocation. Once in the nucleus, dephosphorylated NFATc1 proteins have been shown to be rephosphorylated by one or more priming kinases that create a phospho-recognition site for glycogen synthase-3 kinase (GSK3) resulting in their translocation back to the cytoplasm and termination of calcineurin-regulated transcription. NFATc3 has also been shown to be phosphorylated in the nucleus by *Jun*-amino-terminal kinase (JNK) and the combination of MEK kinase-1 (MEKK1) and casein kinase-1a (Rao et al., 1997). Observations correlate with *in vitro* studies demonstrating the role for NFATc2 in myoblast fusion and for NFATc3 in myoblast differentiation (Abbott et al., 1998). The role for calcineurin/NFAT signalling pathway in the regulation of skeletal muscle slow-to-fast fibre type switch have also been demonstrated by *in vitro* and *in vivo* analysis (Abbott et al., 1998). It has been proposed that phosphorylation stimulates nuclear export of NFATs by exposing a nuclear export sequence or

regulating the nuclear import sequence. The plethora of kinases and phosphatases that act on NFAT proteins provides multiple potential targets for pharmacologic manipulation of NFAT-dependent cellular responses.

### 1.2.3.3. $Ca^{2+}$/calmodulin/calcineurin/NFAT pathway

The $Ca^{2+}$/calcineurin/NFAT signalling pathway was initially defined in T lymphocytes. In activated T cells, NFAT proteins are substrates of calcineurin, translocating into the nucleus following removal of phosphate groups by calcineurin activity (Rao et al., 1997). Although the pathway is simple, multiple levels of regulation impinge upon it, making it adaptable for many functions in a wide variety of cell types. In T lymphocytes, antigen recognition by the T-cell receptor (TcR) causes an increase in intracellular $Ca^{2+}$, which activates calmodulin and CnB to bind to $Ca^{2+}$. Growth factors such as IGF-1 have also been reported to activate calcineurin (Musaro et al., 2001;DeVol et al., 1990;Coleman et al,1995). Activated calmodulin binding to calcineurin leads to a conformational change which allows the auto-inhibitory domain of CnA to move away from the catalytic active site of calcineurin, and the phosphatase activity of calcineurin is activated (Masuda et al., 1998). Activated calcineurin binds and dephosphorylates members of the NFAT family of transcription factors. In resting cells where $Ca^{2+}$ concentration is low, calcineurin, which exists in an inactive form, is unable to bind calmodulin. Thereafter, NFAT proteins are phosphorylated and retained in the cytoplasm. Increases in intracellular calcium concentrations within a cell allow binding of calcium to the calmodulin-calcineurin complex thereby increasing the complex's phosphatase activity (Rao et al., 1997). In signalling pathways that lead to a rise in intracellular $Ca^{2+}$concentration, activated calcineurin dephosphorylates a conserved serine in the amino terminus of NFAT proteins, which, after removal of phosphate, are translocated into the nucleus to serve as subunits of transcription factor complexes (Crabtree and Olson, 2002;Graef et al., 2001). NFAT transcription factors contain the RSD that is sufficient for DNA recognition and cooperative binding interactions with other transcription factors, such as activator protein-1 (AP-1) (Crabtree, 1999). T cell activation leads to enhanced-transcription of the T cell gene encoding IL-2 (Crabtree, 1999;Crabtree, 2001;Crabtree, 2002).

### 1.2.3.4. Calcineurin and Myocyte Enhancer Factor-2 (MEF2)

There are four vertebrate MEF2 genes - MEF2A, MEF2B, MEF2C and MEF2D. MEF2 proteins are expressed, at high levels in both muscle cell and neurons, and at lower levels in many tissues

and a wide range of cell types, however, it is only in the developing cardiac, skeletal and smooth muscle that MEF2 activates transcription and act as a target for many signalling pathways involving calcium (Seale and Rudnicki, 2000). In skeletal muscle, transcriptional activation of slow muscle-specific genes is mediated by calcineurin-dependent activation of NFAT and MEF2 transcription factors (McKinsey et al., 2002;Naya et al., 1999;Wu et al., 2000;Wu et al., 2001). An essential role for MEF2 factors has been implicated in the formation of slow twitch skeletal muscle fibres. At a molecular level, MEF2 transcriptional activity can be stimulated by calcineurin either directly by dephosphorylation of MEF2 or indirectly by the association of active NFAT with MEF2 bound to DNA (Liu et al., 1997). Upon dephosphorylation by calcineurin, NFATc2 translocates to the nucleus where it directly associates with MEF2A and MEF2D (Blaeser et al., 2000;Youn et al., 2000). MEF2-NFATc2 interactions appear to play crucial roles in the control of slow twitch fibre genes in skeletal muscle (Chin et al., 1998). In addition to calcineurin, other $Ca^{2+}$-dependent signalling pathways, such as the $Ca^{2+}$-calmodulin-dependent protein kinase (CaMK), have been shown to control MEF2 activity and affect muscle phenotype. An indirect target of calcineurin activity, through MEF2 activation, is the up-regulation of the peroxisome proliferator-activated receptor gamma coactivator-1 (PGC-1α) promoter (Czubryt et al., 2003;Handschin et al., 2003). PGC-1α, also known as Pgc-1 and Ppargc-1, was shown to induce mitochondria biogenesis, respiration in cultured cells. When PGC-1α was overexpressed in the fast muscles of transgenic mice, an increase in slow muscle fibres was observed (Lin et al., 2002). During embryogenesis and in adult tissues, MEF2 genes are expressed in myogenesis and morphogenesis of striated and nonstriated muscle cell types. MEF2 binds directly to the promoters or enhancers of the majority of muscle-specific genes and interacts with members of the MyoD family of basic helix-loop-helix (bHLH) proteins to activate the skeletal muscle differentiation program (Black and Olson, 1998; Perry and Rudnicki, 2000).

### 1.2.3.5. Calcineurin expression in skeletal muscle

#### *1.2.3.5.1. Calcineurin expression in skeletal muscle differentiation*

Calcineurin activity is essential for activation of the skeletal muscle differentiation programme, which involves irreversible withdrawal of myoblasts from the cell cycle, fusion to form multinucleate myotubes, and transcriptional activation of muscle-specific genes (Berchtold et al.,

2000;Delling et al., 2000;Friday et al., 2000). NFAT transcription factors are differentially translocated from the cytoplasm to the nucleus at different stage of myoblast differentiation in response to distinct signals in the cytoplasm. Upon fusion, myoblasts cease to proliferate and differentiate by activating a set of muscle-specific genes to become myotubes, which are further remodelled into myofibres. The myogenic basic helix-loop-helix transcription factors, MyoD, myogenin, Myf5, and MRF4, are up-regulated in forming myotubes to initiate and maintain the expression of muscle-specific genes (Molkentin and Olson, 1996). Expression of Myf5, MyoD, and myogenin has been shown to be regulated by calcineurin activity at the level of gene transcription (Friday et al., 2003;Friday and Pavlath, 2001). In response to injury, adult skeletal muscle has a remarkable ability to regenerate. Quiescent reserved cells, satellite cells, become activated and migrate to the site of injury where they proliferate, differentiate, and fuse to form new myofibres. The role of calcineurin in regeneration has been studied using CsA administration following injury. Studies showed inhibition of formation of new myofibres and that calcineurin activity is needed for muscle precursor cell differentiation. In these studies, expression of calcineurin and dephosphorylated NFATc1 was markedly increased in regenerating muscle, although calcineurin activity was not measured (Abbott et al., 1998;Friday et al., 2000;Sakuma et al., 2003).

#### *1.2.3.5.2. Calcineurin expression and skeletal muscle size*

The role of calcineurin as a mediator in skeletal muscle growth and hypertrophy is controversial and has been a matter of debate (Biring et al., 1998;Bodine et al., 2001b;Dunn et al., 2000;Dunn et al., 2002;Dupont-Versteegden et al., 2002;Musaro et al., 1999;Semsarian et al., 1999;Serrano et al., 2001;Spangenburg et al., 2001). The role of calcineurin during muscle atrophy is also unclear (Glass, 2003a;Glass, 2003b). Several studies reported that skeletal muscle hypertrophy was mediated by a $Ca^{2+}$-dependent calcineurin signalling pathway (Dunn et al., 1999; Dunn et al.,2000;Dunn et al., 2002;Dupont-Versteegden et al., 2002;Mitchell et al., 2002;Olson and Williams, 2000a;Semsarian et al., 1999). However, other published data indicated that calcineurin did not appear to control muscle growth (Glass, 2003a; Glass, 2003b;Serrano et al., 2001). Strong support suggesting that calcineurin does not influence myofibre size came from studies of transgenic mice expressing activated calcineurin in skeletal muscle in which there was no evidence of hypertrophy (Naya et al., 2000;Wu et al., 2001). Bodine *et al.* (2001b) provided evidence that the calcineurin pathway was not activated during hypertrophy *in vivo*, and the pharmacological inhibitors of calcineurin activity did not blunt hypertrophy or atrophy. Several

studies have shown variable effects on muscle hypertrophy and growth when administrating CsA (Bigard et al., 2000;Biring et al., 1998). Whereas some groups have reported that CsA inhibits compensatory hypertrophy (Dunn et al., 1999), others have seen no effect (Musaro et al., 2001;Serrano et al., 2001;Dupont-Versteegden et al., 2002). One explanation for the conflicting results is the recent finding that the dose of drug, length of treatment, and muscle type are critical parameters to consider when analysing the effect of CsA on muscle size (Mitchell et al., 2002). However, *in vitro* inhibition of calcineurin-mediated nuclear translocation of NFAT using CsA did not result in an inhibition of IGF-1-mediated hypertrophy of myotubes (Rommel et al., 2001), and several groups were able to deliver sufficient levels of CsA *in vivo* so as to inhibit other markers of calcineurin activity in skeletal muscle, and yet inhibition of hypertrophy was not detected (Musaro et al., 2001;Serrano et al., 2001;Dupont-Versteegden et al., 2002).

#### *1.2.3.5.3. Calcineurin expression determines slow muscle fibre type gene expression*

Transcriptional activation of slow muscle fibre-specific transcription is mediated by a combinatorial mechanism involving proteins of the NFAT and MEF2 families (Chin et al, 1998). NFAT acts in concert with MEF2 transducing the calcineurin signal to the slow muscle fibre type specific promoters (Wu et al., 2000). Moreover, calcineurin induces the required binding of MEF2 to activate slow muscle fibre-specific gene promoters. The requirement of MEF2 is based on the fact that the mutation of the NFAT binding motif is insufficient to completely inhibit transcriptional regulation by calcineurin (Chin et al., 1998 ;Calvo et al, 1999;Esser et al., 1999). Within slow muscle gene promoters, exists a binding motif, which contains a MEF2 binding site within the A/T rich elements, an NFAT binding site (Nakayama et al.,1996, Calvo et al., 1999). It has been found that mutation of the MEF2 binding element results in a loss of muscle specific gene expression of the slow muscle gene promoter (Calvo et al., 1999). It has also been found that a constitutively active calcineurin in transfected C2C12 myoblasts increased the transactivating function of MEF2 (Wu et al., 2000). Activation of NFAT, alone, is not as effective as NFAT and MEF2 acting in concert to regulate slow muscle fibre-specific genes. $Ca^{2+}$/calmodulin/calcineurin/NFAT pathway plays an important role in controlling slow muscle gene expression (Kubis et al., 1997;Schiaffino and Serrano, 2002). It has been shown that rapid, repetitive, high-amplitude calcium transients associated with skeletal muscle stimulation, activation, and contraction are sufficient to activate NFAT translocation and subsequently transform fibres to a slow muscle gene program (Kubis et al., 2003;Abbott et al., 1998). Ras signalling through a mitogen-activated protein kinase (MAPK)/extracellular signal-regulated

kinase (ERK) pathway is another important mediator of slow muscle fibre-specific gene activation (Buckingham, 2001;Murgia et al., 2000;Schiaffino and Serrano, 2002). Ras-MAPK/ERK signalling has been shown to be involved in promoting nerve-activity-dependent differentiation of slow muscle fibre *in vivo* (Schiaffino and Serrano, 2002). Increased neuromuscular activity regulates the dephosphorylation of NFAT by calcineurin and eventually results in an alteration in MyHC isoform expression (Schiaffino and Serrano, 2002). A major contributing factor to the establishment of skeletal muscle fibre type is neural control. Long-term effects of motor neurons on skeletal muscle fibre phenotype are mediated by two distinct mechanisms: transmission of electrical activity and release of specific neural factors (Schiaffino and Serrano, 2002). Signals of electrical activity modulate calcium concentrations in myofibre. Calcium signalling plays a crucial role in determining, maintaining, and transforming muscle fibre types. Cytosolic calcium sensor could potentially distinguish skeletal muscle electrical activity, which affects globally the whole muscle fibre by influencing MyHC isoform gene expression. Since $Ca^{2+}$ is released into the cytosol from the sarcoplasmic reticulum during skeletal muscle contraction, a decreased number of $Ca^{2+}$ release events could act as a signal for reduced electrical activation (Talmadge, 2000). The protein calcineurin could act in concert with calmodulin as a calcium sensor in skeletal muscle (Chin et al., 1998). Thus, increased muscle contractile activity and the resulting sustained elevations in cytosolic $Ca^{2+}$ could potentially lead to altered fibre type-specific gene expression via the calcineurin signalling. Slow muscle fibres are characterised by a high, sustained calcium concentration, whereas short transient calcium elevations are found in fast muscle fibres. A sustained graded increase in intracellular calcium is necessary and sufficient to induce NFAT nuclear accumulation whereas transient pulses were not (Crabtree, 1999;Dolmetsch et al., 1997;Dolmetsch et al., 1998;Li et al., 1998;Timmerman et al., 1996). Translocation of NFAT has also been demonstrated to be sensitive to changes in intracellular calcium concentration that are evoked by stimulation patterns typically experienced by slow skeletal muscle (Liu Y et al., 2001). A number of *in vivo* and *in vitro* studies have provided evidence that calcineurin activity is required for induction and maintenance of the oxidative slow muscle gene program (Bigard et al., 2000;Higginson et al., 2002;Naya et al., 2000;Parsons et al., 2003;Serrano et al., 2001;Wu et al., 2001;Chin et al., 1998). Studies have shown that the translocation of NFAT activates many muscle fibre-specific genes such as, Myf5, myoglobin, MyHC, sarcomeric mitochondrial creatine kinase and slow isoform of troponin I (TnIs). Muscle fibre-specific proteins encoded by these genes, which are expressed in higher amounts in slow muscle fibres, contain NFAT response elements (NREs) in the regulatory regions of their specific genes (Chin et al., 1998). A unique difference between the primary DNA

elements responsible for regulating the slow muscle fibre-specific troponin I (TnIs) and the fast muscle fibre-specific troponin I (TnIf), or for regulating the slow upstream regulatory element (SURE) and fast intronic regulatory element (FIRE), is the inclusion of a consensus NFAT response elements (NRE) in the SURE element that is omitted from FIRE. Thus, the SURE element could confer $Ca^{2+}$-sensitivity to the TnIs gene via the NRE, resulting in enhanced transcription of the TnIs gene under conditions of elevated cytosolic $Ca^{2+}$ (e.g., increased contractile activity) (Abbott et al., 1998). In the presence of activated calcineurin, the MyHC IIa upstream promoter show a greater activation compared to the upstream region of MyHC IIb, suggesting that calcineurin may play a role in transition between fast subtypes (Allen et al., 2001;Allen and Leinwand, 2002). Other studies performed in skeletal muscle tissue culture demonstrate that calcineurin activates the slow fibre-specific myosin (Delling et al., 2000;Meissner et al., 2001), as well as promoting expression of oxidative proteins, such as myoglobin (Chin et al., 1998). Some studies suggest that elevated neuromuscular activity, induced by exercise, can decrease the activities of glycogen synthase kinase-3 (GSK-3) (Markuns et al., 1999), an enzyme that has been reported to phosphorylate NFAT within the nucleus (Beals et al., 1997), resulting in NFAT translocation out of the nucleus. Thus, neuromuscular activity may enhance NFAT binding to nuclear DNA by enhancing its translocation into the nucleus (via dephosphorylation by calcineurin) and by inhibiting nuclear export (via inhibition of rephosphorylation by GSK-3).

## 1.3. MICROARRAY TECHNOLOGY

Over the past few years, muscle biology has seen increasing application of microarray technology. Studies using microarrays have described various gene expression profiles of skeletal muscle in different biological contexts, such as the microarray study of molecular pathophysiology and targeted therapeutics for muscular dystrophy (Hoffman and Dressman, 2001), and the microarray detection of activation of a myogenic transcription program (Khan *et al.*,1999). However, the underpinning knowledge of molecular pathways regulating skeletal muscle developmental, physiological and pathological processes has so far not been fully revealed.

## 1.3.1. GENERAL DESCRIPTION OF DNA MICROARRAYS

An eukaryotic gene is a combination of deoxyribonucleic acid (DNA) segments that together constitute an expressible unit. The segments of a gene consist of a transcription unit and regulatory sequences. Gene expression refers to the process by which a gene's coded information is converted into the structures that present and operate in a cell. Expressed genes include those that are transcribed into messenger ribonucleic acids (mRNAs) and then translated into proteins and those that are transcribed into RNAs but not translated into proteins, for instance, transfer RNAs (tRNAs) and ribosomal RNAs (rRNAs). Due to alternative splicing and post-translational modifications, one gene can produce a variety of proteins.

A major goal of gene expression profiling studies is to determine the pattern of genes expressed under specific circumstances or in a specific cell. One of the contributions of these studies has been to help us understand genes and their product functions and interactions, and most importantly of all, how all of these make organisms function the way they do. The primary approach to measuring gene expression has been to focus on the levels of mRNAs rather than proteins. The protein-based approaches are generally more difficult, less sensitive and have a lower throughput than RNA-based ones. More importantly, mRNA levels are immensely informative about cell state and the activity of genes, and for most genes, changes in mRNA abundance are related to changes in protein abundance (Lockhart and Winzeler, 2000). Traditional techniques for the study of the regulation of gene expression are constrained by the limited amount of data obtained from one experiment and are time consuming to perform. To study simultaneously the expression of thousands of genes in a cell or tissue, and furthermore, to enable global comparisons between biological systems rather than detailed examination of single genes, high-throughput experimental methodologies combined with statistical and computational analysis of the results need to be applied to the study of gene regulatory networks and pathways (Hieter and Boguski, 1997;Emmert-Buck et al., 2000;Lee and whitmore, 2002). The application of microarray technology has met these challenges. Generally speaking, a microarray is a tool that enables parallel analysis of the vast information content resident in complex biochemical target samples (Schena et al., 1995;Marcotte et al., 2001). The term microarray refers to a microscopic, hybridisation-based, ordered array of nucleic acids, proteins, small molecules, cells or other substances that are chemically attached or synthesized as probe onto a substrate. This substrate can be a coated microscope glass slide, a silicon chip, a nylon membrane, or a small,

microsphere-sized bead. According to the arrayed material, microarrays can be classified into different categories, such as DNA microarrays, protein microarrays, small molecule microarrays, cell microarrays, tissue microarrays and chemical microarrays, etc (Lander, 1999;Southern et al., 1999). Microarray technology has led to a rapid increase in the amount of information available about gene expression profiles and, hence, enhances our understanding of diverse biologic and pathophysiologic processes at the molecular level (Blohm and Guiseppi-Elie, 2001). As the goal of this project was to develop a microarray for gene expression profiling studies, DNA microarrays shall be the focus of the following part of this chapter, especially cDNA microarrays.

## 1.3.2. TYPES OF DNA MICROARRAYS

A DNA microarray is an ordered array of DNAs (termed the probes) gridded and attached onto a miniaturised solid-state matrix. There are several names for this technology — DNA microarrays, DNA arrays, DNA chips, gene chips, and others. Sometimes a distinction is made between these names but in fact they are all synonyms as there are no standard definitions for which type of DNA microarray should be called by which name. According to the number of probes immobilised on a solid matrix, DNA microarrays can be classified into three categories: high-density, medium-density and low-density arrays. Each high-density DNA array contains many tens of thousands of genes, whereas medium- and low-density contain on the order of between a few thousand and a handful of genes for each array. The high- and medium-density DNA microarrays are currently the most widely used tools for simultaneous, large-scale analysis of gene expression. Therefore, in this thesis, the term DNA microarray refers to the high- and medium-density microarray in most circumstances. DNA microarrays can also be divided into two groups, according to the arrayed material: complementary DNA (cDNA) and oligonucleotide microarrays. These two types of arrays will be reviewed in the following sections. DNA microarrays make use of the sequence resources created by the genome projects and other sequencing efforts to answer the question, what genes are expressed in a particular cell type of an organism, at a particular time, under particular conditions. For instance, they allow comparison of gene expression between normal and diseased cells, or between early-stage disease tissues and late-stage disease tissues. In gene expression studies, DNA microarrays can be exposed to labelled nucleic acids (termed the targets) from biological samples for the

detections of hybridisation. Through image analysis, the amount of target that hybridises to one of the microarray probes gives a measure of the abundance of that particular transcript within the target sample. Thus, expression patterns of many different genes can be studied simultaneously with DNA microarrays.

### 1.3.2.1. cDNA microarrays

The cDNA microarray is one technological approach that has the potential to accurately measure changes in global mRNA expression levels in various tissues. A cDNA microarray comprises a collection of gene sequences which are usually purified PCR products ranging in size from 100-2,000 bp derived from cDNA libraries, cDNA clone collections or expressed sequence tag (EST) clones. Now, the question arises as to what cDNA, cDNA library and EST are. A cDNA is a single stranded DNA molecule with a nucleotide sequence that is complementary to an mRNA molecule (Bowtell, 1999;Schulze and Downward, 2001). A theoretical complete cDNA library represents all of the genes that are expressed in a particular tissue or organism, at a particular time. The prevalence of a particular cDNA clone in the library is indicative of the abundance of the corresponding mRNA and therefore the expression level of the coding sequences of a specific gene. ESTs are partial gene sequences of cDNA fragments, generated through single read, but error- prone sequencing (Devaux et al., 2001;Southern et al., 1999). ESTs often, but not necessarily represent the cDNAs they derived from. It is well known that RNA molecules are exceptionally labile and difficult to amplify in their natural form. Unlike an mRNA, a cDNA can be easily propagated and sequenced. For this reason, the information encoded by the mRNA is converted into cDNA and then is inserted into a self-replicating vector. There are six basic steps in constructing a cDNA library: (1) purification of mRNA using chemical extraction and an oligo-dT cellulose column. (2) first strand cDNA synthesis from purified mRNA template by the action of viral RNA-dependent DNA polymerase called reverse transcriptase, with the help of oligo-dT primers, random hexanucleotide primers, or gene-specific primers. (3) second strand cDNA synthesis requiring *E. coli* RNase H and DNA polymerase I for a priming event (4) blunting cDNA termini and ligating adaptor oligos (5) ligating cDNA into vector (6) Packaging. Bacteriophages are widely used as cloning and expression vectors. Bacteriophages (also called phages) are any viruses that infect bacteria. When phages infect bacteria, only the phage DNA enters the bacterial host cell and initiates the replication events that lead to the production of several hundred progeny viruses in every infected cell. Lyses of infected bacteria is detected by the appearance of plaques in a bacterial 'lawn' grown on solid media or by the inhibition of

bacterial growth in liquid cultures. Once the information is available in the form of a cDNA library, individual processed segments of the original genetic information can be isolated and examined with relative ease (Forozan et al., 1997).

cDNA microarrays are produced by robotic deposition of cDNA sequences or ESTs that are applied individually to precise locations on a solid matrix, usually nylon or glass. Normally, a few nanolitres of PCR-amplified clone inserts are arrayed. Necessary sequencing information on the cDNAs is not required. Inserts are amplified using either vector-specific or gene-specific primers. PCR products are purified to remove unwanted salts, nucleotides, detergents, primers and proteins presenting in the PCR mixture. Purified PCR products, which are typically 100-500μg/ml, are printed at specified sites on either glass or membrane matrices using high-precision arraying robots (arrayers). Computer-controlled robots are designed to automatically collect samples simultaneously from microtitre plates with multiple pins. Each pin collects between 250 and 500 nanolitres of solution and deposits 0.25-1 nanolitres onto each slide. Robots are programmed so that successive spots are spaced avoiding contact with adjacent spots. Spots are typically 50-300 μm in size and are spaced about the same distance apart (Duggan et al., 1999). DNA is cross-linked to the solid support by ultraviolet irradiation, chemical linkers or baking at 80°C. The state of bound cDNA is ill-defined. It is deposited in double-stranded form, intra-strand cross-linked to some extent, and may well have multiple constraining contacts with the matrix along its length. Therefore, a cDNA microarray is probably not the best hybridisation probe (Southern *et al.*,1999). The cDNA microarrays can be subsequently hybridised to two differentially fluorescently labelled targets. The targets are pools of cDNAs, which are generated after isolating mRNA from cells or tissues in two states that one wishes to compare. The use of long target sequences (≤2 kbp) can increase detection sensitivity for cDNA microarrays. The advantage of cDNA microarray technology is that it is relatively accessible and cost-effective. cDNA microarray hybridisation does not need specialized equipment, and data capture can be carried out using equipment that is very often already available in a laboratory (Cheung et al., 1999). Prefabricated cDNA microarrays are relatively cheap, and in-house production of cDNA microarrays is within the reach of many researchers, affording flexibility of design to meet the specific goals of different scientific experiments. On the other hand, there are several disadvantages to this type of biological tool. (1) One of the weaknesses is, as previously described, in the state of double-stranded cDNAs on a microarray. (2) Sequence homologies between clones representing different closely related members of the same gene family may

result in a failure to specifically detect individual genes. However, closely related genes can often be distinguished by using probes corresponding to the 3'-untranslated region of an mRNA, as these regions often display gene-specific sequence diversity. (3) As each cDNA fragment must be synthesized, purified, and stored before array construction, the curation of extensive clone sets is a critical factor in microarray fabrication. According to the previously published assessment, even the best maintained clone stocks for commercial manufacture of cDNA microarrays are prone to contamination with incorrect plasmids, and mix-ups over clones of different identities (Halgren et al., 2001).

### 1.3.2.2. Oligonucleotide microarrays

The term oligonucleotide refers to a short length of single-stranded polynucleotide chain that is usually less than 30 residues long. Obviously, an oligonucleotide microarray is a very large set of oligonucleotide probes, which are attached to a solid support. This type of array differ from other formats in that the probe is synthesised in situ on the surface of a matrix as opposed to being generated separately and then spotted on the surface. Oligonucleotide microarrays are effective tools for profiling gene expression, and monitoring single nucleotide polymorphisms (SNPs) or mutations (Lipshutz et al., 1999;Southern et al., 1999). A SNP is a position in a genome where a single base (Adenine, Cytosine, Guanine, or Thymine) is altered, so that some individuals have one DNA base whilst others have a different base resulting in DNA sequence variation. SNPs and point mutations are structurally identical, differing only in their frequency. Variations that occur in 1% or less of a population are considered point mutations, and those occurring in more than 1% are SNPs. Single base insertion/deletion variants are not formally considered to be SNPs. SNPs may be responsible for many inheritable differences between individuals. Some SNPs are the cause of genetic diseases. To prepare high-density oligonucleotide microarrays, short 20-mer to 25-mer are chosen from the mRNA reference sequence of each gene, and are synthesised in situ, either by photolithography onto silicon wafers or by ink-jet technology. For low-density arrays, pre-synthesised oligonucleotides can be printed onto glass slides just like long probes (Cunningham, 2000;Helmberg, 2001). Two techniques, photolithography and solid-phase DNA synthesis, have been used in light-directed synthesis for the construction of high-density DNA arrays that display a multitude of oligonucleotides. Affymetrix, which developed this method, attaches synthetic linkers, modified with photo-chemically removable protecting groups, to a solid support, and direct ultraviolet light through holes of masks in order to deprotect and activate selected sites on the matrix. Synthesis of oligonucleotides involves both

light-directed removal of blocking groups (deprotection) from the end of the growing base chain, and coupling of one nucleotide at a time with the base chain at the activated sites. Repetition of this process with different masks allows the complete array of thousands of short oligonucleotides to be constructed (Lipshutz et al., 1999;Gerhold et al., 1999). Methods based on synthetic oligonucleotides offer the advantage that because sequence information alone is sufficient to generate the DNA to be arrayed, no time-consuming handling of cDNA resources is required. Also, probes can be designed to represent the most unique part of a given transcript, making the detection of closely related genes or splice variants possible. Although limited binding affinity of short oligonucleotides may result in less specific hybridisation and reduced sensitivity, the arraying of pre-synthesised longer oligonucleotides (50-100 mers) has been developed to counteract these disadvantages (Granjeaud et al., 1999).

### 1.3.3. JUSTIFICATION OF USE OF MICROARRAYS IN COMPARISON WITH mRNA DIFFERENTIAL DISPLAY AND REPRESENTATIONAL DIFFERENCE ANALYSIS

DNA microarrays are used to study simultaneously the expression of thousands of genes in a cell or tissue, and furthermore, to enable global comparisons between biological systems rather than detailed examination of single genes. cDNA clone stocks for microarray construction can provide full length or at least good length cDNA clones for further functional study. mRNA differential display technology allows detection and isolation those genes that are differentially expressed in various cells or under altered conditions by systematic amplification of the 3' terminal portions of mRNAs and resolution of those fragments on a DNA sequencing gel (Liang and Pardee, 1992). Using anchored oligo-dT primers designed to bind to the 5' boundary of the poly-A tails for the reverse transcription, followed by PCR amplification with additional upstream primers of arbitrary sequences, mRNA sub-populations are visualised by denaturing polyacrylamide electrophoresis. This allows direct side-by-side comparison of most of the mRNAs between or among related cells. This method is thus far unique in its potential to visualise all the expressed genes in a eukaryotic cell in a systematic and sequence-dependent manner by using multiple primer combinations. More importantly, this method enables the recovery of sequence information and the development of probes to isolate their cDNA and genomic DNA for further molecular and functional characterisations. Representational difference analysis (RDA) is a technique for the identification of specific differences between

two mRNA populations (Lisitsyn et al., 1993). Genomics or cDNA sequences from two samples are PCR amplified and differences between two complex sets of genomes analysed using subtractive DNA hybridisation. This method, allows the selective amplification and cloning of transcripts that differ in abundance between two populations.

## 1.4. JUSTIFICATION OF WORK

The major goal of the study described in this thesis was to construct a porcine skeletal muscle cDNA microarray. It was anticipated that the completed porcine cDNA microarray could be utilised for profiling high throughput gene expression, identifying simultaneously alterations in the transcript level of thousands of transcriptomes, and investigating different molecular pathways related to porcine skeletal muscle in various biological contexts. The microarray construction and the subsequent utilisation are described in the following chapters of this thesis.

The porcine cDNA microarray was to be assembled from two porcine skeletal muscle cDNA libraries. In the absence of a known porcine genome, this approach was expected to allow the construction of a valid tool for profiling large-scale gene expression in porcine skeletal muscles. The recombinant plasmid DNAs, polymerase chain reaction (PCR) products, and purified PCR products, to be used for the construction of the porcine skeletal muscle cDNA microarray, would be characterised to ensure that relevant cDNA fragments were present. The purified, PCR-amplified cDNA fragments would then be used to construct the microarray which would be used for subsequent experiments.

Once constructed, the porcine cDNA microarray would be evaluated to optimise the experimental conditions for use. The porcine cDNA microarray would also be evaluated for its effectiveness for high throughput gene expression profiling. Two experiments would be carried out to analyse differential gene expression. One would aim at revealing molecular mediators regulating phenotypic differences between porcine *psoas* red and *longissimus dorsi* white skeletal muscle. The other would aim at investigating ionomycin-regulated genes involved in porcine skeletal muscle.

# CHAPTER TWO

# CONSTRUCTION OF A PORCINE SKELETAL MUSCLE cDNA MICROARRAY

# 2.1. INTRODUCTION

Construction of human skeletal muscle cDNA microarray has previously been reported (Noguchi et al., 2003; Campanaro et al., 2002). To date, development of porcine skeletal muscle DNA microarrays appear not to have been described. One reason for this could be that there is insufficient sequence information on pigs for designing a comprehensive DNA microarray (Davoli et al., 1999;Davoli et al., 2002). This chapter describes the construction of a porcine skeletal muscle cDNA microarray, which was the major goal of this project. Skeletal muscle biological processes are controlled by various cell-signalling pathways coordinating the action of thousands of genes. To progress towards a better understanding of molecular basis underlying skeletal muscle biology, questions about skeletal muscle developmental, physiological and pathological processes are being addressed with DNA microarray approach, which has provided a means to simultaneously measure mRNA abundance for tens of thousands of genes in parallel in a single experiment. cDNA microarrays have been commercially available for muscle in other species (Campanaro et al., 2002;Noguchi et al., 2003), but no skeletal muscle specific cDNA microarray has yet been described for porcine, which is both an important target farm animal species and an invaluable large animal experimental model for skeletal muscle research. To evaluate gene expression at large scale and allow identification of differentially expressed genes in skeletal muscles, a porcine microarray containing 5,500 cDNA fragments was developed by this project for the following potential uses. The fundamental prospective uses of this microarray include profiling temporal muscle gene expression from embryo to adult, characterising spatial gene expression between phenotypically distinct muscles within the same animal, profiling changes in gene expression under different metabolic status, and providing underpinning knowledge of molecular mechanisms of skeletal muscle diseases. This cDNA microarray can also be used to identify known and unknown genes that associate with particular muscle quality traits, so that selection of animals can be facilitated by genotyping based on levels of gene expression. This chapter is about the design and *de novo* construction of this cDNA microarray.

# 2.2 MATERIALS AND METHODS

## 2.2.1. MATERIALS

### 2.2.1.1. cDNA libraries

Complementary DNA (cDNA) libraries represent the information encoded in the messenger RNA (mRNA) of a particular tissue or organism. The construction of the porcine skeletal muscle cDNA microarray was based on the use of two developmentally distinct, directionally cloned, representative porcine skeletal muscle lambda ZAP Express® cDNA libraries, which were previously made in the Molecular Medicine Laboratory, Department of Veterinary Pathology, University of Glasgow Veterinary School. One of the libraries was derived from the *longissimus dorsi* muscle of a 50-day-old Meishan × Large White porcine foetus; the other was made from the *gastrocnemius* muscle of a 3-day-old Meishan × Large White pig. The *longissimus dorsi* muscle extends the length of the spinal column on either side of the vertebrae, while the *gastrocnemius* muscle extends from the distal femur to the calcaneus of the hock joint. Both cDNA libraries were not normalised nor subtracted. The morphological and physiological properties of both muscles are similar. No other cDNA library was available at the starting point of the microarray construction. Construction of both cDNA libraries was carried out using the Zap Express® cDNA Synthesis Kit and Gigapack® III Gold Cloning Kit (Stratagene). First strand cDNA was synthesised by reverse transcription using oligo (dT) linker-primer that contained a *Xho*I recognition site within it. Following double-stranded cDNA synthesis, *Eco*RI adapters were ligated to the blunt ends, and the samples were digested with *Xho*I. The result was cDNA fragments with an *Eco*R I sticky end on one side and a *Xho*I sticky end on the other. These cDNAs were ligated directionally in the ZAP Express® vectors. The vectors were then packaged using Gigapack III Gold packaging extracts and were plated on the *Escherichia coli* (*E. coli*) XL1-Blue MRF' cells. Both cDNA libraries, each with approximately $1\times10^6$ primary plaques, have been extensively characterised by sequencing and screening and shown to be highly representative (unpublished data). They had been used to isolate several full-length cDNA clones, including porcine myosin heavy chains (MyHCs) (6.0kb) and transcription factors, such as the Nuclear Factor of Activated T cells (NFAT2) and GATA binding protein 2 (GATA2) (Beuzen et al., 2000;Chang et al., 2003;Sun et al., 2001). The amplified cDNA libraries were kept as aliquots in 7% [volume/volume (v/v)] sterile filtered dimethyl sulphoxide (DMSO) (Sigma), at -80°C. To start the process of microarray construction, aliquots of each cDNA library contained in vials were removed from the -80°C freezer, thawed at room temperature, and were then ready for the following mass excision of pBK-CMV phagemid vector from ZAP Express® vector.

### 2.2.1.2. Bacteria and culture media

#### *2.2.1.2.1. Bacteria*

Two strains of *E. coli* (XL1-Blue MRF' and XLOLR) were used in this study. Stratagene supplied both. Detailed information about their origin and properties is described in the instruction manual of the ZAP Express® cDNA synthesis kit (Catalogue #200403, Stratagene). Their practical features are summarised in Table 2:1 below.

**Table 2:1** Summary of the main features of XL1-Blue MRF' cells and XLOLR cells

| XL1-Blue MRF' cells | XLOLR cells |
|---|---|
| *E. coli* strain | *E. coli* strain |
| XL1-Blue MRF' cells are for amplifying libraries and plating amplified libraries. XL1-Blue MRF' cells allow the amplified ZAP Express® cDNA library to grow very efficiently on the XL1-Blue MRF' strain. | XLOLR cells are lambda bacteriaphage resistant nonsuppressing *E. coli* host strain for plating in vivo excised phagemids. XLOLR cells are resistant to lambda phage infection. |
| LB-tetracycline agar plates for XL1-Blue MRF' bacterial streak | LB-tetracycline agar plates for XLOLR bacterial streak |

#### *2.2.1.2.2. Culture media*

Media used throughout the study was based on *Luria-Bertani* (LB) broth. LB-tetracycline agar plates were used for maintenance of the *E. coli* cells. LB-kanamycin agar plates were used for selecting the transformed XLOLR cells containing the kanamycin-resistant pBK-CMV plasmid vector and cDNA insert, if one was present. Details of these media are described in the Appendix.

### 2.2.1.3. Phage strains

Two phage strains (ZAP Express® vector [Fig. 2:1] and ExAssist® interference-resistant helper phage) were used in this study. Stratagene supplied both. Detailed information about their origin and properties is given in the instruction manual of the ZAP Express® cDNA synthesis kit (Catalog #200403). Their main features are summarised in Table 2:2.

**Figure 2:1** Expression cassette in ZAP Express® and pBK vectors

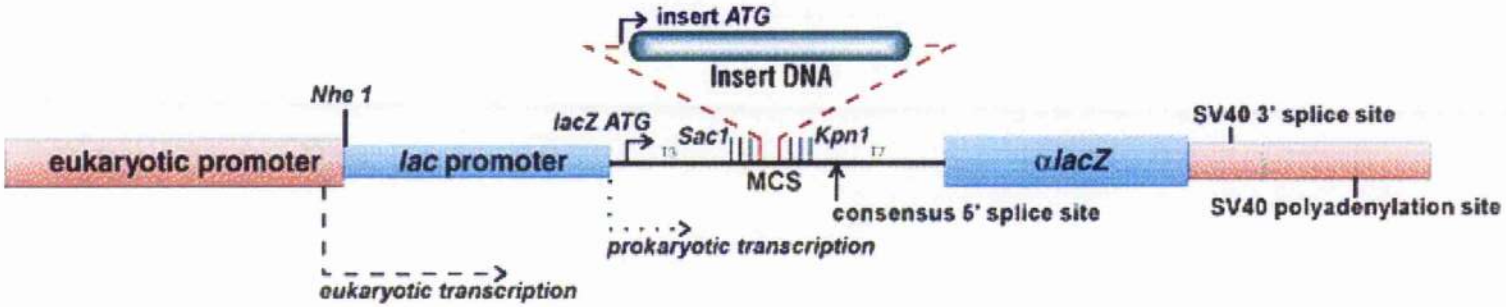


(Downloaded from website http://www.stratagene.com)

ZAP Express® vector combines the high efficiency of a lambda vector system with the versatility of a plasmid system. Fragments cloned into the ZAP Express vector can be excised with ExAssist® helper phage to generate subclones in the pBK-CMV phagemid. Expression of ZAP Express® vector is driven lacZ promoter in bacteria and CMV immediate early promoter in eukaryotic cells.

**Table 2:2** Summary of main features of ZAP Express® vector and ExAssist® interference-resistant helper phage

| **ZAP Express® vector** | **ExAssist® interference-resistant helper phage** |
|---|---|
| • The ZAP Express® vectors are pre-digested with *Eco*R I and *Xho* I by the manufacturer.<br>• The unidirectional cloning sites of the ZAP Express® vectors are *Eco*R I-*Xho* I.<br>• Inserts are cloned in sense orientation as *Eco*R I-*Xho* I fragments into the ZAP Express® vectors. | |
| **ZAP Express® vector**<br><br>• Combines lambda bacteriophage vector system with pBK-CMV phagemid/plasmid system.<br>• Allows both eukaryotic and prokaryotic gene expression.<br>• Has 12 unique cloning sites.<br>• Can accommodate DNA inserts from 0 to 12 kb in length.<br>• Inserts cloned into the ZAP Express® vectors can be excised out of the lambda bacteriophage to generate subclones in the kanamycin-resistant pBK-CMV phagemid vector. | **ExAssist® interference-resistant helper phage**<br><br>• Is filamentous (M13) interference-resistant helper phage.<br>• This helper phage with XLOLR strain is designed to efficiently excise the pBK-CMV phagemid vector from the ZAP Express® vector.<br>• Contains an amber mutation that prevents replication of the helper phage genome in a nonsuppressing *E. coli* strain such as XLOLR cells.<br>• Allows only the excised pBK-CMV phagemid to replicate in the *E. coli* XLOLR host cells, removing the possibility of co-infection from the ExAssist® interference-resistant helper phage. |
| **pBK-CMV phagemid/plasmid vector**<br><br>• Has 17 unique cloning sites flanked by T3 and T7 promoters.<br>• Has T7 primer binding site and T3 primer binding site for DNA sequencing.<br>• Can infect *E. coli* and replicate autonomously as plasmid DNA.<br>• Carries kanamycin-resistance gene for stable selection of the plasmid clones. | |

#### 2.2.1.4. Restriction endonucleases

Two restriction endonucleases, *Eco*R I (GibcoBRL, UK) and *Xho* I (GibcoBRL, UK) were used in this study for digestion of pBK-CMV plasmid DNAs. Both *Eco*R I and *Xho* I are 10U/μl in concentration, and use 10× SuRE/CUT buffer H for enzyme digestion.

#### 2.2.1.5. Commercial kits

The commercial kits used in this study and their uses are summarised in Table 2:3

## 2.2.2. METHODS

The process of construction of the microarray includes the actual construction process and its associated quality assurance process. The important methods used in this study to produce the porcine skeletal muscle cDNA microarray from the two porcine skeletal muscle cDNA libraries are set out in Figure 2:2. The main construction process refers to the following eleven steps: (1) mass excision of pBK-CMV phagemid vector from ZAP Express® vector, (2) colony blot hybridisation, (3) colony selection, (4) cultivation of the selected colonies in 96-well flat-bottom blocks, (5) plasmid DNA extraction in 96-well plate format for the selected colonies, (6) storage and naming of the plasmid DNAs, (7) PCR in 96-well plate format for amplification of the cDNA inserts contained in plasmid DNAs of the selected colonies, (8) PCR purification in 96-well plate format, (9) storage and naming of the purified PCR products, (10) Microarray printing, (11) storage of the microarray slides. The associated quality assurance process refers to the following eight steps: (1) individual bacterial culture of randomly picked colonies, (2) plasmid DNA extraction from the randomly picked colonies, (3) Southern blot hybridisation, (4) detection of presence of the cDNA fragments by restriction enzyme digestion and agarose gel electrophoresis, (5) sequencing of plasmid DNAs derived from the selected colonies, (6) dot blot hybridization, (7) microarray hybridisation using Cy3 labelled T7 primer target, (8) microarray hybridisation using both Cy3 labelled target and Cy5 labelled target.

**Table 2:3** The commercial kits used in this study and their uses

| **Commercial kits** | **Use of the kits** |
|---|---|
| ZAP Express® cDNA synthesis kit (Stratagene) | Part of this kit was used for mass excision of pBK-CMV phagemid vector from ZAP Express® vector. |
| Dynabeads mRNA Direct™ kit (Dynal LTD) | This kit was used for mRNA extraction from skeletal muscle tissues or cells. |
| Reverse Transcription System (Promega) | This kit was used for single-stranded cDNA synthesis. |
| Random Primers DNA labelling System (Life Technologies) | This kit was used for labelling [$\alpha$ - $^{32}$P] to cDNA probes. The [$\alpha$ - $^{32}$P] labelled cDNA probes were applied to colony blot hybridisations, Southern blot hybridisations and dot blot hybridisation. |
| QIAprep Spin Miniprep kit (QIAGEN) | This kit was used for individual extraction of plasmid DNAs, which were for quality assurance during the microarray construction. |
| QIAprep 96 Turbo Miniprep kit (QIAGEN) | This kit was used for 96-well plate format plasmid DNA extraction. |
| HotStarTaq Master Mix kit (QIAGEN) | This kit was used for the 96-well plate format hot start PCR. |
| QIAquick 96 PCR Purification kit (QIAGEN) | This kit was used for 96-well plate format purification of PCR products. |
| QIAvac 96 Vacuum Manifold (QIAGEN) | This kit was used along with a vacuum pump for providing negative vacuum environment, which was required by both QIAprep 96 Turbo Miniprep Kit and QIAquick 96 PCR Purification kits. |
| Thermo Sequenase Cycle Sequencing kit (Amersham Life Science) | This kit was used for sequencing reactions. |

**Figure 2:2** The entire process of microarray construction in this study

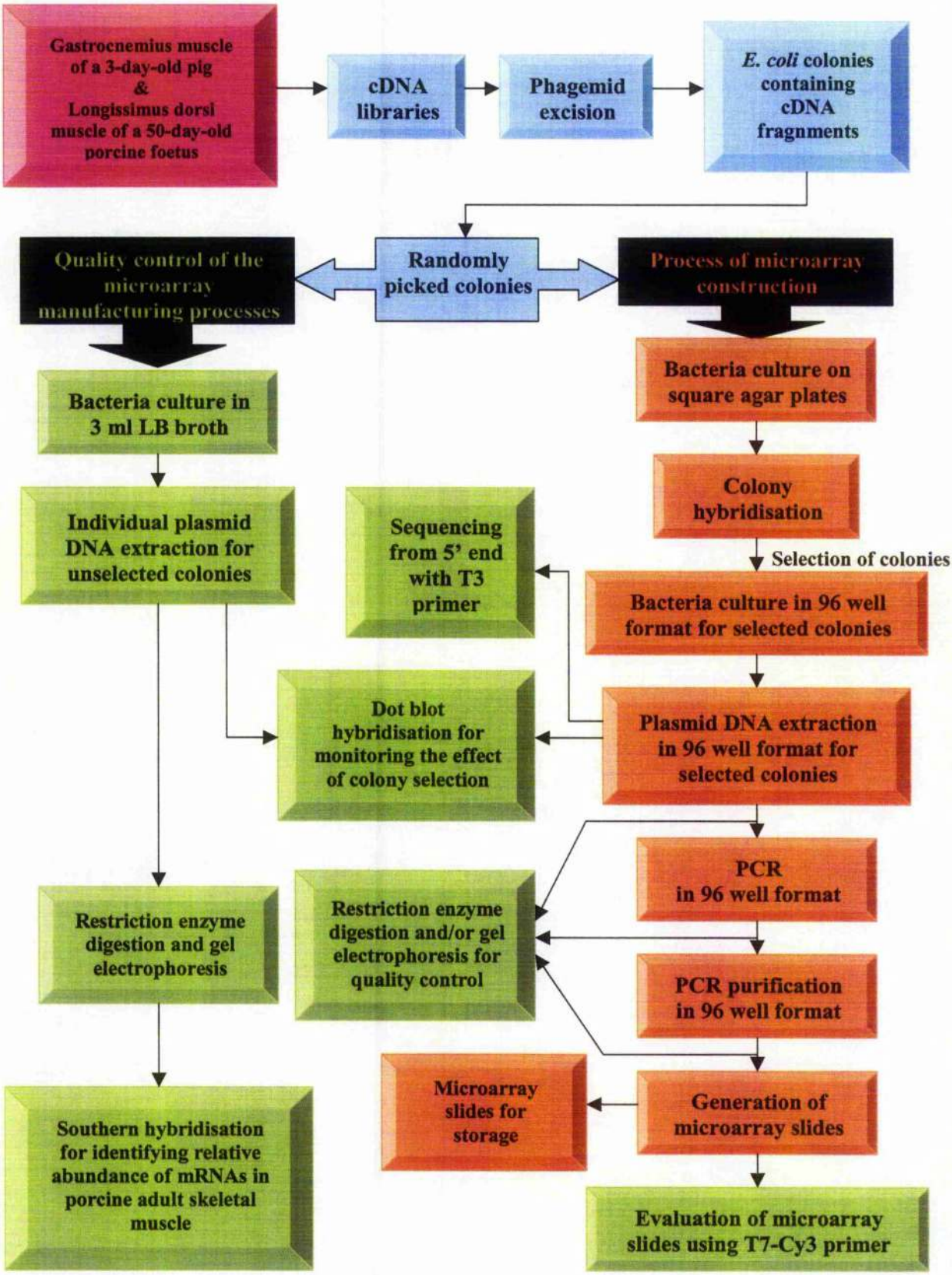

### 2.2.2.1. *In vivo* mass excision of pBK-CMV phagemid vector from ZAP Express® vector

A large number of isolated cDNA fragments are crucial for constructing a cDNA microarray. However, each cDNA fragment of the two cDNA libraries used in this study was a recommbinant insert contained within the multiple cloning site of pBK-CMV sequence, which combined with the sequence of the ZAP Express® vector. In order to obtain isolated cDNA fragments from both cDNA libraries, in vivo mass excision was carried out following manufacturer's protocol. Through in vivo mass excision, linear pBK-CMV sequences containing cDNA inserts were converted to circular pBK-CMV phagemids containing the cDNA inserts (Fig. 2:3). These phagemids were later transformed into *E.coli* XLOLR cells.

The ZAP Express® vector, which contains pBK-CMV sequence and lambda DNA, is designed to insert cDNA fragment within the pBK-CMV sequence. During in vivo mass excision, *E.coli* XL1-Blue MRF' cells are simultaneously infected with both the ZAP Express® vector and the ExAssist® interference-resistant helper phage (Stratagen, UK). Inside each infected XL1-Blue MRF' cell, proteins from the helper phage recognise initiator and terminator domains within the ZAP Express® vector, and new single-stranded DNA fragments are then synthesised. Each of these synthesised DNA molecules includes the complete sequence of pBK-CMV phagemid vector and the sequence of the insert, if one is present. The synthesised DNA molecules are circularised by the gene II product from the helper phage, "packaged" into phagemid particles, and secreted from the XL1-Blue MRF' cell. These phagemids become plasmids after infecting *E. coli* XLOLR cells. Colonies of the transformed XLOLR cells containing pBK-CMV plasmids grow in the presence of kanamycin on LB agar plates as the pBK-CMV vector contains the kanamycin-resistance gene.

XL1-Blue-MRF' cells were cultured overnight in LB broth, which was supplemented with 0.2 % (w/v) maltose and 10 mM $MgSO_4$ at 30°C with shaking at 200 rpm in a Gallenkamp Orbital Incubator. XLOLR cells were cultured overnight in NZY broth without supplementation under the same conditions. XL1-Blue-MRF' and XLOLR cells were harvested separately by spinning at 1000×g in Beckman GPR Centrifuge (Beckman, UK), and resuspended in 10 mM $MgSO_4$. In order to obtain a final concentration of $8\times10^8$ cells/ml, which was equal to an optical density (OD) of 1.0 at 600 nm, the concentration of the suspension was determined

**Figure 2:3** ZAP Express® vector excision

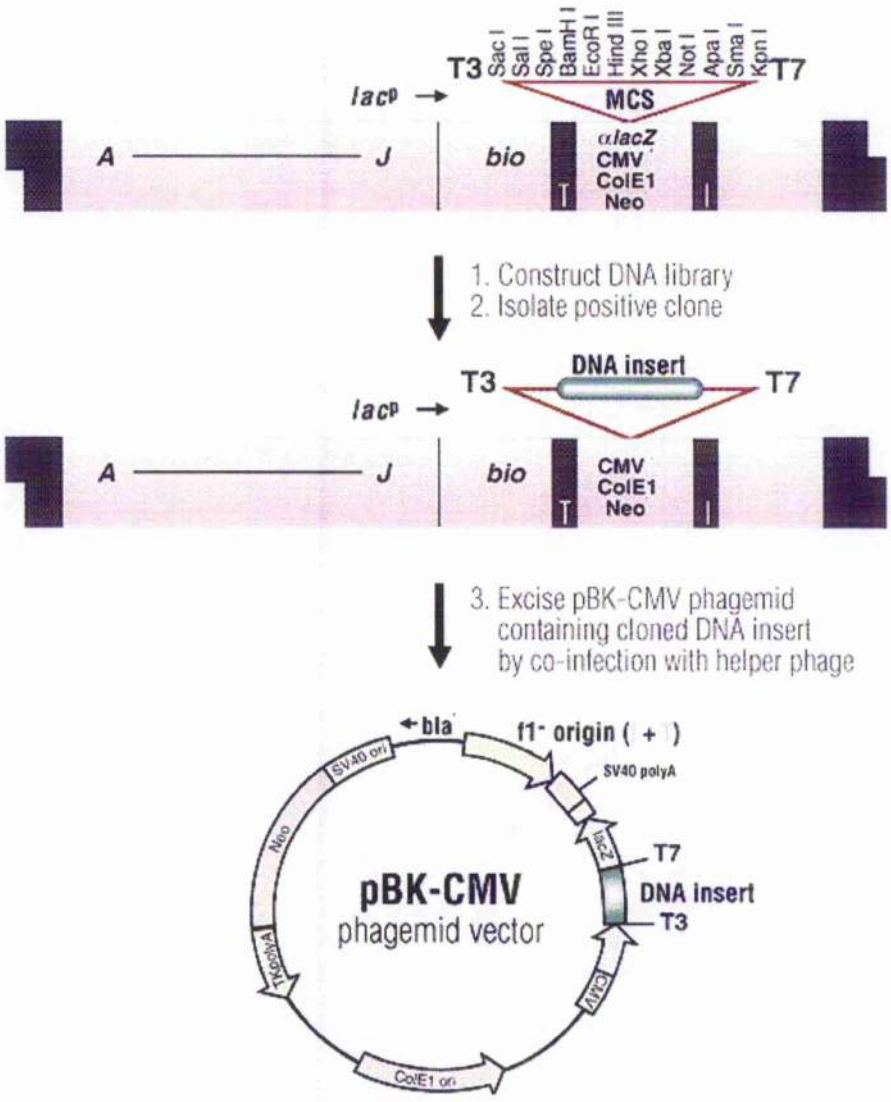


(Downloaded from website http://www.stratagene.com

Individual lambda phage or an amplified library are allowed to infect *E. coli* cells which are co-infected with filamentous helper phage. Inside the cell, trans-acting proteins from the helper phage recognise initiator (I) and terminator (T) domains within the ZAP Express® vector arms. Both of these signals are recognised by the helper phage gene II protein and a new DNA strand is synthesised, displacing the existing strand. The displaced strand is circularised and packaged as a filamentous phage by the helper phage proteins, and secreted from the cell. pBK plasmids are recovered by infecting an F' strain and growing in the presence of kanamycin.

using a Beckman DU® 640 spectrophotometer (Beckman Coulter, Inc., USA) at a wave length of 600nm.

A portion of the amplified ZAP® Express cDNA library was combined with XL1-Blue-MRF' cells at a multiplicity of infection (MOI) of 1:10 lambda phage-to-cell ratio in a 50-ml Falcon tube (Becton Dickinson Labware). In order to ensure statistical representation of the excised clones, 10- to 100-fold more lambda phage than the size of the primary library was excised. ExAssist® interference-resistant helper phage was then added to the tube at a ratio of 10 helper phage to 1 cell to ensure that every XL1-Blue-MRF' cell was co-infected with ZAP® Express lambda phage and ExAssist® interference-resistant helper phage. The 50 ml Falcon tube containing the mixture of lambda phage, XL1-Blue MRF' cells and helper phage, was incubated at 37°C for 15 minutes to allow absorption. After incubation, 20 ml of NZY broth was added to the mixture, and the Falcon tube was incubated for 2.5-3 hours at 37°C with shaking at 200 rpm in an Orbital Incubator SI 50 (Stuart Scientific). After incubation, the Falcon tube containing the mixture was heated at 65-70°C for 20 minutes in a waterbath (Grant Instruments Ltd). The debris was spun down at 1000×g for 10 minutes, and the supernatant was decanted into a new 50 ml Falcon tube.

The concentration of the excised phagemids was determined by combining 1 µl of the supernatant with 200 µl of the previously prepared XLOLR cells in a 1.5-ml microcentrifuge tube. This microcentrifuge tube was then incubated at 37°C for 15 minutes. After incubation, 40 µl of 5× concentrated NZY broth was added to this 1.5 ml microcentrifuge tube, which was then incubated at 37°C for 45 minutes. A hundred microlitres of the incubated cell mixture was plated onto each LB-kanamycin agar plate using sterile plastic spreaders, which contained 50 µg/ml kanamycin (Sigma-Aldrich), in 90 mm petri dishes (Bibby Sterilin Ltd). The LB-kanamycin agar plates were incubated overnight at 37°C. Colonies appearing on these plates were XLOLR cells, each of which contained the pBK-CMV double-stranded plasmid. ExAssist® interference-resistant helper phage would not grow since the helper phage was unable to replicate in XLOLR cells and did not contain kanamycin-resistance genes. XLOLR cells were also resistant to lambda phage infection, thus preventing the ZAP Express® lambda phage contamination after excision. At this stage, the XLOLR bacterial colonies on the LB-kanamycin plates could be

selected for plasmid DNA extraction and, for further bacterial culture in downstream colony hybridisation.

### 2.2.2.2. Colony blot hybridisations

After in vivo mass excision, cDNA fragments contained in the ZAP Express® vectors were converted into pBK-CMV phagemids, which were transformed into *E. coli* XLOLR cells to become pBK-CMV plasmids. In order to select cDNA inserts for the cDNA microarray construction, colony blot hybridisations were carried out on 17,600 bacterial colonies of transformed *E. coli* XLOLR cells, immobilised on 40 nylon membranes. Colony selection was then performed based on the intensity of hybridisation signals on autoradiograph films, as an indication of expression copies of each mRNA transcript in the two skeletal muscles from which the cDNA libraries were made. The process of colony hybridisation was divided into three steps: (1) preparation of nylon membranes on which *E. coli* XLOLR bacterial colonies were immobilised; (2) the preparation of [$\alpha$ - $^{32}$P] labelled porcine skeletal muscle cDNA probes (this step included mRNA extraction from muscle tissues, single-stranded cDNA synthesis using reverse transcription reaction, and [$\alpha$ - $^{32}$P] labelling of the synthesised cDNA); (3) the [$\alpha$ - $^{32}$P] labelled cDNA probe obtained from the step (2) was hybridised to nylon membranes obtained from the step (1).

#### *2.2.2.2.1. Membrane preparation for colony blot hybridisations*

The transformed *E. coli* XLOLR cells were plated onto LB-kanamycin agar plates (90 mm Sterilin Petri, Dishes Bibby Sterilin Ltd). From these plates, individual bacterial colonies were randomly picked using autoclaved toothpicks, and transferred immediately onto new LB-kanamycin agar plates in 243×243×25 mm square Bio-Assay dishes (Nalge Nunc International). Approximately, 17,600 colonies in total were randomly picked from the 90 mm Sterilin Petri Dishes, and transferred onto 40 LB-kanamycin agar plates in 243×243×25 mm square Bio-Assay dishes, with 440 colonies on each square agar plate, for overnight bacterial culture at 37°C. Before starting this process of bacterial transfer, a paper grid with 440 sub-grids numbered from 1 to 440 (Fig. 2:4) was attached on the underside of each 243×243×25 mm square Bio-Assay plate. Hence, the surface of each square agar plate was divided into 440 sub-grids. During the process of bacterial transfer, each randomly picked colony was transferred individually to the

**Figure 2:4** A paper grid, which has 440 sub-squares labelled with numbers from 1 to 440, was attached to the underside of the 243×243×25 mm Bio-Assay dish

| 1 | 2 | 3 | 4 | 5 | 6 | 7 | 8 | 9 | 10 | 11 | 12 | 13 | 14 | 15 | 16 | 17 | 18 | 19 | 20 |
|---|---|---|---|---|---|---|---|---|---|---|---|---|---|---|---|---|---|---|---|
| 21 | 22 | 23 | 24 | 25 | 26 | 27 | 28 | 29 | 30 | 31 | 32 | 33 | 34 | 35 | 36 | 37 | 38 | 39 | 40 |
| 41 | 42 | 43 | 44 | 45 | 46 | 47 | 48 | 49 | 50 | 51 | 52 | 53 | 54 | 55 | 56 | 57 | 58 | 59 | 60 |
| 61 | 62 | 63 | 64 | 65 | 66 | 67 | 68 | 69 | 70 | 71 | 72 | 73 | 74 | 75 | 76 | 77 | 78 | 79 | 80 |
| 81 | 82 | 83 | 84 | 85 | 86 | 87 | 88 | 89 | 90 | 91 | 92 | 93 | 94 | 95 | 96 | 97 | 98 | 99 | 100 |
| 101 | 102 | 103 | 104 | 105 | 106 | 107 | 108 | 109 | 110 | 111 | 112 | 113 | 114 | 115 | 116 | 117 | 118 | 119 | 120 |
| 121 | 122 | 123 | 124 | 125 | 126 | 127 | 128 | 129 | 130 | 131 | 132 | 133 | 134 | 135 | 136 | 137 | 138 | 139 | 140 |
| 141 | 142 | 143 | 144 | 145 | 146 | 147 | 148 | 149 | 150 | 151 | 152 | 153 | 154 | 155 | 156 | 157 | 158 | 159 | 160 |
| 161 | 162 | 163 | 164 | 165 | 166 | 167 | 168 | 169 | 170 | 171 | 172 | 173 | 174 | 175 | 176 | 177 | 178 | 179 | 180 |
| 181 | 182 | 183 | 184 | 185 | 186 | 187 | 188 | 189 | 190 | 191 | 192 | 193 | 194 | 195 | 196 | 197 | 198 | 199 | 200 |
| 201 | 202 | 203 | 204 | 205 | 206 | 207 | 208 | 209 | 210 | 211 | 212 | 213 | 214 | 215 | 216 | 217 | 218 | 219 | 220 |
| 221 | 222 | 223 | 224 | 225 | 226 | 227 | 228 | 229 | 230 | 231 | 232 | 233 | 234 | 235 | 236 | 237 | 238 | 239 | 240 |
| 241 | 242 | 243 | 244 | 245 | 246 | 247 | 248 | 249 | 250 | 251 | 252 | 253 | 254 | 255 | 256 | 257 | 258 | 259 | 260 |
| 261 | 262 | 263 | 264 | 265 | 266 | 267 | 268 | 269 | 270 | 271 | 272 | 273 | 274 | 275 | 276 | 277 | 278 | 279 | 280 |
| 281 | 282 | 283 | 284 | 285 | 286 | 287 | 288 | 289 | 290 | 291 | 292 | 293 | 294 | 295 | 296 | 297 | 298 | 299 | 300 |
| 301 | 302 | 303 | 304 | 305 | 306 | 307 | 308 | 309 | 310 | 311 | 312 | 313 | 314 | 315 | 316 | 317 | 318 | 319 | 320 |
| 321 | 322 | 323 | 324 | 325 | 326 | 327 | 328 | 329 | 330 | 331 | 332 | 333 | 334 | 335 | 336 | 337 | 338 | 339 | 340 |
| 341 | 342 | 343 | 344 | 345 | 346 | 347 | 348 | 349 | 350 | 351 | 352 | 353 | 354 | 355 | 356 | 357 | 358 | 359 | 360 |
| 361 | 362 | 363 | 364 | 365 | 366 | 367 | 368 | 369 | 370 | 371 | 372 | 373 | 374 | 375 | 376 | 377 | 378 | 379 | 380 |
| 381 | 382 | 383 | 384 | 385 | 386 | 387 | 388 | 389 | 390 | 391 | 392 | 393 | 394 | 395 | 396 | 397 | 398 | 399 | 400 |
| 401 | 402 | 403 | 404 | 405 | 406 | 407 | 408 | 409 | 410 | 411 | 412 | 413 | 414 | 415 | 416 | 417 | 418 | 419 | 420 |
| 421 | 422 | 423 | 424 | 425 | 426 | 427 | 428 | 429 | 430 | 431 | 432 | 433 | 434 | 435 | 436 | 437 | 438 | 439 | 440 |

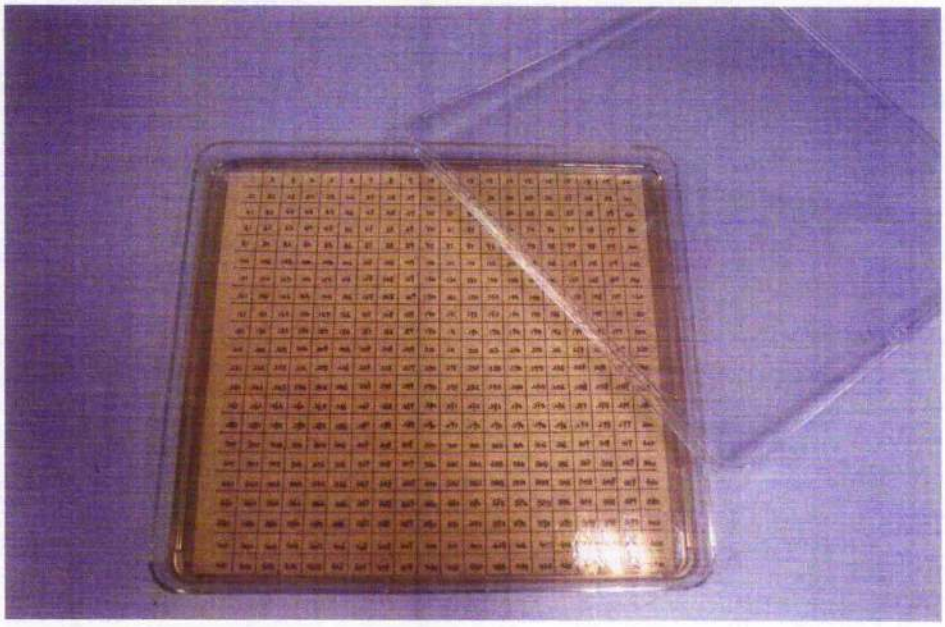

centre of each sub-grid. Each transferred colony was spaced about 1 cm distance apart from neighbouring colonies. After overnight bacterial culture, a 200×200 mm Hybond-N+ nylon membrane (Amersham Pharmacia Biotech) was laid gently onto the surface of each square agar plate, and then peeled back slowly. The bacteria-attached nylon membranes were air dried, with the bacteria side facing up, on a piece of Whatman chromatography paper (Whatman International Ltd) for 2-3 hours. Finally, the attached colonies were immobilised on the nylon membranes using ultraviolet (UV) crosslinking for about 15 seconds in a XL-1500 UV crosslinker (Spectronics Corporation).

#### *2.2.2.2.2. Probe preparation for colony hybridisations*

##### *2.2.2.2.2.1. mRNA extraction*

Direct isolation of messenger RNA (mRNA) from the *longissimus dorsi* muscle of a 50-day-old Meishan × Large White porcine foetus, and from the *gastrocnemius* muscle of a 3-day-old Meishan × Large White pig were carried out separately using the Dynabeads® mRNA DIRECT™ Kit (Dynal Biotech). All skeletal muscle tissues used for the mRNA extractions were stored in liquid nitrogen since obtained. The use of the Dynabeads® mRNA DIRECT™ Kit relies on the base pairing between the poly A tails of most mRNAs and the oligo dT sequences bound to the Dynalbeads® surfaces. Dynabeads® are the monodisperse polymer particles, which exhibit magnetic properties when placed within a magnetic field, but have no residual magnetism when removed from the magnetic field. Dynabeads® oligo $(dT)_{25}$ combine oligo dT sequences with magnetic properties of the Dynabeads®. Using a magnet like the Dynal Magnetic Particle Concentrator (Dynal MPC®), Dynabeads® oligo $(dT)_{25}$ can be used to isolate mRNA directly from crude extracts of animal tissues.

Each frozen muscle tissue was freeze-fracture pulverized rapidly to a powder while frozen in liquid nitrogen using mortar and pestle, which were previously baked at 80°C for 24 hours and pre-cooled with liquid nitrogen before use. The frozen powdered muscle tissue was weighed rapidly into approximately 50 mg portions using AB54 Analytical Balance (Mettler Toledo), foil and forceps pre-cooled with liquid nitrogen. The muscle was kept frozen throughout this aliquoting process to avoid mRNA degradation. Each portion of the frozen powdered muscle tissue was transferred immediately to a 2 ml RNAase-free microcentrifuge tube, which had been

pre-cooled in dry ice. One millilitre Lysis/Binding Buffer was added into each microcentrifuge tube containing muscle fragments, and the mixture was homogenised using T8.01 Netzgerat Homogeniser (Janke & Kunkel Gmbtt & Co., IKA Labortechnik) for about one minute until complete lysis was obtained. The lysate was spun for one minute in a Biofuge Pico Microcentrifuge (Heraeus Instruments) to remove debris. The supernatant was used in combination with Dynabeads® oligo $(dT)_{25}$.

Dynabeads® oligo $(dT)_{25}$ was supplied as a suspension in phosphate-buffered saline (PBS) in a stock tube. The Dynabeads® oligo $(dT)_{25}$ was resuspended by thorough shaking the stock tube before use. Two hundred and fifty microlitre suspension containing Dynabeads® oligo $(dT)_{25}$ was transferred from the stock tube to a 1.5 ml RNAase-free microcentrifuge tube placed in a Dynal MPC® magnet. When the suspension was clear, supernatant was removed from the tube and discarded. The tube was removed from the Dynal MPC®, and the Dynabeads® oligo $(dT)_{25}$ left inside the tube was resuspended in 200 µl Lysis/Binding Buffer. This tube was then returned to the Dynal MPC®. When the suspension was clear, supernatant was removed from the tube and discarded. The Dynabeads® oligo $(dT)_{25}$ left inside the tube was ready for combination with the clarified muscle tissue lysate.

The muscle tissue lysate was added into the tube containing the washed Dynabeads® oligo $(dT)_{25}$. The lysate was mixed with the Dynabeads® oligo $(dT)_{25}$ by rotating the tube on a Denley A600 Rocker (Denley-Tech Ltd) for six minutes at room temperature to allow mRNA and oligo dT sequence to aneal. This tube was then placed in the Dynal MPC®. When the suspension was clear, supernatant was removed from the tube and discarded. The Dynabeads® oligo $(dT)_{25}$, with captured mRNA, was washed twice with Washing Buffer A (see Apendix) (1 ml Washing Buffer A was used each time), then, once with Washing Buffer B (see Apendix) (1 ml Washing Buffer B was used), and finally, once with 1× concentration Reverse Transcription Buffer (1 ml 1×Reverse Transcription Buffer was used) at room temperature using the Dynal MPC®. Twenty-one microlitre 10 mM Tris-HCl (pH 7.5) was mixed with the Dynabeads® oligo $(dT)_{25}$ left inside the tube for elution of the captured mRNA from the Dynabeads® oligo $(dT)_{25}$. The tube containing the mixture was incubated at 65°C water bath (Grant Instruments Ltd) for 2 minutes, and then placed in the Dynal MPC®. When the suspension was clear, the supernatant containing mRNA was transferred to a new 1.5 ml RNAase-free microcentrifuge tube, ready for cDNA synthesis.

*2.2.2.2.2.2. Single-stranded cDNA syntheses*

Single-stranded cDNA was synthesised from the poly(A)+ mRNA using a reverse transcription system (Promega). Nine microlitres (about 2 μg) poly(A)+ mRNA extracted from the muscle tissue were placed in a sterile 1.5 ml microcentrifuge tube. The poly(A)+ mRNA contained in the tube was incubated at 70°C in a water bath (Grant Instruments Ltd) for 10 minutes, spun briefly in a Biofuge pico microcentrifuge (Heracus Instruments), and was then placed on ice. Prior to setting up a 40 μl reverse transcription reaction, a 31 μl reagent mixture including water, buffer, dNTPs, $MgCl_2$, primers, Recombinant RNasin® Ribonuclease Inhibitor, and AMV Reverse Transcriptase was set up in a new sterile 1.5 ml microcentrifuge tube (see Table 2:4). The mixture was added into and mixed with the poly(A)+ mRNA kept in the microcentrifuge tube, which had been placed on ice, to set up a 40 μl reverse transcription reaction. The reaction was first incubated at room temperature for 10 minutes, and then at 42°C for 15 minutes. The incubation at room temperature was to allow extension of the primers so they remained hybridised when the temperature was raised to 42°C. After incubation, the reaction was heated at 99°C in a heat block (Techne Dri-Block) for 5 minutes, and then incubated on ice for 5 minutes. The AMW reverse transcriptase was inactivated. At this stage, the synthesised single-stranded cDNA was ready to be labelled with [$\alpha$-$^{32}$P]. The synthesised single-stranded cDNA could be stored at –20°C in a freezer for future use.

**Table 2:4** Reverse transcription reaction for single-stranded cDNA synthesis

| **Reverse transcription reaction component** | **Amount** | | |
|---|---|---|---|
| $MgCl_2$ (25 mM) | 8.0 | μl | |
| Reverse Transcription Buffer (10xconcentration) | 4.0 | μl | |
| dNTP Mixture (10 mM) | 4.0 | μl | |
| Recombinant RNasin® Ribonuclease Inhibitor | 1.0 | μl | |
| AMV Reverse Transcriptase (high concentration) | 1.5 | μl | (≈ 30 U) |
| Random Primers (0.5μg/μl) | 2.0 | μl | (≈ 1 μg) |
| Poly(A)+ mRNA | 9.0 | μl | |
| Nuclease-Free Water | 10.5 | μl | |
| Final volume | 40.0 | μl | |

*2.2.2.2.2.3. Labelling single-stranded cDNAs with [α-$^{32}$P]*

Single-stranded cDNAs, synthesised by reverse transcription reactions, were labelled with [α-$^{32}$P] using Random Primers DNA labelling Systems (Life Technologies). The [α-$^{32}$P] labelled cDNAs were used as radioactive probes in colony blot hybridisation. To set up a labelling reaction, a 1.5 ml microcentrifuge tube containing 5 µl (approximately 25 nanograms) synthesised cDNA was removed from the -20°C freezers. The cDNA was thawed on ice, and 18 µl of autoclaved double distilled water (dd$H_2O$) was added into the tube. The diluted cDNA was denatured by heating the tube at 100°C for 5 minutes in a heat block (Techne Dri-Block). The tube was immediately placed on ice. On ice, The labelling mixture which contained 2µl dATP solution, 2µl dGTP solution, 2µl dTTP solution, 15µl Random Primers Buffer Mixture, 1µl Klenow Fragment and 5 µl 370 MBq/ml [α-$^{32}$P]dCTP (Amersham Pharmacia Biotech) (approximately 1.85 MBq in total), was gently mixed, centrifuged briefly at 5000 rpm in a Biofuge Pico Centrifuge (Heraeus Instruments), and incubated at 37°C in a waterbath (Grant Instruments Ltd) for 3 hours. In order to separate labelled probe from unincorporated nucleotides, the labelling mixture was purified using a Nick™ Column (Amersham Pharmacia Biotech) following the manufacturer's protocol. First of all, the NICK™ Column was equilibrated twice by allowing 3 ml distilled water to enter the gel bed of the column each time. Then, the labelling mixture, which was 27 µl in total, and 473 µl of distilled water was made to enter the gel bed in turn. The purified sample was eluted by another 400 µl of distilled water. Two microlitres of the purified labelling mixture was mixed in a plastic scintillation vial with 5 ml of Ecoscint™ A scintillation solution (National Diagnostics). The average count per minute (cpm) of the 2 µl aliquot contained in the vial, which represented the proportion of the radionucleotide incorporated into the probe cDNA, was counted using a LS1801 Beckman Counter (Beckman).

***2.2.2.2.3. Colony blot hybridisations***

A total of forty 200×200 mm Hybond-N+ nylon membranes, carrying immobilised bacterial colonies, were hybridised with [α-$^{32}$P] labelled cDNA probe, derived from the same muscle type and stage of development as that used for the library construction. All colony hybridisations were carried out in Schott GL45 glass hybridisation tubes (Stuart Scientific) in a hybridisation

oven (Stuart Scientific) with a rotating speed of 10 revs/minute. Each nylon membrane was first washed inside the hybridisation tube at 55°C for 30 minutes with about 200 ml washing buffer containing 5×SSC and 0.5% SDS. The washing buffer was decanted, and the tube was replaced with 20 ml prehybridisation buffer [50% formamide, 5×SSC, 5×Denhardt's, 0.1M EDTA, 1% SDS, 50mM sodium phosphate buffer (pH7.0) and 200 μg/ml sheared salmon sperm DNA] (see Appendix). The membrane was prehybridised with prehybridisation buffer at 65°C for 1 hour followed by overnight hybridisation at 60°C soaked in the same 20 ml prehybridisation buffer with an addition of [$\alpha$-$^{32}$P]dCTP labelled cDNA probe, at a concentration of $2\times10^6$ cpm/ml. The hybridised membrane was washed with washing buffer which contains 2×SSC and 0.1% SDS, at 55°C for 3-4 times, each time for 40 minutes with about 200 ml washing buffer. After washing, the membrane was exposed to a Hyperfilm™ MP high performance autoradiograph film (Amersham Pharmacia Biotech) in a Kodak X-Omatic cassette (Eastman Kodak Company) at -80°C for about 3 days. The film was then developed using a Compact X4 automatic x-ray film processor (Xograph Imaging Systems Ltd).

#### 2.2.2.3. Clone selection

Colonies were selected based on relative signal intensity found on the Hyperfilm™ MP high performance autoradiograph films. Selection emphasis was on those colonies with weak to moderate hybridisation signals. About 10 colonies with strong hybridisation signals was also selected from each square agar plate. On average, about 100-200 weakly to moderately expressed colonies and 10 highly expressed colonies were selected from each LB-kanamycin square Bio-Assay agar plate. The reasons for this selection are given in the discussion of this chapter. These selected colonies were transferred using sterile pipette tips (Sarstedt) from the square Bio-Assay plates to the 96-well flat-bottom blocks for bacterial cultivation.

#### 2.2.2.4. Bacterial culture of selected clones in 96-well flat-bottom blocks

Five thousand five hundred separate bacterial cultures of the selected colonies, which mostly gave weak to moderate hybridisation signals, were carried out using terrific broth (GIBCOBRL, Life Technologies) (see Appendix) in 96-well flat-bottom blocks (QIAGEN) [Fig. 2:5 (A)]. One millilitre of 50 mg/ml kanamycin was added into 1000 ml terrific broth using a sterile Plastipak® syringe (Becton Dickinson). The broth containing kanamycin was mixed gently and poured into

**Figure 2:5** QIAGEN 96-well flat-bottom block and QIAGEN 96-well format filter plate

**(A)**

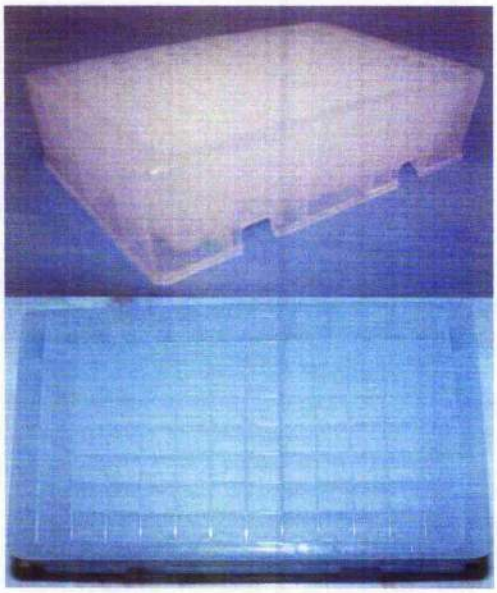

Picture (A) shows a QIAGEN 96-well flat-bottom block used for bacterial culture during microarray construction. The difference in the colour of the flat-bottom blocks in picture (A) is because the two photographs were taken using two different cameras.

**(B)**

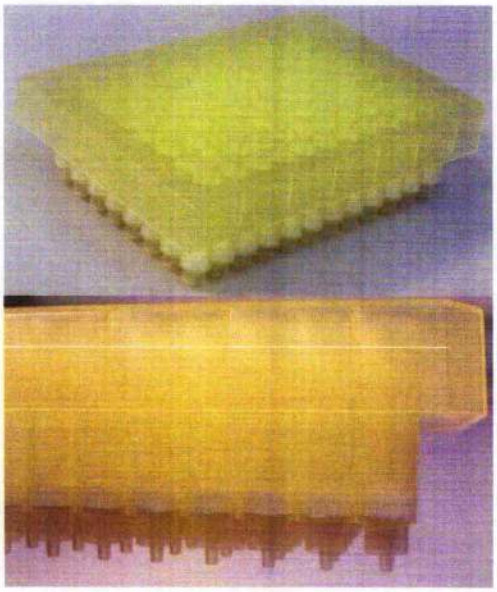

Picture (B) shows a QIAGEN 96-well format filter plate, its silica-gel membranes and nozzles. All TurboFilter 96 plates, QIAprep 96 plates and QIAquick 96-well plates are in the same form as this 96-well format filter plate shown in picture (B)

a sterile plastic disposable reagent reservoir (Sigma) for dispensing by a multichannel pipette (Eppendorf). Each well of a 96-well flat-bottom block was filled with 1.3 ml of the terrific broth, and was then inoculated with a single bacterial colony on a 243×243×25 mm Bio-Assay plate using a sterile yellow pipette tip (Sarstedt). The wells of each block were sealed with plastic adhesive tape (QIAGEN). Five to six holes were pierced in the tape with a sterile BD microlance™ 3 needle (Becton Dickinson) above each well for aeration during culture. The cultures were incubated for 24 hours at 37°C with shaking at 300 rpm in an Orbital Incubator SI 50 (Stuart Scientific). After incubation, the block was sealed by the addition of a new plastic adhesive tape, and bacterial cells in the block were harvested by centrifugation for 5 minutes at 1500× g in a Sorvall Legend RT centrifuge (Heraeus). After centrifugation, the plastic adhesive tapes were peeled off. The media in all wells were removed by quickly inverting the block over a waste container. Any remaining droplets of media were removed by tapping the inverted block firmly on a stack of absorbent paper. The bacterial pellets in the 96-well flat-bottom blocks were ready for plasmid DNA isolation.

#### 2.2.2.5. Plasmid DNA extraction in 96-well plate format

A total of 5,500 plasmid DNAs was extracted separately from the selected colonies using QIAprep 96 Turbo Miniprep Kits (QIAGEN) [Figs 2:5 (B) and 2:6] following the manufacturer's protocol. QIAprep 96 plates combined the convenience of multiwell technology with the selective binding properties of silica-gel membrane [Fig. 2:5 (B)]. The isolation of plasmid DNAs using the QIAprep 96 Turbo Miniprep Kits was based on alkaline lysis of bacterial cells followed by adsorption of DNA onto silica-gel membrane in the presence of high salt. The procedure for plasmid DNA extraction consisted of three basic steps: (1) preparation and clearing of bacterial lysate (2) adsorption of DNA onto the silica-gel membrane of the QIAprep 96 plate (3) washing and elution of plasmid DNA. The materials used in the isolation of plasmid DNAs in 96-well plate format are given in Table 2:5.

##### *2.2.2.5.1. Preparation and clearing of bacterial lysates*

Two hundred and fifty microliters of Buffer P1 containing 100μg/ml RNAase A were added to each bacterial pellet in the 96-well flat-bottom block. The block was then sealed with a plastic adhesive tape. The bacterial pellets in the block were resuspended by vortexing until no cell

**Figure 2:6** QIAGEN QIAvac 96 Vacuum Manifold

A

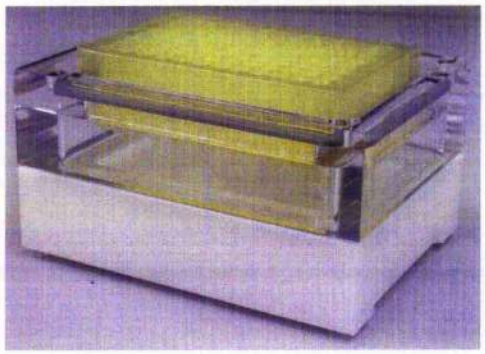

Figure 2:4 (A) shows a QIAvac 96 Vacuum Manifold with a 96-well format filter plate sitting on its top. Figure 2:4 (B) shows a QIAvac 96 Vacuum Manifold connected with vacuum regulator and vacuum pump.

B

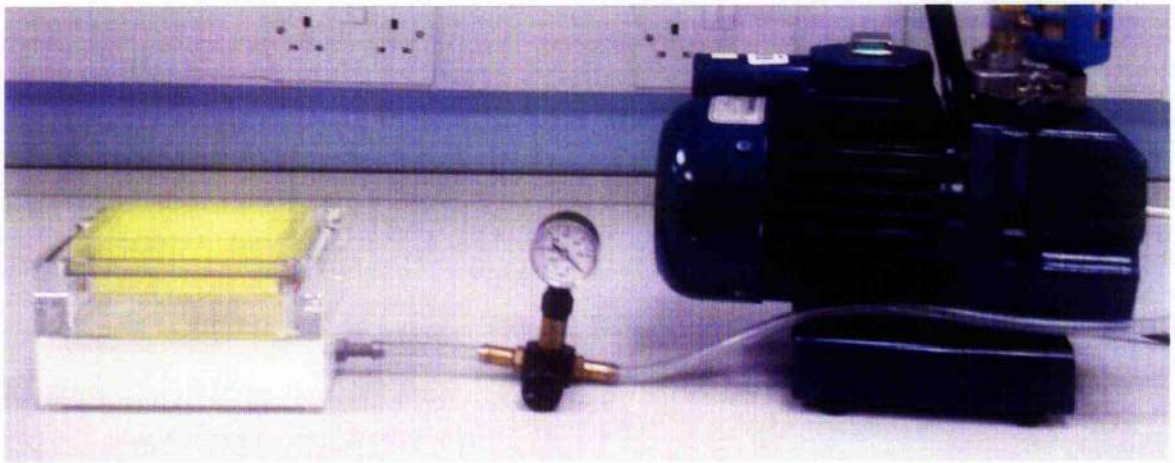

clumps were visible. The plastic adhesive tape was then removed from the block, and 250 µl Buffer P2 was added to each sample in the block. The block was sealed with a new plastic adhesive tape, and each sample in the block was mixed by gently inverting the block until the solutions became viscous and began to clear. After the block was incubated at room temperature for 5 minutes, the plastic adhesive tape was removed from the block, and 350 µl Buffer N3 was added to each sample in the block. The block was then sealed with a new plastic adhesive tape, and each sample in the block was mixed by gently inverting the block until the solutions became cloudy. The plastic adhesive tape was then removed from the block.

The TurboFilter 96 plate was placed in the QIAvac top plate, while the QIAprep 96 plate was positioned under the TurboFilter 96 plate. The bacterial lysates in the 96-well flat-bottom block, each of which was approximately 850 µl, were transferred to the TurboFilter 96 plate using a multichannel pipette (Eppendorf). Vacuum pressure [-200 millibar (mbar) to -600 mbar] generated by the vacuum pump was applied to the TurboFilter 96 plate until all lysates passed through the filters of TurboFilter 96 plate with a flow rate of 1-2 drops/second. The vacuum regulator connected with the vacuum pump was used to regulate the flow rate. The flow-through of the TurboFilter 96 plate was collected in wells of the QIAprep 96 plate. The TurboFilter 96 plate was then discarded.

#### *2.2.2.5.2. Adsorption of DNA onto silica-gel membrane of QIAprep 96 plate*

The QIAprep 96 plate containing the cleared lysates was placed in the QIAvac top plate, while a waste tray was positioned under the QIAprep 96 plate. Vacuum pressure (-200 mbar to -600 mbar) was applied to the QIAprep 96 plate until all lysates passed through the silica-gel membranes of the QIAprep 96 plate. The flow-through was collected in the waste tray and discarded. Nine hundred microliters of Buffer PB were added to each well of the QIAprep 96 plate. Vacuum pressure (-200 mbar to -600 mbar) was then applied to the QIAprep 96 plate. The flow-through was collected in the waste tray and discarded.

#### *2.2.2.5.3. Washing and elution of plasmid DNAs*

The QIAprep 96 plate was washed twice with Buffer PE. Each time, 900 µl of Buffer PE was added to each well of the QIAprep 96 plate. The vacuum pressure (-200 mbar to -600 mbar) was

**Table 2:5** Materials used in plasmid DNA extraction in 96-well plate format

| **QIAprep 96 Turbo Miniprep Kit (QIAGEN)** | |
|---|---|
| **Kit components** | **Uses of the components** |
| 96-well flat-bottom block with 2 ml square wells | 96-well flat-bottom blocks are for growing, harvesting, and lysing bacterial cultures prior to plasmid DNA extraction. |
| TurboFilter 96 plates (96-well plate format) | TurboFilter 96 plates are for filtering and clearing bacterial lysate. |
| QIAprep 96 plates (96-well plate format) | QIAprep 96 plates contain silica-gel membranes for adsorption of DNA in the presence of high salt. |
| Ribonuclease A (100mg/ml) | Ribonuclease A (RNase A) is for the digestion of RNA. |
| Buffer P1 | Buffer P1 is for re-suspending bacteria. |
| Buffer P2 | Buffer P2 is for lysis of bacteria. |
| Buffer N3 | Buffer N3 is for neutralization of the bacteria lysate. |
| Buffer PB | Buffer PB provides the correct salt concentration and pH for adsorption of DNA to the silica-gel membrane of the QIAprep 96 plate. |
| Buffer PE | The ethanol-containing Buffer PE washes salts away from the silica-gel membranes. |
| Buffer EB | Elution of plasmid DNAs from the silica-gel membranes was performed with low-salt Buffer EB. |

applied to the QIAprep 96 plate, and the flow-through was collected in the waste tray and discarded. After Buffer PE in all wells had passed through the silica-gel membranes of the QIAprep 96 plate, maximum vacuum was applied to the QIAprep 96 plate for an additional 10 minutes to remove residual Buffer PE from the membranes. The vacuum pressure was then switched off, and the QIAvac 96 top plate with the QIAprep 96 plate sitting in it was lifted from the QIAvac base and vigorously rapped on a stack of absorbent paper until no drops came out. The nozzles of the QIAquick 96 plate were blotted with clean absorbent paper. Each DNA

sample adsorbed on the silica-gel membrane was eluted by adding 110 µl of Buffer EB (10 mM Tris·Cl, pH 8.5) to the centre of the silica-gel membrane. The QIAprep 96 plate was left to stand for a minute, and maximum vacuum was then applied to the QIAprep 96 plate for 5 minutes in order to remove residual Buffer PE, which may interfere with subsequent enzymatic reactions. The flow-through of the QIAprep 96 plate, which was about 70 µl for each well, was collected in a Microtest™ U-Bottom 96-well plate (Becton Dickinson), which had been placed under the QIAprep 96 plate. Vacuum source was switched off once the process of elution was finished. Concentrations of 20 eluted DNAs were determined separately using a Beckman DU® 640 spectrophotometer (Beckman Coulter, Inc.).

#### 2.2.2.6. Storage and accounting of plasmid DNAs

Thirty-five microliters of each eluted DNA were transferred using a multichannel pipette to the corresponding well of a new Microtest™ U-Bottom 96-well plate to produce two sets of the plasmid DNA stock. One set was kept as an archive; the other was used as templates for PCR in 96-well plate format for the microarray construction. Each 96-well plate was labelled with its unique plate identity and sealed with a plastic adhesive tape to avoid cross-contamination and evaporation. All 96-well plates containing the recombinant plasmid DNAs were kept at -20°C in a freezer.

#### 2.2.2.7. PCR in 96-well plate format

Five thousand five hundred individual polymerase chain reactions (PCR) to amplify the cDNA inserts contained in the plasmid DNAs, derived from the two cDNA libraries, were carried out in 96-well plate format using HotStarTaq Master Mix kit (QIAGEN). Insert amplification of each pBK-CMV vector based plasmid clone was performed with T7 and T3 primers (Table 2:6). The HotSarTaq Master Mix contained HotStarTaq DNA polymerase, PCR Buffer with 3 mM $MgCl_2$, 400 µM dATP, 400 µM dTTP, 400 µM dGTP and 400 µM dCTP. HotStarTaq DNA polymerase, which provided hot-start PCR for higher PCR specificity, was provided in an inactive state with no polymerase activity at ambient temperatures. This prevents the formation of misprimed products and primer-dimers at low temperatures. HotStarTaq DNA Polymerase is activated by a 15-minute, 95°C incubation step. To carry out PCR reactions in 96-well plate format, reaction mixture was made up for 106 PCR reactions using Rainin pipette tips with hydrophobic filters

(Rainin Instrument) to minimise cross-contamination. Each individual PCR was performed in 100 µl volumes, using 10 µl of diluted plasmid DNA, which was equivalent to about 15 ng miniprep plasmid DNA of original concentration (Table 2:7). All PCR reactions were conducted for 35 cycles with denaturation at 94°C for one minute, continued with annealing at 55°C for 45 seconds, followed by elongation at 72°C for 3.5 minutes. All PCR reactions started with an initial activation step of 95°C for 15 minutes, and ended with an additional elongation step of 72°C for 10 minutes. All PCR reactions were performed using PCR Plate 96 low volume (0.2 ml) (Eppendorf) on an Eppendorf Mastercycler Gradient PCR machine (Eppendorf). Half of the total PCR amplification products, which were 2750 individual PCR products, were checked routinely for DNA yield and size by agarose gel electrophoresis.

**Table 2:6** T7 and T3 primers used for insert amplification by PCR

| Primer name | Manufactorature | Melting temperature (Tm) | Primer length | Primer sequences |
|---|---|---|---|---|
| T7 | MWG Biotech, Germany | 58.4°C | 22-mer | 5'-GTAATACGACTCACTATAGGGC-3' |
| T3 | MWG Biotech, Germany | 58.9°C | 23-mer | 5'-CGAAATTAACCCTCACTAAAGGG-3' |

**Table 2:7** Reaction mixture for each PCR in 96-well plate format

| PCR in 96-well format | | |
|---|---|---|
| | Reaction mixture for a single PCR reaction | Reaction mixture for 106 PCR reactions |
| Diluted plasmid DNA(s) | 10 µl | — |
| T7 primer (20 pmol/µl) | 4 µl | 424 µl |
| T3 primer (20 pmol/µl) | 4 µl | 424 µl |
| HotStarTaq Master Mix | 50 µl | 5300 µl |
| Distilled water | 32 µl | 3392 µl |
| Total volume | 100 µl | |

### 2.2.2.8. Purification of PCR product in 96-well plate format

All 5,500 PCR products were purified in 96-well plate format using QIAquick 96 PCR Purification kit which included Buffer PB, Buffer PE, Buffer EB, and QIAquick 96-well plates (QIAGEN). The QIAquick 96-well plates are in 96-well plate format and contain silica-gel membrane for adsorption of DNA in the presence of high salt. Unwanted primers and impurities, such as salts, enzymes, unincorporated nucleotides, and detergents (e.g. DMSO) were removed from the PCR products through the purification step. All PCR products, each of which was 100 µl, were transferred using a multichannel pipette from the wells of PCR Plate 96 low volume (0.2 ml) (Eppendorf Scientific) into the wells of QIAquick 96-well plate, which was placed in the QIAvac 96 top plate. Each 100 µl PCR product was then mixed with 500 µl Buffer PB. Vacuum pressure (-200 to -600 mbar) generated by the vacuum pump was applied to the QIAquick 96 plate until all the mixtures passed through the membranes of the QIAquick 96 plate. The following purification procedure was the same as that described in section 2.2.2.5. of this chapter for plasmid DNA extraction. The flow-through of each QIAquick 96 plate, which was about 50 µl for each well, were collected in the wells of a Microtest™ U-Bottom 96-well plate, which was placed under the QIAquick 96 plate. Vacuum source was switched off once the process of elution was finished. Concentrations of the eluted, purified DNAs were determined using Beckman DU® 640 spectrophotometer (Beckman Coulter, Inc.).

### 2.2.2.9. Storage and accounting of purified PCR products

Twenty-five microlitres of each eluted DNA was transferred using multichannel pipette to the corresponding well of a new Microtest™ U-Bottom 96-well plate to produce two sets of the purified PCR products stock. One set was kept as an archive; the other was used for microarray printing. Each Microtest™ U-Bottom 96-well plate was labelled with its unique identity and sealed with plastic adhesive tape to avoid cross-contamination and evaporation (Fig. 2:7). All the Microtest™ U-Bottom 96-well plate containing the purified, PCR amplified cDNA fragments were kept at -20°C in a freezer.

**Figure 2:7** Clone stock plates for microarray construction and clone tracking


Two sets of purified PCR products contained in Microtest™ U-Bottom 96-well plate were kept at -20°C. One set was kept as an archive; the other was used for microarray printing.

### 2.2.2.10. Printing microarray slides

After PCR purification, the purified cDNA fragments were transferred from the Microtest™ U-Bottom 96-well plates to v-bottom 384-well plates (Genetix) using a Hydra96 Microdispenser (Robbins Scientific) for microarray printing. The cDNAs in the 384 well plates were resuspended in spotting buffer which contained 600 mM phosphate buffer (pH 8.5) and 0.4% SDS. Medium-density, gridded microarrays were generated on 25mm×75mm, #40004 non-barcoded, non-sterile Corning® CMT-GAPS™ Coated glass slides (Corning Microarray Technology, Corning Incorporated) using a Microgrid II arrayer (Biorobotics Ltd) with a 48 print pin tool. The Corning® CMT-GAPS™ Coated slides have a uniform coating of pure gamma amino propyl silane reacted onto each slide. During microarray printing, the temperatures inside and outside the Microgrid II arrayer were 17°C and 19°C, respectively; the environmental moisture inside and outside the arrayer was 76% and 69%, respectively. All DNA samples including cDNA fragments and landing lights were printed in duplicate on each microarray slide. After microarray printing, the microarray slides were air-dried at room temperature. The spotted DNA fragments were then immobilised to the glass slides by baking at 80°C in a Gallenkamp incubator for two hours. A total of 5,500 selected clones were printed onto glass slides, of which 3,500 colonies derived from the 3-day-old porcine skeletal muscle library and 2,000 colonies derived from the 50-day-old porcine foetal skeletal muscle library.

The fluorescent landing lights used for the microarray printing in this study were cyanine 3 (Cy3)-labelled pGEM-T vector sequences and cyanine 5 (Cy5)-labelled pGEM-T vector sequences, both of which were about 160-170 base pairs. Both Cy3 and Cy5 are fluorescence cyanine dye (CyDye). Cy3 gives red fluorescence whilst Cy5 produces green fluorescence. The landing lights used in this study were included in the microarray, and spotted together with the cDNA fragments, which derived from the two skeletal muscle cDNA libraries, onto the glass slides for identifying orientation of the completed microarray. The landing lights printed on the microarray slides would be fluorescent whenever the microarray slides were detected for either Cy3 or Cy5 fluorescent images using a laser scanner. All landing lights used in this study were previously prepared using PCR by the PIC/Sygen Laboratory, Department of Pathology, Cambridge University. The microarray printing of this study was also performed in Cambridge University. The landing lights were stored at –20°C. When the microarray printing was to be conducted, the vials containing the landing lights were removed from the –20°C freezer, thawed

on ice, and spotted together with the porcine skeletal muscle cDNA fragments onto the microarray slides.

#### 2.2.2.11. Storage of microarray slides

After being baked at 80°C for 2 hours, the immobilised microarray slides were protected from light by storing in microscope slide boxes (VWR international), which were kept in a dark and dry enviroment at room temperature (20-25°C) for use at a later date. Direct contact with the surfaces of the slides, on which the DNA fragments had been printed, was always avoided.

#### 2.2.2.12. Quality controls

Throughout the main process of construction of the microarray, samples were taken to monitor the nature, purity and identities of the plasmid DNAs or cDNA fragments. The stages from which samples were taken and the procedures carried out are shown diagrammatically in the flow chart of Figure 2:2.

##### *2.2.2.12.1. Individual bacterial culture of unselected clones*

Randomly picked unselected bacteria colonies prepared were to be used in two processes (Southern blot hybridisation and dot blot hybridisation). About 300 transformed *E. coli* strain XLOLR colonies obtained through the in vivo mass excision were randomly picked from the previously prepared bacterial cultures on the LB-kanamycin agar plates in 90 mm Sterilin round petri dishes (see section 2.2.2.1. of this chapter). Each picked colony, which contained the recombinant pBK-CMV plasmid vector, was inoculated and grew overnight in 3 ml LB broth containing 50 μg/ml kanamycin (Sigma-Aldrich Co) in a 30 ml sterile plastic tube at 37°C with shaking at 200 rpm in a SI50 orbital incubator (Stuart Scientific). After incubation, the bacterial suspension in each tube was spun at 2,500 rpm for 5 minutes using a Beckman GPR centrifuge (Beckman) to obtain the bacteria pellet, which was used straight for individual isolation of the plasmid DNA.

### *2.2.2.12.2. Individual plasmid DNA extraction*

Individual isolation of plasmid DNAs from the randomly picked unselected bacteria colonies was carried out using QIAprep Spin Miniprep Kit (QIAGEN) following the manufacturer's protocol. QIAprep spin columns provided by this kit are individual columns containing silica-gel membrane for adsorption of DNA in the presence of high salt. All buffers provided by the QIAprep Spin Miniprep Kit are the same as that provided by the QIAprep 96 Turbo Miniprep Kit (see section 2.2.2.5. of this chapter). Each bacterial pellet kept in the 30 ml sterile plastic tube was resuspended by adding 250 µl Buffer P1 into the tube. The suspension was transferred to a sterile 1.5 ml microcentrifuge tube, and mixed with the added 250 µl Buffer P2 by gently inverting the tube 4-6 times. The solution in the tube was later mixed with the added 350 µl Buffer N3 by gently inverting the tube 4-6 times, followed by centrifuging the tube at 10,000×g for 10 minutes using a Heraeus Biofuge Pico microcentrifuge to form pellet. The supernatant was applied using an eppendorf pipette to a QIAprep spin column, which was then spun at 10,000×g for one minute. The flow-through of the column was discarded. The QIAprep spin column was washed two times, firstly with 0.5 ml Buffer PB and secondly with 0.75 ml Buffer PE, both of which were followed by centrifugation for one minute. The flow-through of the column from either wash was discarded. The column was then spun for an additional minute to remove residual Buffer PE. In order to elute plasmid DNA, the QIAprep spin column was placed in a new sterile 1.5 ml microcentrifuge tube while 50 µl Buffer EB was added onto the centre of silica-gel membrane of the column, which was later left to stand for one minute and then centrifuged for one minute. The extracted plasmid DNA was used in two ways (Fig. 2:2). One portion was subjected to restriction enzyme digestion and gel electrophoresis for Southern blot hybridisation. The other was used for dot blot hybridisation and compared with plasmid DNAs, which derived from the selected colonies for microarray construction.

### *2.2.2.12.3. Southern blot hybridisation*

After *in vivo* mass excision and before carrying out colony hybridisations, Southern blot hybridisation was performed to identify the relative abundance of different mRNA transcripts in porcine skeletal muscles. Plasmid DNAs used in Southern blot hybridisation were extracted from randomly picked colonies, which were derived from the 3-day-old porcine skeletal muscle cDNA library. All ninety-one plasmid DNAs, which derived from the randomly picked

unselected bacterial colonies, were doubly digested using restriction endonucleases *Eco*RI and *Xho*I. A 15 µl reaction of the restriction enzyme digestion was set up for each plasmid DNA by adding the DNA template, water, buffer and restriction endonucleases into a sterile 1.5 ml microcentrifuge tube (Table 2:8). The tube containing the reaction mixture was incubated at 37°C for 3 hours in a water bath (Grant Instruments). After incubation, all digested samples were subjected to agarose gel electrophoresis. Each digested sample, which was 15 µl in total, was mixed with 2.5 µl loading buffer of 6× concentration (see Appendix) and then loaded onto 0.8% [weight/volume (w/v)] agarose gel containing 0.2 µg/ml ethidium bromide (EB) (see Appendix). One microlitre of 1 µg/µl 1kb DNA ladder ($G_{IBCO}$BRL), which was used as size marker, was mixed with 14 µl $ddH_2O$ and 2.5 µl loading buffer of 6× concentration, and loaded onto the same gel. The agarose gel electrophoresis was conducted in Tris-acetate (TAE) buffer with electric power of 60 voltages for 3 hours. Using an ultraviolet transilluminator, DNA was visualised.

**Table 2:8** Reaction of restriction enzyme digestion

| | | |
|---|---|---|
| Plasmid DNA | | 1.5 µl |
| *Eco*RI (10U/µl) | ($G_{IBCO}$BRL) | 0.8 µl (=8U) |
| *Xho*I (10U/µl) | ($G_{IBCO}$BRL) | 0.8 µl (=8U) |
| 10× SuRE/CUT buffer H | (Boehringer Mannheim) | 1.5 µl |
| $ddH_2O$ | | 10.4 µl |
| Total volume | | 15.0 µl |

For Southern blot analysis, the DNA fragments in the agarose gel were denatured by immersing the gel in denaturing buffer, followed by neutralisation in neutralisation buffer. Southern blot hybridisation was conducted by hybridising the Hybond-N+ nylon membranes, on which the DNA fragments had been immobilised, to the [$\alpha$-$^{32}$P] labelled cDNA probe derived from the *gastrocnemius* muscle of a 3-day-old pig. The method used for the Southern blot hybridisation was that described for the colony blot hybridisation in section *2.2.2.2.3.* of this chapter.

#### *2.2.2.12.4. Detection of cDNA inserts during microarray construction*

Samples were taken at three stages of microarray construction to monitor the presence of cDNA fragments in the materials intended for inclusion in the microarray. The first sampling stage (Fig.

2:2) was prior to PCR amplification in 96-well plate format when the material sampled was still in the form of plasmid DNA. Two hundred of recombinant plasmid DNAs were detected by performing restriction enzyme digestion using *Eco*R I and *Xho* I. The digested samples were subjected to agarose gel electrophoresis to ascertain the presence of cDNA fragments and evaluate the quantity and quality of the cDNA fragments. Further samples were taken following PCR amplification and after the PCR purification step (Fig. 2:2). Half of the 5,500 PCR products and half of the 5,500 purified PCR products for microarray incorporation were detected by performing agarose gel electrophoresis to ascertain the presence of cDNA fragments and evaluate the quantity and quality of the cDNA fragments. The materials and methods used for restriction enzyme digestion and agarose gel electrophoresis have previously been described in the procedures of Southern blot hybridisation (see section *2.2.2.12.3.* of this chapter).

#### *2.2.2.12.5. Sequencing of plasmid DNAs derived from selected clones*

Sequencing reactions were performed using a Thermo Sequenase fluorescence cycle sequencing Kit (Amersham Life Science). In this sequencing kit, the enzyme, reaction buffer and nucleotides were pre-mixed and found in four separate tubes called reagent A, reagent C, reagent G and reagent T. In order to prepare a sequencing reaction, 5 µl (2-3 µg) plasmid DNA, 1 µl 2 pmol/µl T3 primer and 2 µl of reagent A, C, G or T were mixed thoroughly in a 0.2 ml tube. The sequencing reaction started with an initial pre-denaturation step of 95°C for 5 minutes, then the sequencing reaction was conducted for 25 cycles with denaturation at 95°C for 30 seconds, continued with annealing at 55°C for 30 seconds, followed by elongation at 72°C for 30 seconds. At the completion of the cycling programme, 2 µl formamide loading dye was added to each sequencing reaction. The sample was mixed thoroughly, and then denatured for 2 minutes at 90°C prior to gel electrophoresis. One and a half microlitres of each sequencing reaction product was subjected to gel electrophoresis. Sequencing reaction products were analysed on a LI-COR DNA sequencer model 4000L (LI-COR Corporation) for 140 plasmid DNAs, derived from the selected bacterial colonies. Each cDNA fragment inserted in the plasmid DNA was amplified by sequencing reaction with T3 primer, which sequenced from the 5' end of the insert. The purpose of this sequencing effort was to identify the range of genes represented in the microarray. However, the location of each clone in the 96-well stock plates was not recorded. To make 4% gel mixture solution, 25.2 g of Urea (Fisher Chemicals), 4.8 ml National Diagnostic Gel Mix Concentrate Solution and 7.2 ml 10× Tris-boric acid (TBE) buffer (see Appendix) were mixed in

a beaker. The TBE buffer contained 10.78% (w/v) Tris Base (Sigma), 5.5% (w/v) Boric Acid (Sigma) and 0.74% (w/v) EDTA (Sigma). The volume of the gel mixture was brought to 60 ml with $ddH_2O$. The solution was stired well with magnetic stirrer, and was allowed to cool in fridge. Two 66-cm plates were prepared by washing with 100% ethanol (Bamford laboratories) and 100% isopropanol (BDH). The plates were polished off until the surface of each plate was dry before they were assembled and placed into gel pouring stand. 400 µl ammonium persulphate (APS) (Sigma) and 40 µl N, N, N', N'-tetramethylethylenediamine (TEMED) (GIBCOBRL) were mixed with the gel solution before pouring the gel. The comb was carefully placed at the top of the gel to create wells. The gel was left to set for 2 hours before being inserted into LI-COR machine and loading samples to the wells. The gel was run with a high voltage of 2000V for 18-20 hours to get 800-100 bases of sequence from the gel. The sequences provided by the machine were stored digitally for analysis. The identity for sequencing was obtained by carrying out blast searches.

#### *2.2.2.12.6. Dot blot hybridisation*

To evaluate the effectiveness of colony selection, dot blot hybridisation was carried out using 192 individual plasmid DNAs. Half of these plasmid DNAs were extracted from 96 selected *E. coli* strain XLOLR colonies, derived from the 3-day-old skeletal muscle cDNA library, and intended for incorporation in the microarray. The other half were derived from 96 randomly picked unselected colonies studied in the quality assurance process (Fig. 2:2). In order to dilute the plasmid DNAs, 46 µl $ddH_2O$ was added into each well of two 96-well PCR Plates (Eppendorf). One of the plates was labelled plate A, the other plate B. Four microlitres of each plasmid DNA were added to each well of the 96-well PCR Plates containing $ddH_2O$. The 96 randomly picked unselected plasmid DNAs were transferred to plate A, whilst the 96 selected plasmid DNAs were transferred to plate B. The final volume of each diluted plasmid DNA was 50 µl. All diluted plasmid DNAs were denatured at 95°C for 10 minutes using the Eppendorf Mastercycler Gradient PCR machine (Eppendorf), followed by adding 50 µl 20×SSC (see Appendix) into each denatured DNA sample. The mixtures in plate A were transferred to wells of a Scotlab 96-well vacuum manifold (Scotlab) (Fig. 2:8). Negative vacuum generated by

**Figure 2:8** Scotlab 96-well format vacuum manifold and Hybaid™ blot processing pump used for dot blot hybridisation

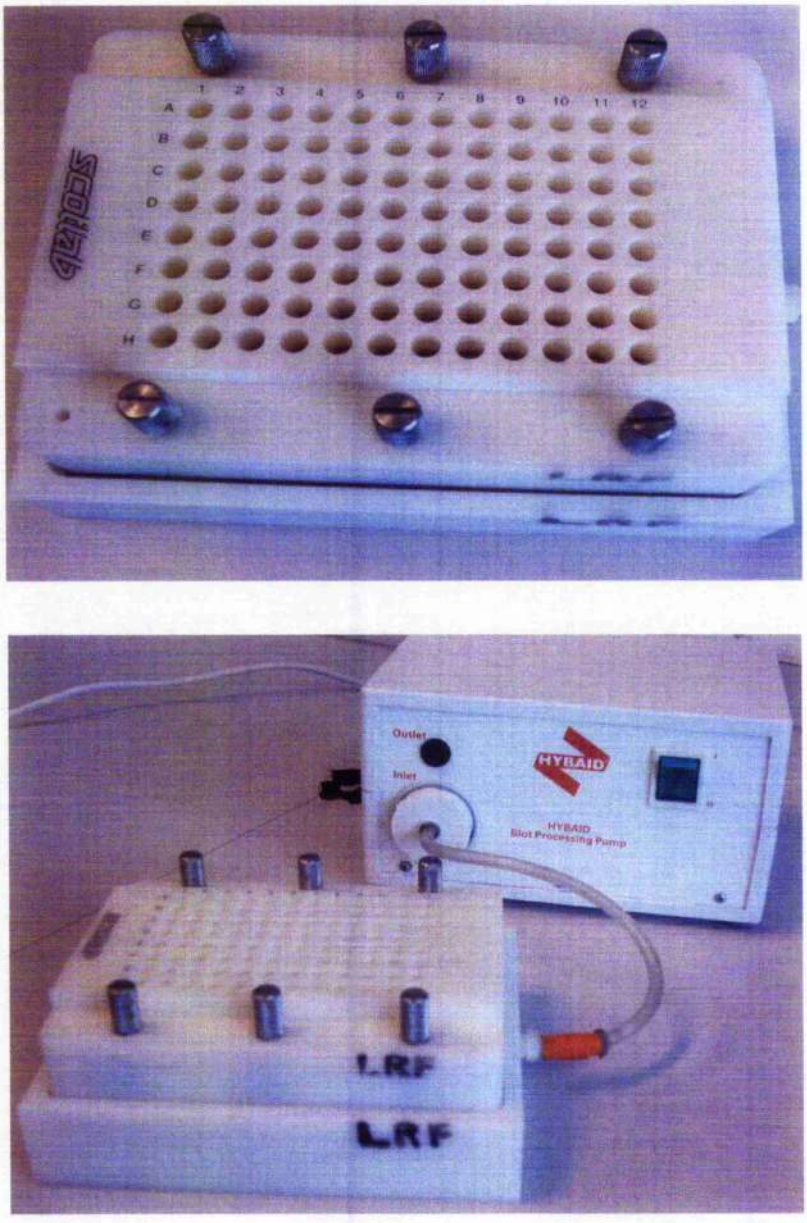

Hybaid™ Blot Processing Pump (Hybaid) (Fig. 2:8) was switched on throughout the transferring process, and then switched off once all the samples from plate A had been transferred onto a 80mm×115mm Hybond-N+ nylon membrane wetted with 10×SSC (see Appendix) placed inside the vacuum manifold. The nylon membrane was removed from the vacuum manifold, labelled, washed with 10×SSC, and air-dried for 2 hours on a piece of Whatman chromatography paper. The transferred plasmid DNAs were immobilised on the nylon membrane using ultraviolet (UV) crosslinking for about 15 seconds in a XL-1500 UV crosslinker (Spectronics Corporation). The same procedure followed for plate B. Both nylon membranes, which carried the immobilised plasmid DNAs derived from the 3-day-old skeletal muscle cDNA library, were hybridised to the [$\alpha$-$^{32}$P] labelled cDNA probe derived from muscle of the same muscle type and stage of development. The method used for dot blot hybridisation was that described for colony blot hybridisation in section *2.2.2.2.3.* of this chapter.

#### *2.2.2.12.7. Microarray hybridisation using Cy3 labelled T7 primer target*

The microarray printing process was evaluated by carrying out microarray hybridisation using T7 primer, which was labelled with FluoroLink™ Cyanine 3 fluorescent dye (Amersham Pharmacia Biotech), as target to hybridise to the cDNA probes immobilised on the microarray slide. The microarray hybridisation was performed at early stage of the microarray printing process in the PIC/Sygen Laboratory, Department of Pathology, Cambridge University. The sequence and manufacturer of the T7 primer used for the hybridisation were that described in Table 2:6.

A freshly printed microarray slide was air dried inside the Microgrid II arrayer, and then removed from the arrayer to be baked at 80°C-90°C for 2 hours on a heat block (Techne Dri-Block). After baking, the microarray slide was immersed in 95°C-100°C dd$H_2O$ for 2 minutes in a sterile glass beaker, followed by immersing the slide in 100% ethanol kept at room temperature in a 50 ml Falcon tube. The slide was dried by centrifugation at low speed for 2 minutes. The preparation of the 20 µl T7-Cy3 primer target mixture, which was later applied to the microarray slide in order to perform the microarray hybridisation, is detailed in Table 2:11. The slide was then covered with a BDH glass coverslip, and placed in a hybridisation chamber that could be tightly sealed. The hybridisation reaction performed on the microarray slide was incubated at 37°C for 30 minutes in a water bath. After hybridisation, the slide was removed from the

hybridisation chamber, and then immersed in 3×SSC contained in a 50 ml Falcon tube to remove the coverslip. The slide was washed twice by immersed firstly in washing buffer containing 3×SSC and 0.1% SDS, and secondly in 4×SSC. Both washing buffers were kept in 50 ml Falcon tubes. Following the washing step, the slide was dried by centrifugation at low speed for 2 minutes, and then scanned using GenePix 4000A scanner (Axon Instruments, Inc.).

The scanned image of the hybridised microarray was used for evaluating the effectiveness of the microarray printing process through assessing the quality of the microarray slides (i.e. the presence of DNA in every location on the slide for spotting) and the quantity of DNA present. As all the cDNA probes immobilised on the microarray slide had been obtained through PCR using T7 and T3 primers, the sequence of every single cDNA fragment incorporated in the microarray should hybridise with the T7-Cy3 primer target. Thus, after scanning the microarray slide, according to the amount of spots giving out fluorescence and the fluorescent signal intensity of each spot, the effectiveness of the microarray printing process and the amount of DNA per spot could be evaluated.

**Table 2:9** The T7-Cy3 primer target mixture prepared for the microarray hybridisation

| **The T7-Cy3 primer target mixture prepared for the microarray hybridisation** | |
|---|---|
| 20×SSC | 5 µl |
| Salmonsperm DNA | 1 µl |
| 10% SDS | 1 µl |
| $ddH_2O$ | 12 µl |
| T7-Cy3 primer (1 µM) | 1 µl |
| Final volume | 20 µl |

### *2.2.2.12.8. Dual-colour microarray hybridisation*

To evaluate hybridisation efficiency of the printed microarray slides, dual-colour microarray hybridisation was carried out using both Cy3 labelled cDNAs derived from 91-day-old porcine foetal skeletal muscle and Cy5 labelled cDNAs derived from porcine kidney. Both target cDNA samples were prepared in the Molecular Medicine Laboratory, Department of Veterinary Pathology, University of Glasgow. The hybridisation was performed in the PIC/Sygen Laboratory, Department of Pathology, Cambridge University. The method used for mRNA extraction and cDNA synthesis was the same as that described in section *2.2.2.2.2.* of this chapter.

Table 2:10 shows details of the cyanine dye labelling reaction for preparation of microarray hybridisation target. Cyanine dye labelling reaction was incubated first at 65°C for 5 minutes, then at 42°C for 2 minutes. Two microlitres of 200 U/µl Superscript™ II RNase H - Reverse Transcriptase (GIBCOBRL, Life Technologies) were then added to each cyanine dye labelling reaction. The mixture was incubated at 42°C for one hour. At the completion of the incubation, 5µl 500 mM EDTA was added to the mixture to stop the labelling reaction. The Cy3-labelled target and the Cy5-labelled target were mixed thoroughly. Pre-hybridisation was carried out by immersing a porcine skeletal muscle cDNA microarray slide in pre-hybridisation solution, which contained 1% (0.5 g) BSA and 3×SSC. The pre-hybridisation was incubated at 65°C for 15 minutes. Following pre-hybridisation, the microarray slide was washed briefly first with $ddH_2O$, then with 100% ethanol, and dried by centrifugation. In order to perform microarray hybridisation, the dual-CyeDye labelled cDNA target mixture was added to the microarray slide. The microarray hybridisation reaction was incubated overnight at 65°C. At the completion of the incubation, 5 µl 500 mM EDTA was added to the microarray slide to stop hybridisation reaction. Following hybridisation, the microarray slide was washed at room temperature for 5 minutes with washing buffer containing 0.5× SSC and 0.01% SDS, and then immersed briefly in 0.06× SSC. Immediately after washing, the microarray slide was dried by centrifugation, and scanned using GenePix 4000A scanner (Axon Instruments, Inc.) to capture the image. Image processing was performed using GenePix Pro 3.0 software (Axon Instruments, Inc.).

**Table 2:10** Cyanine dye labelling reaction for preparation of microarray hybridisation target

| **Content of the cyanine dye labelling reaction** | **91-day-old porcine foetal skeletal muscle** | **Porcine kidney** |
|---|---|---|
| Oligo dT (500 ng/µl) | 2.0 µl | 2.0 µl |
| First strand buffer (5× concentration) | 8.0 µl | 8.0 µl |
| dNTPs (10× low concenreation) | 2.0 µl | 2.0 µl |
| FluoroLink™ Cy3-dCTP (Amersham Pharmacia Biotech) | 2.0 µl | — |
| FluoroLink™ Cy5-dCTP(Amersham Pharmacia Biotech) | — | 2.0 µl |
| DTT (0.1 M) | 2.0 µl | 2.0 µl |
| RNAsin | 0.5 µl | 0.5 µl |
| DEPC $H_2O$ | 16.5 µl | 16.5 µl |
| mRNA | 5.0 µl (≈1 µg) | 5.0 µl (≈1 µg) |
| Total volume | 38.0 µl | 38.0 µl |

# 2.3. RESULTS

The entire process of microarray construction included the construction process itself and its associated quality controls. Results presented are divided into two sections: results of the construction process and results of the quality controls. Results of the construction process are divided into seven parts: (1) *in vivo* mass excision of pBK-CMV phagemid vector from lambda ZAP Express® vector, (2) colony hybridisations, (3) clone selection, (4) plasmid DNA preparation of selected clones, (5) PCR in 96-well plate format for amplification and purification of the cDNA inserts, (6) microarray printing, (7) clone accounting. Results of the quality controls are divided into the six parts: (1) Southern blot hybridisation, (2) detection of cDNA fragments by restriction enzyme digestion and agarose gel electrophoresis, (3) sequencing of plasmid DNAs derived from selected clones, (4) dot blot hybridisation, (5) microarray hybridisation using Cy3 labelled T7 primer target, (6) dual-colour (Cy3 and Cy5) microarray hybridisation.

## 2.3.1. RESULTS OF MICROARRAY CONSTRUCTION PROCESS

### 2.3.1.1. *In vivo* mass excision of pBK-CMV phagemid vector from ZAP Express® vector

To obtain *E. coli* colonies for microarray construction, *in vivo* mass excision of pBK-CMV phagemid vector from λ ZAP Express® vector was carried out based on the two porcine skeletal muscle cDNA libraries. One of the libraries was derived from the *longissimus dorsi* muscle of a 50-day-old Meishan × Large White porcine foetus; the other was made from the *gastrocnemius* muscle of a 3-day-old Meishan × Large White pig. Each cDNA library stored at -20°C in 1.5 ml microcentrifuge tubes was thawed successfully. This step was the starting point for construction of the composite microarray in this study. As a direct consequence of the *in vivo* mass excision of pBK-CMV phagemid vector from λ ZAP Express® vector, transformed kanamycin-resistant *E. coli* strain XLOLR bacterial colonies were obtained. Some difficulties were experienced at controlling density of the bacterial colonies on each LB-kanamycin agar plate, which turned out to be too high or too low. High density of bacteria on each plate made it difficult for picking individual colonies because cross-contamination was likely to happen. Low bacterial density, which brought about scarce colonies on each plate, required the use of a large number of such plates in order to obtain thousands of colonies for microarray construction. This requirement was

considered expensive and time-consuming. The difficulties were due to lacking of practical experience of standard method of ten-fold serial dilution for titrating bacterial concentration. Countermeasure to solve the problem was the effort to test repeatedly different dilutions and plating volumes of inoculums for achieving consistent colony yield on LB-kanamycin agar plates and obtaining the desirable bacterial density. About 50 of such attempts had been made until an idea bacterial density (around 500 colonies/per plate) was repeatedly achieved when 30 µl of inoculum was used for each agar plate. Although some of the colonies were still close together with this density (around 500 colonies/per plate), individual colonies were obtained with relative ease in sufficient number without the risk of cross-contamination. Eventually, a total of 17,900 *E. coli* colonies derived from the two cDNA libraries were randomly picked for Southern hybridisation, colony hybrdisations and dot blot hybridisation.

### 2.3.1.2. Colony blot hybridisations

Colony hybridisations were carried out for approximately 17,600 randomly picked bacterial colonies immobilised on 40 nylon membranes. The membranes were probed with [$\alpha$-$^{32}$P] labelled cDNAs derived from the same muscle type and stage of development as that used for the library construction. Each nylon membrane had 440 bacterial colonies transferred to it. Figure 2:9 shows estimates of porcine *longissimus dorsi* muscle mRNAs extracted for probe labelling using agarose gel containing ethidium bromide. Figure 2:10 shows two representative autoradiographs with various hybridisation signals. Intense signals represented cDNA clones that were derived from highly expressed genes, while faint signals represented cDNA clones from weakly expressed genes. Intermediate signals represented cDNA clones from moderately expressed genes. The absence of a signal could be due to a weakly expressed clone or absence of cDNA insert. According to its location on the paper grid, each spot on the autoradiographs was able to be traced to the corresponding bacterial colony on the LB-kanamycin agar plate in BioAssay square dish. Results of the colony hybridisations confirmed the presence of recombinant cDNAs in the transformed *E. coli* strain XLOLR bacterial colonies. Furthermore, the strong, moderate and weak expression profiles of porcine skeletal muscle genes were revealed on autoradiograph films in the form of hybridisation signals of randomly picked colonies. The images of hybridsation signals reflected the similarity of mRNA abundance between the two skeletal muscles cDNA libraries used in this study. The results of colony hybridisations made it feasible to perform the following colony selection step, and more importantly, allowed the construction of the microarray to proceed.

**Figure 2:9** Estimation of porcine *longissimus dorsi* muscle mRNAs extracted for $^{32}P$-probe labelling in colony hybridisations using agarose gel containing ethidium bromide

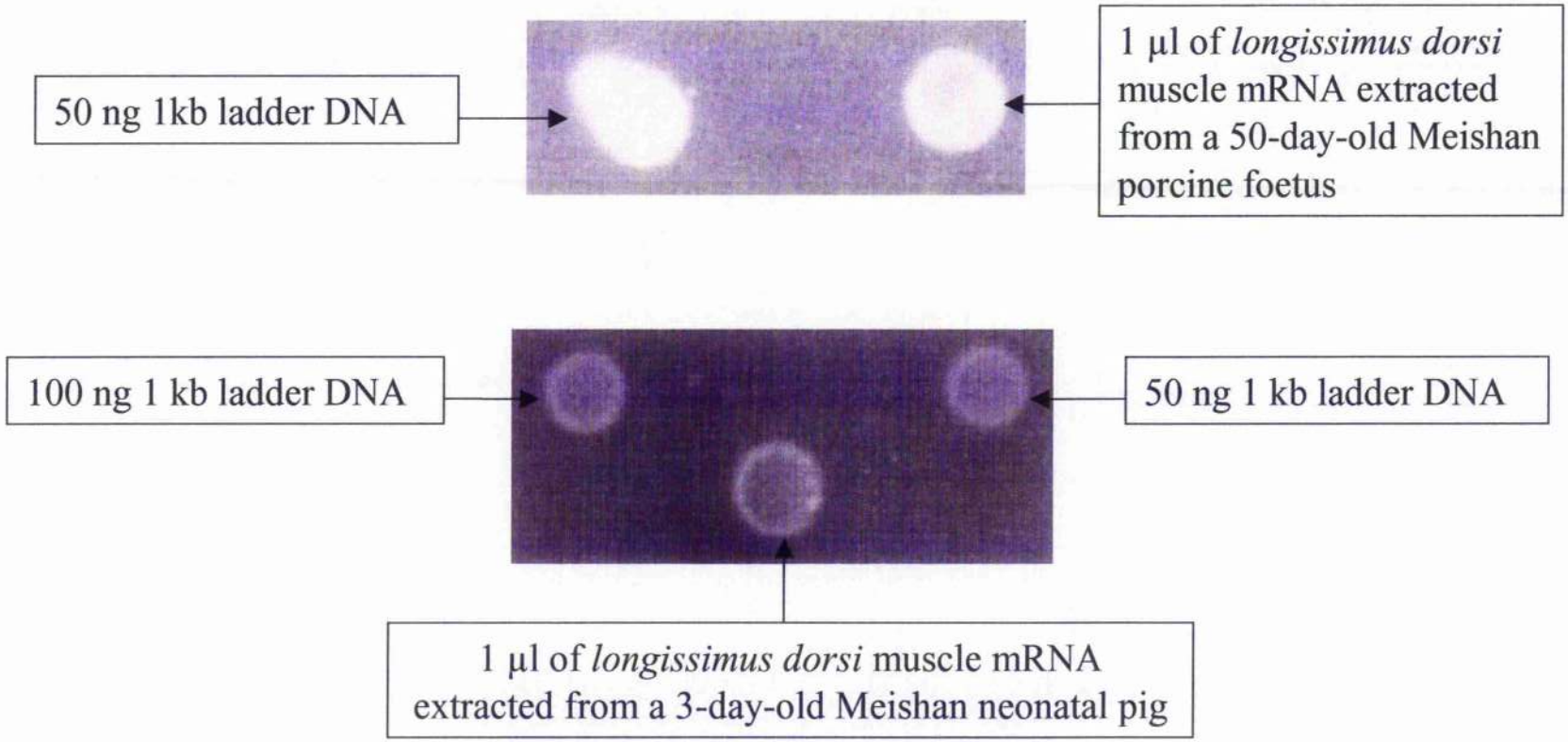

**Figure 2:10** Colony hybridisations

A

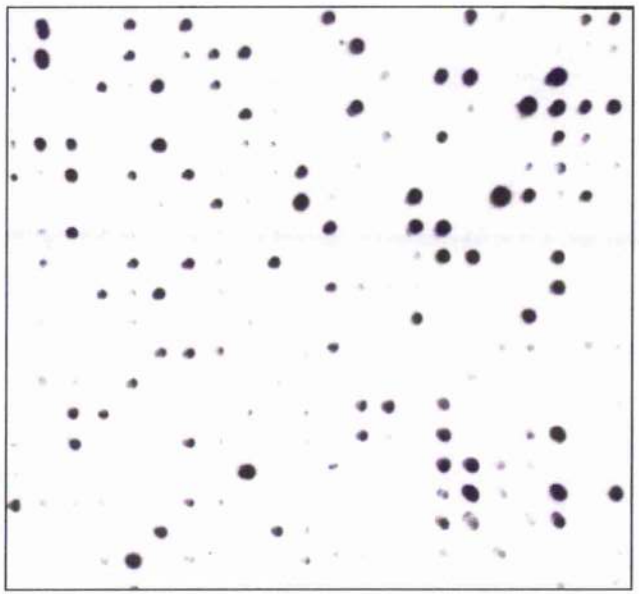

A:
Probe: 3-day-old neonatal porcine skeletal muscle total cDNA

Immobilised colonies: derived from 3-day-old porcine skeletal muscle cDNA library

B

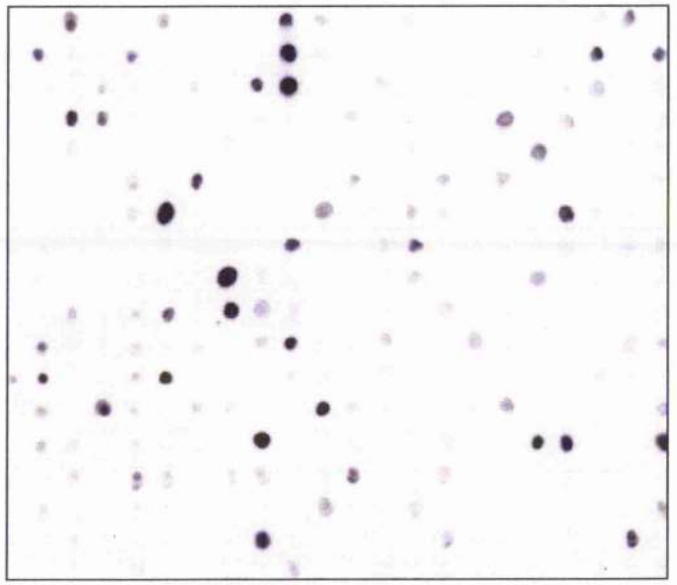

B:
Probe: 50-day-old porcine foetal skeletal muscle total cDNA

Immobilised colonies: derived from 50-day-old porcine foetal skeletal muscle cDNA library

### 2.3.1.3. Clone selection

Selection of the transformed *E. coli* strain XLOLR bacterial colonies from the LB-kanamycin agar BioAssay square dishes for microarray assembly was based on the signal intensity on autoradiograph films of the colony hybridisations. To attempt to assemble a cDNA microarray with a wide range of different cDNA clones, priority of colony selection was given to colonies with weak to moderate signals while colonies with strong signals were largely avoided. On average, about a quarter of the colonies on each LB-kanamycin agar BioAssay square dishes were selected/picked for the microarray assembly. A total of 5,500 colonies were selected/picked, of which 3,500 colonies derived from the 3-day-old porcine neonatal skeletal muscle library and 2,000 colonies derived from the 50-day-old porcine foetal skeletal muscle library.

### 2.3.1.4. Plasmid DNA extraction

The 5,500 selected bacterial colonies were inoculated individually into a total of fifty-seven 96-well flat-bottom blocks containing LB-kanamycin broth. Five thousand five hundred individual plasmid DNAs were obtained from their corresponding bacterial cultures. The average concentration of 20 eluted plasmid DNAs, which were randomly chosen, was 80 ng/µl as determined by spectrophotometry. In order to ensure the largest reliability of the constructed microarray, the presence of cDNA inserts in the pBK-CMV vector was evaluated by restriction enzyme digestion and agarose gel electrophoresis as part of the quality control outlined in Figure 2:2. Sample gels from the evaluation are given in Figure 2:11. The inserts ranged in size from 100 bp to 4 kb, predicted according to the known molecular weight standard (1 kb DNA ladder). The majority of the digestion samples produced two bands. The vector without insert would be the larger (4518 bp) of the two, and the insert the smaller. Some digestion samples of the recombinant plasmids produced three bands: two insert bands and one vector band. This may indicate that there was a restriction enzyme recognition site (*Eco*R I site or *Xho* I site) within each of these cDNA inserts. Of the total number of clones evaluated, about 10% were clones that did not show insert band on 0.8% agarose gel. This could be due to absence of cDNA insert in the pBK-CMV vector, or containing cDNA inserts of small size that was difficult to detect using 0.8% agarose gel.

### 2.3.1.5. PCR and purification of PCR products in 96-well plate format

All PCR amplification were performed in 96-well plate format, using T7 and T3 primers, on the plasmid DNAs extracted from the transformed and selected *E. coli* colonies. When evaluated by agarose gel electrophoresis for half of the 5,500 PCR products as part of the quality control outlined in Figure 2:2, the presence of the amplified cDNA fragments was found in all the PCR products evaluated. Purification of all PCR products was performed in 96-well plate format. The concentrations of 20 eluted purified PCR products, which were randomly selected, ranged from 0.054 μg/μl to 0.271 μg/μl with the average concentration of 0.137 μg/μl. When evaluated by agarose gel electrophoresis for half of the 5,500 PCR purification products as part of the quality control outlined in Figure 2:2, the presence of the amplified and purified cDNA fragments was found in all the PCR purification products evaluated. A sample gel from the evaluation is given in Figure 2:12. The presence of double bands in some of the purified PCR products (e.g., Lanes 4 and 5 in Fig. 2:12) could be due to non-specific priming. The purified PCR products were divided into two identical sets of 96-well plates ready to be spotted onto Corning® CMT-GAPS™ Coated slides. Figure 2:13 shows three types of stock plates kept at -20°C for the construction of porcine skeletal muscle cDNA microarray and clone tracking.

### 2.3.1.6. Printing microarray slides

Printing of microarray slides was carried out in the PIC/Sygen Laboratory, Department of Pathology, Cambridge University. Purified, PCR amplified cDNA fragments were transferred from fifty-seven 96-well plates (Plate1-Plate57) to fifteen 384-well plates (QB1-QB15). An additional 384-well plate (QB16) of Cy3 labelled landing lights, Cy5 labelled landing lights and printing buffer was included for the printing process. Table 2:11 shows the link between the 384-well stock plates, the 96-well stock plates and the two porcine cDNA libraries. All printed materials were transferred and spotted onto glass slides by robots from these sixteen 384-well plates. The microarray printed on each glass slide was arranged in 48 squares organised in 4 meta-rows and 12 meta-columns (Fig. 2:14). Each square was composed of 256 individual printed spots arranged as 16 rows and 16 columns (Figure 2:15). Therefore, a total of 12288 spots including landing lights and printing buffer were printed on each slide. Every single spot was printed in duplicate. Each printed spot and its corresponding duplicate were located in the

**Figure 2:11** Insert detection of selected clones by restriction enzyme digestion with *Eco*R I and *Xho* I and agarose gel electrophoresis

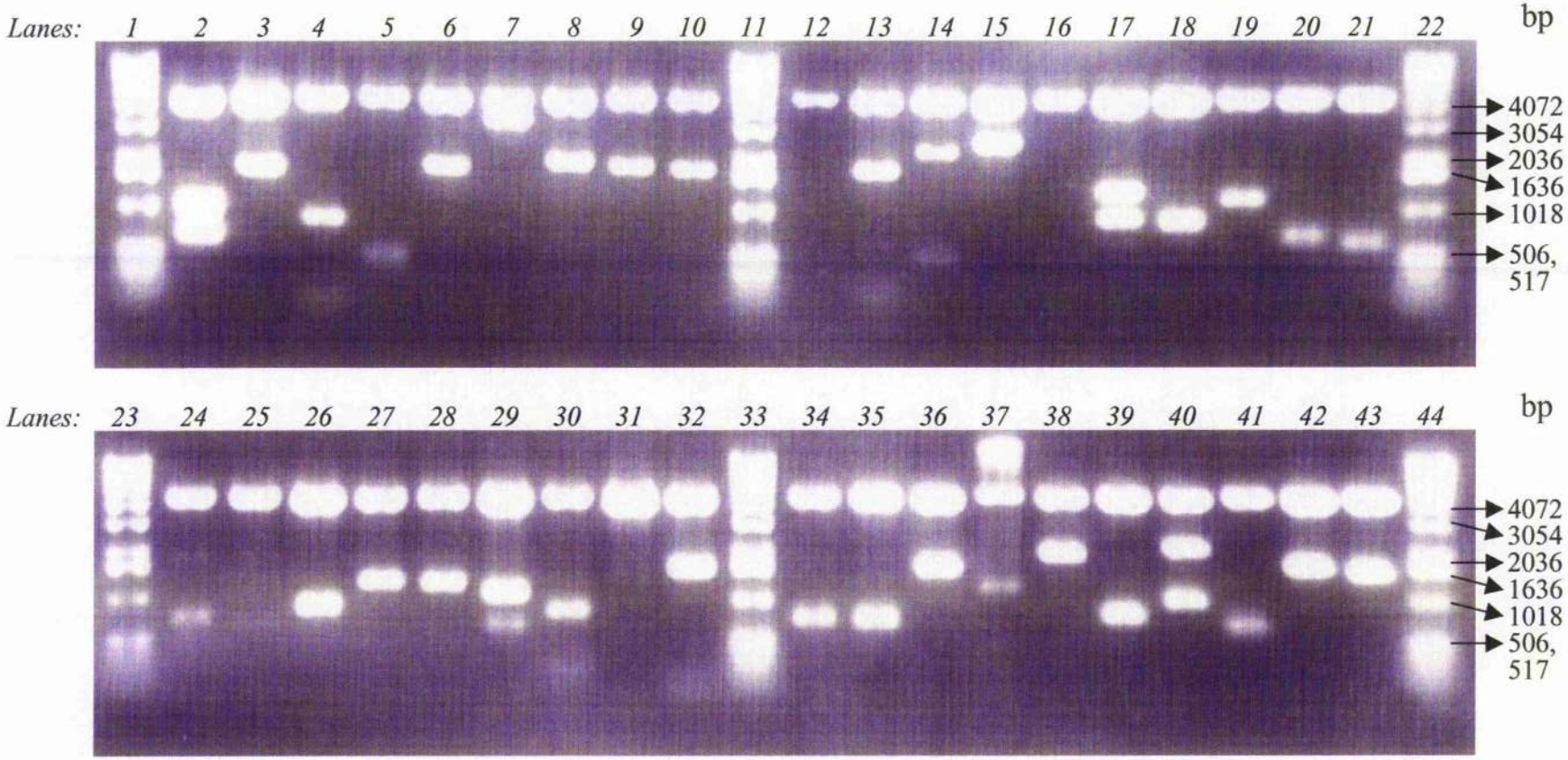


*Lanes 1, 11, 22, 23, 33, and 44* were 1 kb DNA ladder. *Lanes 2-10,12-21, 24-32, 34-43* were selected recombinant DNA digested with *Eco* R I and *Xho* I, which showed the bands of plasmid DNA and inserts.

**Figure 2:12** Detection of purified PCR-amplified cDNA inserts

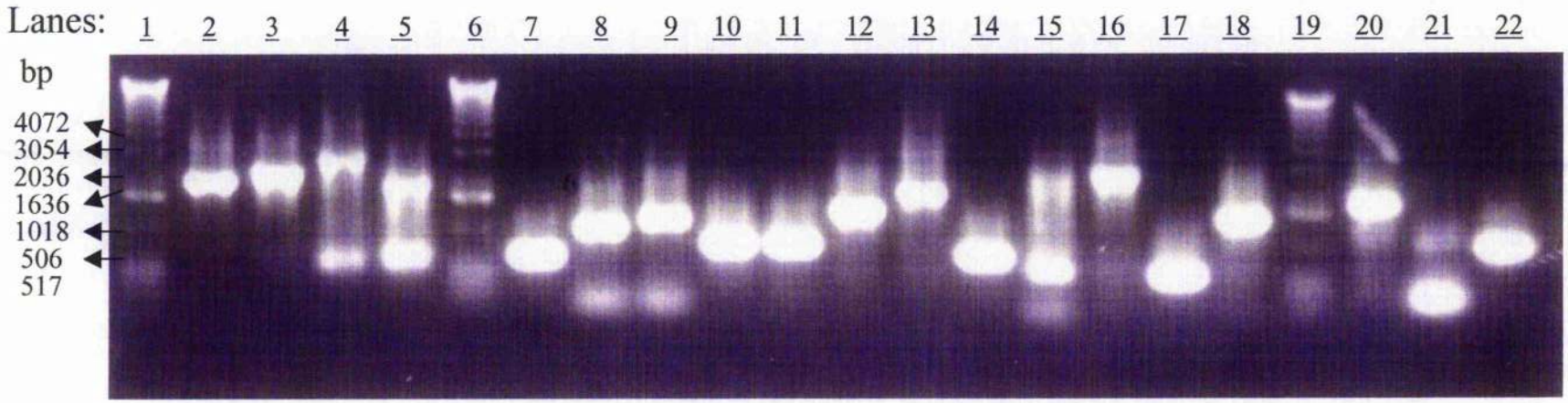


Lanes 1, 6 and 19 were molecular weight standards (1 kb DNA ladder).
Lanes 2-5,7-18, and 20-22 were purified PCR amplified cDNA inserts.

**Table 2:11** The link between 384-well plates, 96-well plates and the two porcine cDNA libraries

| 384-well plates | | 96-well plates | cDNA Library |
|---|---|---|---|
| **QB 1** | contains whole plates of : | Plate **1** & Plate **2** & Plate **3** & Plate **4** | 3-day-old pig |
| **QB 2** | contains whole plates of : | Plate **5** & Plate **6** & Plate **7** & Plate **8** | 3-day-old pig |
| **QB 3** | contains whole plates of : | Plate **9** & Plate **10** & Plate **11** & Plate**12** | 3-day-old pig |
| **QB 4** | contains whole plates of : | Plate **13** & Plate **14** & Plate**15** & Plate**16** | 3-day-old pig |
| **QB 5** | contains whole plates of : | Plate **17** & Plate **18** & Plate**19** & Plate**20** | 3-day-old pig |
| **QB 6** | contains whole plates of : | Plate **21** & Plate **22** & Plate**23** & Plate**24** | 3-day-old pig |
| **QB 7** | contains whole plates of : | Plate **25** & Plate **26** & Plate**27** & Plate**28** | 50-day-old foetus |
| **QB 8** | contains whole plates of : | Plate **29** & Plate **30** & Plate**31** & Plate**32** | 50-day-old foetus |
| **QB 9** | contains whole plates of : | Plate **33** & Plate **34** & Plate**35** & Plate**36** | 50-day-old foetus |
| **QB 10** | contains whole plates of : | Plate **37** & Plate **38** & Plate**39** & Plate**40** | 50-day-old foetus |
| **QB 11** | contains whole plates of : | Plate **41** & Plate **42** & Plate**43** & Plate**44** | 50-day-old foetus |
| **QB 12** | contains whole plates of : | Plate **45** & Plate **46** & Plate**47** & Plate**48** | 50-day-old foetus |
| **QB 13** | contains whole plates of : | Plate **49** & Plate **50** & Plate**51** & Plate**52** | 50-day-old foetus |
| **QB 14** | contains whole plates of : | Plate **53** & Plate **54** & Plate **55** & Plate**56** | 50-day-old foetus |
| **QB 15** | contains whole plates of : | Plate **57** | |

**Figure 2:13** Three types of stock plates kept at -20°C for the construction of porcine skeletal muscle cDNA microarray and clone tracking

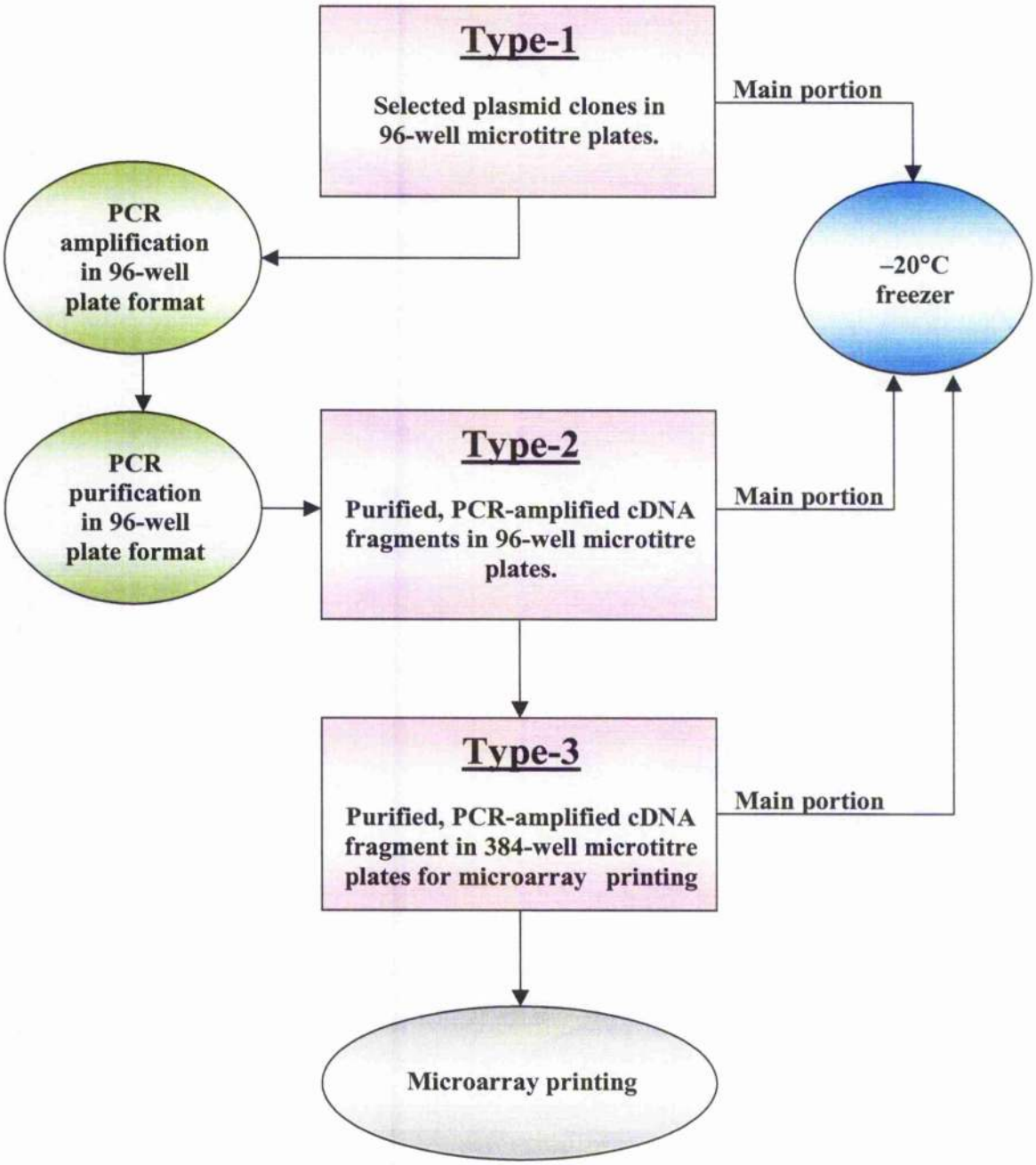

**Figure 2:14** The 48 printed squares of a hybridised microarray slide

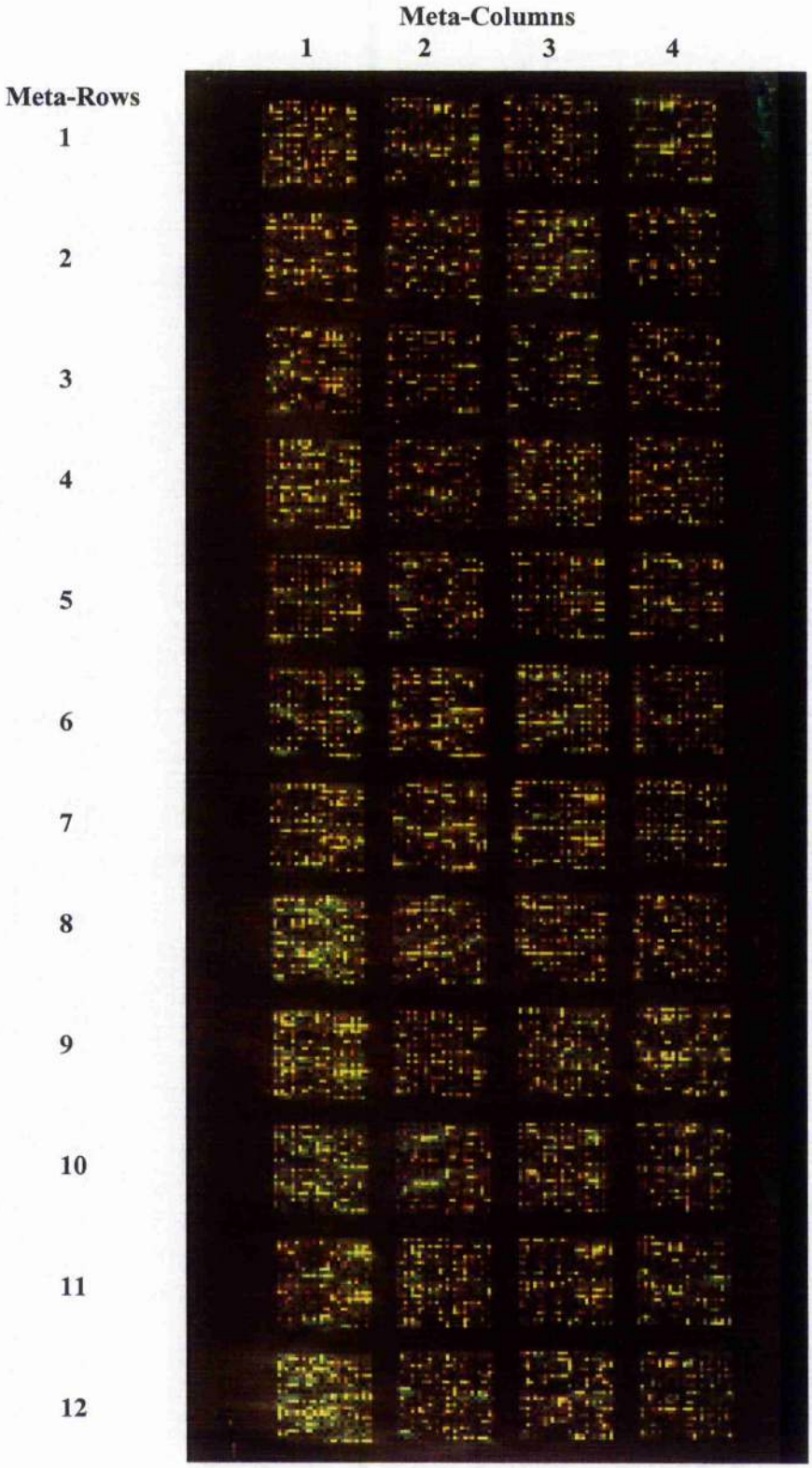

**Figure 2:15** Printing format for each square (16 spots × 16 spots) on the microarray slide

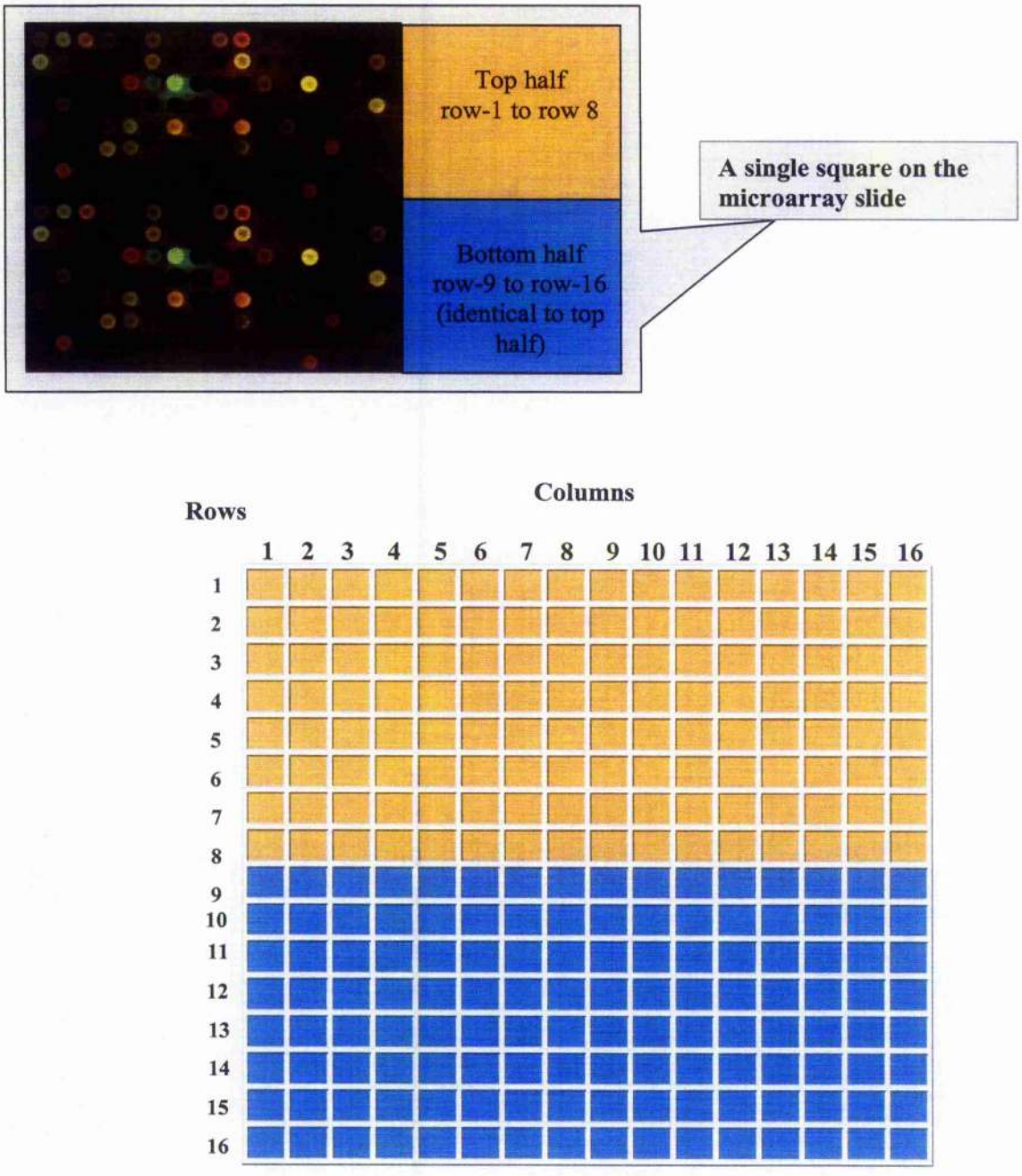


Each square of the microarray printing format containing 256 spots (16 spots × 16 spots).
The yellow section represents spots printed in the top half of each square. The blue section represents spots printed in the bottom half of each square, which is the duplicate of the spots in the yellow (top half) section.

same square. For each of the 48 squares, the spots located from row 9 to row 16 were orderly repeats of spots in rows 1 to 8 in the same square (Figures 2:14 and 2:15). All 48 squares were printed in the same format by using a preset computer programme for controlling the arraying robot (also called arrayer). Fifty-seven Corning® CMT-GAPS™ Coated slides were initially printed. All slides were stored for future use under the conditions specified in the Materials and Methods (see section 2.2.2.11. of this chapter). The quality of the printed porcine skeletal muscle cDNA microarray slides was monitored by both single-colour (Cy3) microarray hybridisation and dual-colour (Cy3 and Cy5) microarray hybridisation in the quality monitoring process (see sections *2.2.2.12.7.* and *2.2.2.12.8.* of this chapter).

### 2.3.1.7. Clone accounting

#### *2.3.1.7.1. Clone identification system for microarray slides*

The location of each printed spot was identified through the meta-row, meta-column, row and column of the spot on the microarray slide constructed in this study (Figs. 2:14 and 2:15). Every printed clone was given a unique gene name (Fig. 2:16). A total of 6144 different gene names labelled as "KC 1" to "KC 6144" were used.

#### *2.3.1.7.2. Clone identification system for stock plates*

All 96-well and 384-well stock plates were kept at -20°C in a freezer. The 96-well stock plates were of two types: plasmid DNA plates and PCR purification product plates. PCR purification products were transferred from 96-well plates to 384-well plates prior to printing. All plates were labelled sequentially. Each cDNA clone was given a unique "KC" number. Each cDNA spot on the microarray slide and its duplicate spot located in the same square but different row had an identical and unique "KC" number. The location of each cDNA clone on the 96-well stock plate was identified as "P", which was followed by the plate category, plate number, row, and column. The location of each clone on the 384-well stock plate was identified as "QB", which was followed by the plate category, plate number, row, and column. Every cDNA clone printed on the microarray slide could be traced to all types of stock plates. An Excel file was set up for all the printed spots to link together the clone location in 96-well stock plates and in 384-well stock plates (Fig 2:17). Each cDNA clones used for the microarray construction could be

**Figure 2:16** An example of gene naming and plate identity system of cDNA clones

| Gene name | Meta-Row | Meta-Column | Row | Column | Spot Location |
|---|---|---|---|---|---|
| KC1 | 1 | 1 | 1 | 1 | 1,1,1,1 |
| KC1 | 1 | 1 | 9 | 1 | 1,1,9,1 |
| KC16 | 1 | 1 | 1 | 16 | 1,1,1,16 |
| KC16 | 1 | 1 | 9 | 16 | 1,1,9,16 |
| KC128 | 1 | 1 | 8 | 16 | 1,1,8,16 |
| KC128 | 1 | 1 | 16 | 16 | 1,1,16,16 |
| KC129 | 1 | 2 | 1 | 1 | 1,2,1,1 |
| KC129 | 1 | 2 | 9 | 1 | 1,2,9,1 |
| KC6144 | 12 | 4 | 8 | 16 | 12,4,8,16 |
| KC6144 | 12 | 4 | 16 | 16 | 12,4,16,16 |

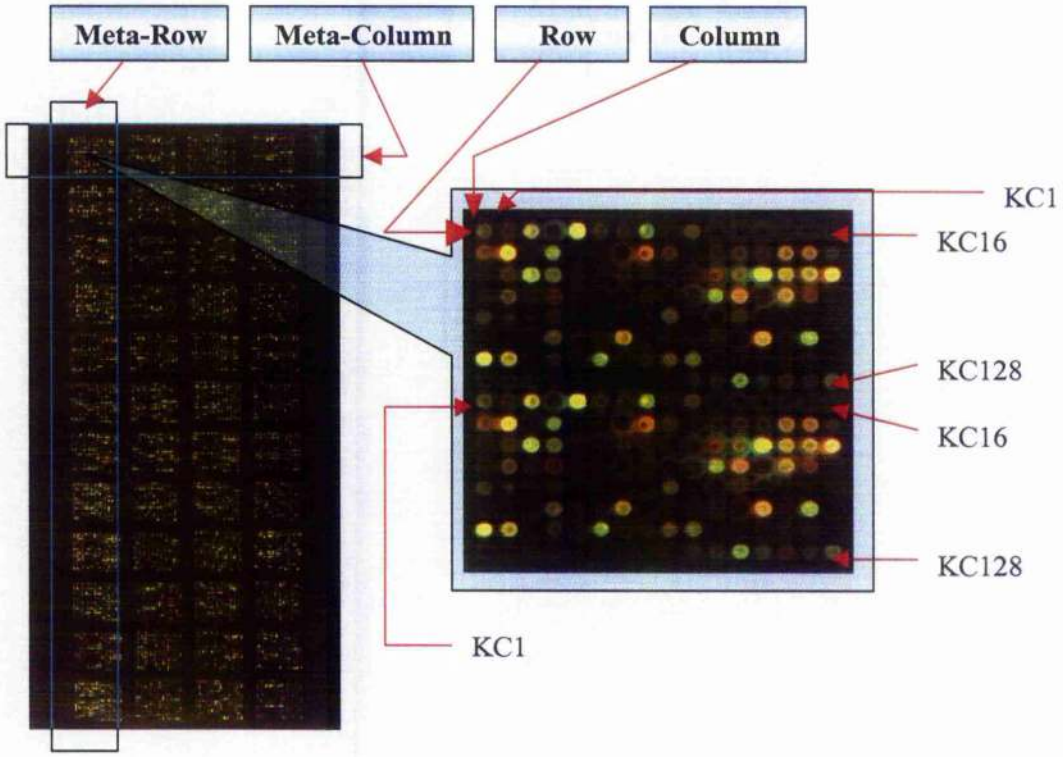


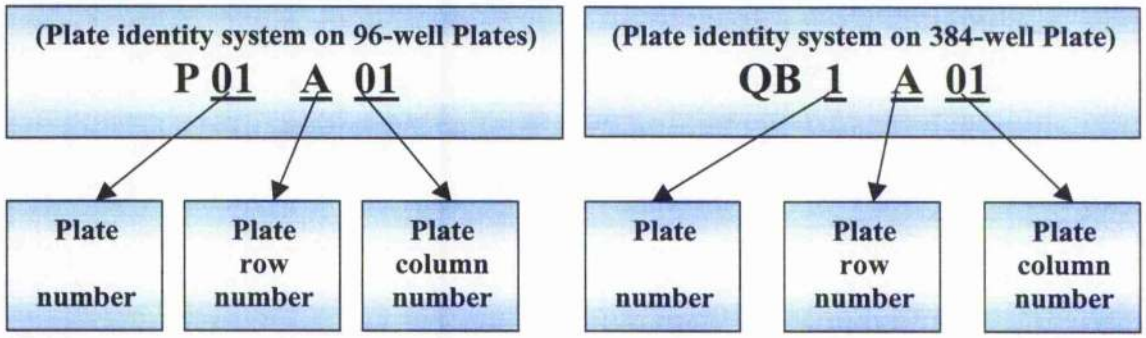

**Figure 2:17** A sample of the Excel file established for tracking each gene name back to the location of a plasmid clone or a cDNA insert in stock plates

| Image Meta-Row | Image Meta-Column | Image Row | Image Column | Identity on 384-well Plates | Identity on 96-well Plates |
|---|---|---|---|---|---|
| 12 | 4 | 16 | 16 | QB14_I12 | P54_E06 |
| 12 | 4 | 15 | 16 | QB12_I12 | P46_E06 |
| 12 | 4 | 14 | 16 | QB10_I12 | P38_E06 |
| 12 | 4 | 13 | 16 | QB8_I12 | P30_E06 |
| 12 | 4 | 12 | 16 | QB6_I12 | P22_E06 |
| 12 | 4 | 11 | 16 | QB4_I12 | P14_E06 |
| 12 | 4 | 10 | 16 | QB2_I12 | P06_E06 |
| 12 | 4 | 9 | 16 | Landlights | Cy3 Landlights |
| 12 | 4 | 8 | 16 | QB14_I12 | P54_E06 |
| 12 | 4 | 7 | 16 | QB12_I12 | P46_E06 |
| 12 | 4 | 6 | 16 | QB10_I12 | P38_E06 |
| 12 | 4 | 5 | 16 | QB8_I12 | P30_E06 |
| 12 | 4 | 4 | 16 | QB6_I12 | P22_E06 |
| 12 | 4 | 3 | 16 | QB4_I12 | P14_E06 |
| 12 | 4 | 2 | 16 | QB2_I12 | P06_E06 |
| 12 | 3 | 7 | 2 | QB14_B12 | P55_A06 |
| 12 | 3 | 6 | 2 | QB12_B12 | P47_A06 |
| 12 | 3 | 5 | 2 | QB10_B12 | P39_A06 |
| 12 | 3 | 4 | 2 | QB8_B12 | P31_A06 |
| 12 | 3 | 3 | 2 | QB6_B12 | P23_A06 |
| 12 | 3 | 2 | 2 | QB4_B12 | P15_A06 |
| 12 | 3 | 1 | 2 | QB2_B12 | P07_A06 |
| 12 | 2 | 16 | 15 | QB14_O12 | P54_H06 |
| 12 | 2 | 15 | 15 | QB12_O12 | P46_H06 |
| 12 | 2 | 14 | 15 | QB10_O12 | P38_H06 |
| 12 | 2 | 13 | 15 | QB8_O12 | P30_H06 |
| 12 | 2 | 12 | 15 | QB6_O12 | P22_H06 |
| 12 | 2 | 11 | 15 | QB4_O12 | P14_H06 |
| 12 | 2 | 10 | 15 | QB2_O12 | P06_H06 |
| 12 | 1 | 8 | 9 | QB15_H12 | P57_H12 |
| 12 | 1 | 7 | 9 | QB13_H12 | P51_D06 |
| 12 | 1 | 6 | 9 | QB11_H12 | P43_D06 |
| 12 | 1 | 5 | 9 | QB9_H12 | P35_D06 |
| 12 | 1 | 4 | 9 | QB7_H12 | P27_D06 |
| 12 | 1 | 3 | 9 | QB5_H12 | P19_D06 |
| 12 | 1 | 2 | 9 | QB3_H12 | P11_D06 |

**Figure 2:18** Microarray clone tracking system

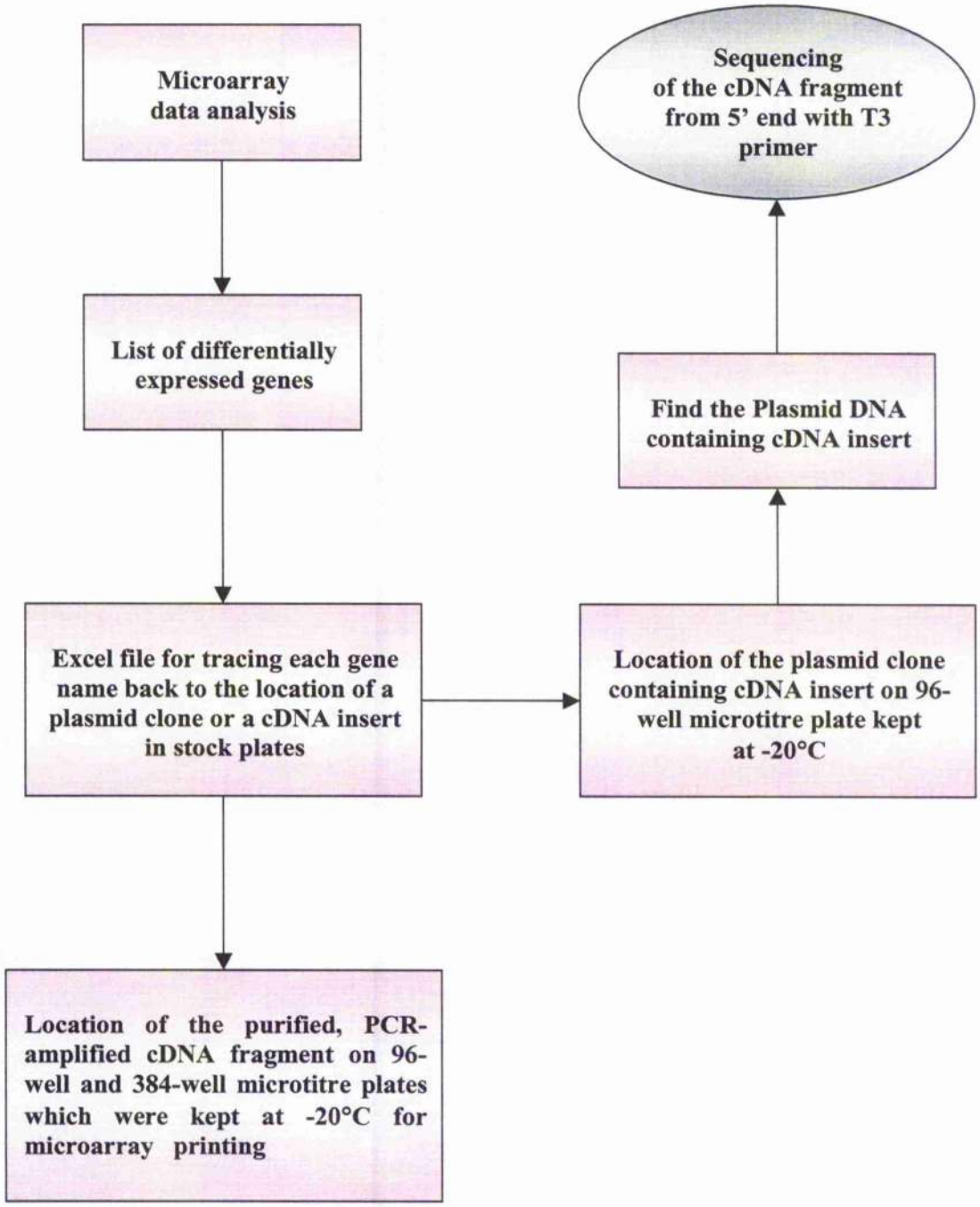

tracked from its spot location on the microarray slide back to its corresponding DNA materials in the stock plates (Tables 2:11; Figures 2:13, 2:16 and 2:18).

## 2.3.2. QUALITY CONTROLS

### 2.3.2.1. Southern blot hybridisation

As part of the quality control outlined in Figure 2:2, Southern blot hybridisation was performed for the purpose of identifying the expression patterns of different types of mRNA transcripts (e.g., weakly, moderately and highly expressed mRNAs) in total mRNAs of porcine skeletal muscle, and therefore, providing the theoretical basis for the subsequent selection of clones according to the colony hybridisation results. In order to carry out Southern blot hybridisation, 91 unselected plasmid clones, derived from the 3-day-old porcine cDNA library, were first subjected to restriction enzyme digestion with *Eco*R I and *Xho* I, followed by agarose gel electrophoresis. A sample gel is given in Figure 2:19. All the digested plasmid DNAs produced cDNA insert bands on 0.8% agarose gel. These cDNA fragments were transferred to nylon membranes and hybridised to the [$\alpha$-$^{32}$P] labelled cDNA probe derived from 3-day-old porcine neonatal skeletal muscle. On the agarose gels for examining the digested plasmid clones (Fig. 2:19), a signal band, between 4072 bp and 5090 bp in size, was visible in each sample lane. It was likely that these bands represented the pBK-CMV plasmid vector, which should be of 4518 bp. All vector bands produced signals on the autoradiograph films of the Southern blot hybridisation. This could be due to non-specific hybridisation. The 1 kb DNA ladder, which bands were visible on the agarose gels (Fig. 2:19), did not produce signals on the autoradiograph films of Southern hybridisation (Fig. 2:20). On the autoradiograph films of Southern hybridisation, the majority of cDNA inserts produced clear signal bands. However, some cDNA inserts, which did not produce distinct band (e.g., Lanes 10 and 20 in Fig. 2:20) when a short exposure (e.g., 23 hours) was used at –70 °C for the autoradiograph films (Fig. 2:21), became readily seen when a longer exposure (e.g., 41 hours) was used at -70 °C for the autoradiograph films (Fig 2:21). The signal intensities of cDNA inserts on the autoradiograph films of Southern blot hybridisation were grouped into 3 categories: intense, intermediate and weak signals. cDNAs producing intense, intermediate and weak hybridisation signals represented the highly,

moderately and weakly expressed mRNA transcripts, respectively. Two sample autoradiograph films of the Southern blot hybridisation are shown in Figure 2:20. Intense hybridisation signals were produced by 33 cDNA clones, which comprised 36.3% of the 91 cDNA clones evaluated. Intermediate hybridisation signals were produced by 26 cDNA clones, which comprised 28.6% of the 91 cDNA clones evaluated. Weak hybridisation signals were produced by 32 cDNA clones, which comprise the 35.2% of 91 cDNA clones evaluated (Table 2:12). The expression patterns of different types of cDNA clones demonstrated by Southern blot hybridisation was similar to that demonstrated by colony blot hybridisations (Section 2.3.1.2. of this chapter).

**Table 2:12** Results of Southern blot hybridisation

| **Signal intensity of cDNA insert on autoradiograph films** | **Number of plasmids** | **Relative abundance (percentage)** |
|---|---|---|
| Intense | 33 | 36.3% |
| Intermediate | 26 | 28.6% |
| Weak | 32 | 35.2% |
| Total | 91 | 100% |

**Figure 2:19** Restriction enzyme digestion of unselected clones with both *Eco*R I and *Xho* I prior to Southern blot hybridisation

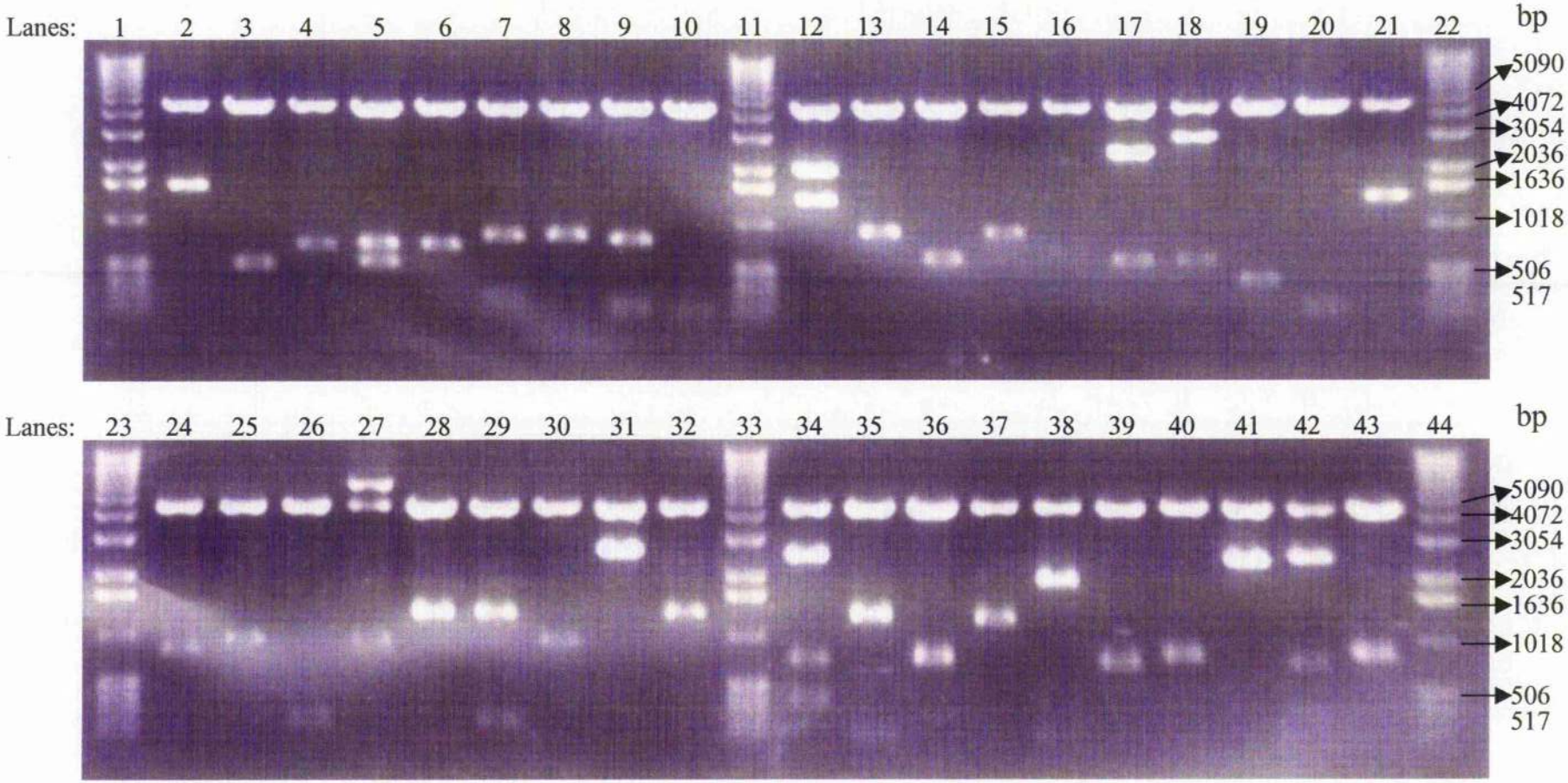


Lanes 1, 11, 22, 23, 33, and 44 were 1 kb DNA ladder. Lanes 2-10,12-21, 24-32, 34-43 were unselected recombinant DNA digested with *Eco*R I and *Xho* I, which showed the bands of plasmid DNA and inserts.

**Figure 2:20** Southern blot hybridisation using [$\alpha$-$^{32}$P] labelled cDNA probe derived from 3-day-old neonatal porcine skeletal muscle for unselected clones

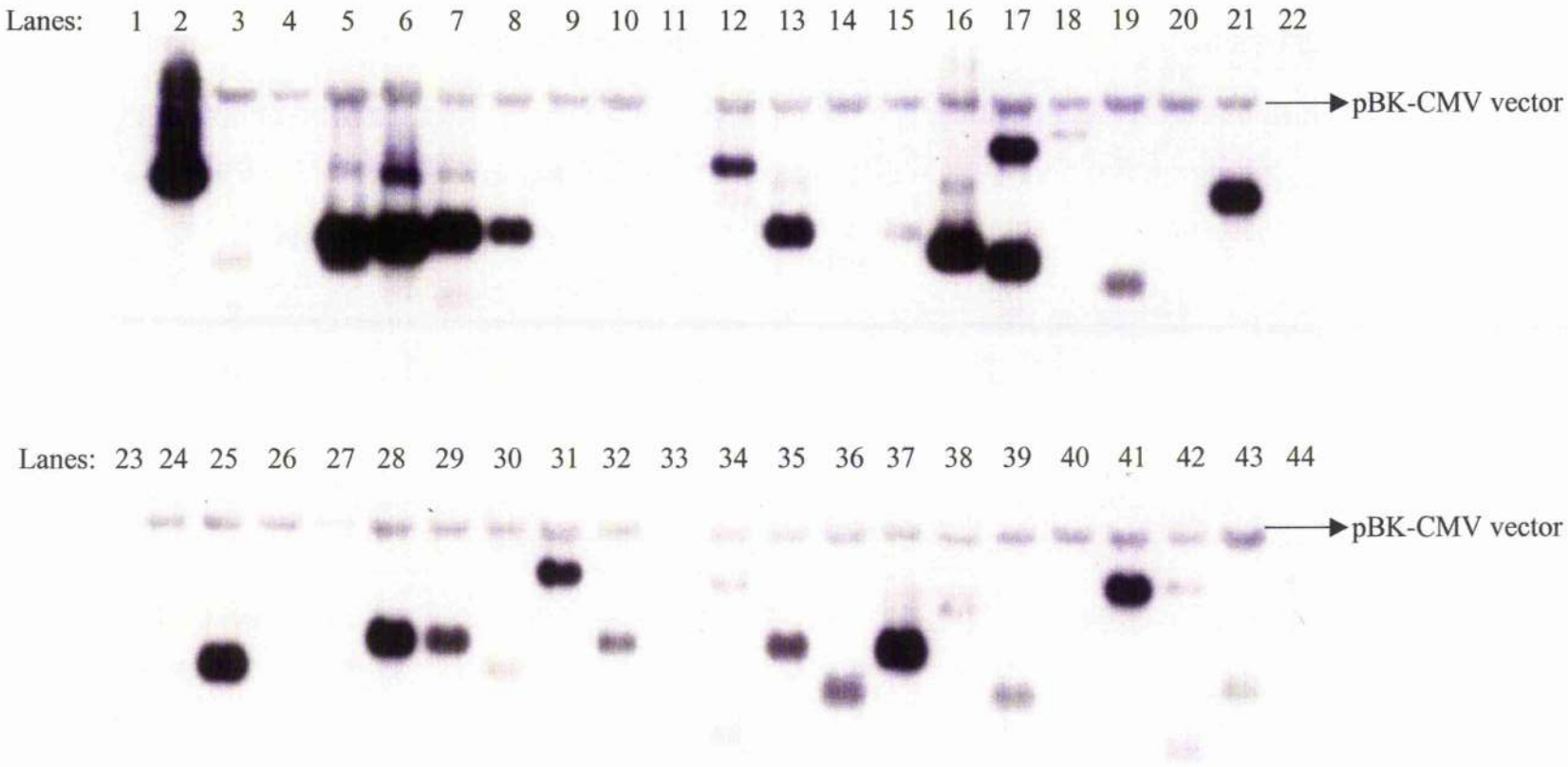


Lanes 1, 11, 22, 23, 33, and 44 were 1 kb DNA ladder. Lanes 2-10,12-21, 24-32, 34-43 were recombinant DNA digested with *Eco*R I and *Xho* I, which showed the presence of plasmid DNA and inserts. The 1 kb DNA ladder did not produce signals on the autoradiograph film of Southern hybridisation. This autoradiograph film was exposed for 23 hours at –70 °C.

**Figure 2:21** Southern blot hybridisation using [$\alpha$-$^{32}$P] labelled cDNA probe derived from 3-day-old neonatal porcine skeletal muscle for unselected clones

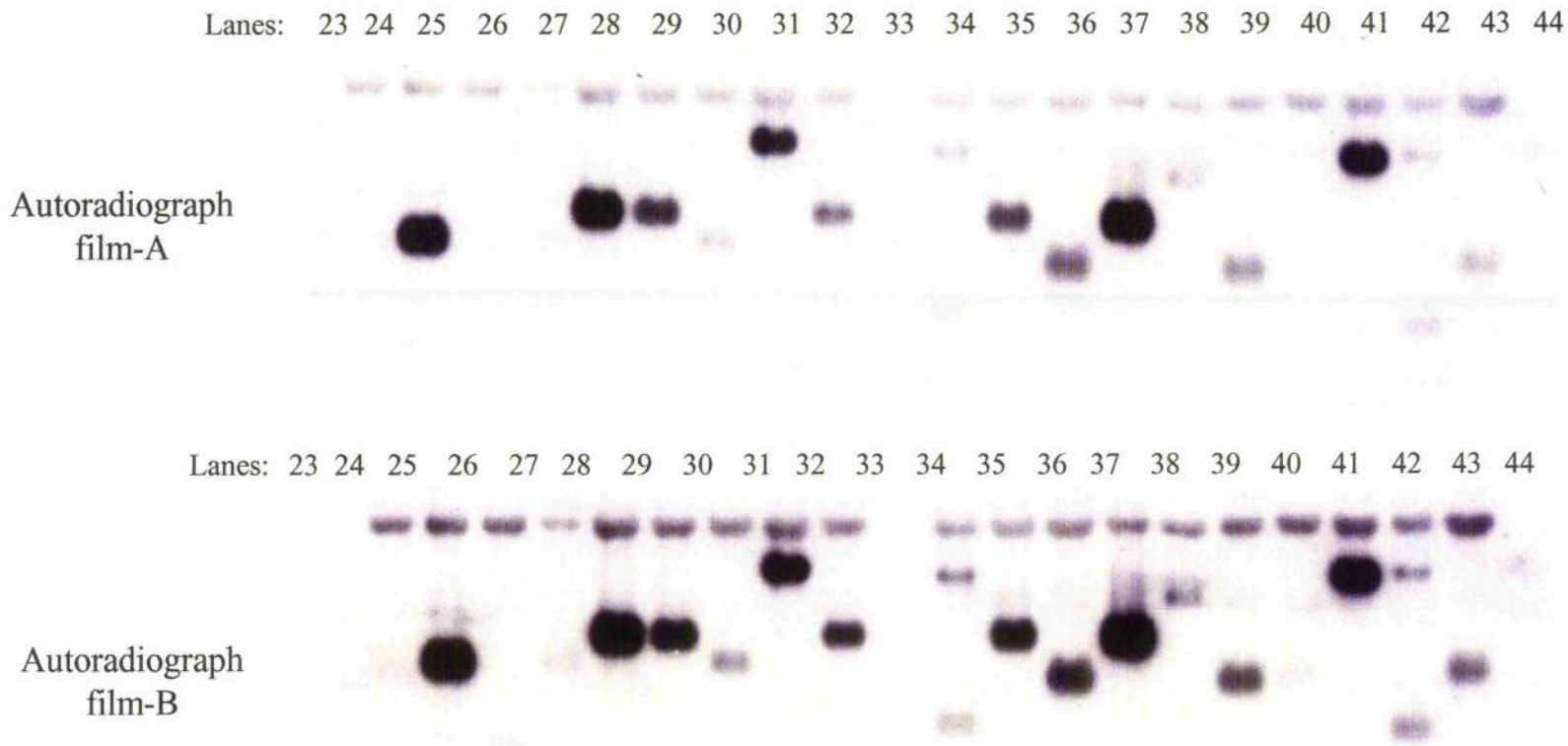


Autoradiograph film A was exposed for 23 hours at –70 °C. Film B was exposed for 41 hours at –70 °C. Bands of cDNA inserts that were very faint in Film-A can be readily seen on Film-B.

### 2.3.2.2. Sequencing of plasmid DNAs derived from selected clones

One hundred and forty cDNA fragments from the 3-day-old porcine cDNA library were sequenced to evaluate the range of genes present in the selected clones. The putative identity of each clone is listed in Table 2:13. Description of putative identity was based on the nucleotide sequence database provided by NCBI Standard nucleotide-nucleotide BLAST service. The GeneBank accession number, homology, function and property of each gene were also described in Table 2:13. The sequencing result confirmed the presence of a wide range of different genes represented by the selected clones for microarray incorporation.

Among the 140 selected cDNA clones detected by random sequencing, 65 cDNA clones appeared only once and represented 65 different genes, the majority of which were involved in various cell signalling pathways [e.g., IGF-2 (for Insulin-like Growth Factor 2), MAP3K7 (for Mitogen-Activated Protein Kinase Kinase Kinase 7), PTK9L (for Protein Tyrosine Kinase-9 like), GPS2 (for G Protein Pathway Suppressor 2), CDK2 (for Cyclin-Dependent Kinase 2), CKMT2 (for Creatine Kinase Mitochondrial 2)]. In Table 2:13, there were 18 duplicate clones representing 9 genes, which included ribosomal protein L7a, ribosomal protein S5, laminin receptor 1, cytochrome *c* oxidase subunit Vib, myosin binding protein H, cardiac alpha tropomyosin, troponin I, sarcolipin, and heat shock protein. These 9 genes were found twice, each by sequencing. There were four identical clones representing enolase 3 gene, whilst another four identical clones were found to represent skeletal alpha actin gene. There were five identical clones found to represent mitochondrion partial genome. Among the 140 cDNA clones, 11 clones were pBK-CMV plasmid vectors without cDNA insert; 15 clones were unknown cDNA sequences without clear open reading frame; 18 clones were unknown cDNA sequences with clear open reading frame that had very low homology to any information of the nucleotide databases provided by the NCBI Standard nucleotide-nucleotide BLAST services. In summary, sequencing analysis of the 140 cDNA clones gave the results of a wide range of genes representing a wide range of different gene transcripts for the microarray incorporation.

**Table 2:13** Sequencing of plasmid DNAs derived from the selected colonies

| Closest putative identity and length of fragment in base pairs | GeneBank accession # | Homology | # of clone | Functions and properties |
|---|---|---|---|---|
| Human ribosomal protein L4 (RPL4) mRNA, Length =1445 bp | BC005817 | 310/331 (93%) | 1 | Protein synthesis |
| Human ribosomal protein L6 (RPL6) mRNA, Length = 925 bp | XM_012260 | 237/260 (91%) | 1 | Protein synthesis |
| Human ribosomal protein L7a (RPL7A) mRNA, Length = 885 bp | XM_015622 | 299/334 (89%)<br>208/228 (91%) | 2 | Protein synthesis |
| Bovine ribosomal protein S28-like protein mRNA, partial cds, Length= 203 bp | AF307320 | 72/79 (91%) | 1 | Protein synthesis |
| Bovine ribosomal protein S2 mRNA, partial cds, Length = 918 bp | AF013215 | 567/663 (85%) | 1 | Protein synthesis |
| Human ribosomal protein S5 (RPS5) mRNA, Length = 706 bp | XM_009371 | 356/386 (92%) | 2 | Protein synthesis |
| Human ribosomal protein L23 (RPL23) mRNA, Length = 474 bp | XM_015407 | 382/418 (91%) | 1 | Protein synthesis |
| *Macaca fascicularis* (Monkey) ribosomal protein S11 (RPS11) mRNA, Length = 557 bp | AB093675 | 448/484 (92%) | 1 | Protein synthesis |
| Human laminin receptor 1 (ribosomal protein SA, 67kD) mRNA, (LAMR1), Length =1045 bp | BC010418<br>NM_174379 | 629/684(91%)<br>692/759 (91%) | 2 | Mediates the effects laminin |
| Bovine COX6A mRNA for cytochrome *c* oxidase subunit VIa, Length = 344 bp | X56857 | 284/309 (91%) | 1 | The enzyme cytochrome c oxidase is a transmembrane protein found in the mitochondrion. |
| Bovine mRNA for cytochrome *c* oxidase subunit VIb (AED), Length = 359 bp | X15112 | 259/274 (94%)<br>243/259 (93%) | 2 | Cytochrome c oxidase is a transmembrane protein found in the mitochondrion. |
| Porcine lactate dehydrogenase-A (LDH-A) mRNA, Length =1668 bp | U07178 | 492/495 (99%) | 1 | LDH-A catalyses the conversion of L-lactate and NAD to pyruvate and NADH in the final step of |

| | | | | |
|---|---|---|---|---|
| | | | | anaerobic glycolysis. |
| Porcine mitochondrion, partial genome, Length = 15978 bp | AF304200<br>AF304202 | 612/636 (96%)<br>316/316(100%)<br>385/400 (96%)<br>191/192 (99%)<br>457/463 (98%) | 5 | Mitochondrion partial genome |
| Porcine mRNA for myosin heavy chain 2b, Length=5929 bp | AB025261 | 229/230(99%) | 1 | Myofilament component |
| Porcine myosin light chain (MLC-1) mRNA, Length = 859 bp | X94689 | 601/614 (97%) | 1 | Myofilament component |
| Myosin binding protein H (MYBPH) mRNA, Length = 1772 bp | NM_004997<br>XM_001686 | 676/744 (90%)<br>250/288 (86%) | 2 | Binds to myosin; may be involved in interaction with thick myofilaments in the a-band. |
| Porcine skeletal alpha actin gene, Length = 5157 bp | U16368 | 254/256 (99%)<br>312/314 (99%)<br>254/256 (99%)<br>297/299 (99%) | 4 | Myofilament component |
| Human capping protein (actin filament) muscle Z-line, alpha 2 (CAPZA2) mRNA, Length = 918 bp | XM_004969 | 427/450 (94%) | 1 | Myofilament component |
| Human cardiac muscle alpha actin mRNA, Length=1549 bp | BC009978 | 269/290 (92%) | 1 | Myofilament component |
| Porcine mRNA for cardiac alpha tropomyosin, Length = 1207 bp | X66274 | 799/800 (99%)<br>499/503 (99%) | 2 | Myofilament component |
| Porcine partial mRNA for type III collagen (col3a1 gene), Length = 287 bp | AJ289758 | 75/87 (86%) | 1 | Connective tissue |
| Porcine mRNA for sarcolipin, Length = 324 bp | Z98820 | 315/324 (97%)<br>276/285 (96%) | 2 | Sarcolipin is an integral membrane protein. Sarcolipin regulates the sarcoplasmic reticulum Ca-ATPase in fast-twitch skeletal muscle. |
| Domestic rabbit mRNA for myosin light chain 2 (MLC2), type I, Length=645 bp | X54042 | 498/548 (90%) | 1 | Myofilament component |
| Human actinin, alpha 2 (ACTN2), mRNA, Length = 4161 bp | XM_002047 | 267/288 (92%) | 1 | Actin-binding protein.It is localised to skeletal muscle Z-disc and helps |

| | | | | |
|---|---|---|---|---|
| | | | | anchor myofibrillar actin filaments. |
| Domestic rabbit mRNA for troponin I, Length = 701 bp | X14190 | 352/398 (88%)<br>502/548 (91%) | 2 | Myofilament component |
| Dog triadin mRNA, Length = 2349 bp | AF165916 | 544/583 (93%) | 1 | Sarcoplasmic reticulum glycoprotein |
| Human NAC alpha mRNA (Naca muscle-specific factor), Length = 829 bp | AY034001 | 526/555 (94%) | 1 | Muscle-specific transcriptional factor |
| Human aldolase A, fructose-bisphosphate (ALDOA), mRNA, Length = 1461 bp | XM_008117 | 386/417 (92%) | 1 | Striated muscle contraction; fructose metabolism |
| Human triosephosphate isomerase (TIM), mRNA, Length = 1225 bp | XM_208215 | 93/109 (85%) | 1 | TIM is an important enzyme in the glycolytic pathway |
| Human isopentenyl-diphosphate delta isomerase (IDI1), mRNA, Length = 1807 bp | NM_004508 | 194/227 (85%) | 1 | Intramolecular oxidoreductases transposing C=C bonds;converts isopentenyl diphosphate to dimethylallyl diphosphate |
| Human heterogeneous nuclear ribonucleoprotein L (HNRPL), mRNA, Length = 2033 bp | NM_001533 | 83/87 (95%) | 1 | This protein is a component of the heterogenous nuclear ribonucleoprotein complexes, which provide substrate for the processing events that pre-mRNAs undergo before becoming functional, translatable mRNAs in the cytoplasm. |
| Domestic sheep glycogen myophosphorylase, mRNA, Length = 2869 bp | AF001899 | 422/455 (92%) | 1 | This enzyme is needed for the breakdown of glycogen. |
| Human phosphorylase kinase, gamma 1 (muscle) (PHKG1), mRNA, Length = 1377 bp | NM_006213 | 293/324 (90%) | 1 | Phosphorylase kinase is a regulatory enzyme of glycogen metabolism |
| Human enolase 3, (beta, muscle) (ENO3), mRNA, Length = 1389 bp | XM_008524<br>BC017249 | 497/550 (90%)<br>339/370 (91%)<br>352/384 (91%) | 4 | Glycolytic enzyme |

| | | | | |
|---|---|---|---|---|
| LIM and cysteine-rich domains 1 (LMCD1), mRNA,Length = 1724 bp | XM_003181 | 423/474 (89%)<br>379/416 (91%) | 1 | LIM protein is transcription factor |
| Human apolipoprotein B mRNA editing enzyme, catalytic polypeptide-like 2 (APOBEC2), mRNA, Length = 1164 bp | NM_006789 | 83/93 (89%) | 1 | Glycolysis |
| Porcine mRNA for insulin-like-growth factor 2 (IGF-2), Length = 1225 bp | X56094 | 694/709 (97%) | 1 | Cell signalling |
| Human HLA class III region containing NOTCH4 gene, partial sequence, homeobox PBX2 (HPBX) gene, receptor for advanced glycosylation end products (RAGE) gene, complete cds, and 6 unidentified cds, Length = 62944 bp | U89336 | 157/183 (85%) | 1 | Cell signalling |
| House mouse integral membrane glycoprotein (Img), mRNA, Length = 4822 bp | NM_008377 | 100/124 (80%) | 1 | An integral component of a membrane |
| Domestic rabbit elongation factor 1 A2 (EEF1A-2), mRNA, Length = 1749 bp | AF035178 | 316/328 (96%) | 1 | Eukaryotic translation |
| (1) Human integral membrane protein 2B (ITM2B), mRNA, Length = 1844 bp<br>(2) Human putative transmembrane protein E3-16, mRNA, Length = 1896 bp | (1) XM_012311<br>(2) AF136973 | 314/341 (92%)<br>314/341 (92%) | 1 | An integral component of a membrane |
| (1) Human laminin, gamma 1 (formerly LAMB2) (LAMC1), mRNA, Length = 7923 bp<br>(2) Porcine mRNA for heat shock protein 70, Length= 2518 bp<br>(3) Porcine heat shock protein 72 mRNA, Length = 1461 bp | (1) NM_002293<br>(2) X68213<br>(3) M29506 | 470/501(93%)<br>19/19 (100%)<br>19/19 (100%) | 2 | Heat shock proteins are induced when a cell undergoes environmental stresses |
| (1) Human tripartite motif protein TRIM5 isoform alpha,beta,gamma ,delta,epsilon (TRIM5) mRNA, complete cds; alternatively spliced<br>(2) Human stimulated trans-acting factor (50 kDa) (STAF50), mRNA, Length = 2809 bp | (1) AF220025-AF220029<br>(2) XM_015243 | 184/223 (82%)<br>76/83 (91%) | 1 | TRIM proteins share a common function: by means of homo-multimerisation they identify specific cell compartments. |

| | | | | |
|---|---|---|---|---|
| Human diacylglycerol kinase 3 (DAGK3) gene, exon 10, Length = 418 bp | AF020931 | 22/23 (95%) | 1 | Transcription factor |
| Human presenilin 1 (Alzheimer disease 3; apoptosis) (PSEN1), mRNA, Length = 2764 bp | XM_007441 | 287/329 (87%) | 1 | The encoded protein is predicted to be an integral membrane protein |
| Human kelch-like protein C3IP1 (C3IP1), mRNA, Length = 2013 bp | XM_010659 | 373/404 (92%) | 1 | Protein-protein interaction |
| Porcine mRNA for heparin-binding epidermal growth factor-like protein, Length = 627 bp | Y15731 | 425/437 (97%) | 1 | Cell signalling |
| Human ankyrin 1, erythrocytic (ANK1), mRNA, Length = 1179 bp | XM_011727 | 364/408 (89%) | 1 | Attach integral membrane proteins to cytoskeletal elements |
| (1) Human upregulated by 1,25-dihydroxyvitamin D-3 (VDUP1), mRNA, Length = 2688 bp<br>(2) Mouse thioredoxin interacting factor (Vdup1) gene, Length = 5529 bp | (1) XM_002093<br>(2) AF282825 | 152/162 (93%)<br>152/167 (91%) | 1 | Stress response gene, which could have a unique role in epidermis regulating the conversion of postmitotic cells to differentiating ones. |
| *Lynx lynx* (wild feline) H19 RNA gene, partial cds, Length = 879 bp | AF190056 | 166/195 (85%) | 1 | Not clear |
| Human cyclin-dependent kinase 2 (CDK2), mRNA, Length = 1297 bp | NM_001798 | 182/198 (91%) | 1 | Cell signalling; Transcription factor |
| Human creatine kinase, mitochondrial 2 (sarcomeric) (CKMT2), mRNA,Length = 1585 bp | XM_011329 | 405/459 (88%) | 1 | Transcription factor |
| Human seven transmembrane domain protein mRNA, Length = 878 bp | BC001118 | 476/514 (92%) | 1 | Cell signalling |
| (1) Porcine adenine nucleotide translocator 1 (ANT1) gene, exons 2 and 3, partial cds, Length = 1042 bp<br>(2) Bovine ADP/ATP translocase T1 mRNA, Length = 1194 bp | (1)AF055633<br>(2)M24102 & J02845 | 145/145(100%)<br>322/335 (96%) | 1 | Adenine nucleotide translocase (ANT) is responsible for the stoichiometric exchange of ATP and ADP across the inner mitochondrial membrane. |
| Human apoptosis inhibitory protein 5, | XM_208445 | 235/287 (81%) | 1 | Inhibit apoptosis |

| | | | | |
|---|---|---|---|---|
| mRNA, Length = 3665 bp | | | | |
| Human mitogen-activated protein kinase kinase kinase 7 (MAP3K7), mRNA, Length = 2769 bp | XM_004499 | 348/371 (93%) | 1 | MAP3K7 is involved in JNK signal transduction pathway. |
| Human zinc finger protein 259, mRNA, Length = 1199 bp | XM_018293 | 452/501 (90%) | 1 | Transcription factor |
| Human protein tyrosine kinase 9-like (A6-related protein) (PTK9L), mRNA, Length = 1574 bp | XM_003237 | 395/434 (91%) | 1 | Transcription factor |
| Human G protein pathway suppressor 2 (GPS2), mRNA, Length = 1189 bp | NM_004489 | 530/576 (92%) | 1 | G protein pathway suppressor |
| (1) Human long form transcription factor C-MAF (c-maf proto-oncogene) mRNA, complete cds, Length = 2145 bp<br>(2) Human v-maf musculoaponeurotic fibrosarcoma (avian) oncogene homolog (MAF), mRNA, Length = 2145 bp | (1) AF055377<br>(2) NM_005360 | 279/287 (97%)<br>279/287 (97%) | 1 | Oncogene |
| Porcine glyceraldehyde 3-phosphate dehydrogenase (GAPDH), mRNA, Length = 1419 bp | AF017079 | 318/330 (96%) | 1 | Mammalian GAPDH is involved in membrane fusion, microtubule bundling, phosphotransferase activity, nuclear RNA export, prostate cancer progression, programmed neuronal cell death, DNA replication, and DNA repair. |
| Domestic rabbit pyruvate kinase mRNA, partial cds, Length = 1593 bp | U44751 | 342/374 (91%) | 1 | Pyruvate kinase is an enzyme that helps in the conversion of glucose to energy when there is not adequate oxygen. |
| (1) Human calmodulin 1 (phosphorylase kinase, delta) (CALM1) mRNA, Length = 1525 bp<br>(2) Human, calmodulin 2 (phosphorylase kinase, delta), mRNA, Length= 1058 bp | (1)XM_00738 5<br>(2)BC000454 | 302/326 (92%)<br>301/326 (92%) | 1 | Transcription factor |

| | | | | |
|---|---|---|---|---|
| Porcine gene for skeletal muscle ryanodine receptor (RyR1), Length = 29699 bp | X69465 | 184/199 (92%) | 1 | The ryanodine receptor is the channel responsible for the release of calcium from the sarcoplasmic reticulum in muscle cells. |
| (1) Porcine rotavirus mRNA for RGD-containing collagen associated protein, Length = 2819 bp<br>(2) Human transforming growth factor, beta-induced, 68kDa (TGFBI), mRNA, Length = 2691 bp | (1) D55717<br>(2) NM_000358 | 484/501 (96%)<br>97/112 (86%) | 1 | (1) Porcine rotavirus mRNA<br>(2) transcription factor |
| Bovine low molecular mass ubiquinone-binding protein mRNA, Length = 681 bp | L06665 | 301/332 (90%) | 1 | Ubiquinone-binding protein |
| House mouse casein kinase 2 beta subunit (gMCK2) gene, partial cds. | AF109719 | 100% | 1 | Transcription factor |
| House mouse adult male kidney cDNA, RIKEN full-length enriched library, clone:0610010G04, full insert sequence, Length = 993 bp | AK002470 | 184/214 (85%) | 1 | Not clear |
| Human mRNA for KIAA0353 gene, partial cds, Length = 6651 bp | AB002351 | 297/367 (80%) | 1 | The protein encoded by this gene is an intermediate filament family member, which forms a linkage between desmin and the extracellular matrix, and provides an important structural support in muscle. |
| Human CGI-92 protein (LOC51117), mRNA, Length= 1548 bp | NM_016035 | 320/363 (88%) | 1 | Ubiquinone biosynthesis protein |
| Human upregulated by 1,25-dihydroxyvitamin D-3 (VDUP1), mRNA, Length = 2704 bp | NM_006472 | 387/420 (92%) | 1 | An stress response gene |
| Human, clone MGC: 2198, mRNA, Length = 657 bp | BC000587 | 221/259 (85%) | 1 | Not clear |
| Human myomesin (M-protein) 2 (MYOM2) mRNA,Length = 4921 bp | XM_005198 | 159/180 (88%) | 1 | 165 kDa titin-associated protein |
| Human C9orf10 protein (C9orf10: | XM_011758 | 435/487 (89%) | 1 | Not clear |

| | | | | |
|---|---|---|---|---|
| chromosome 9 open reading frame10) mRNA, Length = 3331 bp | | | | |
| Human hypothetical protein HSPC152 (HSPC152), mRNA, Length = 612 bp | NM_016404 | 302/356 (84%) | 1 | Not clear |
| (1) Bovine BAP 1 mRNA, Length = 1367<br>(2) Human APEX nuclease, clone MGC:4057 IMAGE:2823545, mRNA, Length = 1450 bp | (1) X56685<br>(2) BC019291 | 832/917 (90%)<br>733/821 (89%) | 1 | Human APEX nuclease is a multifunctional DNA repair enzyme. |
| House mouse mRNA for hypothetical protein (ORF1) clone Telethonin (Italy_B41)_Strait03708_FL626, Length=905 bp | AJ277212 | 128/143 (89%) | 1 | Not clear |
| cDNA sequences (with clear open reading frame) that had very low homology to any information of the nucleotide databases provided by the NCBI Standard nucleotide-nucleotide BLAST services. | None | Not Match | 18 | Not clear |
| cDNA sequences (without clear open reading frame) that had very low homology to any information of the nucleotide databases provided by the NCBI Standard nucleotide-nucleotide BLAST services | None | Not Match | 15 | Not clear |
| Shuttle expression vector pBK-CMV, Length = 4518 bp (Plasmid DNA without insert) | U37573 | 100% homology | 11 | pBK-CMV plasmid vector |

"cds" is abbreviated from "coding sequence"; "bp" is abbreviated from "base pairs"

### 2.3.2.3. Dot blot hybridisation

The efficiency of the clone selection was assessed by dot blot hybridisation, which was performed to compare 96 plasmid DNAs extracted from the selected colonies with 96 plasmid DNAs extracted from the unselected colonies. All cDNA inserts in the plasmids for dot blot

hybridisation were derived from the 3-day-old porcine cDNA library. On the autoradiograph films of the dot blot hybridisation, much less number of intense signals (dark spots) appeared in the hybridisation image of selected clones than in the hybridisation image of unselected clones (Fig. 2:22). These intense signals (dark spots) represented cDNA inserts converted from highly expressed mRNA transcripts. The reduction in the number of intense signals in the hybridisation image of selected clones indicated that the clone selection method had substantially reduced cDNAs representing highly expressed genes and consequently increased the number of cDNAs representing weakly and moderately expressed genes.

#### 2.3.2.4. Microarray hybridisation using Cy3 labelled T7 primer target

Effectiveness of the microarray printing process was evaluated by microarray hybridisation with the Cy3 labelled T7 primer target. The fluorescent image of every single hybridised microarray cDNA spot, which was obtained by scanning the hybridised microarray slide, was round, clear and bright (image not shown). The signal intensities of all hybridised cDNA spots printed on the microarray slide were similar. This image indicated that all the printed cDNA fragments, which had previously been amplified using T7 and T3 primers, hybridised successfully with the Cy3 labelled T7 primer. The result of this single-colour (Cy3) microarray hybridisation confirmed that all the cDNA fragments obtained for microarray incorporation were effectively printed and immobilised onto the surface of the Corning CMT-GAPS™ Coated slides.

#### 2.3.2.5. Dual-colour microarray hybridisation

Following microarray printing, one of the completed microarray slides was evaluated by cohybridisation of Cy3 labelled cDNA target derived from 91-day-old porcine foetal *longissimus dorsi* muscle and Cy5 labelled cDNA target derived from porcine kidney. The scanned image was processed using ImaGene™ v4.2 (BioDiscovery) computational software to show the two colour (red and green) fluorescent image (Fig. 2:23). Microarray cDNA spots, which hybridised with both Cy3 labelled targets and Cy5 labelled targets, were yellow or orange in colour. The result of this dual-colour (Cy3 and Cy5) microarray hybridisation showed that the cDNA microarray constructed in this study was appropriate for simultaneous hybridisation with the mixture of Cy3 labelled and Cy5 labelled targets.

**Figure 2:22** Dot blot hybridisation of both selected and unselected plasmid clones with 3-dayold neonatal porcine skeletal muscle total cDNA probe

Picture A: Unselected

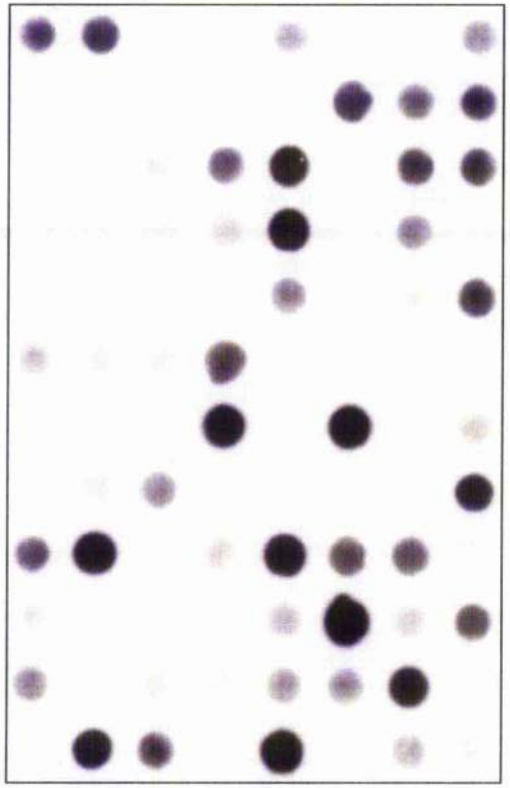

Picture B: Selected

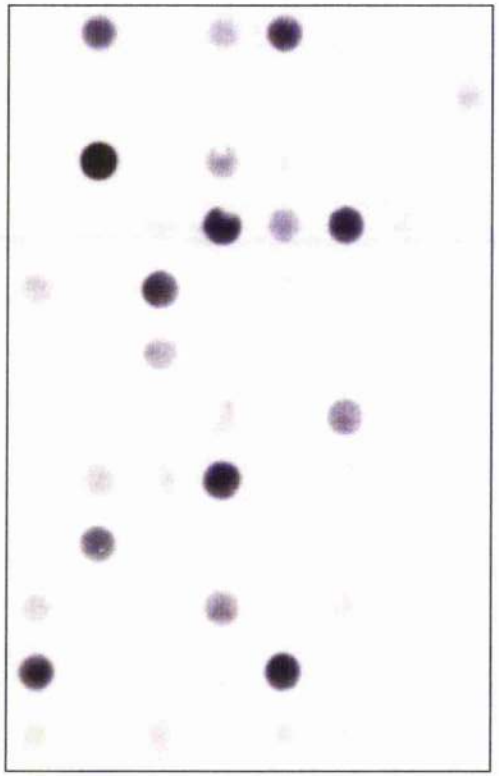

Picture A shows the dot blot hybridisation of unselected plasmid clones. Picture B shows the dot blot hybridisation of selected plasmid clones. Both unselected and selected clones were subjected to the 3-day-old porcine neonatal skeletal muscle total cDNA probe.

**Figure 2:23 Dual-colour microarray hybridisation for monitoring microarray printing process**

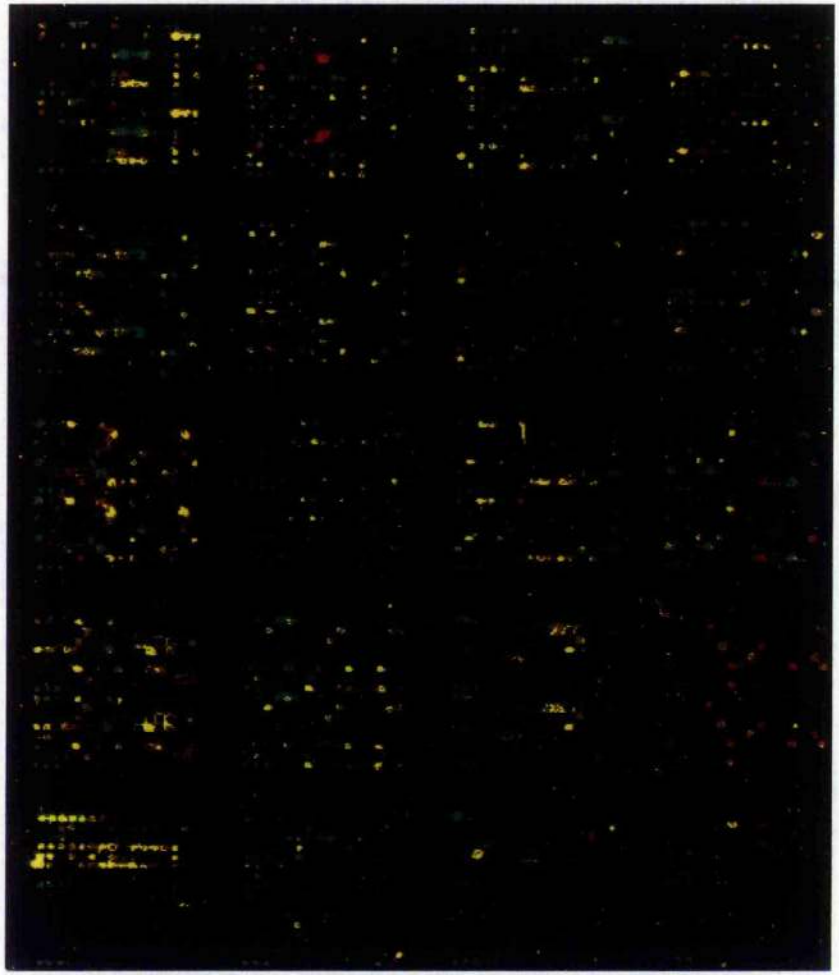

- 91-day porcine foetal skeletal muscle cDNA target was labelled with the red colour Cy3
- Porcine kidney cDNA target was labelled with the green colour Cy5

# 2.4. DISCUSSION

## 2.4.1. CONSTRUCTION OF THE PORCINE SKELETAL MUSCLE cDNA MICROARRAY

An ordinary array design starts with identification of genes to be arrayed. Selecting the right genes and clones to represent these genes is crucial to successful use of in-house designed microarrays. In most cases, sequence information of gene collections for array assembly is obtained from public, proprietary or subscription databases such as human division of UniGene, primate division of GeneBank, etc. Most cDNA microarrays are developed based on DNA fragments with known sequence information. However, at the initial array design stage of this study, sufficient sequence information on porcine skeletal muscle was not available. It was not possible to build an oligonucleotide microarray or a cDNA microarray by adopting conventional approaches. To resolve the problem of lack of necessary sequence information, this study sought to develop a cDNA microarray, the establishment of which was completely based on the selection of unknown cDNA fragments derived from either prenatal or postnatal porcine skeletal muscle cDNA libraries. The two cDNA libraries were chosen for use because understanding alterations of expression patterns of thousands of genes in different developmental stages is critical for enhancing current knowledge of molecular mechanisms involved in skeletal muscle development, ageing, regeneration and degeneration, which remain elusive at this time. In this study, sequencing all the unknown cDNA fragments to be arrayed was deemed impractical because the necessary efforts would have been too long and the cost too high. The non-normalised cDNA libraries used in this study for microarray assembly posed the problem of clone redundancy. Colony hybridisations and the clone selection effectively reduced this problem to a large extent. To date, gene identities of a large number of these arrayed clones have already been obtained by sequencing.

First-hand experience has been gained from this study to enable improvements on the methods used for creating the porcine skeletal muscle cDNA microarray. For example, the clone tracking system included in the microarray construction process had not been established until the microarray printing was finished. Owing to lack of practical experience, the importance of building a clone tracking system at a much earlier stage had not been fully realised when the sequencing efforts had been made as quality assurance for identifying 140 cDNA inserts, which

were later used for the microarray incorporation. The clone tracking system was not established for the 140 cDNA fragments. Consequently, it is impossible to correlate the sequence information on the 140 DNA fragments with spot locations on the completed porcine cDNA microarray. One other experience was also gained during the colony hybridisation and clone selection process for the microarray assembly. The porcine cDNA fragments, ranging from approximately 100bp to 3kb, were labelled with [$\alpha$-$^{32}$P] using random primers and used as radioactive probes subjected to colony hybridisation for clone selection based on signal intensities on autoradiograph films. cDNA to be labelled was first denatured and then mixed with oligonucleotides of random sequence in the presence of [$\alpha$-$^{32}$P] labelled nucleotide(s) and DNA polymerase. These "random oligos" annealed to complementary random sites on the DNA and serve as primers for DNA synthesis during which [$\alpha$-$^{32}$P] label was incorporated. More [$\alpha$-$^{32}$P] label was incorporated into longer cDNA fragments than into shorter cDNA fragments. Therefore, when a long cDNA fragment and a short cDNA fragment, which had similar gene expression levels, were hybridised with their complementary cDNA fragments labelled with [$\alpha$-$^{32}$P], stronger signals were seen for the longer cDNA fragments on autoradiograph films, whilst weaker hybridisation signals were obtained for the shorter cDNA fragments. As colony selection was based on signal intensities, some cDNA fragments representing lowly expressed genes must have been left out by the colony selection process. Because of the nature of the colony selection process, this phenomenon is deemed unavoidable. The results obtained during this study were similar to those described in a published literature which showed that, in human adult skeletal muscle, the abundance of weakly expressed genes accounts for 63.5% of the total genes, while moderately expressed and highly expressed genes account for 27.4% and 9.1% of the total genes respectively (Bortoluzzi et al., 2000).

Apart from the experimental knowledge established, different versions of the microarray construction process could have been adopted for a similar outcome. In order to increase the frequency of occurrence of rare cDNA clones while decreasing the percentage of abundant cDNAs in the two porcine skeletal muscle cDNA libraries, subtraction normalisation by suppression PCR, or normalisation without subtraction, which is based on re-association kinetics can be alternative methods of colony selection (Rink et al., 2002;Patanjali et al., 1991;Soares et al., 1994). The approach of subtraction normalisation by suppression PCR (also called subtractive suppression hybridisation) depends on hybridisation selection with genomic DNA so that the relative abundance of cDNAs would be proportional to the abundance of genes

complementary to that cDNA in genomic DNA (Byers et al., 2000;von Stein, 2001). However, this method was deemed less suitable for microarray clone selection because of its potential to exclude lowly expressed non-muscle specific clones. The re-association reaction kinetics approach, which is by reassociation of single-stranded library plasmids at relatively low $C_0t$ [initial concentration of DNA (mol of nucleotide per litre) × time (sec)] to remove highly expressed clones, depends on the observation that if cDNA reannealing follows second-order kinetics, rarer species will anneal less rapidly and the remaining single-stranded fraction of cDNA will become progressively more normalised during the course of the hybridisation.

## 2.4.2. DIVERSITY AND REDUNDANCY OF CLONES INCORPORATED IN THE PORCINE SKELETAL MUSCLE cDNA MICROARRAY

The approach of colony selection based on mRNA relative abundance, although laborious, has the capability of reducing the repetition of colonies representing highly expressed genes for microarray incorporation. Sequencing of 140 plasmid DNAs derived from the selected colonies contributed to the assurance that the colony selection was appropriate for obtaining diverse cDNA fragments, which represented a broad range of different genes. These genes, including both the skeletal-muscle-specific gene transcripts and transcripts expressed in other tissues. Although the redundancy in the constructed novel microarray was diminished by eliminating multiple cDNA clones belonging to the same transcript, repetition of some genes (e.g. porcine skeletal alpha actin gene, porcine beta-globin gene) was evident in the sequencing results presented in Table 2:14.

## 2.4.3. IMPORTANCE AND NECESSITY OF THE QUALITY ASSURANCE PROCESS

The fabrication of microarray in this study included two processes: the main construction process and the associated quality assurance process. Due to practical limitation, the main construction process was set up with the aim of incorporating 5,000 to 6,000 cDNAs in the microarray. Ideally, this desired number of cDNAs is expected to represent 5,000 to 6,000 different genes, so that the microarray can be highly representative. However, because no sequence information was available on any cDNA insert derived from the two muscle libraries that were used for the

construction, it was unlikely to avoid the presence of some repeat cDNAs in the microarray. The efficiency of colony selection detected through dot blot hybridisation for quality assurance has contributed in part to the success of this construction project. Although the quality assurance steps including restriction enzyme digestion and/or agarose gel electrophoresis were not always included in other construction protocols, it was conducted resolutely in this study on 8,250 samples from three stages (plasmid DNA extractions, PCR reactions and PCR purifications) to monitor the presence of cDNAs in order to complete the microarray of a high quality. Once the cDNAs were printed on slides, hybridisation detection with the Cy3 labelled T7 primer target was used to monitor the printing process. The two-colour (Cy3 and Cy5) microarray hybridisation was used as a first evaluation on the functionality of the microarray.

### 2.4.4. ADVANTAGES AND WEAKNESSES OF THE MICROARRAY CONSTRUCTED IN THIS STUDY

The porcine skeletal muscle cDNA microarray fabricated in-house in this study is the first of its kind. This microarray, in common with many other cDNA microarrays obtained commercially, has a most important advantage of accurately measuring changes in expression levels of a large number of mRNA transcripts in tissues or cells. A major advantage of the *de novo* constructed microarray is the possession of potential full-length cDNA clones, whose inserts were unidirectionally cloned into a CMV-promoter driven expression plasmid (pBK-CMV vector). These clones could be readily used for downstream expression studies. Another advantage of this microarray is the good maintenance and accurate curation of extensive clone stocks for microarray fabrication and gene identification. The clone sets were categorised as concentrated plasmid DNA, diluted plasmid for DNA synthesis by PCR, and purified PCR products. Clones classified into different category were differently labelled whilst all sets of stocks were kept in microtitre plates at -20°C with unique identity for each sample. This system makes it possible to trace the locations of immobilised cDNA on microarray slides back to the correct plasmids or purified PCR products, in microtitre plate. Gene identification could be double-checked with different category of stocks to avoid any possible mix-ups. The clone stocks for the microarray construction can potentially provide several hundred fabricated slides that would be sufficient for various downstream works in skeletal muscle research.

A possible disadvantage of the constructed porcine microarray, at least at the beginning, is the lack of knowledge of the sequence identity of each clone. However, there is, at present, insufficient sequence information on farm animals to design a comprehensive oligonucleotide-based microarray. As the sequence identity of each clone is largely unknown, it is not known for certain how representative the porcine skeletal muscle cDNA microarray is. On the one hand, considering that there might be fewer than 30,000 human genomic DNAs (Venter et al., 2001), and assuming that 50% of all genes are transcriptionally active at one time in a given tissue (Bortoluzzi et al., 2000), it is possible that around 20% of the genes that are expressed in skeletal muscle are found on the constructed microarray (Pietu et al., 1999;Venter et al., 2001). On the other hand, a group of 4080 human skeletal muscle genes, which included both skeletal muscle-specific genes and genes expressed in skeletal muscle as well as in other tissues, was found to correspond to 80% of the total number of genes expressed in skeletal muscle as reported so far in Unigene (including foetal muscle and rhabdomyosarcoma) (Bortoluzzi et al., 2000). Hence the constructed microarray in this project may represent substantially more than 20% of all genes expressed in porcine muscle.

## 2.4.5. POTENTIAL IMPROVEMENTS TO THE MICROARRAY CONSTRUCTED IN THIS STUDY

Future investigations into gene expression patterns will require microarrays with cDNA collections covering most if not all genes expressed in porcine skeletal muscles. In order to improve the in-house constructed novel microarray for future studies, more recombinant clones, containing weakly and moderately expressed cDNAs, can be selected to expand the range of different genes represented in the microarray. Continuing effort is being made to identify, by sequencing analysis, all the cDNA fragments incorporated in the current microarray. Moreover, genes derived from other developmentally distinct porcine skeletal muscle cDNA libraries (e.g. porcine foetus younger than 50 days, and old pigs) can also be included in this microarray.

## 2.4.6. POTENTIAL APPLICATIONS OF THE MICROARRAY AND ITS ASSOCIATED CLONE STOCKS

The porcine cDNA microarray constructed *de novo* in this study has a wide range of potential applications in both industrial and academic research. Industrial research, in which the porcine microarray can be used, includes meat quality control for food production, animal selection for breeding, and the effects of nutrition on the amount and type of fat in meat. For example, the porcine microarray can be used to characterise expression levels of known and unknown genes that associate with particular muscle quality traits, such that specific type of animals can be selected based on levels of gene expression. Comprehensive gene expression analysis with the porcine microarray can potentially provide valuable information about various biological processes, such as alterations in skeletal muscle structure and function as consequences of different stimuli that modify skeletal muscle contractile activity, changes in gene expression under different metabolic status (e.g., different hormone treatment; different type of nutrition), differences at the molecular level between normal and diseased skeletal muscle tissues, and among patients. The transcriptional signalling pathways and the differential gene expression evens involved in these processes can be further recognised using the porcine microarray. Potential utilisation of the porcine microarray also includes the development and validation of new drugs for treatment of skeletal muscle diseases, the identification of drug targets by profiling gene expression of diseased skeletal muscle, and examination of drug side effects on skeletal muscle (e.g. drug toxicity). Therefore, with the porcine skeletal muscle cDNA microarray, the response of a large percentage of the skeletal muscle genome to exercise training, inactivity, and drug treatment is expected to be further characterised.

# CHAPTER THREE

# DIFFERENTIAL GENE EXPRESSION IN RED AND WHITE PORCINE SKELETAL MUSCLES

# 3.1. INTRODUCTION

Skeletal muscle is composed of heterogeneous fibre types that vary in contraction velocity, endurance capability, and metabolic enzyme profile. Skeletal muscle also displays a remarkable ability to adapt at the gene level to alter its structure in response to the demand placed on muscle. Two extremes of skeletal muscle phenotype are the red, oxidative, slow twitch muscle, usually employed in a postural role, and the white, glycolytic, fast twitch muscle, which generally has a locomotive role (Pette and Staron, 1990;Schiaffino and Reggiani, 1996). The physiological differences between red and white muscle have been reviewed in chapter one. The molecular mechanisms underlying these differences have so far not been fully discovered. Understanding the molecular processes that regulate skeletal muscles fibre-type is of agricultural and medical importance. In agriculture, for example, because skeletal muscle fibre characteristics are key determinants of meat quality, molecular insights into factors that affect pig muscle traits are necessary for developments to improve meat quality and production (Essén-Gustavsson, 1993;Karlsson et al., 1999). In medicine, for example, the metabolic profile of red and white muscle may show the development and progression of chronic disease. Individuals with a higher percentage of red fibres are less likely to have chronic metabolic syndromes, such as insulin resistance (Hickey et al., 1995; Kriketos et al., 1996), glucose intolerance (Toft et al., 1998), type 2 diabetes (Nyholm et al., 1997), obesity (Helge et al., 1999; Kriketos et al., 1997; Storlien et al., 1996), and a blood lipid profile associated with an increased risk of cardiovascular disease (Tikkanen et al., 1991). The ability to study gene expression differences with DNA microarrays may enable researchers to determine those genes responsible for the diversity of muscle fibre composition. The main purpose of the study of red and white muscle microarray analysis was to detect the effectiveness of the novel porcine skeletal muscle cDNA microarray for high throughput gene expression profiling. The study aims to develop a gene expression profile of white and red muscles in pigs to gain a better understanding of gene regulation that underlies the differences between muscle fibre types.

# 3.2. MATERIALS AND METHODS

## 3.2.1. MATERIALS

### 3.2.1.1. Porcine tissues

The red and white muscle microarray differential gene expression analysis was carried out using the *psoas* muscle, which was red muscle, and the *longissimus dorsi* (LD) muscle, which was white muscle, of a 22-week-old Berkshire pig named pig 130. Previous study demonstrated that over 90% of *psoas* muscle fibres were red muscle fibres (da Costa et al., 2002;da Costa et al., 2003), whilst over 90% of *longissimus dorsi* muscle fibres were white muscle fibres (da Costa et al., 2002;da Costa et al., 2003). *Psoas* muscles and *longissimus dorsi* muscles taken from another three 22-week-old Berkshire pigs (pig 1, pig 2, and pig 3) were used in real-time quantitative reverse transcription polymerase chain reaction (RT-PCR) for validation of expression levels of specific genes, which were identified as differentially expressed in the microarray analysis. These four pigs (pig 130, pig 1, pig 2, pig 3) were intact males reared under identical husbandry and feeding conditions. These pigs were individually fed (20% protein, 14 megajoules/digestible energy/kg with 1.14% lysine) twice a day at 90% of the predicted adlib feed intake based on body weight. Each type of muscle was sampled from the same anatomical sites of each animal within 30 minutes of slaughter, frozen in liquid nitrogen, and stored at -80°C until further processing (da Costa et al., 2002;da Costa et al., 2003). In addition, eight different porcine tissues including *psoas* muscle, *longissimus dorsi* muscle, heart, brain, uterus, kidney, liver and spleen were taken from of a 7-weeks-old commercial hybrid pig (pig 4) from a local farm. These eight different porcine tissues were used in real-time quantitative RT-PCR for examination of expression levels of specific genes in these tissues.

### 3.2.1.2. Commercial kits, reagents and software

Most of the commercial kits and reagents used in this study are detailed in Table 3:1. Other materials used have been listed in chapter two, or are described under "Methods" below. Commercial software used in this study is detailed in Table 3:2. The ImaGene™ version 4.2 software (BioDiscovery) was used for automating the process of measuring and visualising gene expression level in microarray image analysis. The GeneSpring™ version 4.2 software (Silicon Genetics) was used for performing statistics and ratio operations in microarray data mining. The ABI PRISM™ Primer Express version 1.5 software (Applied Biosystems) was used for designing primers and probes used in real-time quantitative RT-PCR.

**Table 3:1** Commercial kits and reagents

| **Commercial kit and chemical reagent** | **Use of the kit** |
|---|---|
| Dynabeads® mRNA DIRECT™ kit (Dynal LTD) | mRNA extraction from skeletal muscle tissues or cells |
| CyScribe First-Strand cDNA labelling kit (Amersham Pharmacia Biotech) | Synthesis and cyanine dye labelling of single-stranded cDNA |
| Micro Bio-Spin® Chromatography Columns (BIO-RAD Laboratories) | Purification of nucleic acids and proteins (In this study, these columns were used during the calcineurin cellular activity assay.) |
| AutoSeq G-50 columns (Amersham Pharmacia Biotech) | Purification of cyanine dye labelled target cDNAs prepared for microarray hybridisation. |
| GIIB-200 2× microarray hybridisation buffer (Genpak) | Microarray hybridisation. |
| TaqMan® Universal PCR Master Mix (Applied Biosystems, Roche) | Real-time quantitative RT-PCR amplification. |
| ABI Prism BigDye Terminator v3.0 Cycle Sequencing Reaction Kit (Applied Biosystems) | Sequencing PCR. |
| Performa® DTR (Dye Terminator Removal) Gel Filtration Cartridge | Removing dye terminators, dNTPs, and other low molecular weight materials from sequencing reactions before loading PCR products onto ABI PRISM™ 3100 Genetic Analyser for sequencing. |

**Table 3:2** Software used in microarray expression analysis and real-time quantitative RT-PCR

| **Software** | **Use of software** | **Manufacturer** |
|---|---|---|
| ImaGene™ version 4.2 | For automating the process of measuring and visualising gene expression level in microarray image analysis | BioDiscovery, Inc. |
| GeneSpring™ version 4.2 | For performing statistics and ratio operations in microarray data mining | Silicon Genetics |
| ABI PRISM™ Primer Express version 1.5 | For designing primers and probes used in real-time quantitative RT-PCR | Perkin Elmer, Applied Biosystems |

## 3.2.2. METHODS

The experimental design (Figures 3:1 and 3:2) of this study was to use mRNAs from skeletal muscle tissues to generate fluorescent dye labelled cDNA samples (termed targets), which were subsequently hybridised to the cDNA sequences (termed probes) of the porcine cDNA microarray. The hybridisation images were processed, and the data was normalised and analysed.

### 3.2.2.1. Preparation of target cDNA samples for microarray hybridisation

#### *3.2.2.1.1. First strand cDNA synthesis and fluorescent dye labelling*

All skeletal muscle samples used for isolation of mRNA were frozen in liquid nitrogen. Red muscle (*psoas* muscle) and white muscle (*longissimus dorsi* muscle) mRNAs were extracted separately from pig130 using Dynabeads® mRNA DIRECT™ kit (Figures 3:1 and 3:3). The mRNA extraction was as described in chapter two (section *2.2.2.2.2.*). At the beginning of each mRNA extraction, 50 mg frozen skeletal muscle tissue was weighed, homogenised and used for the extraction. At the final stage of each mRNA extraction, 21 µl of 10 mM Tris-HCl (pH 7.5) was used to elute the mRNA from the Dynabeads® oligo $(dT)_{25}$. Concentration of the 21 µl mRNAs from each extraction reaction was estimated to be about 20-25 ng/µl by comparing 1 µl extracted mRNA with 1 µl 50 ng/µl 1 kb ladder DNA on agarose gel containing ethidium bromide (Fig. 3:3). Single-stranded cDNA synthesis and target labelling were performed on red and white muscle mRNAs using a CyScribe First-Strand cDNA labelling kit (Amersham Pharmacia Biotech). To anneal the oligo(dT) and random nonamer primers to muscle mRNA, 9 µl (about 180-225 ng) muscle mRNA, 1 µl random nonamers and 1 µl anchored oligo(dT) were added into a sterile ribonucleases-free 1.5 µl microcentrifuge tube, and mixed gently by pipetting up and down. The mixture was incubated at 70°C for 5 minutes in a water bath (Grant Instruments Ltd), and then left at room temperature for 10 minutes to allow random nonamer primers to anneal to the mRNA template. The mixture was then centrifuged for 30 seconds using a Heraeus Biofuge Pico microcentrifuge. Following annealing step, 4 µl CyScript buffer (5× concentration), 2 µl 0.1 M dithiothreitol (DTT), 1 µl dCTP CyDye-labelled nucleotide, 1 µl nucleotide mix and 1 µl CyScript reverse transcriptase were added to the annealed

**Figure 3:1** Steps taken for the red and white muscle microarray hybridisation

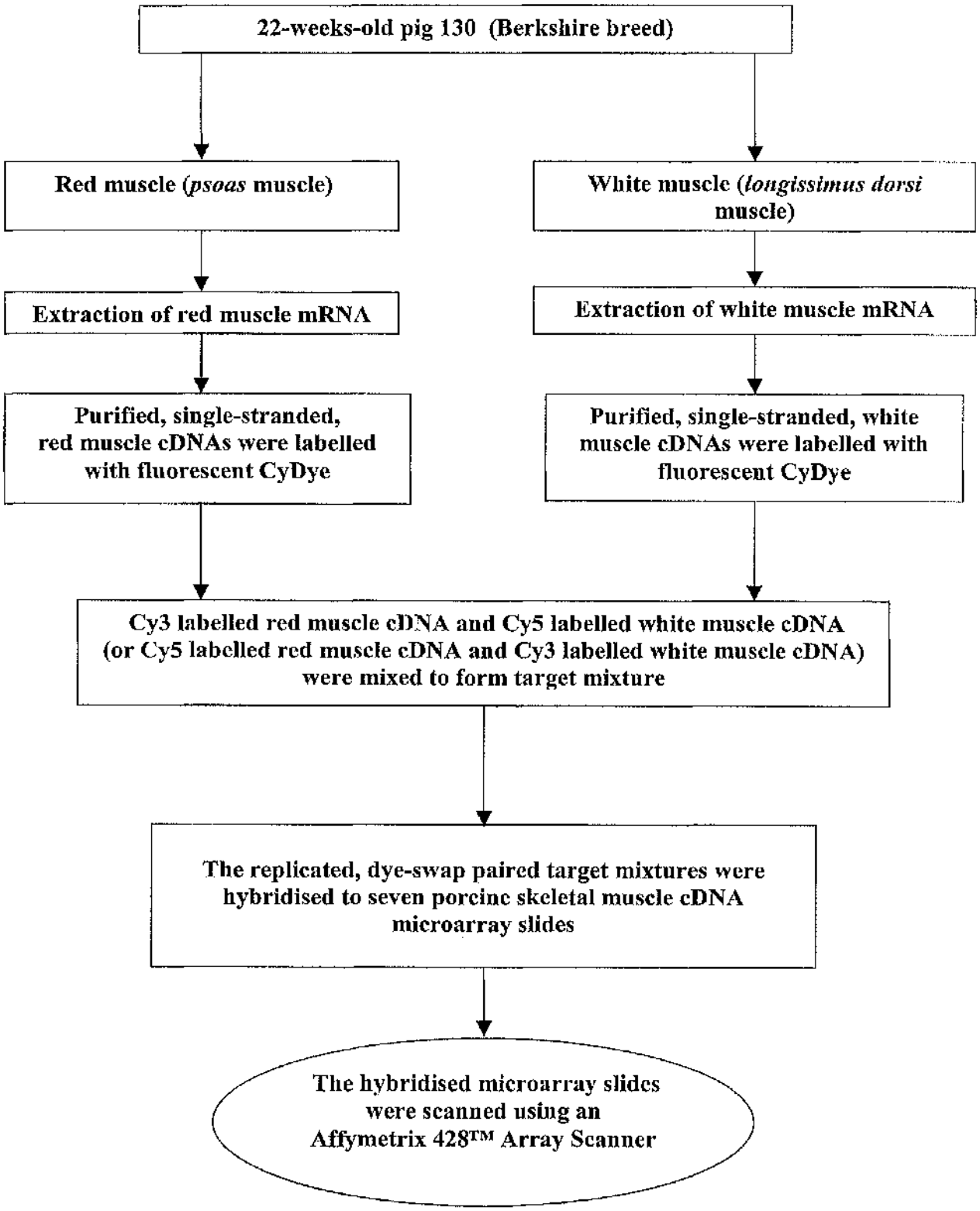

**Figure 3:2** Procedures for microarray image processing, data mining and validation

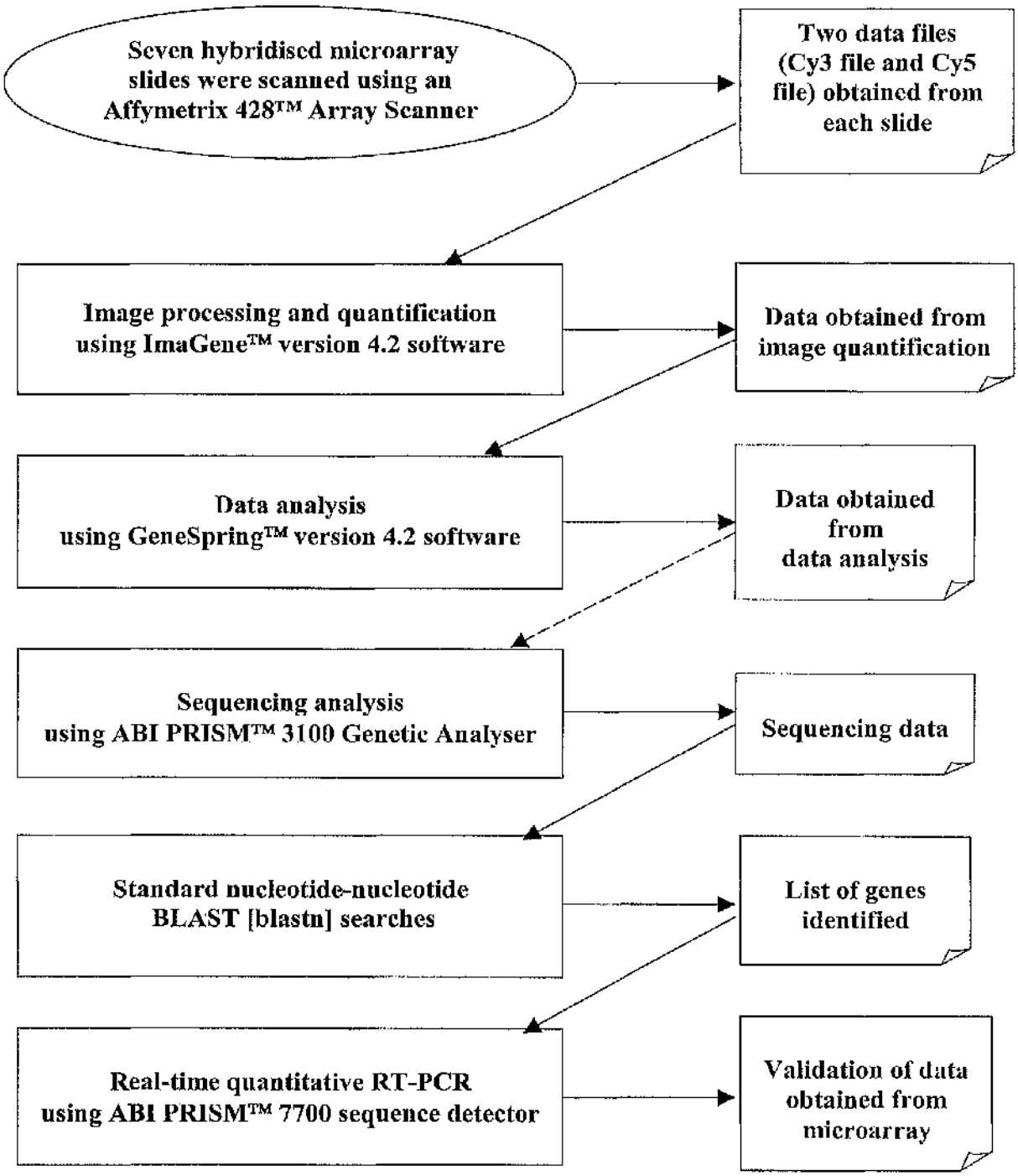

**Figure 3:3** Estimation of mRNAs extracted respectively from *Psoas* red muscle and *longissimus dorsi* white muscle of 22-week-old pig 130 for red-white muscle microarray hybridisations using agarose gel containing ethidium bromide

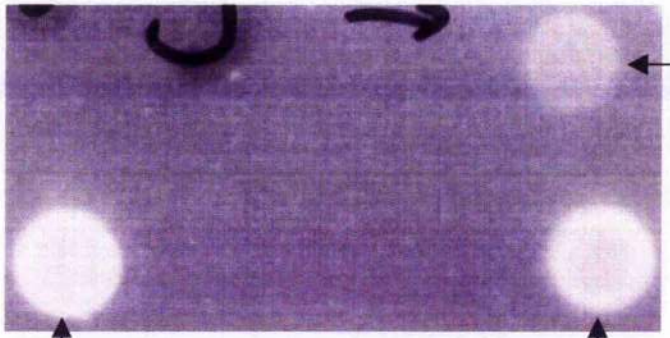

template mRNA in the 1.5 ml microcentrifuge tube which was placed on ice. The final volume of the cDNA synthesis reaction was 20 µl. The reaction components were mixed by vortexing, then centrifuged for 30 seconds, and followed by incubation at 42°C for 1.5 hours in a water bath.

#### *3.2.2.1.2. Target cDNA Purification*

It was necessary to remove unincorporated mRNAs from the synthesised cDNAs by purification to promote hybridisation of target cDNAs to immobilised microarray probes whilst minimising hybridisation with complementary mRNAs. Removal of unincorporated cyanine dye labelled nucleotides (e.g. primers) was necessary for minimising hybridisation background and improving detection sensitivity of targets of low abundance. In order to purify target cDNAs, mRNA was degraded into short oligomers. The short oligomers and unincorporated nucleotides were then removed by spin column chromatography. To degrade mRNA into short oligomers, 2 µl of 2.5 M NaOH was added into each 20 µl labelling reaction, mixed by vortexing, centrifuged for 30 seconds, and then incubated at 37°C for 15 minutes. In order to neutralise all components of the mRNA degradation reaction, 10 µl of 2 M HEPES free acid was added to each reaction solution, mixed by vortexing, and then centrifuged for 30 seconds. At this stage, 32 µl solution was obtained for each target cDNA labelled with cyanine dye. Following centrifugation, AutoSeq G-50 columns (Amersham Pharmacia Biotech) containing Sephadex G-50 DNA grade F were used to remove nucleotides and short oligomers from the cyanine dye labelled single-stranded target cDNAs. The resin in each AutoSeq G-50 column was re-suspended by vortexing gently. The cap of each column was loosened a quarter of a turn, and the bottom closure of each column was snapped off. The columns, which had been placed in a 1.5 ml screw-cap microcentrifuge tube for support, were centrifuged at 2000 ×g for 1 minute. Following centrifugation, each AutoSeq G-50 column was placed in a new 1.5 ml microcentrifuge tube and used immediately for target purification to avoid drying of the matrix. The 32 µl solution of target cDNAs was applied slowly to the centre of angled surface of the compacted resin bed in each AutoSeq G-50 column. The columns were then centrifuged for 1 minute at 2000× g. The purified cDNAs were collected at the bottom of the 1.5 ml microcentrifuge tubes. A final volume of 32 µl was obtained for each purified target cDNAs.

*3.2.2.1.3. Dye-swap pairing*

Following purification, dye-swap pairing was performed for the cyanine dye labelled target cDNAs. Sixteen microlitres of Cy3 labelled *psoas* muscle cDNAs and 16 µl of Cy5 labelled *longissimus dorsi* muscle cDNAs were mixed with 1.0 µl (8.0µg/µl) of poly (dA) oligonucleotide (27-7836, Amersham). The mixture was heated at 95°C for 2 minutes, and then mixed with 33 µl of 2× hybridisation buffer (GHB-200, Genpak) to obtain a final volume of 66 µl. The same procedure was carried out for pairing Cy5 labelled *psoas* muscle cDNAs and Cy3 labelled *longissimus dorsi* muscle cDNAs. The dyes, Cy3 and Cy5 are frequently paired because they are widely separated in their excitation and emission spectra, allowing highly discriminating optical filtration during microarray image capture. Most cDNA microarray experiments show systematic differences in the red and green fluorescent intensities, namely, overall cDNA spots on a microarray exhibit higher fluorescent intensity when incorporated with one dye or the other, regardless of the target sample under study. The red-green bias is due to differences between the labelling efficiencies and scanning properties of the two fluorescent dyes (Cy3 and Cy5). In this study, it was anticipated that the replicated dye-swap pairing method adopted by this study would help to reduce systematic colour bias of fluorescent dyes.

**3.2.2.2. Microarray hybridisations**

Prior to pre-hybridisation, microarray cDNA fragments immobilised on glass slides were denatured at 95°C for 2 minutes by immersing the microarray slides in heated distilled water. Pre-hybridisation was then performed at 65°C for 20 minutes in a plastic 2-slide holder containing 15 ml of 3× SSC (sodium chloride and sodium citrate), 2% bovine serum albumin (B4287, Sigma) and 0.1% SDS. After a brief rinse in distilled water at room temperature, the slides were dehydrated in absolute ethanol and centrifuged at 100× g for 2 minutes. At this stage, the microarray slides were ready to be used for microarray hybridisations. With the red and white muscle fluorescent-dye-tagged cDNA targets, which were not quantified, seven replicate microarray hybridisations were completed, with the dye assignments reversed in three of them. Each microarray slide was layered with 33 µl of hybridisation mixture, then covered with a 22 mm × 64 mm BDH cover glass to exclude air bubbles, and placed in a hybridisation chamber (ArrayIt hybridisation cassette AHC-1). Although 1-2 µg target mRNA was used for each cyanine dye labelling reaction (section *3.2.2.1.1.* of this chapter), only 0.5-1 µg target mRNA

was needed for each microarray slide. The hybridisation reaction was incubated in a dry incubator at 45°C for 24 hours. Following incubation, the microarray slides were washed gently to remove as much as possible the unbound and non-specifically bound target cDNAs. The slides were washed once in a 300 ml of solution containing 1× SSC and 0.2% SDS for 10 minutes at 45°C, twice in 300 ml of solution containing 0.2× SSC and 0.2% SDS for 10 minutes at 45°C, and twice in a 300 ml of solution containing 0.1× SSC for 10 minutes at 37°C. The microarray slides were then dried by centrifugation at 100× g for 2 minutes and ready for microarray image capture.

### 3.2.2.3. Microarray image capture and quantification

On each hybridised microarray slide, the signal intensity of each spot is proportional to the number of dye molecules, and hence the number of probes hybridised with the array (Byers et al., 2000). To obtain information about gene expression levels following hybridisation, each hybridised microarray slides were scanned using a MWG Affymetrix 428™ Array Scanner to facilitate measurement of molecular binding events on the array and generate a quantitative two-dimensional fluorescence image of hybridisation intensity. This scanner was a confocal laser microscope with a flying head, *i.e.* the objective lens scans over the slide. The resulting fluorescence was measured after excitation with two different wavelengths (532 and 635nm) corresponding to the dyes used (Bowtell, 1999). The hybridisation intensity information was captured digitally and imported to ImaGene™ version 4.2 software to extract biological information by adding GeneID files, generating grid, and quantifying dyes. Once the image processing was completed, the quantified image data were saved/stored automatically in text files, which were subsequently imported to GeneSpring™ version 4.2 software to perform data analysis.

### 3.2.2.4. Microarray data analysis

Microarray data analysis, including data normalisation, ratio operation and statistical analysis, was conducted using GeneSpring™ version 4.2 computer software. The purpose of microarray data normalisation was to adjust for any bias which arose from variation in the microarray technology rather than from biological differences between the target samples or the printed

probes. It was necessary to normalise the microarray signal intensities before any subsequent analysis was carried out (Cui and Churchill, 2003).

In this study, three normalisation steps (per spot, intensity-dependent, and per chip/slide) were performed in data mining to achieve data normalisation at gene level (to standardise expression levels between genes) and at chip level (to standardise expression values between arrays). In per spot normalisation, after background subtraction, the fluorescent intensity (e.g. Cy3) of each clone was divided by its control or reference channel intensity (e.g. Cy5). Values of the control channel that fell below 10 were adjusted to 10 prior to taking the ratio between signal and control value. Intensity-dependent normalisation, often called non-linear or Localised Weighted Regression (LOWESS) normalisation, was applied in this study to correct artefacts caused by differential dye incorporation and inconsistency of fluorescence dye intensities. Per chip normalisation was used to take into account intensity variation across the entire slide, by dividing the signal strength of a clone on a slide by the $50^{th}$ percentile signal of all of the measurements taken from the same slide. Chip-wide variations in signal intensity could be due to inconsistent washing, inconsistent sample preparation, or microfluidics imperfections. Additionally, the GeneSpring Global Error Model, based on the replicate measurement samples of all genes on the microarray was applied to estimate differences between medians, the standard errors among the different clones, and the extreme tails of the distribution of differences. Differences among muscles in expression were standardised for different clones by dividing the difference between muscle medians by the square root of the common variance. The Global Error Model is a way to estimate the precision/variability of gene expression measurement by combining measurement variation and sample-to-sample variation. Measurement variation is the lowest level of difference between the expression measurement of a gene on a single chip and the true value that would be achieved by a perfect measurement. Sample-to-sample variation, which represents biological or sampling variability, is the variation between results of replicate microarray hybridisations which are carried out in a same condition (Smyth et al., 2003;Lee et al., 2002).

To identify genes that were more highly expressed in the *psoas* than in the *longissimus dorsi*, clones with normalised *psoas/longissimus dorsi* ratio of 2.0 or more, and with one-sample t-test p-values not more than 0.05 were selected for sequencing. Likewise, clones with a normalised *psoas/longissimus dorsi* ratio of 0.7 or less, and with one-sample t-test p-values not more than 0.05 were selected for sequencing to identify genes that were more highly expressed in the *longissimus dorsi* than in the *psoas*. In the red and white muscle microarray analysis, "Filter

Genes Analysis tools" of GeneSpring version 4.2 was applied to search for genes that were differentially expressed. Genes were filtered by setting normalised *psoas/longissimus dorsi* ratio of 2.0 as minimum fold change to be met, whilst normalised *psoas/longissimus dorsi* ratio of 0.7 the maximum one. To examine the expression levels of genes in the two phenotypical distinct muscles, the "Scatter Plot view" of GeneSpring version 4.2 was applied to represent the experiment values plotted against the control values.

### 3.2.2.5. Sequence analysis to clone identification

Following microarray data analysis, cycle sequencing reaction was performed for each cDNA template (see Table 3:5 and 3:6) using the ABI PRISM® BigDye™ Terminators v3.0 Cycle Sequencing Reaction kit (Applied Biosystems), which provided AmpliTaq DNA polymerase, 5× sequencing buffer and FS Hi-Di formamide. In a 0.2 ml microcentrifuge tube, 6 µl plasmid DNA (about 500 ng), 6 µl sterile dd$H_2O$, 4 µl Big Dye (containing AmpliTaq DNA polymerase), 2 µl of 5× sequencing buffer, and 2 µl 1.6 pmol/µl primer mixture containing T7 and T3 primers, were mixed. The cycle sequencing reaction was performed for 25 cycles. In each cycle, the reaction was first incubated at 96 °C for 10 seconds, then at 50 °C for 10 seconds and finally at 60 °C for 4 minutes. Performa® DTR Gel Filtration Cartridges (EDGE Biosystems) were used for purification of the cycle sequencing reaction products. Each purified cycle sequencing product was resuspended with 25 µl FS Hi-Di formamide. Twenty microlitres of each resuspended sample were used for sequencing and loaded onto the ABI PRISM® 3100 Genetic Analyser (Applied Biosystems). Sequencing data was collected by using the 3100 Data Collection Software version 1.1 (Applied Biosystems). All data obtained from the sequencing step was subjected to BLAST (standard nucleotide-nucleotide Basic Local Alignment Search Tool) searches for gene identification based on the similarity between the sequences obtained in this study with the sequences provided by the database. Sequence information and BLAST search results were made available through this web-accessible database (http://www.ncbi.nlm.nih.gov/BLAST/).

### 3.2.2.6. Validation of gene expression by real-time quantitative RT-PCR

As microarray data does not provide an absolute measure of gene expression, post-analysis validation of microarray gene expression data using real-time quantitative RT-PCR is critical for

confirming biological significance of specific gene results. Continuous, real-time, fluorescence detection of amplification products allows accurate calculation of the quantity of template initially present in a sample. During the exponential phase (also called extension phase) of amplification, there is a highly reproducible relationship between the initial amount of template present in the reaction, and the number of cycles required before a significant increase in fluorescence signal is observed. First, the position of the cycle threshold line must be defined on a graph of "Fluorescence versus Threshold cycle number". The cycle threshold [C(t)] line is often positioned at a point where the fluorescent signals surpass background noise and begin to increase. The threshold cycle for an individual sample is then defined as the cycle at which the sample's fluorescence trace crosses the cycle threshold line. By including quantitation standards with varying initial amounts of template in the run, a standard curve of "Log quantity versus Threshold cycle number" can be plotted. The quantity of initial template in unknown samples can then be calculated by applying the sample's threshold cycle to the standard curve. The higher the initial amount of target template in real-time RT-PCR process, the fewer cycles required before significant fluorescence signal is detected, and the sooner the accumulated product is detected. In this study, an arbitrary cycle threshold line was chosen, placed above the baseline and within the exponential phase of PCR. The threshold cycle value was calculated for each reaction by determining the point at which fluorescence generated exceeded this chosen cycle threshold line/limit. The threshold cycle value was reported as the cycle number at this point (Bustin, 2000;Chuaqui et al., 2002).

#### *3.2.2.6.1. Designing primers and probes for real-time quantitative RT-PCR*

In real-time quantitative RT-PCR, three oligonucleotides (a forward primer, a reverse primer, and a Taqman probe) are used. TaqMan probes (also called hydrolysis probes) are non-extendible fluorogenic probes, which are designed to anneal to an internal region of a PCR product. Each Taqman probe is dual-labelled with a fluorescent reporter dye FAM (6-carboxyfluorescein) at 5' end and a quencher dye TAMRA (6-carboxy-tetramethyl-rhodamin) at 3' end of the sequence. When a Taqman probe is in its free form, the fluorescence of reporter dye is absorbed by quencher dye, and prevented from emission. Once Taqman probe anneal to PCR template, the 5' exonuclease activity of Taq polymerase cleave the Taqman probe and separate reporter and quencher dye. Reporter dye starts to emit fluorescence which increases in each cycle proportional to the quantity of PCR product present. This process occurs every cycle and does not interfere with the exponential accumulation of PCR products. TaqMan probe only emit a

fluorescent signal upon cleavage of this probe by Taq polymerase during exponential phase of PCR reaction. Initial amount of mRNA in cDNA template can be quantified by recording increase in TaqMan probe fluorescence emission at each PCR cycle, which indicates PCR product accumulation. In this study, all primers and TaqMan probes for real-time quantitative RT-PCR were designed using the ABI PRISM™ Primer Express software version 1.5 (Perkin Elmer Applied Biosystems) (Tables 3:3).

**Table 3:3** Primers and TaqMan probes for real-time quantitative RT-PCR

| Gene | Tm | | Sequence 5'→3' |
|---|---|---|---|
| porcine β-actin | 58.2°C | Primer | Sense: CCA GCA CCA TGA AGA TCA AGA TC |
| | 58.0°C | Primer | Antisense: ACA TCT GCT GGA AGG TGG ACA |
| | 63.0°C | TaqMan Probe | Sense: 5' FAM - CCC CTC CCG AGC GCA AGT ACT CC - 3' TAMRA |
| GAPDH | 57.5°C | Primer | Sense: AGG CTC GGG CTC ACT TGA A |
| | 57.8°C | Primer | Antusense: TGC CCA TCA CAA ACA TGG G |
| | 62.0°C | TaqMan Probe | Sense: 5' FAM - AGC CAA AAG GGT CAT CAT CTC TGC CC - 3' TAMRA |
| MyHC IIb | 59.0°C | Primer | Sense: CAC TTT AAG TAG TTG TCT GCC TTG AG |
| | 58.0°C | Primer | Antisense: GGC AGC AGG GCA CTA GAT GT |
| | 63.0°C | TaqMan Probe | Sense: 5' FAM - TGC CAC CGT CTT CAT CTG GTA ACA TAA GAG G - 3' TAMRA |
| bin-1 | 57.3°C | Primer | Sense: GCC AGC AAT GTG CAG AAG AA |
| | 59.4°C | Primer | Antisense: CAT CTG CCT TCC CCA GTT TC |
| | 63.0°C | TaqMan Probe | Antisense: 5' FAM - CCT TCT CCT GCG CGC GAG TGA G -3' TAMRA |
| novel gene kc2725 | 54.0°C | Primer | Sense: TTT TTT CCA TTC CCT GGT TGA |
| | 59.4°C | Primer | Antisense: AGG GAC CCT GTA AGC CAA CA |
| | 64.0°C | TaqMan Probe | Sense: 5' FAM - CCA GTC TGG TGG CCT AGT CAT GCC C - 3' TAMRA |

The choice of probe sequences was made prior to that of primers. All TaqMan probes were systhesised by Transgenomic/Cruachem Limited at 100 pmol/μl, and primers by MWG. All TaqMan probes were designed to have more cytosines than guanines. The total number of

guanines and cytosines in each probe was 30-80%. Guanine was avoided at 5' end of all probes because a guanine adjacent to reporter dye would have suppressed reporter fluorescence even after cleavage. Runs of consecutive identical nucleotides (especially guanine) in all probes were avoided. The primers were designed to be 15-30 bases in length. In order to avoid non-specific priming due to relative instability of the 3' end of primers, the total number of guanines and cytosines in the last five nucleotides at 3' end of all primers was designed not to exceed three. In real-time quantitative PCR, ideal length of template sequences are 50-150 bases because PCR with shorter template sequences is more efficient and more tolerant of reaction conditions, and gives more consistent results. In this study, maximum length of all template sequences was designed not to exceed 200 base pairs (bp). In order to avoid false-positive results due to amplification of contaminating genomic DNA in the cDNA preparation, primers were designed to span exon-exon junctions to avoid the amplification of genomic DNA (Bustin, 2000).

#### *3.2.2.6.2. Selected genes, target templates and endogenous housekeeping gene for normalisation*

Real-time quantitative RT-PCR was performed for four selected genes [GAPDH (for glyceraldehyde-3-phosphate-dehydrogenase), MyHC IIb, bin-1 (for box-dependent MYC-interacting protein-1) and novel gene kc2725] for validation of gene expression levels in *psoas* and *longissimus dorsi* muscles derived from four pigs (pig 1, pig 2, pig 3 and pig 4). A reference cDNA panel, comprising eight different tissue templates (*longissimus dorsi* muscle, *psoas* muscle, heart, brain, uterus, liver, spleen and kidney) of a 7-week-old pig (pig 4) was used to evaluate the quantitative distribution of two selected genes (bin-1 and novel gene kc2725) in different tissue templates.

In real-time quantitative RT-PCR, for an ideal quantification, the start amount of mRNA should be the same for all target templates. Normalisation with an endogenous housekeeping gene helps to minimise the effects of variations in initial amount of target templates input into real-time RT-PCR reaction. An ideal 'housekeeping' gene should be expressed at constant level among different tissues of an organism, at all stages of development, and should not be affected by the experimental treatment. The most common genes used as a housekeeping gene are β-actin, 18S rRNA (ribosomal RNA) and HPRT (hypoxanthine guanine phosphoribosyl tranferase) (Bustin et al., 2000; Rajeevan et al., 2001). Choosing the ideal housekeeping gene for each real-time quantitative RT-PCR experiment is very important to ensure the credibility and reproducibility of the results. β-actin is a highly conserved protein ubiquitously expressed in all eukaryotic cells

as a component of the cytoskeleton and as a mediator of internal cell motility. In this study, in order to compare relative gene expression of a same gene between samples, mRNA of β-actin was quantified as a standard control to normalise results in real-time quantitative RT-PCR.

#### *3.2.2.6.3. Real-time quantitative RT-PCR*

Real-time quantitative RT-PCR was performed in this study using relative standard curve method of quantification (da Costa et al., 2002). In the relative standard curve method, comparisons of relative expressions are only made between samples of the same gene, and it is considered not appropriate to compare expression levels between two different genes. The components of each reaction mixture prepared for real-time quantitative RT-PCR are described in Table 3:4. Microamp Optical 96-well reaction plates (Applied Biosystems) were used for preparation of the reaction mixtures. The amplification of each reaction was performed in a ABI PRISM™ 7700 sequence detector (Perkin Elmer, Applied Biosystems) containing a built-in thermal cycler with 96-well positions, and monitored by the sequence detection system version 1.7 software (Perkin Elmer, Applied Biosystems). The real-time RT-PCR reaction mixture was first incubated at 50°C for 2 minutes, and then denatured at 95°C for 10 minutes. After denaturation, 40 cycles of the amplification were performed for each target template with each cycle started at 95°C for 15 seconds and followed by incubation for one minute at 60°C.

**Table 3:4** Reaction mixture prepared for Real-time quantitative RT-PCR

| Reaction content | Volumn |
|---|---|
| cDNA template derived from skeletal muscle tissue | 5.0 µl |
| Probe (5 pmol/µl) (Cruchem) | 1.0 µl |
| TaqMan™ Universal PCR Master Mix (Applied Biosystems) | 12.5 µl |
| W4502 sterile double distilled $H_2O$ for molecular biology (Sigma) | 1.5 µl |
| Sense primer (900 nM) (MWG) | 2.5 µl |
| Antisense primer (900 nM) (MWG) | 2.5 µl |
| Total volume for each reaction | 25.0 µl |

# 3.3. RESULTS

## 3.3.1. RED AND WHITE MUSCLE MICROARRAY ANALYSIS

To evaluate the performance of the porcine skeletal muscle cDNA microarray, a profiling experiment was conducted to determine the differential expression of genes between red (*psoas*) and white (*longissimus dorsi*) muscle. Replicated, dual-colour hybridisations (e.g., Fig. 3:4) were performed on seven identical porcine cDNA microarray slides. The expression profile of all clones represented on the microarray after hybridisation can be visualised as an Imagene scatter plot. In the Imagene scatterplot images (e.g., Fig. 3:5) that plotted the expression of each clone in the *psoas* muscle against the expression of the same clone in the *longissimus dorsi* muscle, each point is the unnormalised value from only one slide. In the GeneSpring scatterplot image (Fig. 3:6) that plotted the median expression of each clone in the *psoas* muscle against the median expression of the same clone in the *longissimus dorsi* muscle, each point is the median of 14 normalised values (2 replicates per slide, 7 slides per muscle). Most points cluster around the middle line indicating similar levels of expression in both muscles. There were, however, a number of clones falling substantially below the middle line, indicating consistently lower levels of expression in the *psoas* compared with the *longissimus dorsi* muscle. Low signal readings for both dyes may indicate the absence of a cDNA insert. About 12% of the printed clones were found to fall below 50 arbitrary units for both dyes (according to GeneSpring analysis) and were considered to be without cDNA inserts. This value was consistent with the earlier estimate of insertless clones in the cDNA libraries.

### 3.3.1.1. Genes more highly expressed in *psoas* red muscle

A normalised *psoas*/*longissimus dorsi* ratio of 2.0 or more ($P<0.05$) was used as data mining selection criterion to identify genes that were more highly expressed in *psoas* than in *longissimus dorsi* muscle. This ratio represents the top 5% of differences in expression. Seventy clones meeting this criterion were sequenced. The sequences were compared with database sequences by BLAST searching. Table 3:5 is a summary of these genes identified. All the listed genes are

# Figure 3:4 Imagene™ processed image of red-white muscle microarray hybridisation

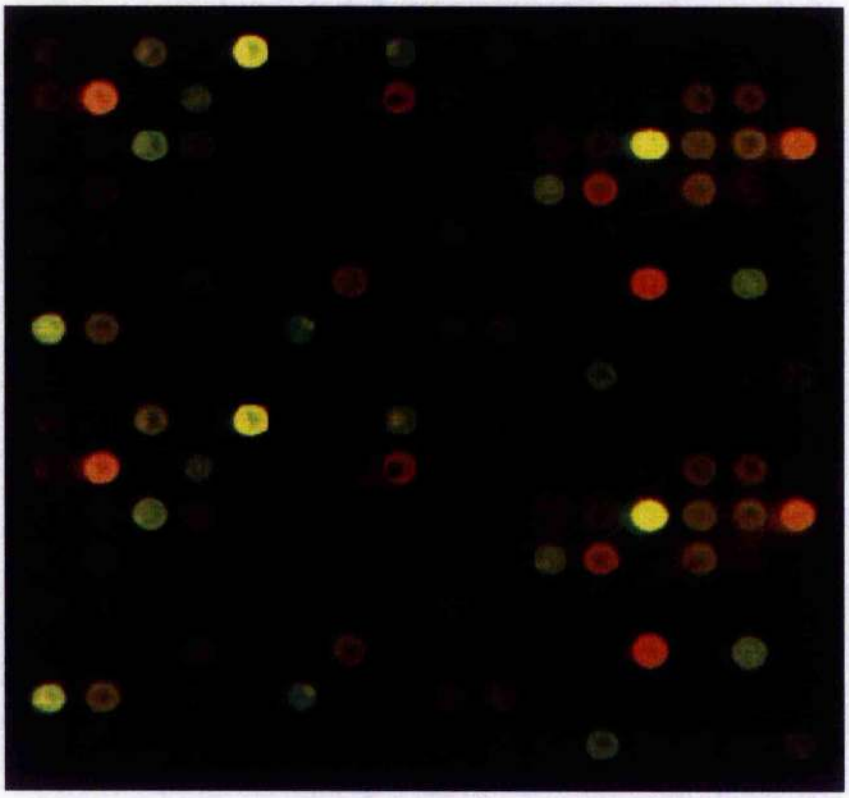

- *Psoas* muscle target was labelled with the red colour Cy3
- *Longissimus dorsi* muscle target was labelled with the green colour Cy5

# Figure 3:5 Imagene™ scatterplot demonstrating differential gene expression in red and white muscles

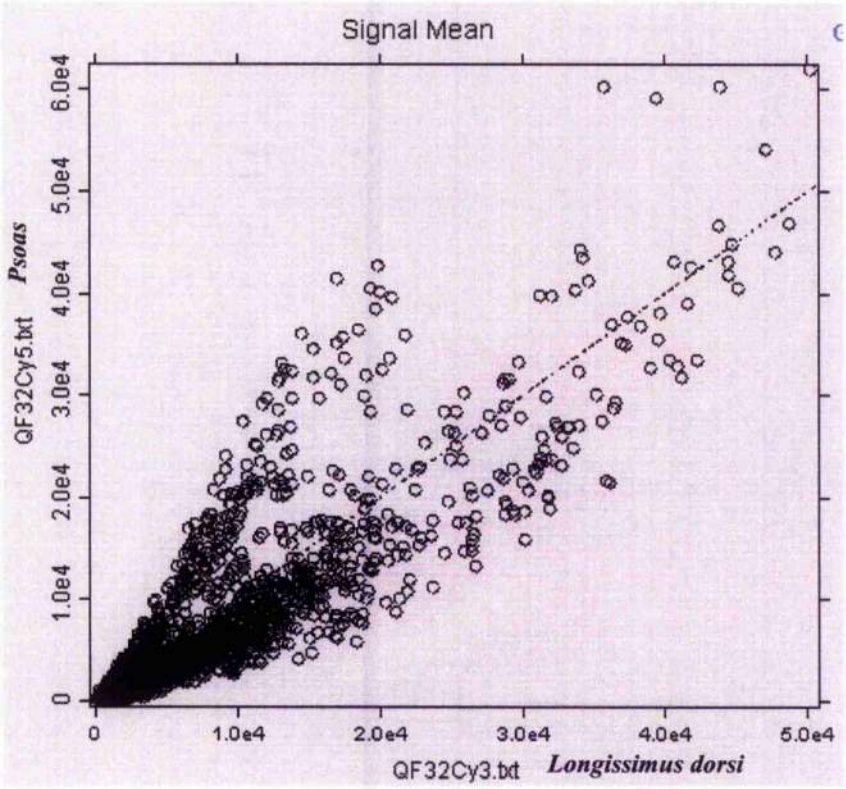

**Figure 3:6 GeneSpring™ Scatterplot of normalised red-white muscle microarray hybridisation data**

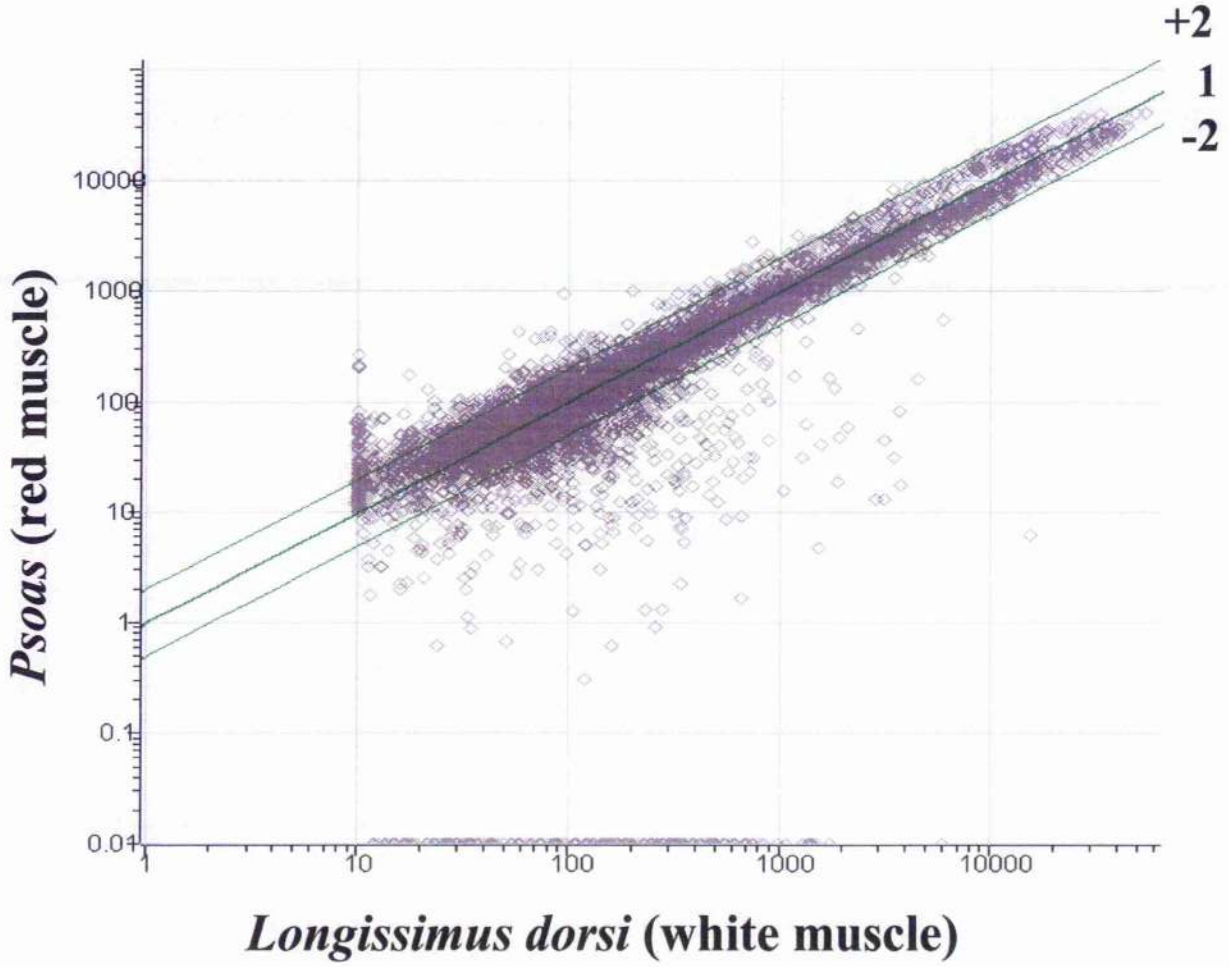

**Table 3:5** Genes more highly expressed in *psoas* red muscle than in *longissimus dorsi* (LD) white muscle

| Gene | *Psoas/LD* | Homology | # of clones | Accession # |
|---|---|---|---|---|
| ***Mitochondrial Origin*** | | | | |
| 16S ribosomal RNA | 2.07 | 97%(P) | 12 | AY011178 |
| 12S ribosomal RNA | 2.18 | 100%(P) | 7 | AY012145 |
| 28S ribosomal RNA | 2.67 | 99%(BR) | 1 | V01270 |
| Ribosomal protein S29 | 4.14 | 94%(B) | 1 | U66372 |
| Ribosomal protein L23 | 30.05 | 92%(H) | 1 | NM_000978 |
| Cytochrome oxidase subunit I | 2.03 | 86%(B) | 2 | AF490529 |
| Cytochrome oxidase subunit III | 2.28 | 81%(SA) | 1 | AF030272 |
| Cytochrome oxidase subunit VIc | 27.97 | 88%(H) | 1 | NM_004374 |
| Cytochrome oxidase subunit VIb | 2.51 | 96%(B) | 1 | X15112 |
| NADH dehydrogenase subunit 2 | 2.51 | 77%(SW) | 1 | AF414121 |
| NADH dehydrogenase subunit 3 | 2.58 | 82%(B) | 7 | AY052631 |
| NADH dehydrogenase subunit 6 | 2.15 | 81%(B) | 4 | AF416451 |
| NADH dehydrogenase subunit B15 | 2.34 | 87%(B) | 1 | X64898 |
| ATP synthase protein 6 | 2.1 | 96%(P) | 2 | AF190813 |
| ATP synthase protein 8 | 2.17 | 100%(P) | 1 | AF039170 |
| ATP synthase protein 9 | 20.55 | 96%(H) | 1 | NM_001689 |
| tRNA | 3.87 | 97%(P) | 2 | AF304202 |
| Adenine nucleotide translocator SLC25A6 | 2.05 | 92%(H) | 1 | XM_114724 |
| ***Non-Mitochondrial Origin*** | | | | |
| *Non-Mitochondrial and sarcomeric/structural* | | | | |
| Ankyrin 1 | 2.23 | 93%(H) | 1 | XM_016774 |
| Tubulin alpha 1 | 2.68 | 94%(H) | 1 | AF14147 |
| *Non-Mitochondrial and non-sarcomeric* | | | | |
| Pituitary tumor-transforming 1 interacting protein (tr) | 2.98 | 84%(H) | 1 | BC031097 |
| Par-6 partitioning defective 6 homolog gamma (tr) | 30.36 | 92%(HM) | 1 | XM_129044 |
| TAFII140, a novel TAF component (TATA-binding protein associated factors) (tr) | 2.16 | 94%(H) | 1 | AJ292190 |
| STAF transcriptional activator (tr) | 2.15 | 88%(H) | 1 | NM_003442 |
| Prefoldin subunit 6 (KE2 protein) (tl) | 2.65 | 85%(HM) | 1 | M65255 |
| EH domain-binding protein, Epsin (s) | 2.23 | 93%(H) | 2 | NM_013333 |
| Beta-catenin (s) | 2.18 | 100%(P) | 1 | AB046171 |
| Casein kinase 2, alpha 1 polypeptide (s) | 6.47 | 87%(H) | 1 | NM_001895 |
| Small muscle protein (smpx) (s) | 7.34 | 88%(H) | 1 | BC005948 |
| Tyrosine kinase 9-like (A6-related protein) (s) | 2.04 | 90%(H) | 1 | BC016452 |
| Fructose-1,6-biphosphatase (m) | 25.07 | 92%(DR) | 1 | AJ272520 |
| Testis intracellular mediator protein (PEAS) (kc3978) (u) | 2.12 | 88%(H) | 1 | BC021546 |
| Hypothetical protein (FLJ12666) (kc5959) (u) | 2.23 | 93%(H) | 1 | NM_024595 |
| Unknown small protein (kc1564) (u) | 3.93 | 94%(H) | 1 | BC005398 |

| | | | | |
|---|---|---|---|---|
| Unknown clone (kc2725), homologous to 3' untranslated region (UTR) of RNA binding protein S1 (u) | 2.57 | 90%(H) | 1 | XM_028847 |
| Unknown clone (kc542), homologous to 3' UTR of enhancer of rudimentary (u) | 2.07 | 81%(H) | 1 | U66871 |
| Unknown clone (kc797), homologous to *Homo sapiens* clone KIAA0513 (u) | 13.21 | 81%(H) | 1 | NM_014732 |
| Unknown clones (kc2668, kc522, kc2469) (u) | 3 | | 3 | |

Possible involvement: (tr), transcriptional; (tl), translational; (s), signalling; (m), metabolic; (u), unknown. Accession # refers to porcine gene or close homologue: (P) = Porcine, (H) = Human, (HM) = House mouse, (DR) = Demestic rabbit, (SA) = Shaggy antelope, (SW) = Sperm whale, (BR) = Brown rat, (B) = Bovine.

categorised into two groups: mitochondrial origin and non-mitochondrial origin. The non-mitochondrial origin category is divided into sarcomeric/structure genes and non-sarcomeric genes. Sixty seven percent of the clones (47 out of 70) sequenced were genes of mitochondrial origin. Of these several were featured more than once on the microarray, namely genes encoding 16S ribosomal RNA, 12S ribosomal RNA, and NADH dehydrogenase subunits 3 and 6. One of the well established distinguishing features of red muscle is its relatively high oxidative phosphorylation capacity, reflected by an abundance of mitochondria in red muscles. It is therefore not surprising that the mitochondrial genome was well represented in the identified population of differentially expressed clones in the *psoas* red muscle. Thirty percent of the clones (21 out of 70) did not show any homology with known mitochondrial or sarcomeric genes in the database. These clones were categorised as non-mitochondrial and non-sarcomeric genes. The function of 9 of these clones was completely unknown. The 9 clones included kc3978, kc5959, kc1564, kc2725, kc797, kc542, kc2668, kc522 and kc2469 (Table3:5). Of the 21 genes in the non-mitochondrial and non-sracomeric category, one gene encoded for fructose-1,6-biphosphatase, an enzyme that is necessary for muscle gluconeogenesis. The function of the remaining 11 clones, which represented 10 different genes, was involved with aspects of transcription, translation or signal transduction, but their functions in skeletal muscle have not been characterised. These 10 genes encoded 10 different proteins including pituitary tumor-transforming 1 interacting protein, par-6 partitioning defective 6 homolog gamma, TATA-binding protein associated factor, STAF transcriptional activator, prefoldin subunit 6, EH domain-binding protein, beta-catenin, alpha 1 polypeptide of casein kinase 2, small muscle

protein and tyrosine kinase 9-like A6-related protein. Of these 10 different genes, three genes, which encoded alpha 1 polypeptide of casein kinase 2, small muscle protein and tyrosine kinase 9-like A6-related protein, were members of the casein kinase 2 signalling pathway. The α1 subunit of casein kinase 2 (CK2) is one half of the holoenzyme (Blanquet, 2000;Faust and Montenarh, 2000). The small muscle protein (smpx) is encoded by a recently discovered X-linked stretch response gene (Kemp et al., 2001). The tyrosine kinase A6-related protein binds ATP and actin, and interacts with protein kinase C zeta (Rohwer et al., 1999). Although the function of the latter two proteins is not known, both were shown to be targets of CK2 phosphorylation. The normalised *psoas/longissimus dorsi* ratios of five genes listed in Table 3:5 were above 20. The proteins encoded by these five genes were ribosomal protein L23, cytochrome oxidase subunit Vic, ATP synthase protein 9, par-6 partitioning defective 6 homolog gamma, and fructose-1,6-biphosphatase. The uncharacteristic high *psoas/longissimus dorsi* ratio could be due to low signal intensities or high levels of noise, which could lead to the occurrence of the false positive.

#### 3.3.1.2. Genes more highly expressed in *longissimus dorsi* white muscle

When the data mining criteria of a normalised *psoas/longissimus dorsi* ratio of 0.5 or less ($P<0.05$), equivalent to *longissimus dorsi/psoas* ratio of 2.0 or more ($P<0.05$), was applied, only 10 significant clones were detected. When the selection criteria were relaxed, clones with a normalised *psoas/longissimus dorsi* ratio of 0.7 or less ($P<0.05$), which represented the most extreme 5% of clones were identified. Forty-five clones were sequenced and examined for homology by BLAST searching. Table 3:6 lists the genes that were more highly expressed in the *longissimus dorsi* than in the *psoas*. All the listed genes are categorised into two groups: mitochondrial origin and non-mitochondrial origin. The non-mitochondrial origin are divided into sarcomeric/structure and non-sarcomeric. Only 4 out of 45 clones listed in Table 3:6 were of mitochondrial origin, and they were different from those expressed more abundantly in the *psoas*. Fast isoforms of sarcomeric structural proteins (myosin heavy chains [MyHCs] IIa, IIx, IIb, myosin regulatory light chain 2, α-actinin 3, fast troponin C, and fast troponin T3) were well represented amongst the sequenced clones identified to be more highly expressed in *longissimus dorsi* muscle. Sarcomeric/structural genes made up nearly half of the total clones (22 out of 45) listed in Table 3:6. The other highly represented group of genes on the list (11 out of 45 clones) were involved in anaerobic glycolysis, such as glyceraldehyde 3-phosphate dehydrogenase (GAPDH), SERCA, phosphoglycerate kinase, phosphoglucomutase, muscle glycogen

**Table 3:6** Genes more highly expressed in *longissimus dorsi* (LD) white muscle than in *psoas* red muscle

| Gene | *LD/Psoas* | Homology | # of clones | Accession # |
|---|---|---|---|---|
| ***Mitochondrial Origin*** | | | | |
| Ribosomal protein L35A | 2.2 | 86%(H) | 1 | AK055653 |
| Ribosomal protein L7a | 1.85 | 90%(H) | 1 | BC005128 |
| Ribosomal protein S23 | 1.91 | 88%(BR) | 1 | X77398 |
| Ribosomal protein S12 | 1.61 | 100%(P) | 1 | X79417 |
| ***Non-Mitochondrial Origin*** | | | | |
| *Non-Mitochondrial and sarcomeric / structural* | | | | |
| Myosin heavy chain fast IIa | 1.91 | 100%(P) | 6 | AB025260 |
| Myosin heavy chain fast IIx | 1.77 | 100%(P) | 2 | AB025262 |
| Myosin heavy chain fast IIb | 1.88 | 97%(P) | 2 | AB025261 |
| Myosin regulatory light chain 2 | 2.95 | 91%(H) | 2 | AF363061 |
| Alpha actinin 3 | 1.47 | 93%(H) | 2 | M86407 |
| S-nexilin | 1.77 | 70%(H) | 1 | AK057954 |
| Fast skeletal troponin C | 1.67 | 94%(DR) | 1 | Y00760 |
| Fast skeletal troponin T (TnT3) | 1.7 | 93%(B) | 3 | AB085599 |
| Alpha-1 skeletal actin (ACTA1) | 1.53 | 93%(H) | 2 | BC012597 |
| Alpha-2 smooth muscle actin (ACTA2) | 1.62 | 96%(H) | 1 | BC017554 |
| *Non-Mitochondrial and non-sarcomeric* | | | | |
| Sarcoplasmic/endoplasmic reticulum calcium ATPase 1 (SERCA1) (g) | 1.54 | 98%(P) | 3 | AY027797 |
| Aldolase A (g) | 1.47 | 87%(H) | 1 | BC010660 |
| Phosphoglycerate kinase (g) | 1.48 | 88%(H) | 1 | V00572 |
| Glyceraldehyde-3-phosphate dehydrogenase (g) | 1.53 | 100%(P) | 1 | X94251 |
| Muscle pyruvate kinase (PKM2) (g) | 1.63 | 91%(H) | 1 | BC007952 |
| Phosphoglucomutase isoform 2 (PGM) (g) | 1.81 | 94%(DR) | 1 | M97664 |
| Muscle glycogen phosphorylase (g) | 1.65 | 92%(DR) | 2 | X04265 |
| Adenylate kinase isozyme 1 (myokinase) (g) | 1.51 | 87%(P) | 1 | E03007 |
| Calsequestrin (c) | 1.7 | 83%(DD) | 2 | J03766 |
| Polyubiquitin (tl) | 1.51 | 90%(DS) | 1 | AF038129 |
| Bridging-integrator protein-1 (bin1) (s) | 2.17 | 85%(H) | 1 | AF001383 |
| Myomegalin-like protein (kc) (u) | 6.94 | 94%(H) | 1 | AB042557 |
| Heat shock cognate protein (HSPA8) (kc) (tr) | 1.77 | 93%(B) | 1 | X53827 |
| Unknown clone (kc), homologous to *Homo sapiens* clone HSPCO40 (kc4590) (u) | 2.08 | 86%(H) | 1 | BC000810 |
| Unknown clone (kc1362), homologous to 3' UTR of *Homo sapiens* actin bundling protein (kc) (u) | 1.99 | 77%(H) | 1 | U09873 |

Associated or possible role: (g), glycolysis; (c), contraction; (tr), transcription; (tl), translation; (s), signalling; (u), unknown. Accession # refers to porcine gene or close homologue: (P) = Porcine, (B) = Bovine, (H) = Human, (DR) = Demestic rabbit, (DS) = Domestic sheep, (BR) = Brown rat, (DD) = Domestic dog.

phosphorylase, aldolase, adenylate kinase, and muscle pyruvate kinase. White muscles comprise predominantly more fast-glycolytic fibres than red muscles. In this study, most of the 45 clones listed in Table 3:6 were either fast isoforms of structural genes, or enzymes connected with anaerobic glycolysis, and these findings were consistent with expectations. The function of two non-sarcomeric genes (kc1362, kc4590) was completely unknown. A few candidate regulatory genes (bin1, polyubiquitin, myomegalin-like, calsequestrin, and HSPA8) were also found. Of particular interest is the tumour suppressor gene bin1 (Sakamuro et al., 1996;Tsutsui et al.,1997; Wechsler-Reya et al.,1998), which has recently been shown to play a role in C2C12 myoblast differentiation (Wechsler-Reya et al., 1998). Myomegalin-like gene, which predominantly expressed in heart, is also expressed in skeletal muscle. Although precise function of the myomegalin-like gene is still unknown, it could play a role in heart development (Soejima et al., 2001). Calsequestrin, which was identified as more highly expressed in *longissimus dorsi* white muscle than in *psoas* red muscle, is the major $Ca^{2+}$-binding protein in the sarcoplasmic reticulum. Polyubiquitin is ATP-dependent selective degradation of cellular proteins. Heat shock proteins are transcription factors, the main function which is to control the accurate folding and translocation of polypeptides at different cellular compartments (Maitra et al., 2002).

Therefore, the use of the newly assembled porcine skeletal muscle cDNA microarray to study differential expression of muscle genes between red and white muscles had generated two distinct lists of differentially expressed genes (Tables 3:5 and 3:6). The microarray results correctly exemplified genes that are known to be more highly expressed in only one muscle type. With highly expressed genes, such as mitochondrial genes and structural genes, there were detectable levels of redundancies (repeats) on the microarray. Reassuringly, in the presence of redundancies, no gene was found to be present on both lists. Crucially, this work has identified a number of candidate regulatory genes, which may play key roles in determining muscle phenotype.

## 3.3.2. VALIDATION OF GENE EXPRESSION BY REAL-TIME RT-PCR

To assess the validity of the microarray approach to identify differentally expressed genes, quantitative real-time RT-PCR (TaqMan) was performed on four representative clones (GAPDH, MyHC IIb, bin 1 and a novel gene kc2725), each normalised to β-actin. Bin 1 was identified by

microarray analysis as being more highly expressed in the *longissimus dorsi* than in the *psoas* (Fig. 3:7). However, this pattern of gene expression was found in only 3 (pig 1, 3, and 4) out of 4 pigs. In pig 2, there was no significant difference in bin 1 expression between *longissimus dorsi* and *psoas* (Fig. 3:7). Bin 1 was previously found to be ubiquitously expressed by Northern analysis (Sakamuro, et al, 1996;Tsutsui, et al, 1997). In this study, quantitative real-time RT-PCR showed that bin 1 expression was between 1 to 2 orders of magnitude greater in the heart and brain than in skeletal muscle. Bin 1 also demonstrated low expression levels in the uterus, liver, spleen and kidney (Fig. 3:8). A novel gene kc2725 of unknown function, found by microarray analysis to be more highly expressed in the *psoas* than in the *longissimus dorsi*, was individually quantified in 4 pigs (pig 1, 2, 3, and 4) (Fig. 3:9). All pigs (pig 1, 2, 3, and 4) gave the same pattern of expression (Fig. 3:9) as that detected on the microarray. Interestingly, expression of kc2725 was ubiquitous and was much more abundant in other tissues (e.g., brain, uterus, liver, spleen, kidney) than that in skeletal muscle (*psoas* and *longissimus dorsi*) (Fig. 3:10). However, the expression of a gene from the same muscle can vary between similar individuals (Figures 3:7, 3:9). In line with functional expectations, previous quantitative work performed has shown that the mRNA expression of GAPDH and MyHC IIb was higher in the *psoas* than in the *longissimus dorsi* within individual animals (da Costa et al, 2002). In this study, the relative levels of GAPDH and MyHC IIb of pooled total cDNA samples from four pigs (pig 1, 2, 3, and 4) were measured (Fig 3:11). The results showed that the differential mRNA expression of GAPDH and MyHC IIb was sufficiently consistent between the *longissimus dorsi* and *psoas* muscles to be detected in the pooled cDNAs. Therefore, in this study, TaqMan real-time quantitative PCR, performed on the selected representative genes (GAPDH, MyHC IIb, bin 1, a novel gene kc2725), not only demonstrated the functional integrity of the newly constructed porcine skeletal muscle cDNA microarray in the appropriate identification of differentially expressed genes between red and white muscles, but also highlighted the existence of variation in muscle gene expression among similar individuals.

## Figure 3:7 Bin 1 relative gene expression levels in *longissimus dorsi* and *psoas* muscles of four pigs

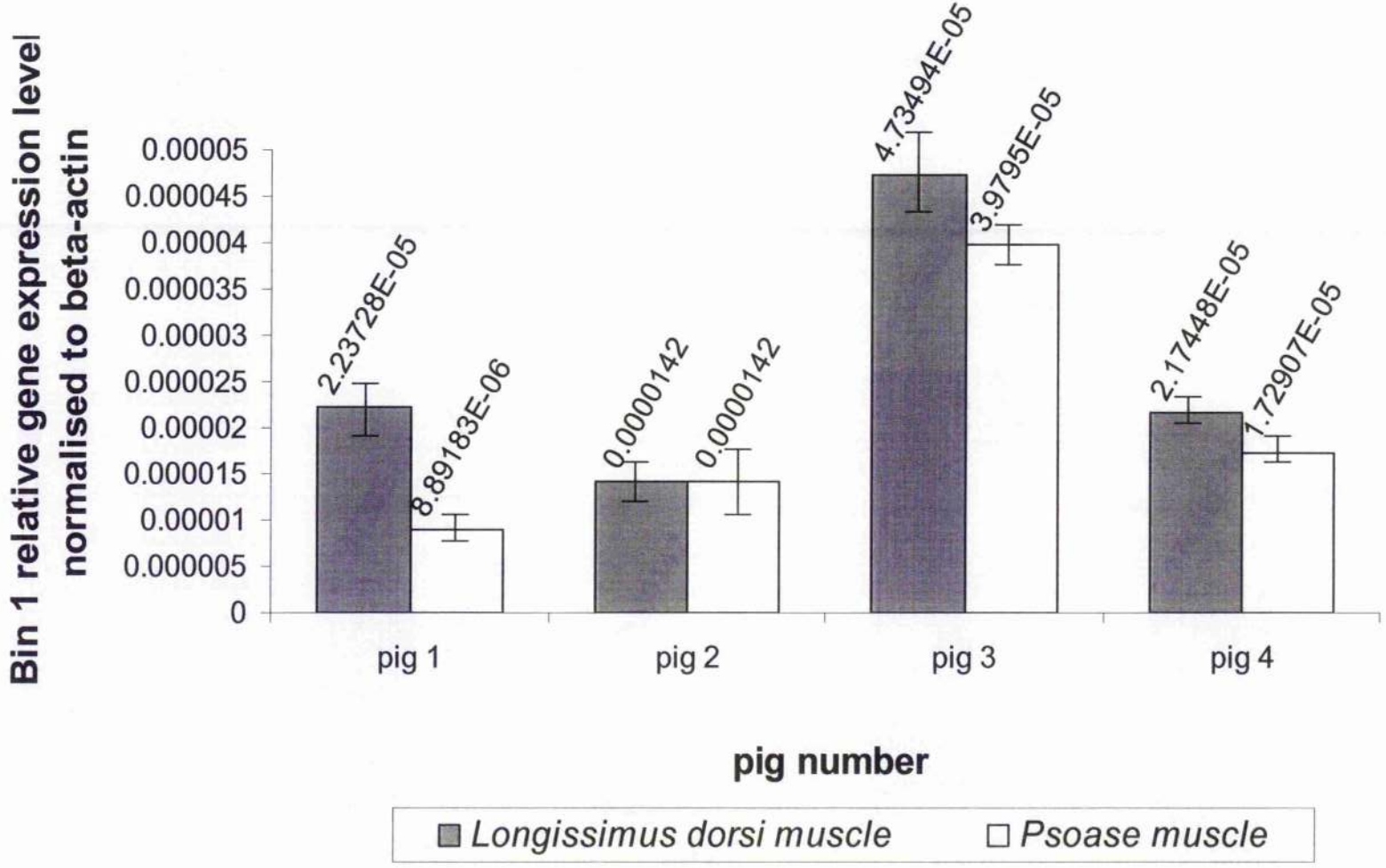

# Figure 3:8 Bin 1 relative gene expression levels in eight different porcine tissues derived from the pig 4

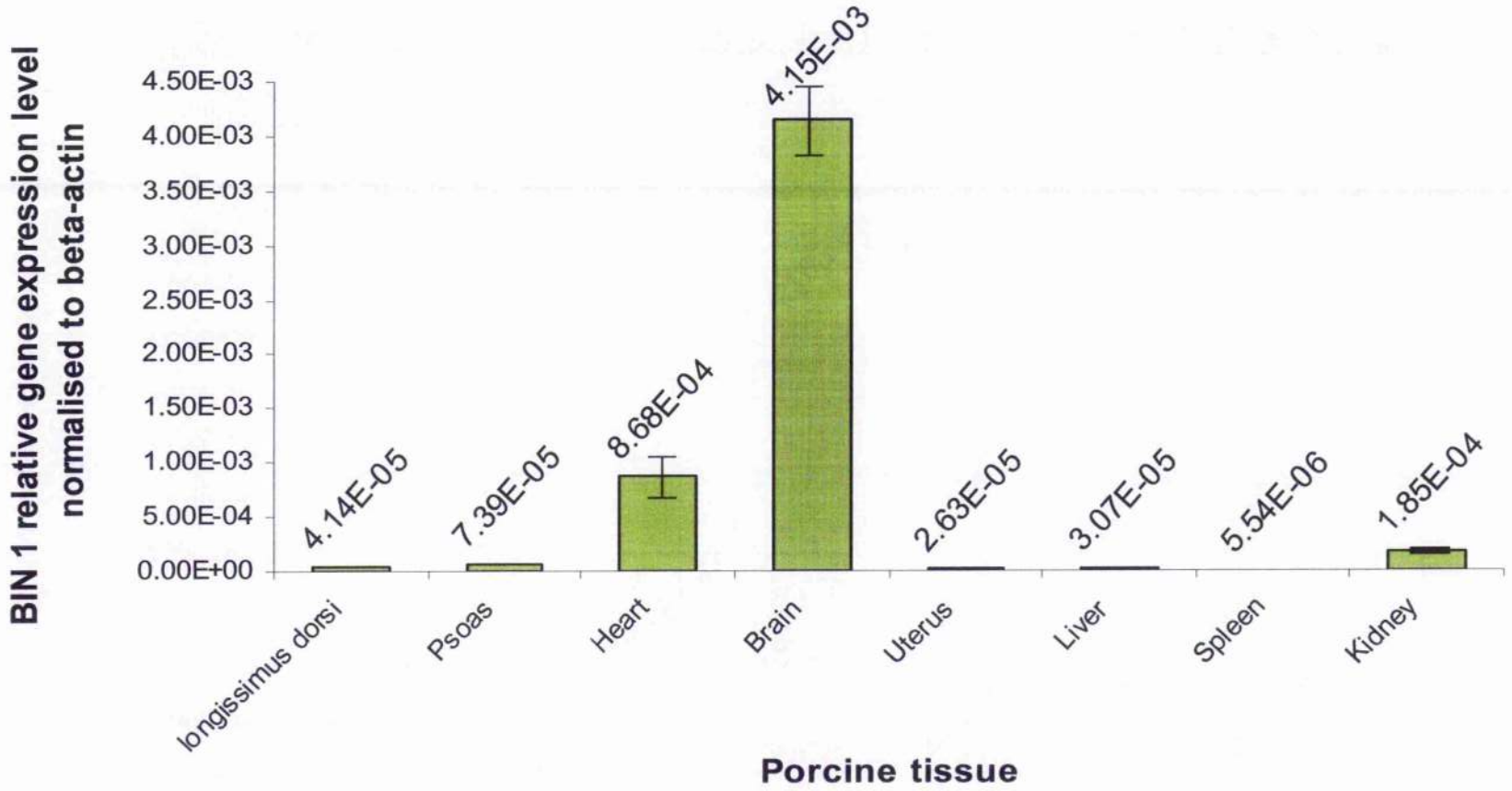

# Figure 3:9 kc2725 relative gene expression levels in *longissimus dorsi* and *psoas* muscles of four pigs

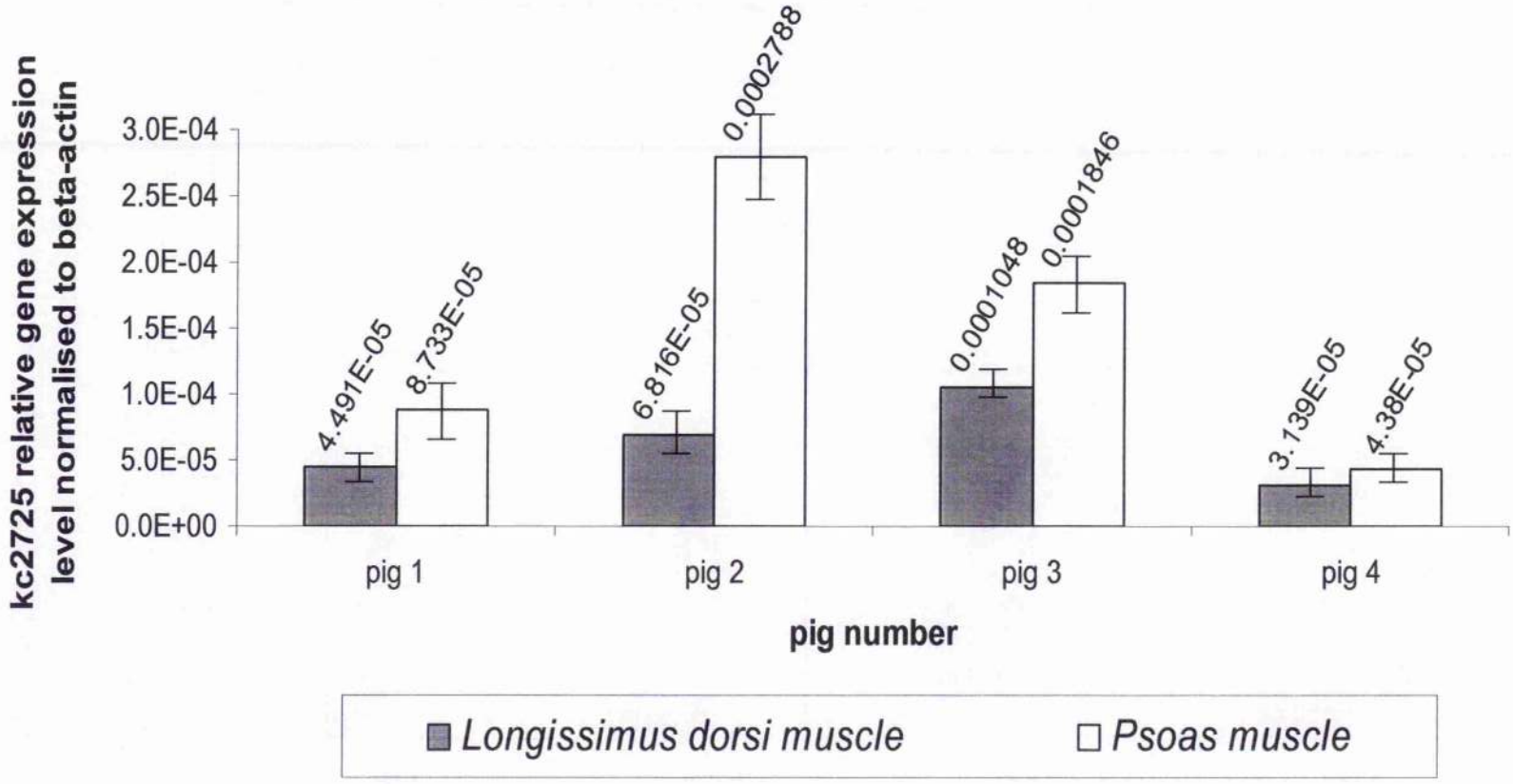

**Figure 3:10 kc2725 relative gene expression levels in eight different porcine tissues derived from the pig 4**

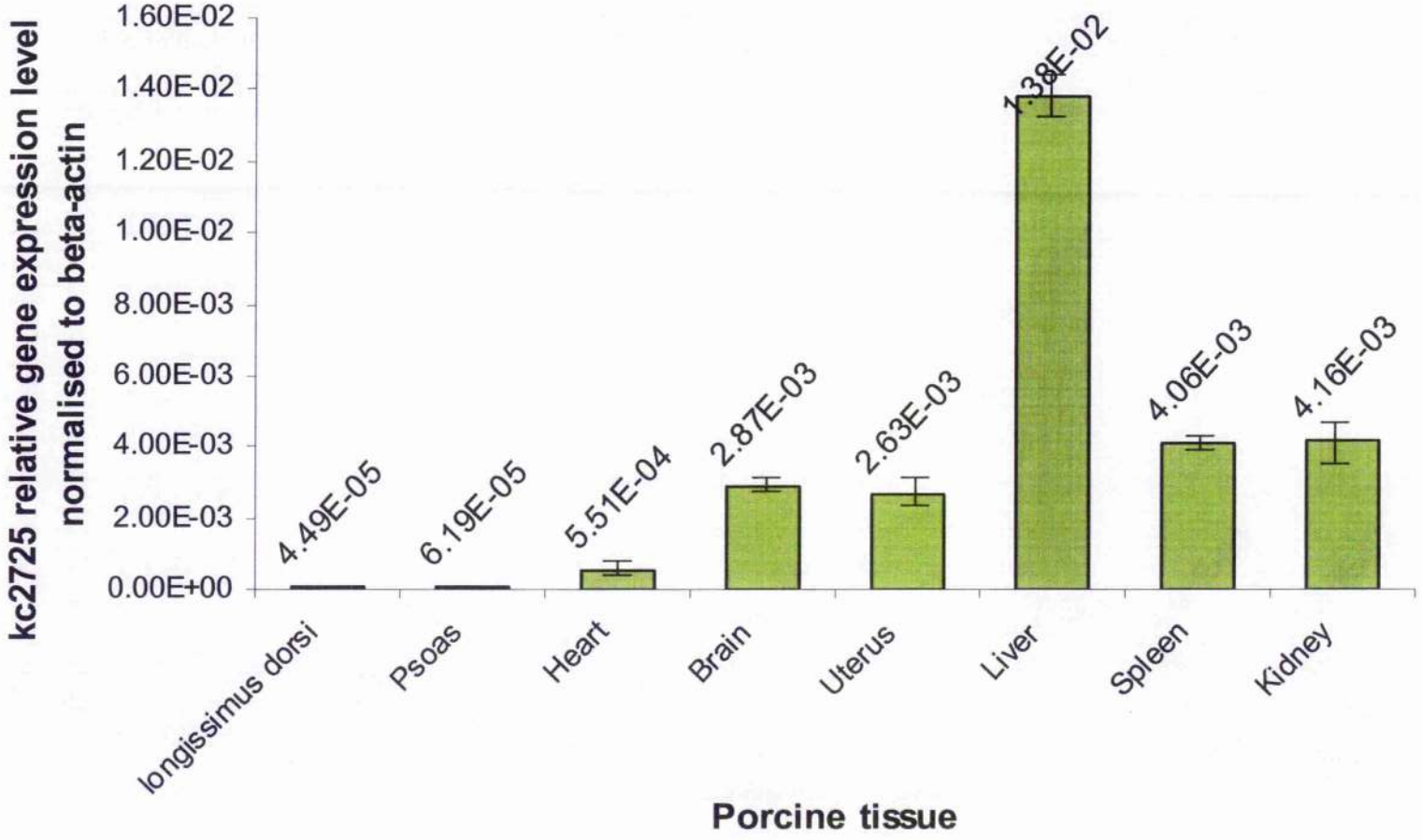

**Figure 3:11 GAPDH and MyHC IIb relative mRNA levels in porcine *psoas* red muscle and *longissimus dorsi* white muscle**

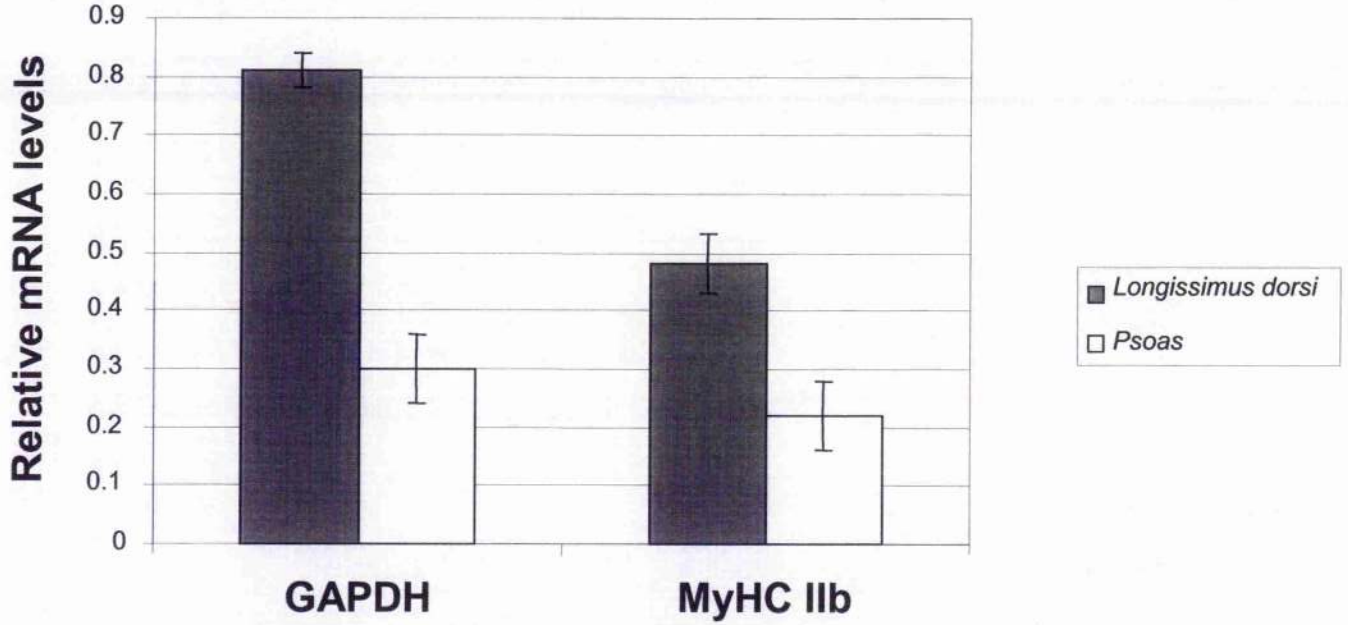

# 3.4. DISCUSSION

The main experimental objective of the red and white muscle microarray gene expression analysis was to evaluate, under experimental conditions, the effectiveness of the in-house constructed porcine skeletal muscle cDNA microarray by profiling the expression patterns in porcine red and white muscles. Two predictable lists of differentially expressed genes were identified by the microarray analysis. Real-time quantitative RT-PCR results were obtained for validating expression levels of the genes selected from the two lists.

The microarray results validated the prior hypothesis of differential gene expression in red and white muscles, thus demonstrating the functional integrity of the newly constructed microarray. One of the well established distinguishing features of red muscle is its relatively high oxidative phosphorylation capacity, reflected by an abundance of mitochondria in red muscles. It is reassuring that genes from the mitochondrial genome were well represented in the red muscle pool of differentially expressed genes (Table 3:5). White muscles comprise predominantly more fast-glycolytic fibres than red muscles. The findings of this study were consistent with expectations, in that most of the 45 clones selected as more highly expressed in white muscle (Table 3:6) were either fast isoforms of structural genes, or enzymes connected with anaerobic glycolysis. With highly expressed genes, such as mitochondrial genes and structural genes, there were detectable levels of redundancies (repeats) on the microarray. However, in the presence of redundancies, no gene was found to be present on both lists. Differentially expressed clones originating from both the foetal and neonatal libraries were found in comparable proportion. A previous report comparing red and white murine skeletal muscles on generic commercial oligonucleotide microarray (Affymetrix GeneChips), which comprised the equivalent of 3,000 different genes, yielded a differential list of 49 known genes (Campbell et al., 2001). In this study, the results of known differentially expressed genes were comparable in both number and in the different types of genes found. One problem underlying the analysis of microarray data is the large number of comparisons required, which can produce false positive results. This study compared the expression of clones in *psoas* and *longissimus dorsi* muscle as the median of 14 comparisons (each microarray clone was printed twice on each slide and 7 slides were used), and restricted further analysis to the clones demonstrating the most consistent and extreme differences. Therefore, the majority of the clones identified in this study are likely to represent real differences between muscles. However, any specific gene assignment should be regarded as

provisional until it can be confirmed in an independent study, such as another microarray or in another assay such as quantitative PCR.

The interpretation of microarray results can be complicated. Firstly, members of the same gene family could cross-hybridise to the same spots on the microarray. Interpretation of differential expression of individual isoforms should therefore be made with caution. In the case of MyHC genes, a plausible interpretation is that fast MyHC mRNA isoforms (IIa, IIx and IIb) were more abundant in the *longissimus dorsi* than in the *psoas*. However, it has previously been found by quantitative real time RT-PCR that in at least 4 out of 6 pigs, of the same sex, age and breed as the one used in the microarray hybridisation, MyHC IIa and IIx were, in fact, more highly expressed in the *psoas* than in the *longissimus dorsi* (da Costa et al., 2002). The 3 fast MyHC isoforms found in Table 3:6 might have been the result of cross hybridisation by the relatively large amounts of MyHC IIb specific probe generated from the *longissimus dorsi* muscle. Secondly, in comparing the profiles of two normal physiological states, such as red and white muscles, large variation in normal gene expression between individual pigs could present a major problem. This variation is mainly attributed to genetic differences that exist between individual pigs; even pigs of the same breed are not genetically the same. The use of pooled porcine mRNA samples could inadvertently increase the genetic variation within each experimental group of animals. Therefore, in the context of porcine red-white muscle microarray analysis, there may be no advantage in pooling mRNAs, derived from the same muscle of several pigs. On the other hand, the use of different muscles from the same pig could minimise the effects of environmental variation, which could exist between individuals. Unlike the use of inbred strains of mice, there is little control over the genetic and metabolic variations that could exist between individual pigs. The use of inbred lines in laboratory rodents largely eliminates the problem of genetic variation between individuals of the same line. Hence, the use of labelled cDNA from pooled inbred individuals would enhance experimental reliability without increasing genetic variation. However, inbred pig strains are not widely available and limited to a few lines of mini-pigs. Whether the microarray probes were derived from an individual or pooled from a group of individuals, extensive validation, such as by quantitative PCR or Northern analysis, is necessary to demonstrate that the differential expression of a gene identified on a microarray is consistent in a wider context.

One important objective of this red and white muscle experiment was to identify a list of candidate regulatory genes that could be involved in determining muscle phenotype, which

includes parameters connected to hypertrophy, differentiation and isoform-specific expression. Indeed, a shortlist of known and unknown candidate regulatory genes was identified. Most of the 10 unknown genes listed as differentially expressed were found with major open-reading frames, suggesting that they code for protein products. Known candidate regulatory genes in the present context are genes with putative identities based on homology comparison. However, with the possible exception of bin1, their functional roles in skeletal muscle are largely unclear. Of the known candidate regulatory genes, CK2 α1 subunit, smpx, and tyrosine kinase A6-related gene were particularly interesting. They were found to be more highly expressed in red muscle and are connected to the casein kinase 2 signalling pathway. CK2 is a protein serine/threonine kinase that has been implicated in cell growth and proliferation (Guerra and Issinger, 1999;Tawfic et al., 2001; Blanquet, 2000) CK2-mediated phosphorylation of Myf-5, a member of a family of myogenic transcription factors, was reported to be required for Myf-5 activity (Winter et al., 1997). Presently, contribution of the CK2 signalling pathway to skeletal muscle function is not known. Its role in muscle phenotype determination deserves evaluation. The gene for heat shock 70kD protein 8 (HSPA8) seemed to be upregulated in white muscle. Heat shock proteins are considered to be molecular chaperones and indicators of cellular stress (Liu and Steinacker, 2001). The same gene was found to be up-regulated in human hypertrophic cardiomyopathy (Lim et al., 2001). It is not clear if this finding was related to cellular stress of myopathy or muscle hypertrophy. Investigations into the function of any candidate gene will need to involve gain-of-function and loss-of-function analysis, such as via *in vitro* transfection studies, using muscle cell lines and primary porcine muscle cells. The results of differential gene expression in red and white muscles exemplify the power of microarray analysis in generating a desirable but substantial list of candidate genes. Its sheer number poses a logistical dilemma for downstream work. The challenge to any investigator is to pick the correct clones to demonstrate their functional significance to the phenotype in question.

Two important questions were considered when evaluating the red-white muscle microarray expression data. The first question was whether the constructed microarray was functional. The second one was whether the microarray results fundamentally described the molecular mechanisms underlying the differences between red and white muscle. The gene expression validation by performing quantitative real-time RT-PCR is not taken as a quality measure of the overall microarray, but as a necessary confirmation of specific gene results. For some of the genes examined in the real-time quantitative RT-PCR in this study, there were significant

quantitative differences, if not contradiction, between the array- and the real-time RT-PCR-based data. Similar observations were also described in other published literature, which argued that genes identified by DNA arrays with a two to fourfold difference in expression should not be accepted as true or false without validation with real-time RT-PCR (Rajeevan et al., 2001a;Rajeevan et al., 2001b;Taniguchi et al., 2001). It has been suggested by the array community that technical questions regarding the differences in accuracy and sensitivity between microarray- and real-time RT-PCR-based methods, and the cost and effect involved in carrying out follow-up studies on a large scale have yet to be thoroughly addressed. Furthermore, obtaining accurate expression measurements involves more than just post-analysis verification of results using an independent laboratory approach. Introduction of artefacts is possible at any time during the array experiment, and so each component of the procedure must be carefully considered.

# CHAPTER FOUR

# MICROARRAY PROFILING OF IONOMYCIN REGULATED GENES

# 4.1. INTRODUCTION

Calcineurin-dependent signalling mechanisms have been characterised extensively in the activation of cytokine gene expression in T and B lymphocytes responding to stimuli that elevate intracellular free calcium concentration ($[Ca^{2+}]_i$). Binding of calcium to a calmodulin-calcineurin complex stimulates serine/threonine phosphatase activity of calcineurin, the major substrates of which are nuclear factor of activated T cells (NFAT) transcription factors. Dephosphorylation of NFATs by calcineurin promotes their translocation from the cytoplasm to the nucleus, where they bind a cognate nucleotide recognition sequence and stimulate transcription of target genes (Crabtree, 1999). Although calcineurin and several NFAT isoforms are abundant in skeletal muscles, target genes that respond to this pathway in skeletal myocytes have not been fully identified previously. Calcineurin activity, tightly regulated by $[Ca^{2+}]_i$, responds preferentially to substained, low-amplitude elevations of $[Ca^{2+}]_i$. The divalent calcium cation $Ca^{2+}$ is used as a major signalling molecule during cell signal transduction to regulate energy output, cellular metabolism, and phenotype. Calcium signals in the cell are generated and highly regulated by ion influx through voltage- and ligand-gated $Ca^{2+}$-permeable ion channels that allow a low resting concentration of $Ca^{2-}$ in the cytosol of the cell, release from internal stores, and sequestration by $Ca^{2+}$ pumps and exchangers. This enables extracellular signals from hormones and growth factors to be transduced as $[Ca^{2+}]_i$ spikes that are amplitude and frequency encoded (Goldring et al., 2002; Hawke and Garry, 2001; Wada et al., 2002). Ionomycin, which has been widely used as a tool to investigate the role of intracellular calcium in cells, has high affinity for calcium, and facilitates the sustained entry of extracellular calcium across biological and artificial membranes by a carrier-type mechanism. Treatment for cells with ionomycin leads to a rise in $[Ca^{2+}]_i$ that allow binding of calcium to the calmodulin-calcineurin complex thereby resulting in the activation of calcineurin. Skeletal muscle satellite cells are undifferentiated mono-nucleate myoblasts, with the capacity to divide extensively and fuse with one another. One objective in this chapter is to further evaluate the effectiveness of the porcine skeletal muscle cDNA microarray by profiling differential gene expression in skeletal muscle myocytes treated with ionomycin or vehicle (dimethyl sulphoxide). This study also aims at identifying transcriptional mediators and target genes related to signalling mechanisms that involve calcium and calcineurin (Rao et al. 1997; Olson and Williams, 2000a; Olson and Williams, 2000b).

# 4.2. MATERIALS AND METHODS

## 4.2.1. TARGET PREPARATION FOR MICROARRAY HYBRIDISATION

### 4.2.1.1. Primary cell culture and ionomycin treatment

The flow diagram in Figure 4:1 shows the methods used in microarray gene expression analysis in this study. In order to obtain skeletal muscle myocytes, a 4-weeks-old Large White cross pig from a local farm was used. *Longissimus dorsi* muscles were removed from the pig, and washed in PBS DULBECCO'S [without (w/o)/lacking calcium, magnesium and sodium bicarbonate] (Gibco™, Invitrogen Corporation) in a 50 ml Falcon tube (Becton Dickinson). The muscle tissues were transferred to a 140 mm sterile Sterilin petri dish (Bibby Sterilin Ltd) in a BioMAT class II microbiological safety cabinet (Medical Air Technology Ltd), and finely dissected using sterile Swann-Morton® disposable scalpels. About 5 ml of the finely minced muscle tissue was transferred to a new 50 ml Falcon tube. Filter-sterilised dispase 1.4 U/ml (Sigma) in PBS DULBECCO'S was added to the minced muscle to obtain a final volume of 50 ml. The mixture of the minced muscle and dispase was incubated at 37 °C for two hours, during which the mixture was shaken fairly vigorously every few minutes. Following incubation, the mixture was centrifuged at 100× g at room temperature for 5 minutes to pellet tissue debris. Debris was removed, and the supernatant was transferred to a new 50 ml Falcon tube using a sterile disposable plastic pipette. Dulbecco's modified Eagle's medium (DMEM) with glutamax-1 (with sodium pyruvate, 4500 mg/l glucose and pyridoxine) (GIBCO™, Invitrogen Corporation), supplemented with 15% [volume/volume (v/v)] heat inactivated foetal bovine serum (Sigma-Aldrich), 50 mg/L penicillin (Invitrogen), 100 mg/L streptomycin (Invitrogen) and 10 µg/ml ciproxin (Bayer), was added to the supernatant to obtain a final volume of 50 ml, followed by centrifugation at 400× g at room temperature for 5 minutes to pellet cells. Following centrifugation, the supernatant was decanted, and the cell pellet was washed with 20 ml DMEM with supplements. The suspension was centrifuged at 400× g for 5 minutes at room temperature to re-pellet cells. Following centrifugation, the supernatant was decanted and the cell pellet was re-suspended in 10 ml DMEM with supplements. The re-suspended cells were filtered using sterile 100-µm nylon cell strainers (Becton Dickinson) into a new 50 ml Falcon tube.

**Figure 4:1** Flow diagram showing methods used for microarray gene expression analysis in this study

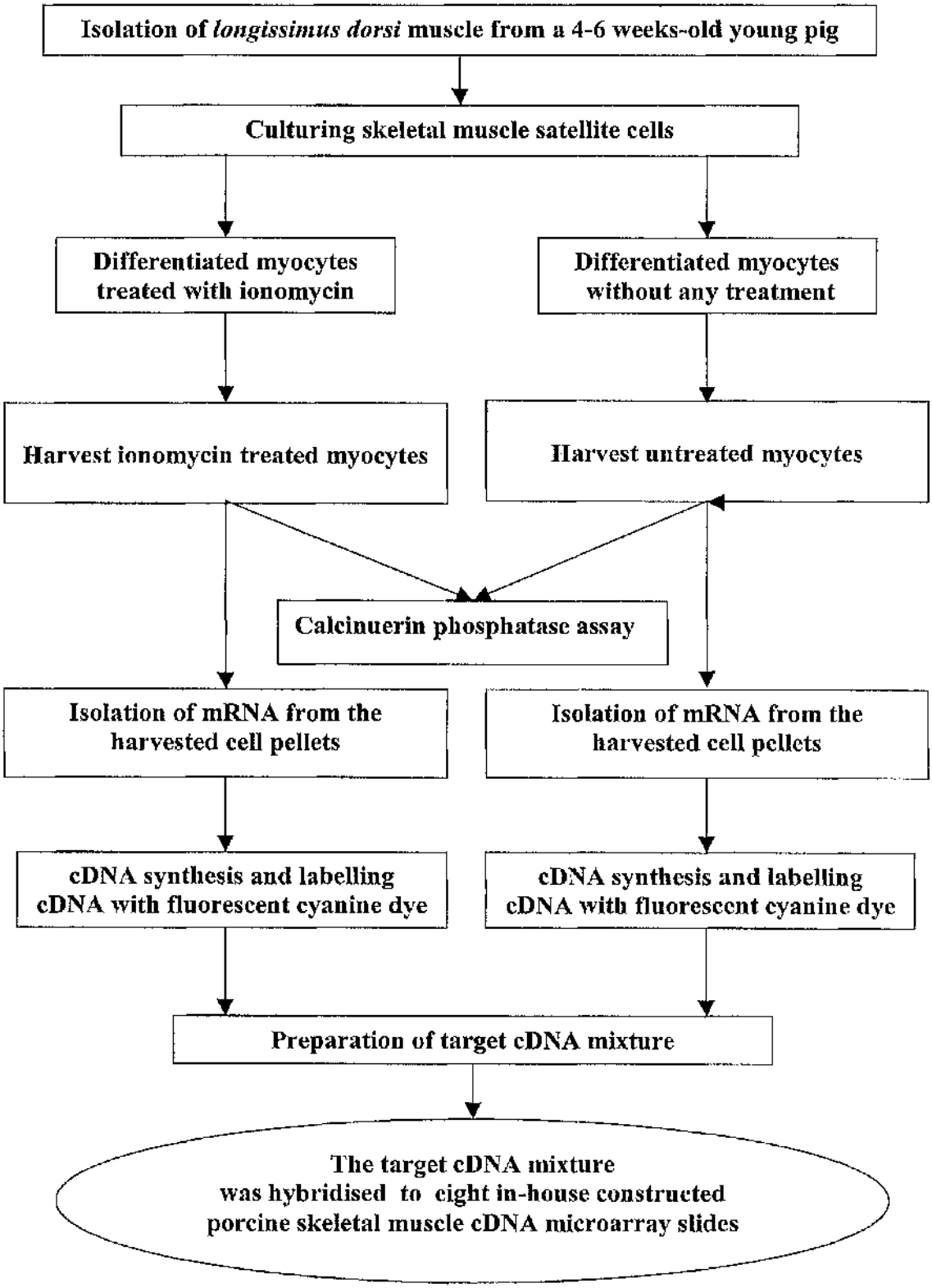

Fifty of sterile Costar® 162 $cm^2$ non-pyrogenic, polystyrene cell culture flasks (Costar®, Corning Incorporated) were used for the primary cell culture. One microlitre of the filtrate was transferred into each of the fifty cell culture flasks. Fifteen microlitres of DMEM, supplemented with 15% (v/v) heat inactivated foetal bovine serum (Sigma-Aldrich), 50 mg/L penicillin (Invitrogen), 100 mg/L streptomycin (Invitrogen) and 10 μg/ml ciproxin (Bayer), was added to the filtrate in each flask. Some cells were plated onto ten chamber glass slides for fixation and morphological analysis and desmin detection. The satellite cells cultured in each 162 $cm^2$ flask was maintained for 48 hours at 37 °C with 5% $CO_2$ in air in a humidified HERA cell incubator (Heraeus). During the culturing process, cells were examined using a Leitz "Labovert FS" trinocular inverted microscope (Leitz). Following incubation, the medium in each flask was discarded. One millilitre of Trypsin-EDTA (1×) in HBSS w/o Ca and Mg w/EDTA.4NA (GIBCO™, Invitrogen Corporation) was added to cells in each flask, incubated at 37°C with 5% $CO_2$ in air in the humidified cell incubator for 5 minutes, and then transferred into a new 50 ml Falcon tube, followed by centrifugation at 1200× g for 5minutes. Cell pellets were re-suspended with 40 ml fresh DMEM with supplements, and transferred into new 162 $cm^2$ flasks. The cells were maintained at 37°C with 5% $CO_2$ in air in the humidified cell incubator for another 120 hours (5 days), during which the medium was replaced every two days. Following five days of incubation, the cells in each flask became about 80-90% confluent. DMEM containing foetal bovine serum in each flask was discarded, and 25 ml of DMEM containing 2% (v/v) heat inactivated horse serum (Sigma-Aldrich), 50 mg/L penicillin, 100 mg/L streptomycin and 10 μg/ml ciproxin were then added to cells. Cells were maintained at 37°C with 5% $CO_2$ in air in the humidified cell incubator for 96 hours (4 days) for differentiation, during which the medium was replaced every two days (Kubis et al., 1997).

After 96 hours of incubation, the medium was removed, and the cells were maintained in 25 ml fresh DMEM with supplements in the absence or presence of ionomycin calcium salt (Sigma-Aldrich). Ionomycin calcium salt was initially dissolved in dimethyl sulphoxide (DMSO) and sterilised using a sterile 0.25 μm filter (Nalgene) to give 1 mM stock solutions. Fifty microlitres of 1mM ionomycin stock solution were diluted with 25 ml DMEM (with supplements) to obtain a final concentration of 2 μM. DMEM (with supplements) containing 2 μM ionomycin calcium salt was added to the myocytes cultured in twenty-five 162 $cm^2$ flaks. The myocytes cultured in the remaining twenty-five 162 $cm^2$ flasks were treated with a vehicle (DMSO) in the absence of ionomycin treatment, serving as a control. DMSO alone had no effect on cultured myocytes at

the concentrations used (0.001-0.05 % v/v) (Scott et al., 1997; Sun et al., 1998). Both cell groups were maintained at 37°C with 5% $CO_2$ in air in the humidified cell incubator for 48 hours prior to harvest.

#### 4.2.1.2. Detection of desmin expression in the cultured cells

##### *4.2.1.2.1. Cell culture on glass slides and methanol/acetone fixation for adherent cells*

Skeletal muscle satellite cells were also cultured on Lab-Tek® II chamber glass slides (Nalge Nunc International). Materials and methods used for the cell culture on chamber glass slides were the same as that described for the cell culture in 162 $cm^2$ flasks (section 4.2.1.1. of this chapter). Following cell culture, the medium was discarded, the glass slides with cells adherent on one side of them were immersed in 1:1 ice-cold methanol:acetone incubated at -20°C in a freezer for 10 minutes. The glass slides were then removed from the -20°C freezer, air-dried at room temperature and then subjected to immunohistochemical staining for desmin.

##### *4.2.1.2.2. Immunohistochemical staining of the cultured cells*

The glass slides with fixed cells on one side were placed in a metal rack and immersed briefly in $ddH_2O$. The glass slides were then placed for 30 minutes in 100 ml methanol containing 0.5% $H_2O_2$, and washed briefly in Tris-buffered Tween. About 1 ml of 1% rabbit serum solution was applied to the cells, and then incubated at room temperature for 30 minutes. Following incubation, 1:500 diluted monoclonal mouse anti-desmin antibody (mouse Ig concentration was 160 mg/L; total protein concentration was 26 g/L) (DAKO), which reacts with intermediate filament protein desmin in skeletal muscle myocytes, was applied to the cells on the glass slides. The cells were incubated at room temperature for 2 hours and then washed with Tris-buffered Tween for three times with 5 minutes for each time. About 1 ml of 1:200 diluted rabbit anti-mouse biotinylated antibody was applied to the cells on the glass slides. The cells were incubated for 45 minutes and then washed with Tris-buffered Tween for three times with 5 minutes each time. About 1 ml of SteptAB Complex/HRP (Dako) was applied to the cells on the glass slides. The cells were incubated for one hour and then washed with Tris-buffered Tween for three times, each time for 5 minutes. A solution of 3,3 diaminobenzidine was applied to the cells on the glass slides, which were examined under the light microscope. The cells were then washed in

$ddH_2O$ to terminate the reaction. The cells on glass slides were placed in Gills Haematoxylin for 30 seconds, then washed in $ddH_2O$. The cells on glass slides were immersed briefly (about 3 dips) in 1% acid alcohol, and then washed in $ddH_2O$. The cells on glass slides were immersed in STWS for staining nuclear, and then washed in $ddH_2O$. The glass slides were placed in methylated spirits, then in absolute alcohol, and finally in citroclear solution. Permanent mountant was then applied to the cells on glass slides.

#### 4.2.1.3. Calcinuerin cellular phosphatase activity assay

##### *4.2.1.3.1. Harvesting skeletal muscle myocytes*

Myocytes, cultured in 162 $cm^2$ flasks and treated with ionomycin or control vehicle, were harvested separately. Before cell harvesting, the myocytes of both category were examined under light microscope to confirm that the cells were about 80-90% confluent. Medium was removed from each flask and discarded. The cells were washed with 20 ml TBS (Tris-buffered saline) (see Appendix) for three times, then scraped off the flasks using a disposable sterile cell scraper (Corning Incorporated) and maintained in TBS on wet ice. Trypsin and PBS were not used in the cell harvesting process in this study because trypsin and PBS contain phosphate, which would have affected the result of the calcineurin cellular phosphatase assay. The cells maintained in TBS were centrifuged using a Heraeus Sorvall Legend RT centrifuge at 1200× g for 5 minutes to pellet cells. The cell pellets were re-suspend with 20 ml fresh TBS. The re-suspended cells were transferred to 2 ml sterile microcentrifuge tubes followed by centrifugation at 1200× g for 5 minutes to pellet cells. The cell pellets were immediately placed on wet ice, then on dry ice, and finally stored in a -80°C freezer. At this stage, the frozen cell pellets were ready for both the assay of calcineurin cellular phophatase activity and the preparation of microarray target mRNAs. Ionomycin-treated cells, which were harvested from five 162 $cm^2$ flasks, and vehicle (DMSO)-treated cells, which were harvested from five 162 $cm^2$ flasks, were both subjected to the assay for calcineurin cellular phosphatase activity. Ionomycin-treated cells, which were harvested from twenty 162 $cm^2$ flasks, and vehicle (DMSO)-treated cells, which were harvested from twenty 162 $cm^2$ flasks, were used to prepare of microarray target mRNAs.

#### *4.2.1.3.2. Preparation of skeletal muscle myocyte extracts*

To determine the effect of ionomycin treatment on the cells cultured in this study, cellular calcineurin phosphatase activity in the cell extracts was measured using CALBIOCHEM® Calcineurin Cellular Activity Assay Kit (Catalogue No. 207007) (Calbiochem-Novabiochem Corporation). Components of this kit included protease inhibitor cocktail tablets, lysis buffer, Green™ reagent, 2× assay buffer, and RII phosphopeptide (full list of components is to be found in the manual of the CALBIOCHEM® Calcineurin Cellular Activity Assay Kit). RII phosphopeptide is the most efficient peptide substrate known for calcineurin. Calcineurin phosphatase activity was measured spectrometrically by detecting free-phosphate released from the calcineurin specific RII phosphopeptide.

The cell pellets, previously harvested using TBS, were removed from -80°C and maintained on dry ice. The protease inhibitor cocktail tablet was added to the lysis buffer (50 mM Tris, 1 mM DTT, 100 µM EDTA, 100 µM EGTA, 0.2% NP-40, pH 7.5) immediately before use, and mixed by vortexing (1 protease inhibitor cocktail tablet per 10 ml lysis buffer). Fifty microlitres of lysis buffer containing protease inhibitors were added to each cell pellet and mixed by pipetting up and down. The mixture was transferred to ultracentrifuge tubes, followed by centrifugation at 100,000 ×g for an hour at 4°C using the TL-100 ultracentrifuge (Beckman). After centrifugation, the debris discarded, the supernatant, which was about 50 µl in each tube, was saved as cell extracts and transferred to sterile 1.5 ml microcentrifuge tubes labelled as "HSS" (high speed supernatant). The quantity of protein in the cell extracts used for each assay was measured by comparing with a protein standard curve (see section *4.2.1.4.3.* of this chapter).The HSS supernatant (cell extracts) was immediately assayed.

#### *4.2.1.3.3. Removal of free phosphate from cell extracts*

A Micro Bio-Spin® Chromatography Column (BIO-RAD Laboratories) was used to remove excess free phosphate and unincorporated nucleotides in the high speed supernatant (HSS). Micro Bio-Spin® Chromatography Columns were inverted sharply several times to re-suspend the settled gel and remove any bubbles. The tip of the column was snapped off and the column was placed in a 2 ml microcentrifuge tube. The top cap of the column was removed to allow the excess packing buffer to drain by gravity to the top of the gel bed. The drained buffer was

discarded and the column was placed back into the 2 ml tube. The Micro Bio-Spin® Chromatography Columns was centrifuged for 2 minutes at room temperature in a Heraeus Biofuge Pico centrifuge at 3,500 rpm [1,000 × (g)] to remove the remaining packing buffer that was later discarded. The column was then placed in a clean 1.5 ml microcentrifuge tube. The HSS supernatant, which was not less than 20 µl was applied directly to the centre of the column. After loading sample, the column was centrifuged at room temprature in a Heraeus Biofuge Pico centrifuge at for 4 minutes at 3,500 rpm [1,000 ×(g)]. Following centrifugation, the column was discarded and the flow through, which was the purified cell extracts, was stored on wet ice for further use. The column retained molecules smaller than the column's exclusion limit. The effective removal of phosphate/nucleotides from the cell extracts was then tested qualitatively by adding 100 µl GREEN™ reagent to 1 µl cell extract and a separate sample of 1 µl of distilled $H_2O$. The GREEN™ reagent is a highly sensitive phosphate detection solution. Free phosphate and unincorporated nucleotides, which are slowly hydrolysed to release free phosphate in the presence of the GREEN™ reagent, is detected visually as a change in colour from yellow to green. If no phosphate/nucleotides were present, both samples should remain yellow in colour over a time period of 30 minutes at room temperature. The development of a visible green colour indicates phosphate contamination, which must be eliminated from the samples before proceeding further. The cell extract flow-through of the column, which was desalted cell lysate material, was collected in the 1.5 ml microcentrifuge tube and frozen on dry ice. About 5 µl purified cell extract was transferred into a new 1.5 ml microcentrifuge tube, to be used for measuring protein concentration.

#### *4.2.1.3.4. Protein quantification*

Eight hundred microlitres of $ddH_2O$ were added to each of twelve plastic cuvettes labelled "cuvette № 1" to "cuvette № 12". Bovine serum albumin (BSA) stock solution (1 mg/ml) was removed from -20°C and thawed at room temperature. In order to obtain a series dilution of the BSA stock solution, 2, 4, 6, 8, 10, 12, 14, 16, and 18 µl of 1 mg/ml BSA stock solution were added respectively to cuvettes № 2, № 3, № 4, № 5, № 6, № 7, № 8, № 9, and № 10. Cuvette № 1 contained distilled $H_2O$ blank. Five microlitres of purified cell extracts from the vehicle (DMSO) treated myocytes were added to cuvette № 11. Five microlitres of purified cell extracts from the ionomycin treated myocytes were added to cuvette № 12. Protein Assay Dye Reagent Concentrate containing phosphoric acid methanol (Bio-Rad) was diluted in a 50 ml Falcon tube

by mixing 12 ml $ddH_2O$ and 3 ml Bio-Rad Protein Assay Dye Reagent Concentrate. One millilitre of the four-times diluted protein assay dye was added to each of the eleven plastic cuvettes containing $ddH_2O$ and the protein samples (BSA or cell extracts). The protein content in each plastic cuvette was measured using a Beckman DU® 640 spectrophotometer (Beckman Coulter, Inc.) at 595 nm absorbance wavelength. The protein concentration standard curve was thus obtained, and the amount of protein used for calcineurin phosphatase activity assay was quantified by comparing with the protein standard curve.

#### *4.2.1.3.5. GREEN™ phosphatase assay*

In order to prepare reagents for the Green™ Phosphatase Assay, all components of the CALBIOCHEM® Calcineurin Cellular Activity Assay Kit were thawed and held on ice, except for the GREEN™ reagent, which was kept at room temperature. Twenty microlitres of calmodulin was added to 980 µl 2× assay buffer. The RII phosphopeptide substrate was reconstituted with distilled $H_2O$ to 750 µM (1.64 mg/ml) by adding 305 µl $ddH_2O$ to a vial containing 0.5 mg RII phosphopeptide (10 µl 1.64 mg/ml RII phosphopeptide were needed per assay well).

In order to prepare phosphate standard curve sample wells, 1:1 serial dilutions of phosphate standard plus a distilled $H_2O$ blank were prepared. Dilutions of 80 µM, 40 µM, 20 µM, 10 µM, 5 µM, 2.5 µM, and 1.25 µM corresponding to 2 nmol, 1 nmol, 0.5 nmol, 0.25 nmol, 0.125 nmol, 0.063 nmol, and 0.031 nmol $PO_4$ were obtained according to the following procedures: (1) fifty microlitres of 80 µM phosphate standard were added to well # 1 of a 96-well microtitre plate. (2) twenty-five microlitres of distilled $H_2O$ were added to wells # 2-8 of the microtitre plate. (3) Twenty-five microlitres of 80 µM phosphate standard were removed from well # 1 and added to well # 2, in which the solution was mixed thoroughly. This process was repeated for wells # 3-7. Finally, 25 µl of the solution in well # 7 was removed and discarded. Well # 8 contained distilled $H_2O$ blank. Twenty-five microlitres of 2× assay buffer were added to each of wells # 1-8, which were used for obtaining the phosphate standard curve. The final volume in each well was 50 µl.

In order to carry out calcineurin total phosphatase activity assay, background wells that did not contain substrate were used as a control for background phosphate/interfering substances. The background wells were set up by adding 20 µl distilled $H_2O$ and 25 µl 2× assay buffer with

calmodulin to each well. The calcineurin total phosphatase activity assay wells used for detecting calcineurin total phosphatase activity in each cell extract sample, were set up by adding 10 µl $dH_2O$ and 25 µl 2× assay buffer with calmodulin to each well. Ten microlitres of phosphopeptide substrate were added to each well of the purified high speed supernatant (HSS) except for the background control. No substrate was added to the phosphate standard curve samples. The microtiter plate was equilibrated to reaction temperature (37°C) for 10 minutes. To initiate the calcineurin assay, 5 µl cell extract was added to each of the appropriate wells. The microtitre plate was incubated at 37°C for 30 minutes. After incubation, the reactions were terminated, by adding 100 µl GREEN™ reagent to each sample including those used for obtaining the phosphate standard curve. The colour was allowed to develop for 20-30 minutes, Absorbance was read for the plate on the microplate reader at 650 nm wavelength, and then data analysis was performed.

#### 4.2.1.4. Preparation of cyanine dye labelled cDNA targets for microarray hybridisations

Messenger RNAs were extracted from ionomycin-treated and control vehicle-treated myocytes, respectively (Fig. 4:2). Materials and methods used for mRNA extraction, single-strand cDNA systhesis, and cyanine dye labelling were the same as those described in Chapter Two and Chapter Three.

## 4.2.2. MICROARRAY HYBRIDISATION AND SEQUENCING ANALYSIS

Materials and methods used for microarray hybridisations and the following image capture, image quantification, data mining, sequencing analysis and BLAST searches were the same as that described in Chapter Three.

# 4.3. RESULTS

## 4.3.1. DESMIN EXPRESSION IN THE CULTURED CELLS

In order to detect presence of desmin in the cells isolated from porcine skeletal muscle, 80-90% confluent cells cultured on chamber glass slides were subjected to monoclonal mouse anti-desmin antibody. About 80-90% of the entire mononucleated cells in porcine cell cultures on chamber glass slides were desmin-positive, suggesting that desmin was synthesised in proliferating porcine satellite cells (Fig. 4:3). The presence of desmin was used as a marker for identifying skeletal muscle satellite cells. Porcine fibroblasts were desmin-negative. Application of desmin staining to porcine satellite cell growth assay indicated that porcine satellite cells cultured in this study were contaminated with porcine fibroblasts at a level that was approximately 15-20% in mature cultures. Desmin is a muscle cytoskeletal protein whose gene belongs to the family of intermediate filament proteins (Lazarides and Hubbard, 1976; Small and Sobieszek, 1977; Geisler and Weber, 1982). Desmin is one of the first muscle-specific proteins to be detected in the mammalian embryo and it is expressed before titin, skeletal muscle actin, myosin heavy chains and nebulin (Hill et al., 1986; Fürst et al., 1989; Babai et al., 1990). Levels of desmin expression in skeletal muscle remain high throughout embryogenesis and in early postnatal life. More than 20 genes are known to be coordinately induced during skeletal myogenic differentiation (Caravatti et al., 1982; Gunning et al., 1987). The expression of the desmin gene differs from most of these genes, which share the property of being repressed in proliferating undifferentiated myoblasts and of being concomitantly expressed with myoblasts fusion. In contrast, desmin expression is initiated in replicating myoblasts and accumulates to a high level as muscle cells differentiate (Pieper et al., 1987; Kaufman and Foster, 1988; Li and Paulin, 1991).

## 4.3.2. CALCINEURIN TOTAL PHOSPHATASE ACTIVITY IN SKELETAL MUSCLE MYOCYTES

The assay for detecting calcineurin total phosphatase activity in the ionomycin-treated or control vehicle (DMSO)-treated myocytes was performed. The calcineurin total phosphatase activity in the ionomycin-treated myocytes (1 nmol phosphate per μg of cell extract protein) was approximately 1.4 times higher than that in the control vehicle-treated myocytes (0.7 nmol

**Figure 4:2** Estimation of mRNAs extracted respectively from ionomycin-treated and vector (DMSO)-treated porcine skeletal muscle myocyte groups using agarose gel containing ethidium brimide

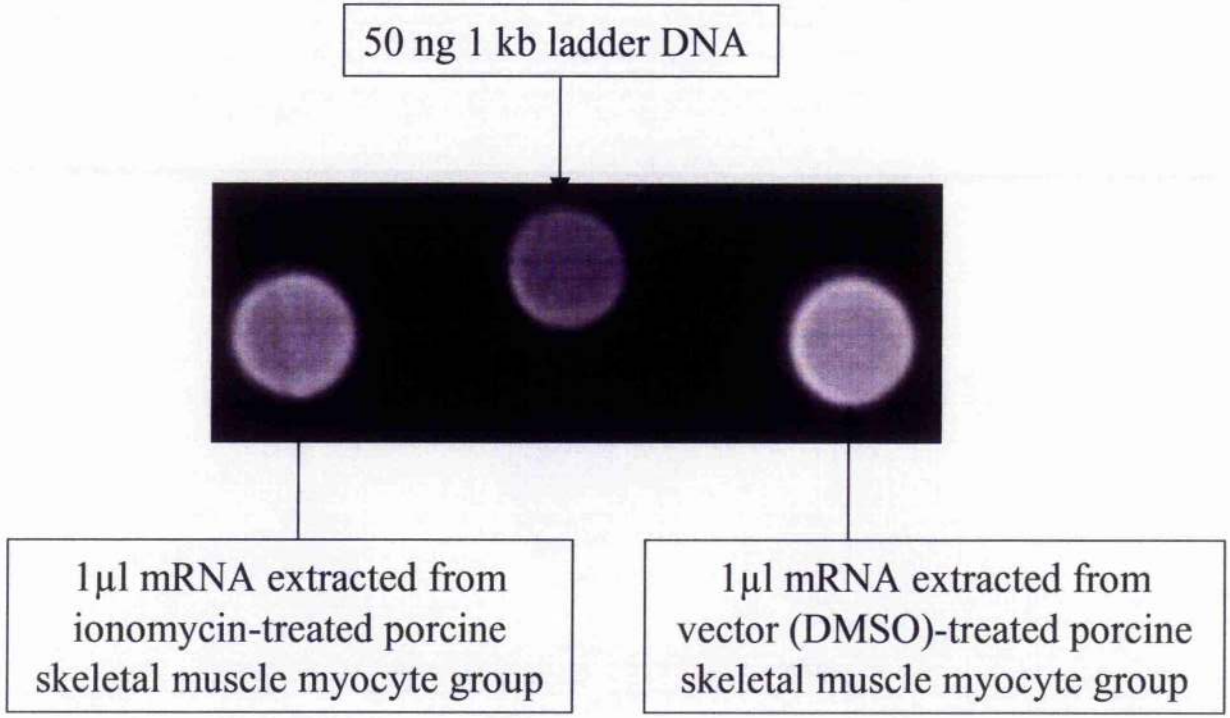

**Figure 4:3 Immunohistochemical staining of porcine skeletal muscle cells with monoclonal mouse anti-desmin antibody**

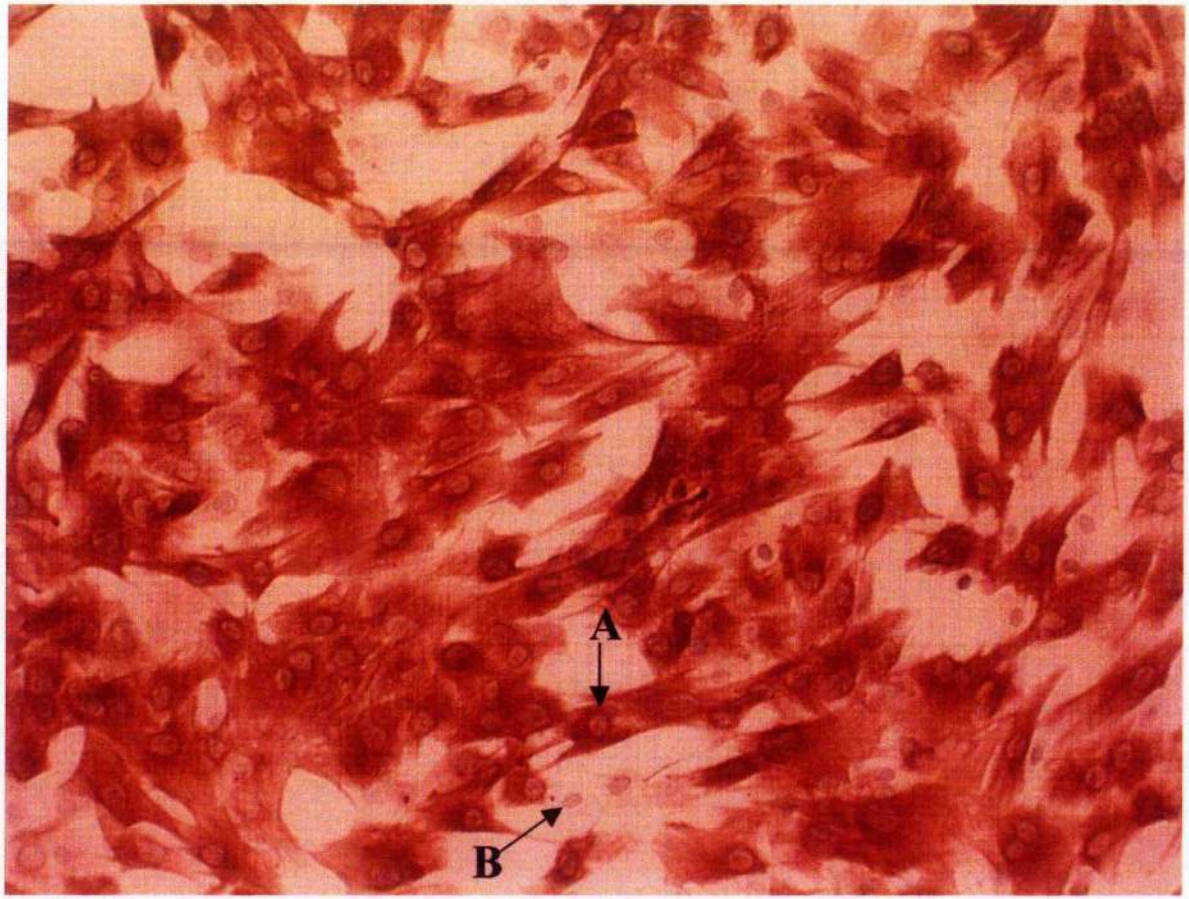


A-Skeletal muscle satellite cells

B-Nucleus of fibroblast

# Fig 4:4 Effects of ionomycin on skeletal muscle myocytes

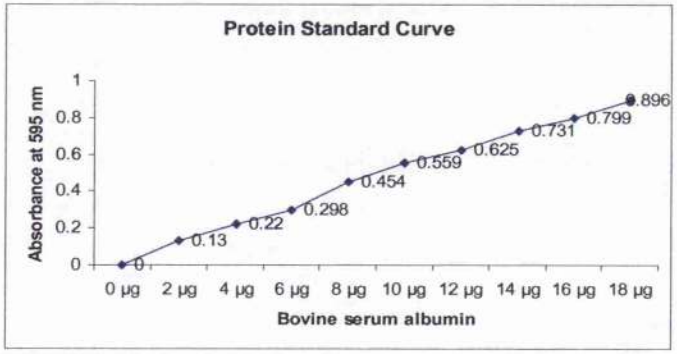


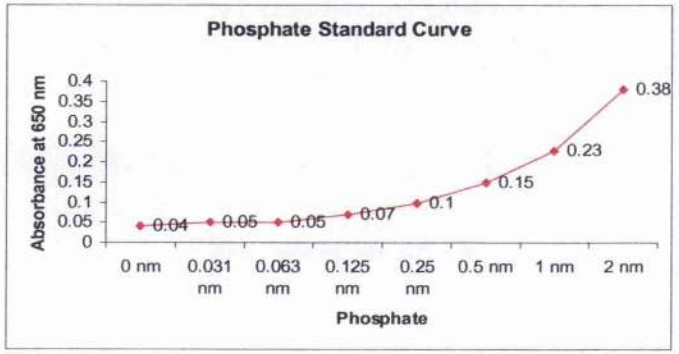


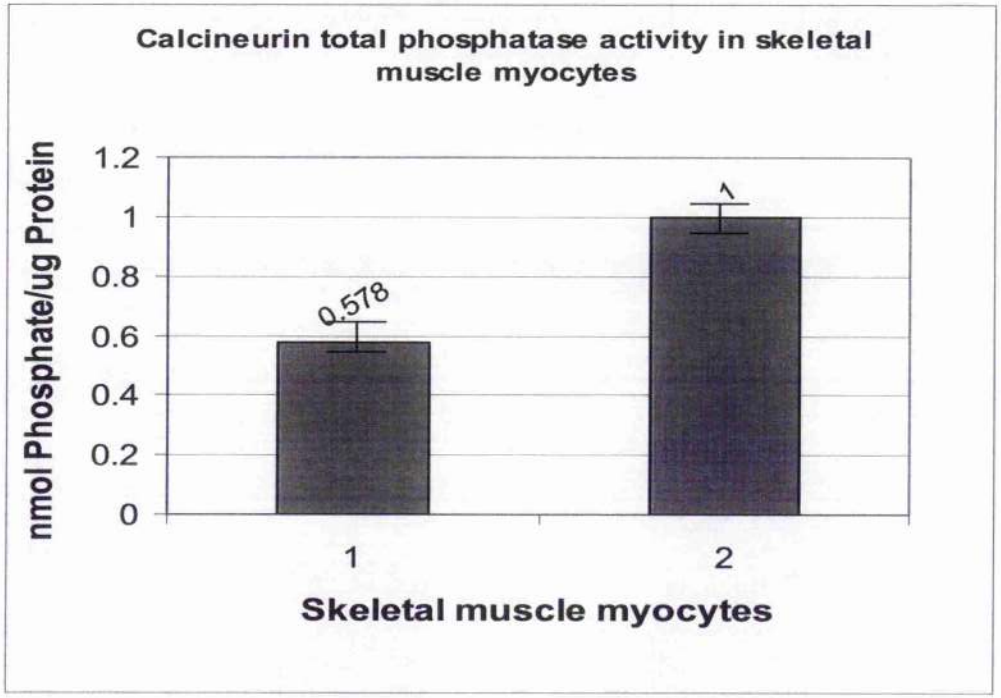


1 Vehicle (DMSO) treated myocytes (control)

2 Ionomycin treated myocytes

phosphate per μg of cell extract protein) (Fig. 4:4), suggesting that calcineurin activity was up-regulated in the myocytes subjected to ionomycin treatment.

## 4.3.3. MICROARRAY IMAGE PROCESSING AND DATA ANALYSIS

Eight dual-coloured array replicates were obtained. Figure 4:5 shows a representative partial hybridised microarray image and ImaGene™ scatter plot. GeneSpring™ scatterplots profiling gene expression patterns in the ionomycin-treated and control vehicle-treated cell groups were obtained by conducting data normalisation and statistical analysis using the GeneSpring™ software. GeneSpring™ scatterplots in Figure 4:6 show separate expression profiles of ionomycin-activated and ionomycin-repressed genes. Figure 4:6 is a derivation of Figure 4:7. Figure 4:7 shows a GeneSpring™ scatterplot profiling expression of total genes including both ionomycin-activated and ionomycin-repressed genes.

## 4.3.4. DIFFERENTIALLY EXPRESSED GENES

### 4.3.4.1. Genes more highly expressed in the myocytes treated with ionomycin

When the data mining criteria of ionomycin-treated/vehicle-treated ratio of 2.0 or more ($P<0.05$), were applied, 68 clones passed the restriction and were detected. They were sequenced and BLAST searches were performed. Table 4:1 is a summary of the genes identified as more highly expressed in the ionomycin treated myocyte group. Of sixty-eight clones characterised, fourteen clones (cytochrome oxidase subunit 1) were of mitochondrial origin; nineteen genes encoded skeletal muscle alpha actin; one gene encoded cardiac alpha actin; nine genes encoded skeletal muscle tropomyosin genes; seven genes encoded cardiac tropomyosin. Other genes such as CD95 (Fas, APO-1)-associated tyrosine phosphatase non-receptor type 13 (PTPN13), polyubiquitin, myotonic dystrophy protein kinase (DMPK) gene, caldesmon 1 (CALD1), muscle cofilin 2, fascin (FSCN), ID3 and fibromodulin (FMOD) were also found in the list of ionomycin-activated genes. Mitochondrial cytochrome oxidase subunit 1 is responsible for aerobic respiration. Polyubiquitin is a protein related to ATP-dependent selective degradation of cellular proteins. Myotonic dystrophy protein kinase (DMPK) is responsible for myotonic dystrophy. Various isoforms of

**Figure 4:5 Microarray image processing**

A

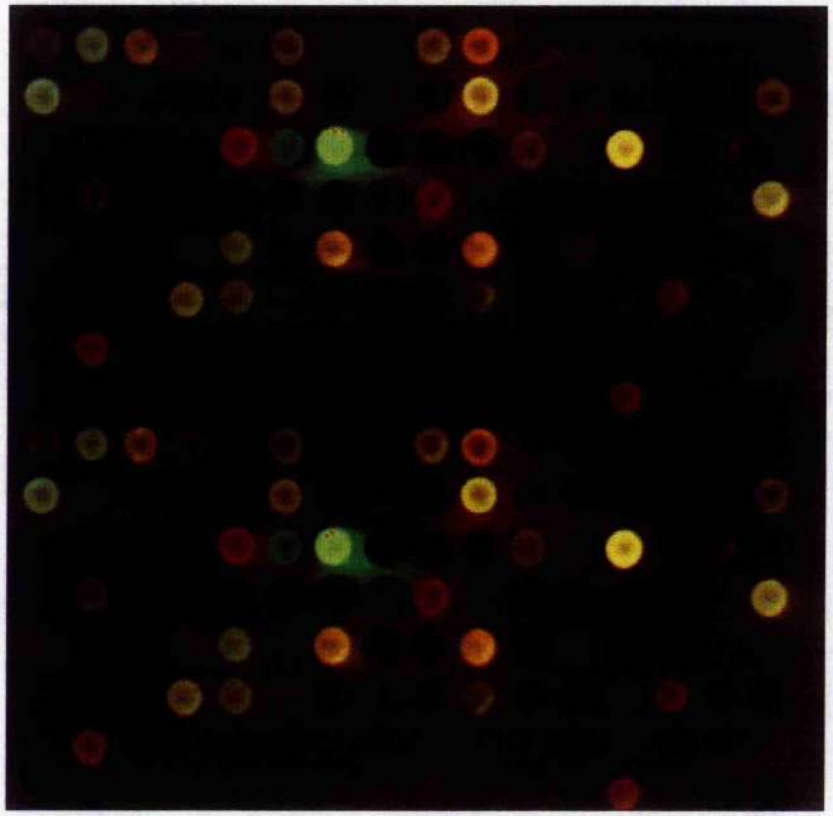

Ionomycin treated  Control vehicle treated

**Microarray image processed using Imagene™ software**

B

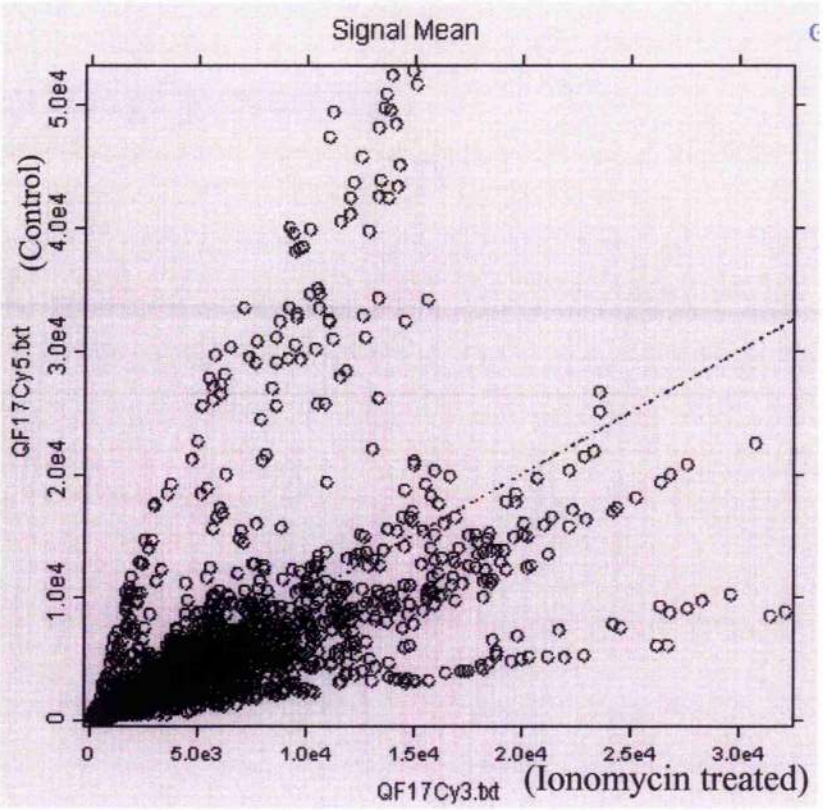


**Imagene™ Scatterplot**

## Figure 4:6 Expression profiling of ionomycin-regulated genes using GeneSpring™ software

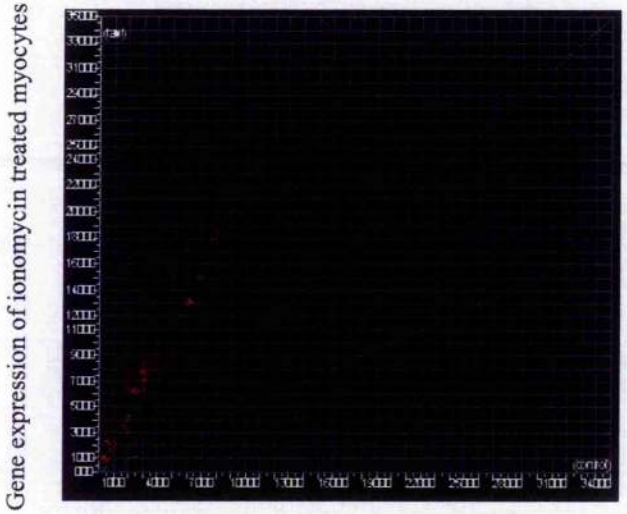


**GeneSpring™ Scatterplot shows the genes up-regulated by ionomycin treatment**

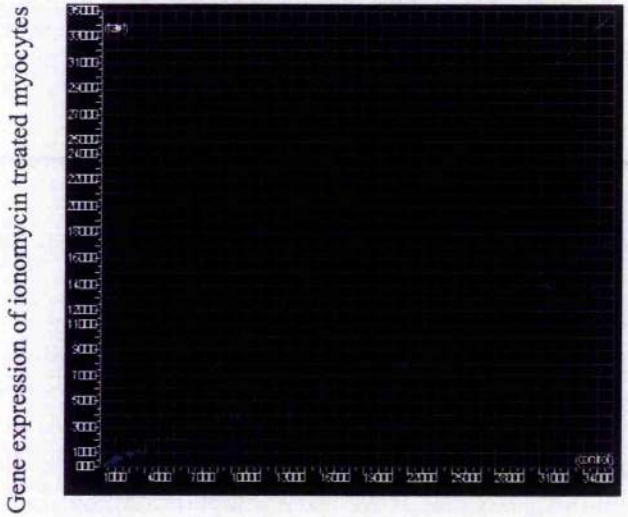


**GeneSpring™ Scatterplot shows the genes down-regulated by ionomycin treatment**

**Figure 4:7 Expression profiling of total genes using GeneSpring™ software**

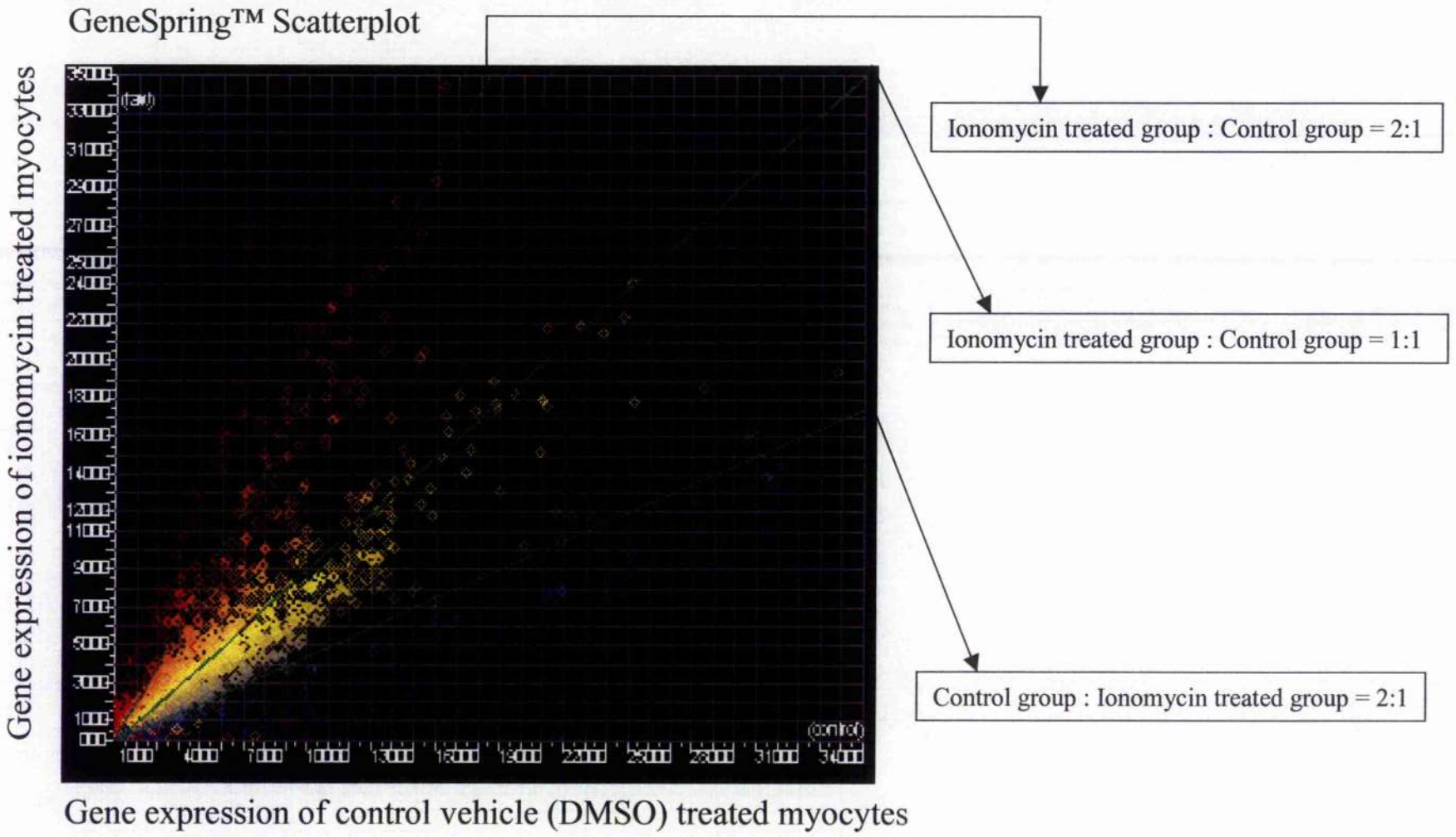

**Table 4:1** Genes that were at least two-fold ($P<0.05$) more highly expressed in the ionomycin-treated myocytes than in the vehicle-treated myocytes

| Closest Putative Identity | Ionomycin-treated /Vehicle-treated | Homology | # of Clone | Accession # |
|---|---|---|---|---|
| Cytochrome oxidase subunit 1 | 2.36 | 100% (P) | 14 | AF030277 |
| NADH dehydrogenase subunit | 2.66 | 97% (H) | 1 | AF493542 |
| Skeletal muscle alpha actin | 2.79 | 93% (H) | 19 | XM_001869 |
| Cardiac alpha actin (Actc1) | 2.83 | 91% (M) | 4 | NM_009608 |
| Fibromodulin(FMOD) | 3.16 | 95% (B) | 2 | X16485 |
| Myosin regulatory light chain | 2.32 | 91% (B) | 1 | AF513721 |
| F-actin binding protein nexilin | 3.21 | 92% (H) | 2 | NM_144573 |
| Cardiac alpha tropomyosin | 2.67 | 98% (P) | 7 | X66274 |
| Skeletal muscle tropomyosin | 2.74 | 92% (H) | 9 | M75165 |
| Fascin homolog 2 (FSCN2), actin-bundling protein | 2.65 | 95% (H) | 1 | NM_012418 |
| Caldesmon 1 (CALD1) | 2.24 | 96% (H) | 1 | XM_058059 |
| Cofilin 2 (muscle) mRNA | 3.01 | 96% (H) | 1 | BC022876 |
| Protein tyrosine phosphatase, non-receptor type 13 (PTPN13) | 2.98 | 86% (H) | 1 | NM_006264 |
| ID3 protein (ID3 gene) | 2.04 | 93% (D) | 1 | AJ271644 |
| Dystrophia myotonica-protein kinase (DMPK) | 2.87 | 83% (H) | 1 | XM_027572 |
| MYB binding protein, mRNA | 2.19 | 94% (H) | 1 | NM_014520 |
| Polyubiquitin | 2.51 | 97% (P) | 1 | M18159 |
| Unknown clones, homologous to *Homo sapiens* chromosome 14 DNA sequence BAC R-137H15 of library RPCI-11 | 2.11 | 87% (H) | 1 | AL135998 |

Accession # refers to porcine gene or close homologue: (P) = Porcine, (B) = Bovine, (H) = Human, (M) = House mouse, (D) = Domestic dog.

DMPK have been reported in skeletal and cardiac muscles. The functional role of DMPK, which has so far not been fully understood, may play an important role in the modulation of the $Ca^{2+}$ homeostasis in skeletal muscle cells. Caldesmon (CALD1) is an actin- and myosin-binding protein implicated in the regulation of actin-myosin interactions, possibly acting as a bridge between myosin and actin filaments in smooth muscles and non-muscle tissues. Although some studies reported that caldesmon was not expressed in skeletal muscle or heart (Wang & Yang, 2000; Mani *et al*, 1992; Ishikawa *et al*, 1992), caldesmon gene was found in this study to be up-regulated in the ionomycin-treated skeletal muscle myocytes. Cofilins are actin-binding proteins and regulate actin assembly. Cofilin 2 (CFL2) is a skeletal muscle actin-modulating protein, which plays an important role in normal muscle function and muscle regeneration (Thirion et al.,

2001). Fascin (FSCN) is an actin-crosslinking protein in the core actin bundles of cell-surface spikes and projections that are implicated in cell motility. Fascin is also a tumor marker with potential diagnostic and therapeutic implications for pancreatic carcinoma (Jawhari et al., 2003; Maitra et al., 2002). Fibromodulin (FMOD) is a collagen binding protein and a key regulator of tendon strength (Hedbom and Heinegard, 1989). FMOD regulates the assembly of collagens into higher-order fibrils in connective tissues and thus aids fibril maturation (Jepsen et al., 2002). The detection of FMOD in this study could be due to the inclusion of fibroblasts in the primary cell culture when isolating skeletal muscle samples from the pigs. The helix-loop-helix (HLH) motif-containing transcription inhibitor ID3 (for Inhibitor of Differentiation-3) inhibits the binding of E2A-containing protein complexes to muscle creatine kinase E-box enhancer. ID3 has been shown to be highly expressed in proliferating myoblasts but down regulated when myoblasts are induced to differentiate (Yeh and Lim, 2000). Moreover, overexpression of ID3 has been shown to inhibit skeletal muscle differentiation program and repress muscle-specific gene expression (Yeh and Lim, 2000; Jen et al., 1992). Enforced expression of ID3 has been found to be a strong inducer of apoptosis in serum-deprived fibroblast cells (Norton and Atherton, 1998).

#### 4.3.4.2. Genes more highly expressed in the myocytes treated with vehicle (DMSO)

When the data mining criteria of vehicle-treated/ionomycin-treated ratio of 2.0 or more ($P<0.05$), equivalent to ionomycin-treated /vehicle-treated ratio of 0.5 or less ($P<0.05$), was applied, 12 clones passed the restriction. They were sequenced and BLAST searches were performed. Table 4:2 is a summary of the genes identified more highly expressed in skeletal muscle myocytes treated with control vehicle (DMSO). Of twelve clones characterised, seven cytochrome oxidase genes were of mitochondrial origin, four genes encoded ribosomal proteins, and one gene encoded S100 calcium binding protein A10 (also called annexin II light chain or calpactin light chain). S100 proteins are a family of calcium binding proteins that function to transmit calcium-dependent cell regulatory signals. S100 proteins have no intrinsic enzyme activity but bind in a calcium-dependent manner to target proteins to modulate target protein function.

**Table 4:2** Genes that were at least two-fold ($P<0.05$) more highly expressed in the vehicle-treated myocytes than in the ionomycin-treated myocytes

| Closest Putative Identity | Vehicle-treated /Ionomycin treated | Homology | # of Cloue | Accession # |
|---|---|---|---|---|
| Cytochrome oxidase subunit 1 | 2.43 | 99% (P) | 7 | AF304202 |
| Ribosomal protein S15a | 2.17 | 92% (H) | 1 | BC030569 |
| Ribosomal protein S3 | 2.62 | 91% (H) | 1 | BC034149 |
| Ribosomal protein S23 (RPS23) | 2.81 | 93% (H) | 1 | NM_001025 |
| Ribosomal protein S2 | 2.09 | 91% (B) | 1 | AF013215 |
| S100 calcium binding protein A10 (S100A10) [annexin II ligand, calpactin I, light polypeptide (p11)] | 2.69 | 94% (H) | 1 | XM_001468 |

Accession # refers to porcine gene or close homologue: (S) = Porcine, (H) = Human, (B) = Bovine.

# 4.4. DISCUSSION

The primary goal of this study was to further assess the effectiveness of the constructed porcine skeletal muscle cDNA microarray for high throughput gene expression profiling. The microarray experiment described in this chapter focused on identifying genes that were differentially expressed in skeletal muscle myocytes in the presence or absence of ionomycin. Results from the eight replicated microarray hybridisations demonstrated that the porcine cDNA microarray was able to generate a list of genes that were at least 2-fold more highly expressed in the ionomycin-treated myocytes.

According to previous published information, treatment for cells with ionomycin led to a rise in intracellular free calcium concentration ($[Ca^{2+}]_i$) that allowed binding of calcium to the calmodulin-calcineurin complex thereby resulting in the activation of calcineurin (Rao et al., 1997). In this study, although the cellular phosphatase activity of calcineurin was up-regulated in the ionomycin-treated myocytes, neither calcineurin nor the targets of calcineurin phosphatase activity (e.g., NF-AT, MEF2) were found in the list of genes that were at least 2-fold more highly expressed in the ionomycin-treated myocytes. Calcineurin activity is essential for activation of the skeletal muscle differentiation program, which involves irreversible withdrawal of myoblasts from the cell cycle, fusion to form multinucleate myotubes, and transcriptional

activation of muscle-specific genes (Berchtold et al., 2000;Delling et al., 2000;Friday et al., 2000). In this study, however, no multinucleate myotubes were found by light microscopy in the primary cultures of satellite cells. It is obvious that in this study the porcine myoblasts did not fuse in either ionomycin-treated or control vehicle-treated primary cell cultures. Even the desmin-positive cells did not have the typical morphology of myoblasts expected to be spindle shaped. Therefore, culture requirements for the porcine skeletal muscle primary cultures require further work that is not possible to be included in this study, due to the restrictions on time limit towards the end of a three-year project. Also, desmin is not an ideal marker for skeletal muscle cells, because even the skeletal myoblasts are expected to synthesise low levels of more specialised myofibrillar proteins such as myosins, troponins and tropomyosin etc. DMSO is a well-known modulator of cell differentiation not only for muscle cells but also for non-muscle cells. For example, Blau and Epstein stated that 2% DMSO inhibits the fusion of myoblasts to form multinucleate myotubes. However, unlike skeletal muscle cells, DMSO is known to promote differentiation of HL60 cells. DMSO alone has no effect on cultured myocytes at the concentrations used (0.001-0.05 % v/v) (Scott et al., 1997; Sun et al., 1998). Although no fused myotubes were observed in the primary cell cultures in this study, it is unlikely that the lack of differentiation is related to the inhibition of differentiation by DMSO, because much lower (0.02% v/v) concentration of DMSO was used in this study. Therefore, DMSO (0.02% v/v) used in this study had no effect on the fusion of myoblasts. Ionomycin is a toxic chemical. Previous published studies showed that toxic chemicals that generated oxidative stress or induced a pathologic increase in cellular calcium levels could target $Ca^{2+}$ signalling processes resulting in a prolonged elevation of $[Ca^{2+}]_i$, depending on the degree of exposure (Trump and Berezesky, 1996;Dypbukt et al, 1994;Raffray and Cohen, 1997;Bonfoco et al, 1995). Elevated cytoplasmic $Ca^{2+}$ levels can cause activation of certain proteases, lipases, and nucleases. Altered physiological properties of skeletal muscle, altered gene transcription and transformation of muscle fibres, necrosis, and apoptosis may be the consequences (Orrenius and Nicotera, 1994;Berchtold et al., 2000). In this study, the effect of prolonged (48 hours) ionomycin treatment on cultured myocytes was likely to be toxic. CD95 (Fas, APO-1)-associated tyrosine phosphatase non-receptor type 13 gene (PTPN13), also known as FAP-1 (Fas-associated phosphatase-1), was up-regulated by the ionomycin treatment (Table 4:1). The protein encoded by PTPN13/FAP-1 is a member of the protein tyrosine phosphatase family, which regulates a variety of cellular processes including cell growth and differentiation (Sato et al., 1995). CD95 (Fas, APO-1) is a cell surface receptor belonging to the tumor necrosis factor receptor superfamily (Inazawa J, 1996). Some published studies reported that tissues and cell lines

resistant to CD95 (Fas, APO-1)-mediated cytotoxicity/apoptosis strongly over-expressed PTPN13/FAP-1, which binds to CD95 (Fas, APO-1) and inhibited CD95 (Fas, APO-1)-induced cytotoxicity/apoptosis and promotes cellular survival (Sato et al., 1995;Westphal and Kalthoff, 2003;Inazawa J, 1996;Yanagisawa et al., 1997; Ivanov et al., 2003). Other studies reported that PTPN13/FAP-1 triggered apoptosis in human breast cancer cells, and this effect was independent of CD95 (Fas, APO-1) but associated with an early inhibition of the IGF-1/PI3K/AKT pathway (Bompard et al., 2002). Apoptosis is a form of programmed cell death occurring during organogenesis and organ remodelling and in adult life to modulate the immune system or to kill transformed and virally infected cells (Kerr et al, 1987;Kerr et al, 1972;Arends and Wyllie, 1991). The mechanisms by which PTPN13/FAP-1 inhibits CD95 (Fas, APO-1)-mediated cell death signalling, or triggers apoptosis remain unclear. In this study, the upregulation of PTPN13/FAP-1 in the ionomycin-treated myocytes could suggest that the skeletal muscle myocytes were resistant to the CD95 (Fas, APO-1)-mediated apoptosis, or could suggest that PTPN13/FAP-1 triggered apoptosis in the ionomycin-treated myocytes. Cells undergoing apoptosis show well-defined morphologic and biochemical changes including cellular and nuclear shrinkage, condensation, margination and fragmentation of chromatin, changes in plasma membrane architecture, and intracellular proteolysis (Kerr et al, 1987; Rudin and Thompson, 1997; Jacobson et al, 1997). However, in this study, when examined by light microscopy, no morphologic changes were found in the myocytes treated with ionomycin. Although this preliminary study showed that the constructed porcine cDNA microarray was able to generate a list of genes differentially expressed in the ionomycin-treated myocytes, the sum of the present data does not provide sufficient information on the involvement of the $Ca^{2+}$/calmodulin/calcineurin signaling pathways in the ionomycin-treated myocytes.

To complement the study described in this chapter, the following experimental designs using the constructed porcine cDNA microarray can be adopted and carried out in the future. The skeletal muscle myocytes can be cultured in the presence or absence of 2 μM ionomycin, and the cells can be harvested at 0, 1, 2, 4, 8, 16, and 24 hours timepoints for microarray differential gene expression analysis. The immunosuppressive agents cyclosporin A (CsA) and tacrolimus (FK506) bind to intracellular immunophilin receptors, cyclophilin (CyP) and FK506 binding protein FKBP), respectively. The complexes of CsA-CyP and of FK506-FKBP both bind to and inhibit the activity of the calcium/calmodulin-dependent serine/threonine phosphatase calcineurin. Therefore, at each of the 5 timepoints (0, 1, 2, 4, 8, 16, and 24 hours) of ionomycin treatment, the transcriptional responses of ionomycin-treated myocytes can be characterised

using the porcine cDNA microarray following stimulation in the absence or presence of cyclosporin A (CsA) or tacrolimus (FK506), hoping to identify target dependent upon calcineurin or specific targets of either CyP or FKBP inhibitable by one drug alone. Furthermore, at each of the 5 timepoints (0, 1, 2, 4, 8, 16, and 24 hours) of ionomycin treatment, dose-dependent effect of ionomycin on skeletal muscle myocytes can also be characterised using the porcine cDNA microarray after treating the myocytes with 0, 0.25, 0.5, 1, and 4 μM ionomycin.

# CHAPTER FIVE

# GENERAL DISCUSSION

# 5.1 IMPORTANCE OF THE PORCINE cDNA MICROARRAY FOR PROFILING DIFFERENTIAL GENE EXPRESSION

The major achievement of this study was the completion of the novel porcine skeletal muscle cDNA microarray, which contained 5,500 cDNA fragments derived from both pre-natal and post-natal porcine skeletal muscle cDNA libraries. The entire process for creating the porcine cDNA microarray, which was composed of the construction process and the quality control process, was successful. The quality control process adopted by this study to ensure uniformity, accuracy and reliability of the microarray was considered to be necessary for achieving the porcine cDNA microarray of a high quality. The red and white muscle microarray gene expression analysis described in Chapter Three optimised experimental conditions peculiar to the utilisation of this *de novo* created microarry (Figures 3:1 and 3:2). The fluorescent images of the microarray hybridisations and the subsequent data mining results uncovered substantial differences in gene expression between red and white muscle (Figures 3:4, 3:5 and 3:6) with a number of these identified, differentially expressed genes [e.g., genes of mitochondrial origin, genes for myosin heavy chain fast isoforms (Tables 3:5 and 3:6)] in either categories well-matched respectively with the physiological characteristics of the two types of the skeletal muscles. The red and white muscle microarray experiment demonstrated the usefulness and reliability of the porcine cDNA microarray by profiling high-throughput differential gene expression, which was in good agreement with prior knowledge of the systems under study (Pette and Staron, 1990;Schiaffino and Reggiani, 1996). Expression patterns of four genes (bin 1, novel gene kc2725, MyHC IIb and GAPDH) validated by real-time quantitative RT-PCR (Figures 3:7, 3:9 and 3:11) were well-matched respectively with their differential gene expression patterns identified by the red-white muscle microarray analysis. Thus, the effectiveness of the porcine cDNA microarray for profiling differential gene expression was confirmed. The experiment described in Chapter Four revealed the alterations in the transcript level of thousands of transcriptomes in the skeletal muscle myocytes treated with ionomycin, and uncovered a number of ionomycin-regulated genes [e.g., PTPN13, DMPK (Tables 4:1)]. This experiment further demonstrated that the porcine cDNA microarray is capable of profiling differential gene expression. In conclusion, the strengths of the study concerning the in-house construction and the subsequent utilisation of the porcine skeletal muscle cDNA microarray include: (1) the availability of a large number of cDNA fragments maintained in the form of plasmid inserts and in the form of PCR-amplified and purified free cDNA fragments, both of which have been maintained as frozen stocks; (2) the ability to print hundreds of the porcine

skeletal muscle cDNA microarray slides; (3) the uniform morphology and high DNA concentration of the printed microarray spots/probes; (4) the clone tracking system established for the porcine cDNA microarray; (5) the hybridisation conditions optimised specifically for the use of the porcine cDNA microarray; (6) the high signal-to-noise ratio and good statistical reproducibility of the microarray hybridisation results obtained with the help of the software tools for image processing and data analysis.

The *de novo* constructed porcine skeletal muscle cDNA microarray has been proved to be a useful biological tool for determining levels of gene expression. Instead of investigating the complexity of skeletal muscle biological effects by analysing single genes of putative importance one after the other, gene expression profiling using the *de novo* constructed porcine cDNA microarray facilitates an experimental approach where alterations in the transcript level of thousands of transcriptomes can be simultaneously detected in various biological contexts. Firstly, this allows one to find out which genes are involved in a biological event and, secondly, it permits detailed analysis of their action or interaction afterwards (Bai et al., 2003;da Costa et al., 2004).

## 5.2 IMPORTANCE OF THE IDENTIFIED CLONES IN SKELETAL MUSCLE RESEARCH

The microarray analysis of red and white muscle, and the access to the microarray clone stocks, allowed a number of differentially expressed genes to be identified [e.g. genes for bin 1, HSPA8, CK2 α1 subunit (Tables 3:5, 3:6)], the function of which had not previously been fully elucidated. These differentially expressed regulatory genes, which could be involved in muscle phenotype determination, should be further investigated to define their roles in skeletal muscle. For example, CK2 α1 subunit, smpx, and tyrosine kinase A6-related gene were found to be more highly expressed in red muscle and are connected to the casein kinase 2 signalling pathway, the contribution of which to skeletal muscle function is not known presently. It would also be important to define the role of the novel gene kc2725 in skeletal muscle in both physiological and pathological situations. PTPN13, which was identified in Chapter Four to be up-regulated in the ionomycin-treated skeletal muscle myocytes, regulates cell growth and differentiation, and is connected to CD95 (Fas, APO-1)-mediated cytotoxicity/apoptosis (Sato et al., 1995; Westphal and Kalthoff, 2003;Inazawa J, 1996). However, the mechanisms by which PTPN13 inhibits

CD95 (Fas, APO-1)-mediated cell death signalling, or triggers apoptosis remain unclear. DMPK was also found to be up-regulated in the ionomycin-treated myocytes. DMPK, the functional role of which in skeletal muscle has not been fully understood, is connected to the modulation of the $Ca^{2+}$ homeostasis in skeletal muscle cells (Benders et al., 1997). In conclusion, the differentially expressed genes identified by this project may play pivotal roles in skeletal muscle biology, and therefore, deserve further evaluation.

## 5.3 FUTURE DIRECTION IN THE UTILISATION OF THE PORCINE cDNA MICROARRAY

High-throughput gene expression analysis with the *de novo* constructed porcine skeletal muscle cDNA microarray could be able to provide in the future valuable information about molecular mechanisms of skeletal muscle physiological and pathological processes, through potential experimental strategies (Yang and Speed, 2002;Churchill, 2002). These biological processes could be alterations in skeletal muscle structure and function as consequences of different stimuli that modify skeletal muscle contractile activity (e.g. low-intensity high-repetitive endurance exercise, high-intensity low-repetitive resistance training, environmental factors such as hypoxia, etc.), mechanisms of skeletal muscle development, gradual changes in skeletal muscle with ageing (Larsson and Ramamurthy, 2000;Hughes and Schiaffino, 1999), skeletal muscle degeneration, degree of progression or interruption of skeletal muscle regeneration, and differences at the molecular level between normal and diseased skeletal muscle tissues, and among patients. The transcriptional signalling pathways and the differential gene expression events involved in these processes could be further recognised using the porcine cDNA microarray. The porcine cDNA microarray could also be used to investigate molecular details of the complex interactions/cross-talk among different signalling pathways [e.g., the MRFs, ubiquitin ligase pathway, IGF-1/PI3K/AKT1/mTOR/p70S6K pathway, $Ca^{2+}$/calmodulin/calcineurin pathway (see reviews in Chapter One)] which are involved in skeletal muscle developmental, physiological and pathological events. The porcine cDNA microarray could also be used in industrial research (e.g., livestock production, meat quality control) to improve the skeletal muscle phenotype of the pig (Klont et al., 1998). Therefore, by using the porcine cDNA microarray, the response of a large percentage of the skeletal muscle genome to exercise training, inactivity, and drug treatment could be characterised; and the transcriptional events influenced by physiological and pathological processes could be identified

in the future. The novel porcine skeletal muscle cDNA microarray could also be used to evaluate high throughput gene expression in porcine models of human skeletal muscle diseases. Furthermore, the current porcine cDNA microarray could also be expanded by incorporating more genes in this biological tool.

# APPENDIX

## (Further Details of Materials and Methods)

## Further details of materials and methods described in this thesis

***40% Acrylamide***
(for DNA sequencing)
Dissolve 380 g of acrylamide (DNA-sequencing grade) and 20 g of *N,N'*-methylenebisacrylamide in a total volume of 600 ml of distilled $H_2O$.

***10% Ammonium persulfate***
To 1 g of ammonium persulfate, add $H_2O$ to 10 ml. The solution may be stored for several weeks at 4°C.

***Antibiotic solutions***
Stock solutions of antibiotics dissolved in $H_2O$ should be sterilised by filtration through a 0.22-micron filter. Antibiotics dissolved in ethanol do not need to be sterilised. Store solutions in light-tight containers.

| | Stock solution | | Working concentration | |
|---|---|---|---|---|
| | concentration | storage | stringent plasmids | relaxed plasmids |
| Ampicillin | 50 mg/ml in $H_2O$ | -20°C | 20 µg/ml | 60 µg/ml |
| Kanamycin | 10 mg/ml in $H_2O$ | -20°C | 10 µg/ml | 50 µg/ml |
| Streptomycin | 10 mg/ml in $H_2O$ | -20°C | 10 µg/ml | 50 µg/ml |
| Tetracycline | 5 mg/ml in ethanol | -20°C | 10 µg/ml | 50 µg/ml |

***Denatured, fragmented salmon sperm DNA***
Salmon sperm DNA (e.g., Sigma type III sodium salt) is dissolved in water at a concentration of 10 mg/ml. If necessary, the solution is stirred on a magnetic stirrer for 2-4 hours at room temperature to help the DNA to dissolve. The concentration of NaCl is adjusted to 0.1 M, and the solution is extracted once with phenol and once with phenol:chloroform. The aqueous phase is recovered, and the DNA is sheared by passing it 12 times rapidly through a 17-gauge hypodermic needle. The DNA is precipitated by adding 2 volumes of ice-cold ethanol. It is then recovered by centrifugation and redissolved at a concentration of 10 mg/ml in water. The $OD_{260}$ of the solution is determined and the extract concentration of the DNA is calculated. The solution is then boild for 10 minutes and stored at –20°C in small aliquots. Just before use, the solution is heated for 5 minutes in a boiling-water bath and then chilled quickly in ice water. Denatured, fragmented salmon sperm DNA should be used at a concentration of 100 µg/ml in prehybridisation solutions.

***Denhardt's reagent***
Denhardt's reagent is usually made up as a 50× stock solution, which is filtered and stored at –20°C. The stock solution is diluted ten-fold into prehybridisation buffer. 50× Denhardt's reagent contains 5 g of Ficoll, 5 g of polyvinypyrrolidone, 5 g of bovine serum albumin (Fraction V), and $H_2O$ to 500 ml.

***1 M Dithiothreitol (DTT)***

Dissolve 3.09 g of DTT in 20 ml of 0.01 M sodium acetate (pH 5.2). Sterilise by filtration. Dispense into 1-ml aliquots and store at –20°C.

***Denaturing buffer***

(For transfer of DNA to nitrocellulose filters)

Per 10 litres

200 g NaOH

876.6 g NaCl

Denaturing buffer contains 1.5 M NaCl and 0.5 N NaOH

***0.5 M disodium ethylenediaminetetra-acetate (EDTA) (pH 8.0)***

Add 186.1 g of disodium ethylenediaminetetra-acetate.$2H_2O$ to 800 ml of $H_2O$. Stir vigorously on a magnetic stirrer. Adjust the pH to 8.0 with NaOH (~ 20 g of NaOH pellets). Dispense into aliquots and sterilise by autoclaving.

***Ethidium bromide (10 mg/ml)***

Add 1 g of ethidium bromide to 100 ml of $H_2O$. Stir on a magnetic stirrer for several hours to ensure that the dye has dissolved. Wrap the container in aluminum foil or transfer the solution to a dark bottle and store at room temperature.

***Ethidium bromide fluorescent quantitation of the amount of double-stranded DNA***

Sometimes there is not sufficient DNA (< 250 ng/ml) to assay spectrophotometrically, or the DNA may be heavily contaminated with other substances that absorb ultraviolet irradiation and therefore impede accurate analysis. A rapid way to estimate the amount of DNA in such samples is to utilise the ultraviolet-induced fluorescence emitted by ethidium bromide molecules intercalated into the DNA. Because the amount of fluorescence is proportional to the total mass of DNA, the quantity of DNA in the sample can be estimated by comparing the fluorescent yield of the sample with that of a series of standards. As little as 1-5 ng of DNA can be detected by this method.

***6×Gel-loading buffer***

0.25% bromophenol blue

0.25% xylene cyanol FF

40% (w/v) sucrose in water

[In this study, 6×Gel-loading buffer type III contained 3 ml glycerol, 7 ml water, 250 µg Xylene cyanole FF (sigma), and 250 µg bromophenol blue (Fisons Scientific Equipment)]

Storage temperature for the 6×Gel-loading buffer is 4°C. Gel-loading buffers serve three purposes: They increase the density of the sample, ensuring that the DNA drops evenly into the well; they add colour to the sample, thereby simplifying the loading process; and they contain dyes that, in an electric field, move toward the anode at predictable rates. Bromophenol blue migrates through agarose gels approximately 2.2-fold faster than xylene

cyanol FF, independent of the agarose concentration. Bromophenol blue migrates through agarose gels run in 0.5× TBE at approximately the same rate as linear double-stranded DNA 300bp in length, whereas xylene cyanol FF migrates at approximately the same rate as linear double-stranded DNA 4 kb in length. These relationships are not significantly affected by the concentration of agarose in the gel over the range of 0.5% to 1.4%.

***HEPES, free acid***

[N-(2-Hydroxyethyl) piperazine N'-(2-ethanesulfonic acid)]

HEPES is a zwitterionic N-substituted aminosulfonic acid buffer, typically referred to as Good's buffer, useful in cell culture media formulations.

***Luria-Bertani (LB) medium***

Per litre:

To 950 ml of deionised $H_2O$, add:

| | |
|---|---|
| Bacto-tryptone | 10 g |
| Bacto-yeast extract | 5 g |
| NaCl | 10 g |

Shake until the solutions have dissolved. Adjust the pH to 7.0 with 5 N NaOH (~ 0.2 ml). Adjust the volume of the solution to 1 litre with deionised $H_2O$. Sterilise by autoclaving for 20 minutes at 15 lb/sq. in. on liquid cycle.

***LB medium containing agar***

Prepare LB medium. Just before autoclaving, add:

bacto-agar 15 g/litre

Sterilise by autoclaving for 20 minutes at 15 lb/sq. in. on liquid cycle. Allow the medium to cool to 50°C before adding thermolabile substances (e.g., antibiotics). Mix the medium by swirling. Plates can then be poured directly from the flask; allow about 30-35 ml of medium per 90-mm plate. In this study, all LB-agar plates used contained 50 µg/ml kanamycin (Sigma-Aldrich).

***Lysis/Binding buffer***

100 mM Tris-HCl, pH 7.5
500 mM LiCl
10 mM EDTA, pH 8.0
1% LiDS
5 mM dithiothreitol (DTT)

***5M NaCl***

Dissolve 292.2 g of NaCl in 800 ml of $H_2O$. Adjust the volume to 1 litre with $H_2O$. Dispense into aliquots and sterilise by autoclaving.

***Neutralisation buffer***

(For transfer of DNA to nitrocellulose filters)

1M Tris (pH 7.4)
1.5 M NaCl

***Phosphate-buffered saline (PBS)***

Dissolve 8 g of NaCl, 0.2 g of KCL, 1.44 g of $Na_2HPO_4$, and 0.24 g of $KH_2PO_4$ in 800 ml of distilled $H_2O$. Adjust the pH to 7.4 with HCl. Add $H_2O$ to 1 litre. Dispense the solution into aliquots and sterilise them by autoclaving for 20 minutes at 15 lb/sq.in. on liquid cycle. Store at room temperature.

***Prehybridisation buffer***

(For Southern blot, Dot blot and colony hybridisations)

Per 500 ml

| | |
|---|---|
| Formamide | 250 ml |
| 20× SSC | 125 ml |
| 50× Denhardt's | 50 ml |
| 0.5 M EDTA | 1 ml |
| 20% SDS | 25 ml |
| 1 M PBS (pH 7.0) | 25 ml |
| 10 mg/ml sheared salmon sperm DNA | 10 ml |

(Sigma Catalogue# D-1626, DNA sodium salt type III from salmon testes)

Prehybridisation buffer contains 50% Formamide, 5× SSC, 5× Denhardt's, 0.1 M EDTA, 1% SDS, 50mM Sodium phosphate buffer (pH 7.0), 200 µg/ml Denatured, fragmented (sheared) salmon sperm DNA (SSS).

***3M Sodium acetate (pH 5.2 and pH 7.0)***

Dissolve 408.1 g of sodium acetate.$3H_2O$ in 800 ml of $H_2O$. Adjust the pH to 5.2 with glacial acetic acid or adjust the pH to 7.0 with dilute acetic acid. Adjust the volume to 1 litre with $H_2O$. Dispense into aliquots. Sterilise by autoclaving.

***20×SSC***

Dissolve 175.3 g of NaCl and 88.2 g of sodium citrate in 800 ml of $H_2O$. Adjust the pH to 7.0 with a few drops of a 10 N solution of NaOH. Adjust the volume to 1 litre with $H_2O$. Dispense into aliquots. Sterilise by autoclaving.

***20×SSPE***

Dissolve 175.3 g of NaCl, 27.6 g of $NaH_2PO_4.H_2O$ and 7.4 g of EDTA in 800 ml of $H_2O$. Adjust the pH to 7.4 with NaOH (~ 6.5 ml of a 10 N solution). Adjust the volume to 1 litre with $H_2O$. Dispense into aliquots. Sterilise by autoclaving.

***1× TAE buffer***

Per 10 litres

| | | |
|---|---|---|
| 48.4 | g | Tris |
| 11.42 | ml | Glacial acetic acid |
| 20 | ml | EDTA (0.5 M, pH 8.0) |

Adjust the volume to 10 litres with $H_2O$

***1× TBE buffer***

Per 10 litres

| | | |
|---|---|---|
| 108 | g | Tris |
| 55 | g | Boric acid |
| 40 | ml | EDTA (0.5 M, pH 8.0) |

Adjust the volume to 10 litres with $H_2O$

***TE buffer***

PH 7.4:
10 mM Tris.Cl (pH 7.4)
1 mM EDTA (pH 8.0)

PH 7.6
10 mM Tris.Cl (pH 7.6)
1 mM EDTA (pH 8.0)

***Transfer buffer***

(For transfer of DNA to nitrocellulose filters)

10× SSC
10 SSPE

***1M Tris***

Dissolve 121.1 g of Tris base in 800 ml of H2O. Adjust the pH to the desired value by adding concentrated HCl.

| pH | HCl |
|---|---|
| 7.4 | 70 ml |
| 7.6 | 60 ml |
| 8.0 | 42 ml |

Allow the solution to cool to room temperature before making final adjustments to the pH. Adjust the volume of the solution to 1 litre with H2O. Dispense into aliquots and sterilise by autoclaving.

***Terrific broth***
(Tartof and Hobbs 1987)

Per liter:

To 900 ml of deionised $H_2O$, add:

| | |
|---|---|
| Bacto-tryptone | 12 g |
| Bacto-yeast extract | 24 g |
| Glycerol | 4 ml |

Shake until the solutes have dissolved and sterilise by autoclaving for 20 minutes at 15 lb/sq. in. on liquid cycle. Allow the solution to cool to 60°C or less, and then add 100 ml of a sterile solution of 0.17 M $KH_2PO_4$, 0.72 M $K_2HPO_4$. (This solution is made by dissolving 2.31 g of $KH_2PO_4$ and 12.54 g of $K_2HPO_4$ in 90 ml of deionised $H_2O$. After the salt have dissolved, adjust the volume of the solution to 100 ml with deionised $H_2O$ and sterilise by autoclaving for 20 minutes at 15 lb/sq. in. on liquid cycle.). In this study, to make 1000 ml terrific broth containing 50 µg/ml kanamycin (Sigma), 47 g terrific broth powder, 4ml glycerol (Sigma) and double distilled $H_2O$ were mixed to get a final volume of 1000ml. The broth was autoclaved at 121°C for 20 minutes.

***Tris-acetate (TAE)***

Working solution (1×TAE): 0.04M Tris-acetate
0.001M EDTA

Concentrated stock solution (50×TAE) (per litre): 242 g Tris base
57.1 ml glacial acetic acid
100 ml 0.5M EDTA (pH 8.0)

***Tris-buffered saline (TBS) (pH 7.2)***

150 mM NaCl
20 mM Tris (pH 7.2)

Dissolve 8 g of NaCl, 0.2 g of KCl, and 3 g of Tris base in 800 ml of distilled $H_2O$. Add 0.015 g of phenol red and adjust the pH to 7.4 with HCl. Add distilled $H_2O$ to 1 litre. Dispense the solution into alliquots and sterilise them by autoclaving for 20 minutes at 15 lb/sq. in. on liquid cycle. Store at room temperature.

***Sequencing gel-loading buffer***

98% deionised formamide
10 mM EDTA (pH 8.0)
0.025% xylene cyanol FF
0.025% bromophenol blue

***2× SDS gel-loading buffer***

100 mM Tris.Cl (pH 6.8)
200 mM dithiothreitol
4% SDS (electrophoresis grade)
0.2% bromophenol blue
20% glycerol

2× SDS gel-loading buffer lacking dithiothreitol can be stored at room temperature. Dithiothreitol should then be added, just before the buffer is used, from a 1 M stock.

***Spectrophotometric Determination of the Amount of DNA or RNA***

For quantitating the amout of DNA or RNA, readings should be taken at wavelengths of 260 nm and 280 nm. The reading at 260 nm allows calculation of the concentration of nucleic acid in the sample. An OD of 1 corresponds to approximately 50 μg/ml for double-stranded DNA, 40 μg/ml for single-stranded DNA and RNA, and ~ 20 μg/ml for single-stranded oligonucleotides. The ratio between the readings at 260 nm and 280 nm ($OD_{260}/OD_{280}$) provides an estimate of the purity of the nucleic acid. Pure preparations of DNA and RNA have $OD_{260}/OD_{280}$ values of 1.8 and 2.0, respectively. If there is contamination with protein or phenol, the $OD_{260}/OD_{280}$ will be significantly less than the values given above, and accurate quantitation of the amount of nucleic acid will not be possible.

***Washing buffer A***

(For nylon membrane washing following Southern blot/Dot blot/Colony blot hybridisations)

1 mM EDTA
0.1% LiDS
10 mM Tris-HCl, pH 7.5
0.15 M LiCl

***Washing buffer B***

(For nylon membrane washing following Southern blot/Dot blot/Colony blot hybridisations)

10 mM Tris-HCl, pH 7.5
0.15 M LiCl
1 mM EDTA

# REFERENCES

Abbott,KL, B B Friday, D Thaloor, T J Murphy, G K Pavlath, 1998, Activation and cellular localization of the cyclosporine A-sensitive transcription factor NF-AT in skeletal muscle cells: Mol.Biol.Cell, v. 9, p. 2905-2916.

Alessi,DR, S R James, C P Downes, A B Holmes, P R Gaffney, C B Reese, P Cohen, 1997, Characterization of a 3-phosphoinositide-dependent protein kinase which phosphorylates and activates protein kinase Balpha: Curr.Biol., v. 7, p. 261-269.

Allen,DL, L A Leinwand, 2002, Intracellular calcium and myosin isoform transitions. Calcineurin and calcium-calmodulin kinase pathways regulate preferential activation of the IIa myosin heavy chain promoter: J.Biol.Chem., v. 277, p. 45323-45330.

Allen,DL, C A Sartorius, L K Sycuro, L A Leinwand, 2001, Different pathways regulate expression of the skeletal myosin heavy chain genes: J.Biol.Chem., v. 276, p. 43524-43533.

Altomare,DA, K Guo, J Q Cheng, G Sonoda, K Walsh, J R Testa, 1995, Cloning, chromosomal localization and expression analysis of the mouse Akt2 oncogene: Oncogene, v. 11, p. 1055-1060.

Amthor,H, B Christ, M Weil, K Patel, 1998, The importance of timing differentiation during limb muscle development: Curr.Biol., v. 8, p. 642-652.

Arends,MJ, A H Wyllie, 1991, Apoptosis: mechanisms and roles in pathology, Int Rev Exp Pathol, v. 32, p. 223-254.

Armand,O, A M Boutineau, A Mauger, M P Pautou, M Kieny, 1983, Origin of satellite cells in avian skeletal muscles: Arch Anat Microsc Morphol Exp, v. 72, p. 163-181.

Arnold,HH, T Braun, 1996, Targeted inactivation of myogenic factor genes reveals their role during mouse myogenesis: a review: Int.J.Dev.Biol., v. 40, p. 345-353.

Asakura,A, 2003, Stem cells in adult skeletal muscle: Trends Cardiovasc Med, v. 13(3), p. 123-128.

Bai,Q, C McGillivray, N da Costa, S Dornan, G Evans, M J Stear, K C Chang, 2003, Development of a porcine skeletal muscle cDNA microarray: analysis of differential transcript expression in phenotypically distinct muscles: BMC.Genomics, v. 4, p. 8.

Bassel-Duby,R, E N Olson, 2003, Role of calcineurin in striated muscle: development, adaptation, and disease: Biochem.Biophys.Res.Commun., v. 311, p. 1133-1141.

Beals,CR, C M Sheridan, C W Turck, P Gardner, G R Crabtree, 1997, Nuclear export of NF-ATc enhanced by glycogen synthase kinase-3: Science, v. 275, p. 1930-1934.

Bendall,AJ, J Ding, G Hu, M M Shen, C Abate-Shen, 1999, Msx1 antagonizes the myogenic activity of Pax3 in migrating limb muscle precursors: Development, v. 126, p. 4965-4976.

Benders,AA, P J Groenen, F T Oerlemans, J H Veerkamp, B Wieringa, 1997, Myotonic dystrophy protein kinase is involved in the modulation of the Ca2+ homeostasis in skeletal muscle cells: J Clin Invest., v. 100(6), p. 1440-1447.

Berchtold,MW, H Brinkmeier, M Muntener, 2000, Calcium ion in skeletal muscle: its crucial role for muscle function, plasticity, and disease: Physiol Rev., v. 80, p. 1215-1265.

Berridge,MJ, M D Bootman, H L Roderick, 2003, Calcium signalling: dynamics, homeostasis and remodelling: Nat.Rev.Mol.Cell Biol., v. 4, p. 517-529.

Berridge,MJ, P Lipp, M D Bootman, 2000, The versatility and universality of calcium signalling: Nat.Rev.Mol.Cell Biol., v. 1, p. 11-21.

Beuzen,ND, M J Stear, K C Chang, 2000, Molecular markers and their use in animal breeding: Vet.J., v. 160, p. 42-52.

Bigard,X, H Sanchez, J Zoll, P Mateo, V Rousseau, V Veksler, R Ventura-Clapier, 2000, Calcineurin Co-regulates contractile and metabolic components of slow muscle phenotype: J.Biol.Chem., v. 275, p. 19653-19660.

Biring,MS, M Fournier, D J Ross, M I Lewis, 1998, Cellular adaptations of skeletal muscles to cyclosporine: J.Appl.Physiol, v. 84, p. 1967-1975.

Bittner,R, C Schofer, K Weipoltshammer, S Ivanova, B Streubel, E Hauser, M Freilinger, H Hoger, A Elbe-Burger, F Wachtler, 1999, Recruitment of bone-marrow-derived cells by skeletal and cardiac muscle in adult dystrophic mdx mice: Anat Embryol, v. 199, p. 391-396.

Black,BL, E C Olson, 1998, Transcriptional control of muscle development by myocyte enhancer factor-2 (MEF2) proteins: Annu. Rev. Cell Dev. Biol., v. 14, p. 167-196.

Blaeser,F, N Ho, R Prywes, T A Chatila, 2000, $Ca^{2+}$-dependent gene expression mediated by MEF2 transcription factors: J.Biol.Chem., v. 275, p. 197-209.

Blanquet,PR, 2000, Casein kinase 2 as a potentially important enzyme in the nervous system: Prog.Neurobiol., v. 60, p. 211-246.

Blau HM, C J Epstein, 1979, Manipulation of myogenesis in vitro: reversible inhibition by DMSO: Cell, v. 17(1), p. 95-108.

Blohm,DH, A Guiseppi-Elie, 2001, New developments in microarray technology: Curr.Opin.Biotechnol., v. 12, p. 41-47.

Bodine,SC, E Latres, S Baumhueter, V K Lai, L Nunez, B A Clarke, W T Poueymirou, F J Panaro, E Na, K Dharmarajan, Z Q Pan, D M Valenzuela, T M DeChiara, T N Stitt, G D Yancopoulos, D J Glass, 2001a, Identification of ubiquitin ligases required for skeletal muscle atrophy: Science, v. 294, p. 1704-1708.

Bodine,SC, T N Stitt, M Gonzalez, W O Kline, G L Stover, R Bauerlein, E Zlotchenko, A Scrimgeour, J C Lawrence, D J Glass, G D Yancopoulos, 2001b, Akt/mTOR pathway is a crucial regulator of skeletal muscle hypertrophy and can prevent muscle atrophy in vivo: Nat.Cell Biol., v. 3, p. 1014-1019.

Bompard,G, C Puech, C Prabois, F Vignon, G Freiss, 2002, Protein-tyrosine phosphatase PTPL1/FAP-1 triggers apoptosis in human breast cancer cells: J Biol Chem., v. 277 (49), p. 47861-47869.

Bonfoco,E, D Krainc, M Ankarcrona, P Nicotera, S A Lipton, 1995, Apoptosis and necrosis: two distinct events induced, respectively, by mild and intense insults with N-methyl-d-aspartate or nitric oxide/superoxide in cortical cell cultures: Proc Natl Acad Sci USA, v. 92, p. 7162-7166.

Bortoluzzi,S, F d'Alessi, C Romualdi, G A Danieli, 2000, The human adult skeletal muscle transcriptional profile reconstructed by novel computational approach: Genome Res., v. 10, p. 344-349.

Borycki,AG, B Brunk, S Tajbakhsh, M Buckingham, C Chiang, C P Emerson, Jr., 1999, Sonic hedgehog controls epaxial muscle determination through Myf5 activation: Development, v. 126, p. 4053-4063.

Bowtell,DD, 1999, Options available--from start to finish--for obtaining expression data by microarray: Nat.Genet., v. 21, p. 25-32.

Braun,T, H H Arnold, 1995, Inactivation of Myf-6 and Myf-5 genes in mice leads to alterations in skeletal muscle development: EMBO J., v. 14, p. 1176-1186.

Brooke,MH, K K Kaiser, 1970, Muscle fibre types: how many and what kind?: Archives of Neurology, v. 23, p. 369-379.

Brunn,GJ, C C Hudson, A Sekulic, J M Williams, H Hosoi, P J Houghton, J C Lawrence, Jr., R T Abraham, 1997, Phosphorylation of the translational repressor PHAS-I by the mammalian target of rapamycin: Science, v. 277, p. 99-101.

Buckingham,M, 2001, Skeletal muscle formation in vertebrates: Curr.Opin.Genet.Dev., v. 11, p. 440-448.

Bustin,SA, 2000, Absolute quantification of mRNA using real-time reverse transcription polymerase chain reaction assays: Journal of Molecular Endocrinology, v. 25, p. 169-193.

Byers,RJ, J A Hoyland, J Dixon, A J Freemont, 2000, Subtractive hybridization--genetic takeaways and the search for meaning: Int.J.Exp.Pathol., v. 81, p. 391-404.

Calvo,S, P Venepally, J Cheng, A Buonanno, 1999, Fiber-type-specific transcription of the troponin I slow gene is regulated by multiple elements: Mol.Cell Biol., v. 19, p. 515-525.

Campanaro,S, C Romualdi, M Fanin, B Celegato, B Pacchioni, S Trevisan, P Laveder, C De Pitta, E Pegoraro, Y K Hayashi, G Valle, C Angelini, G Lanfranchi, 2002, Gene expression profiling in dysferlinopathies using a dedicated muscle microarray: Hum.Mol.Genet., v. 11, p. 3283-3298.

Campbell,WG, S E Gordon, C J Carlson, J S Pattison, M T Hamilton, F W Booth, 2001, Differential global gene expression in red and white skeletal muscle: Am.J.Physiol.-Cell Physiol., v. 280, p. C763-C768.

Chang,KC, N D Beuzen, A D Hall, 2003, Identification of microsatellites in expressed muscle genes: assessment of a desmin (CT) dinucleotide repeat as a marker for meat quality: Vet.J., v. 165, p. 157-163.

Chang,KC, 2000, Critical regulatory domains in intron 2 of a porcine sarcomeric myosin heavy chain gene: J.Muscle Res.Cell Motil., v. 21, p. 451-461.

Chang,KC, K Fernandes, 1997, Developmental expression and 5' end cDNA cloning of the porcine 2x and 2b myosin heavy chain genes: DNA Cell Biol., v. 16, p. 1429-1437.

Chang,KC, K Fernandes, M J Dauncey, 1995, Molecular characterization of a developmentally regulated porcine skeletal myosin heavy chain gene and its 5' regulatory region: J.Cell Sci., v. 108 ( Pt 4), p. 1779-1789.

Chang,KC, K Fernandes, G Goldspink, 1993, In vivo expression and molecular characterization of the porcine slow-myosin heavy chain: J.Cell Sci., v. 106 ( Pt 1), p. 331-341.

Chen,WS, P Z Xu, K Gottlob, M L Chen, K Sokol, T Shiyanova, I Roninson, W Weng, R Suzuki, K Tobe, T Kadowaki, N Hay, 2001, Growth retardation and increased apoptosis in mice with homozygous disruption of the Akt1 gene: Genes Dev., v. 15, p. 2203-2208.

Cheung,VG, M Morley, F Aguilar, A Massimi, R Kucherlapati, G Childs, 1999, Making and reading microarrays: Nat.Genet., v. 21, p. 15-19.

Chikuni,K, S Muroya, I Nakajima, 2004, Absence of the functional Myosin heavy chain 2b isoform in equine skeletal muscle: Zoolog Sci., v. 21 (5), p. 589-596.

Chin,ER, E N Olson, J A Richardson, Q Yang, C Humphries, J M Shelton, H Wu, W Zhu, R Bassel-Duby, R S Williams, 1998, A calcineurin-dependent transcriptional pathway controls skeletal muscle fibre type: Genes Dev., v. 12, p. 2499-2509.

Chuaqui,RF, R F Bonner, C J Best, J W Gillespie, M J Flaig, S M Hewitt, J L Phillips, D B Krizman, M A Tangrea, M Ahram, W M Linehan, V Knezevic, M R Emmert-Buck, 2002, Post-analysis follow-up and validation of microarray experiments: Nat.Genet., v. 32 Suppl, p. 509-514.

Churchill,GA, 2002, Fundamentals of experimental design for cDNA microarrays: Nat.Genet., v. 32 Suppl, p. 490-495.

Coleman,ME, F DeMayo, K C Yin, H M Lee, R Geske, C Montgomery, R J Schwartz, 1995, Myogenic vector expression of insulin-like growth factor I stimulates muscle cell differentiation and myofiber hypertrophy in transgenic mice: J.Biol.Chem., v. 270, p. 12109-12116.

Cossu,G, R Kelly, S Tajbakhsh, S Di Donna, E Vivarelli, M Buckingham, 1996, Activation of different myogenic pathways: myf-5 is induced by the neural tube and MyoD by the dorsal ectoderm in mouse paraxial mesoderm: Development, v. 122, p. 429-437.

Crabtree,GR, 1999, Generic signals and specific outcomes: signaling through $Ca^{2+}$, calcineurin, and NF-AT: Cell, v. 96, p. 611-614.

Crabtree,GR, 2001, Calcium, calcineurin, and the control of transcription: J.Biol.Chem., v. 276, p. 2313-2316.

Crabtree,GR, E N Olson, 2002, NFAT signaling: choreographing the social lives of cells: Cell, v. 109 Suppl, p. S67-S79.

Cross,DA, D R Alessi, P Cohen, M Andjelkovich, B A Hemmings, 1995, Inhibition of glycogen synthase kinase-3 by insulin mediated by protein kinase B: Nature, v. 378, p. 785-789.

Cui,X, G A Churchill, 2003, Statistical tests for differential expression in cDNA microarray experiments: Genome Biol., v. 4, p. 210.

Cunningham,MJ, 2000, Genomics and proteomics: the new millennium of drug discovery and development: J.Pharmacol.Toxicol.Methods, v. 44, p. 291-300.

Czubryt,MP, J McAnally, G I Fishman, E N Olson, 2003, Regulation of peroxisome proliferator-activated receptor gamma coactivator 1 alpha (PGC-1 alpha ) and mitochondrial function by MEF2 and HDAC5: Proc.Natl.Acad.Sci.U.S.A, v. 100, p. 1711-1716.

da Costa,N, R Blackley, H Alzuherri, K C Chang, 2002, Quantifying the temporospatial expression of postnatal porcine skeletal myosin heavy chain genes: J.Histochem.Cytochem., v. 50, p. 353-364.

da Costa,N, C McGillivray, K C Chang, 2003, Postnatal myosin heavy chain isoforms in prenatal porcine skeletal muscles: insights into temporal regulation: Anat.Rec., v. 273A, p. 731-740.

da Costa, N, C McGillivray, Q Bai, J D Wood, G Evans, K C Chang, 2004, Restriction of dietary energy and protein induces molecular changes in young porcine skeletal muscles: Journal of Nutrition, v. 134(9) p. 2191-2199.

Damen,JE, L Liu, P Rosten, R K Humphries, A B Jefferson, P W Majerus, G Krystal, 1996, The 145-kDa protein induced to associate with Shc by multiple cytokines is an inositol tetraphosphate and phosphatidylinositol 3,4,5-triphosphate 5-phosphatase: Proc.Natl.Acad.Sci.U.S.A, v. 93, p. 1689-1693.

Davoli,R, L Fontanesi, P Zambonelli, D Bigi, J Gellin, M Yerle, J Milc, S Braglia, V Cenci, M Cagnazzo, V Russo, 2002, Isolation of porcine expressed sequence tags for the construction of a first genomic transcript map of the skeletal muscle in pig: Anim Genet., v. 33, p. 3-18.

Davoli,R, P Zambonelli, D Bigi, L Fontanesi, V Russo, 1999, Analysis of expressed sequence tags of porcine skeletal muscle: Gene, v. 233, p. 181-188.

De Angelis,L, L Berghella, M Coletta, L Lattanzi, M Zanchi, M G Cusella-De Angelis, C Ponzetto, G Cossu, 1999, Skeletal myogenic progenitors originating from embryonic dorsal aorta coexpress endothelial and myogenic markers and contribute to postnatal muscle growth and regeneration: J Cell Biol, v. 147, p. 869-877.

Delfini,M, E Hirsinger, O Pourquie, D Duprez, 2000, Delta 1-activated notch inhibits muscle differentiation without affecting Myf5 and Pax3 expression in chick limb myogenesis: Development, v. 127, p. 5213-5224.

Delling,U, J Tureckova, H W Lim, L J De Windt, P Rotwein, J D Molkentin, 2000, A calcineurin-NFATc3-dependent pathway regulates skeletal muscle differentiation and slow myosin heavy-chain expression: Mol.Cell Biol., v. 20, p. 6600-6611.

DeRisi,JL, V R Iyer, 1999, Genomics and array technology: Curr.Opin.Oncol., v. 11, p. 76-79.

Devaux,F, P Marc, C Jacq, 2001, Transcriptomes, transcription activators and microarrays: FEBS Lett., v. 498, p. 140-144.

DeVol,DL, P Rotwein, J L Sadow, J Novakofski, P J Bechtel, 1990, Activation of insulin-like growth factor gene expression during work-induced skeletal muscle growth: Am.J.Physiol, v. 259, p. E89-E95.

Dietrich,S, F R Schubert, C Healy, P T Sharpe, A Lumsden, 1998, Specification of the hypaxial musculature: Development, v. 125, p. 2235-2249.

Dolmetsch,RE, R S Lewis, C C Goodnow, J I Healy, 1997, Differential activation of transcription factors induced by Ca2+ response amplitude and duration: Nature, v. 386, p. 855-858.

Dolmetsch,RE, K Xu, R S Lewis, 1998, Calcium oscillations increase the efficiency and specificity of gene expression: Nature, v. 392, p. 933-936.

Duggan,DJ, M Bittner, Y Chen, P Meltzer, J M Trent, 1999, Expression profiling using cDNA microarrays: Nat.Genet., v. 21, p. 10-14.

Dunn,SE, J L Burns, R N Michel, 1999, Calcineurin is required for skeletal muscle hypertrophy: J.Biol.Chem., v. 274, p. 21908-21912.

Dunn,SE, E R Chin, R N Michel, 2000, Matching of calcineurin activity to upstream effectors is critical for skeletal muscle fiber growth: J.Cell Biol., v. 151, p. 663-672.

Dunn,SE, A R Simard, R A Prud'homme, R N Michel, 2002, Calcineurin and skeletal muscle growth: Nat.Cell Biol., v. 4, p. E46-E47.

Dupont-Versteegden,EE, M Knox, C M Gurley, J D Houle, C A Peterson, 2002, Maintenance of muscle mass is not dependent on the calcineurin-NFAT pathway: Am.J.Physiol Cell Physiol, v. 282, p. C1387-C1395.

Dypbukt,JM, M Ankarkrona, M Burkitt, A Sjoholm, K Strom, S Orrenius, P Nicotera, 1994, Different prooxidant levels stimulate growth, trigger apoptosis, or produce necrosis of insulin-secreting RINm5F cells: the role of intracellular polyamines: J Biol Chem, v. 269, p. 30553-30560.

Eizema,K, M van den Burg, A Kiri, E G Dingboom, H van Oudheusden, G Goldspink, W A Weijs, 2003, Differental expression of equine myosin heavy chain mRNA and protein isoforms in a limb muscle: J Histochem Cytochem, v. 51 (9), p. 1207-1216.

Emmert-Buck,MR, R L Strausberg, D B Krizman, M F Bonaldo, R F Bonner, D G Bostwick, M R Brown, K H Buetow, R F Chuaqui, K A Cole, P H Duray, C R Englert, J W Gillespie, S Greenhut, L Grouse, L W Hillier, K S Katz, R D Klausner, V Kuznetzov, A E Lash, G Lennon, W M Linehan, L A Liotta, M A Marra, P J Munson, D K Ornstein, V V Prabhu, C

Prange, G D Schuler, M B Soares, C M Tolstoshev, C D Vocke, R H Waterston, 2000, Molecular profiling of clinical tissue specimens: feasibility and applications: Am.J.Pathol., v. 156, p. 1109-1115.

Epstein,CB, R A Butow, 2000, Microarray technology - enhanced versatility, persistent challenge: Curr.Opin.Biotechnol., v. 11, p. 36-41.

Essén-Gustavsson,B, 1993, Muscle-fiber characteristics in pigs and relationships to meat-quality parameters- review, in E Puolanne and DI Demeyer (eds), Pork quality: genetic and metabolic factors: Wallingford UK, CAB International, p. 140-159.

Esser,K, T Nelson, V Lupa-Kimball, E. Blough, 1999, The CACC Box and the myocyte enhancer factor-2 sites within the myosin light chain 2 slow promoter cooperate in regulating nerve-specific transcription in skeletal muscle: J Biol Chem, v. 274, p. 12095-12102.

Faust,M, M Montenarh, 2000, Subcellular localization of protein kinase CK2. A key to its function?: Cell.Tissue Res., v. 301, p. 329-340.

Ferrari,G, G Cusella-De Angelis, M Coletta, E Paolucci, A Stornaiuolo, G Cossu, F Mavilio, 1998, Muscle regeneration by bone marrow-derived myogenic progenitors: Science, v. 279, p. 1528-1530.

Forozan,F, R Karhu, J Kononen, A Kallioniemi, O P Kallioniemi, 1997, Genome screening by comparative genomic hybridisation: Trends.Genet., v. 13, p. 405-409.

Friday,BB, V Horsley, G K Pavlath, 2000, Calcineurin activity is required for the initiation of skeletal muscle differentiation: J.Cell Biol., v. 149, p. 657-666.

Friday,BB, P O Mitchell, K M Kegley, G K Pavlath, 2003, Calcineurin initiates skeletal muscle differentiation by activating MEF2 and MyoD: Differentiation, v. 71, p. 217-227.

Friday,BB, G K Pavlath, 2001, A calcineurin- and NFAT-dependent pathway regulates Myf5 gene expression in skeletal muscle reserve cells: J.Cell Sci., v. 114, p. 303-310.

Gerhold,D, T Rushmore, C T Caskey, 1999, DNA chips: promising toys have become powerful tools: Trends Biochem.Sci., v. 24, p. 168-173.

Gingras,AC, S P Gygi, B Raught, R D Polakiewicz, R T Abraham, M F Hoekstra, R Aebersold, N Sonenberg, 1999a, Regulation of 4E-BP1 phosphorylation: a novel two-step mechanism: Genes Dev., v. 13, p. 1422-1437.

Gingras,AC, B Raught, N Sonenberg, 1999b, eIF4 initiation factors: effectors of mRNA recruitment to ribosomes and regulators of translation: Annu.Rev.Biochem., v. 68, p. 913-963.

Gingras,AC, B Raught, N Sonenberg, 2004, mTOR signaling to translation: Curr.Top.Microbiol.Immunol., v. 279, p. 169-197.

Glass,DJ, 2003a, Molecular mechanisms modulating muscle mass: Trends Mol.Med., v. 9, p. 344-350.

Glass,DJ, 2003b, Signalling pathways that mediate skeletal muscle hypertrophy and atrophy: Nat.Cell Biol., v. 5, p. 87-90.

Goberdhan,DC, N Paricio, E C Goodman, M Mlodzik, C Wilson, 1999, Drosophila tumor suppressor PTEN controls cell size and number by antagonizing the Chico/PI3-kinase signaling pathway: Genes Dev., v. 13, p. 3244-3258.

Goldring,K, T Partridge, D Watt, 2002, Muscle stem cells: J.Pathol., v. 197, p. 457-467.

Gomes,MD, S H Lecker, R T Jagoe, A Navon, A L Goldberg, 2001, Atrogin-1, a muscle-specific F-box protein highly expressed during muscle atrophy: Proc.Natl.Acad.Sci.U.S.A, v. 98, p. 14440-14445.

Graef,IA, F Chen, G R Crabtree, 2001, NFAT signaling in vertebrate development: Curr.Opin.Genet.Dev., v. 11, p. 505-512.

Granjeaud,S, F Bertucci, B R Jordan, 1999, Expression profiling: DNA arrays in many guises: Bioessays, v. 21, p. 781-790.

Gress,TM, J D Hoheisel, G G Lennon, G Zehetner, H Lehrach, 1992, Hybridization fingerprinting of high-density cDNA-library arrays with cDNA pools derived from whole tissues: Mamm.Genome, v. 3, p. 609-619.

Guerra,B, O G Issinger, 1999, Protein kinase CK2 and its role in cellular proliferation, development and pathology: Electrophoresis, v. 20, p. 391-408.

Gussoni,E, Y Soneoka, C D Strickland, E A Buzney, M K Khan, A F Flint, L M Kunkel, R C Mulligan, 1999, Dystrophin expression in the mdx mouse restored by stem cell transplantation: Nature, v. 401, p. 390-394.

Haddad,F, R R Roy, H Zhong, V R Edgerton, K M Baldwin, 2003a, Atrophy responses to muscle inactivity. I. Cellular markers of protein deficits: J.Appl.Physiol, v. 95, p. 781-790.

Haddad,F, R R Roy, H Zhong, V R Edgerton, K M Baldwin, 2003b, Atrophy responses to muscle inactivity. II. Molecular markers of protein deficits: J.Appl.Physiol, v. 95, p. 791-802.

Halgren,RG, M R Fielden, C J Fong, T R Zacharewski, 2001, Assessment of clone identity and sequence fidelity for 1189 IMAGE cDNA clones: Nucleic Acids Res., v. 29, p. 582-588.

Handschin,C, J Rhee, J Lin, P T Tarr, B M Spiegelman, 2003, An autoregulatory loop controls peroxisome proliferator-activated receptor gamma coactivator 1alpha expression in muscle: Proc.Natl.Acad.Sci.U.S.A, v. 100, p. 7111-7116.

Hara,K, K Yonezawa, M T Kozlowski, T Sugimoto, K Andrabi, Q P Weng, M Kasuga, I Nishimoto, J Avruch, 1997, Regulation of eIF-4E BP1 phosphorylation by mTOR: J.Biol.Chem., v. 272, p. 26457-26463.

Hardt,SE, J Sadoshima, 2002, Glycogen synthase kinase-3beta: a novel regulator of cardiac hypertrophy and development: Circ.Res., v. 90, p. 1055-1063.

Hasty,P, A Bradley, J H Morris, D G Edmondson, J M Venuti, E N Olson, W H Klein, 1993, Muscle deficiency and neonatal death in mice with a targeted mutation in the myogenin gene: Nature, v. 364, p. 501-506.

Hawke,TJ, D J Garry, 2001, Myogenic satellite cells: physiology to molecular biology: J.Appl.Physiol, v. 91, p. 534-551.

Hedbom,E, D Heinegard, 1989, Interaction of a 59-kDa connective tissue matrix protein with collagen I and collagen II: J.Biol.Chem., v. 264, p. 6898-6905.

Helge,JW, A M Fraser, A D Kriketos, A B Jenkins, G D Calvert, K J Ayre, L H Storlien, 1999, Interrelationships between muscle fibre type, substrate oxidation and body fat: Int J Obes Relat Metab Disord, v. 23, p. 986-991.

Helmberg,A, 2001, DNA-microarrays: novel techniques to study aging and guide gerontologic medicine: Exp.Gerontol., v. 36, p. 1189-1198.

Hickey,MS, W D Weidner, K E Gavigan, D Zheng, G L Tyndall, J A Houmard, 1995, The insulin action-fibre type relation-ship in humans is muscle group specific: Am J Physiol Endocrinol Metab, v. 269, p. E150-E154.

Hieter,P, M Boguski, 1997, Functional genomics: it's all how you read it: Science, v. 278, p. 601-602.

Higginson,J, H Wackerhage, N Woods, P Schjerling, A Ratkevicius, N Grunnet, B Quistorff, 2002, Blockades of mitogen-activated protein kinase and calcineurin both change fibre-type markers in skeletal muscle culture: Pflugers Arch., v. 445, p. 437-443.

Hirsinger,E, D Duprez, C Jouve, P Malapert, J Cooke, O Pourquie, 1997, Noggin acts downstream of Wnt and Sonic Hedgehog to antagonize BMP4 in avian somite patterning: Development, v. 124, p. 4605-4614.

Hirsinger,E, P Malapert, J Dubrulle, M C Delfini, D Duprez, D Henrique, D Ish-Horowicz, O Pourquie, 2001, Notch signalling acts in postmitotic avian myogenic cells to control MyoD activation: Development, v. 128, p. 107-116.

Hoffman,EP, D Dressman, 2001, Molecular pathophysiology and targeted therapeutics for muscular dystrophy: Trends.Pharmacol.Sci., v. 22 (9), p. 465-470.

Houzelstein,D, G Auda-Boucher, Y Cheraud, T Rouaud, I Blanc, S Tajbakhsh, M E Buckingham, J Fontaine-Perus, B Robert, 1999, The homeobox gene Msx1 is expressed in a subset of somites, and in muscle progenitor cells migrating into the forelimb: Development, v. 126, p. 2689-2701.

Huang,H, C J Potter, W Tao, D M Li, W Brogiolo, E Hafen, H Sun, T Xu, 1999, PTEN affects cell size, cell proliferation and apoptosis during Drosophila eye development: Development, v. 126, p. 5365-5372.

Hughes,SM, S Schiaffino, 1999, Control of muscle fibre size: a crucial factor in ageing: Acta Physiol.Scand., v. 167, p. 307-312.

Hughes,TR, D D Shoemaker, 2001, DNA microarrays for expression profiling: Curr Opin Chem Biol, v. 5(1), p. 21-25.

Inazawa,J, T Ariyma, T Abe, T Druck, 1996, PTPN13, a Fas-associated protein tyrosin phosphatase, is located on the long arm of chromosome 4 at band q21.3.: Genomics, v. 31, p. 240-242

Ivanov,VN, Lopez Bergami P, Maulit G, Sato TA, Sassoon D, Ronai Z, 2003, FAP-1 association with Fas (Apo-1) inhibits Fas expression on the cell surface: Mol Cell Biol., v. 23(10), p. 3623-35.

Jacobson,MD, M Weil, M C Raff, 1997, Programmed cell death in animal development: cell, v. 88, p. 347-354.

Jagoe,RT, A L Goldberg, 2001, What do we really know about the ubiquitin-proteasome pathway in muscle atrophy?: Curr.Opin.Clin.Nutr.Metab Care, v. 4, p. 183-190.

Jagoe,RT, S H Lecker, M Gomes, A L Goldberg, 2002, Patterns of gene expression in atrophying skeletal muscles: response to food deprivation: FASEB J., v. 16, p. 1697-1712.

Jawhari,AU, A Buda, M Jenkins, K Shehzad, C Sarraf, M Noda, M J Farthing, M Pignatelli, J C Adams, 2003, Fascin, an actin-bundling protein, modulates colonic epithelial cell invasiveness and differentiation in vitro: Am.J.Pathol., v. 162, p. 69-80.

Jen,Y, H Weintraub, R Benezra, 1992, Overexpression of Id protein inhibits the muscle differentiation program: in vivo association of Id with E2A proteins: Genes Dev., v. 6, p. 1466-1479.

Jepsen,KJ, F Wu, J H Peragallo, J Paul, L Roberts, Y Ezura, A Oldberg, D E Birk, S Chakravarti, 2002, A syndrome of joint laxity and impaired tendon integrity in lumican- and fibromodulin-deficient mice: J.Biol.Chem., v. 277, p. 35532-35540.

Jones,PF, T Jakubowicz, B A Hemmings, 1991, Molecular cloning of a second form of rac protein kinase: Cell Regul., v. 2, p. 1001-1009.

Kandel,ES, N Hay, 1999, The regulation and activities of the multifunctional serine/threonine kinase Akt/PKB: Exp.Cell Res., v. 253, p. 210-229.

Karlsson,AH, R E Klont, X Fernandez, 1999, Skeletal muscle fibres as factors for pork quality: Livest.Prod.Sci., v. 60, p. 255-269.

Kashishian,A, M Howard, C Loh, W M Gallatin, M F Hoekstra, Y Lai, 1998, AKAP79 inhibits calcineurin through a site distinct from the immunophilin-binding region: J Biol Chem, v. 273 (42), p. 27412-27419.

Kemp,TJ, T J Sadusky, M Simon, R Brown, M Eastwood, D A Sassoon, G R Coulton, 2001, Identification of a novel stretch-responsive skeletal muscle gene (*Smpx*): Genomics, v. 72, p. 260-271.

Kerr JFR, A H Wyllie, A R Currie, 1972, Apoptosis: a basic biological phenomenon with wide-ranging implications in tissue kinetics: Br J Cancer, v. 26, p. 239-257.

Kerr,JFR, J Searle, B V Harmon, C J Bishop, 1987, Apoptosis: Perspectives on Mammalian Cell Death (Potten CS, ed): Oxford University Press, p. 93-128.

Kerr,MK, G A Churchill, 2001, Experimental design for gene expression microarrays: Biostatistics., v. 2, p. 183-201.

Khan, J, M L Bittner, L H Saal, U Teichmann, D O Azorsa, G C Gooden, W J Pavan, J M Trent, P S Meltzer, 1999, cDNA microarrays detect activation of a myogenic transcription program by the PAX3-FKHR fusion oncogene: Proc.Natl.Acad.Sci.U.S.A., v. 96, p. 13264-13269.

Khrapko,KR, Y Lysov, A A Khorlyn, V V Shick, V L Florentiev, A D Mirzabekov, 1989, An oligonucleotide hybridization approach to DNA sequencing: FEBS Lett., v. 256, p. 118-122.

Klont,RE, L Brocks, G Eikelenboom, 1998, Muscle fibre type and meat quality: Meat Sci., v. 49, p. S219-S229.

Kocamis,H, J Killefer, 2002, Myostatin expression and possible functions in animal muscle growth: Domest.Anim Endocrinol., v. 23, p. 447-454.

Krempler,A, B Brenig, 1999, Zinc finger proteins: watchdogs in muscle development: Mol.Gen.Genet., v. 261, p. 209-215.

Kriketos,AD, L A Baur, J O'Connor, D Carey, S King, I D Caterson, L H Storlien, 1997, Muscle fibre type composition in infant and adult populations and relationships with obesity: Int J Obes Relat Metab Disord, v. 21, p. 796-801.

Kriketos,AD, D A Pan, S Lillioja, G J Cooney, L A Baur, M R Milner, J R Sutton, A B Jenkins, C Bogardus, L H Storlien, 1996, Interrelationships between muscle morphology, insulin action, and adiposity: Am J Physiol Regulatory Integrative Comp Physiol, v. 270, p. R1332-R1339.

Kubis,HP, E A Haller, P Wetzel, G Gros, 1997, Adult fast myosin pattern and Ca2+-induced slow myosin pattern in primary skeletal muscle culture: Proc.Natl.Acad.Sci.U.S.A, v. 94, p. 4205-4210.

Kubis,HP, N Hanke, R J Scheibe, J D Meissner, G Gros, 2003, Ca2+ transients activate calcineurin/NFATc1 and initiate fast-to-slow transformation in a primary skeletal muscle culture: Am.J.Physiol Cell Physiol, v. 285, p. C56-C63.

LaBarge,MA, H M Blau, 2002, Biological progression from adult bone marrow to mononucleate muscle stem cell to multinucleate muscle fiber in response to injury: Cell, v. 111, p. 589-601.

Lai,MM, P E Burnett, H Wolosker, S Blackshaw, S H Snyder, 1998, Cain, a novel physiologic protein inhibitor of calcineurin: J Biol Chem, v. 273 (29), p. 18325-18331.

Lander,ES, 1999, Array of hope: Nat.Genet., v. 21, p. 3-4.

Larsson,L, B Ramamurthy, 2000, Aging-related changes in skeletal muscle: Drugs Aging, v. 4, p. 303-316.

Lecker,SH, 2003, Ubiquitin-protein ligases in muscle wasting: multiple parallel pathways?: Curr.Opin.Clin.Nutr.Metab Care, v. 6, p. 271-275.

Lecker,SH, V Solomon, S R Price, Y T Kwon, W E Mitch, A L Goldberg, 1999, Ubiquitin conjugation by the N-end rule pathway and mRNAs for its components increase in muscles of diabetic rats: J.Clin.Invest, v. 104, p. 1411-1420.

Lee,ML, F C Kuo, G A Whitmore, J Sklar, 2000, Importance of replication in microarray gene expression studies: statistical methods and evidence from repetitive cDNA hybridizations: Proc.Natl.Acad.Sci.U.S.A, v. 97, p. 9834-9839.

Lee,ML, G A Whitmore, 2002, Power and sample size for DNA microarray studies: Stat.Med., v. 21, p. 3543-3570.

Li,W, J Llopis, M Whitney, G Zlokarnik, R Y Tsien, 1998, Cell-permeant caged InsP3 ester shows that Ca2+ spike frequency can optimize gene expression: Nature, v. 392, p. 936-941.

Liang,P. A B Pardee, 1992, Differential display of eukaryotic messenger RNA by means of the polymerase chain reaction: Science, v. 257, p. 967-971.

Lim,DS, R Roberts, A J Marian, 2001, Expression profiling of cardiac genes in human hypertrophic cardiomyopathy: insight into the pathogenesis of phenotypes: Journal of the American College of Cardiology, v. 38, p. 1175-1180.

Lin,J, H Wu, P T Tarr, C Y Zhang, Z Wu, O Boss, L F Michael, P Puigserver, E Isotani, E N Olson, B B Lowell, R Bassel-Duby, B M Spiegelman, 2002, Transcriptional co-activator PGC-1 alpha drives the formation of slow-twitch muscle fibres: Nature, v. 418, p. 797-801.

Lipshutz,RJ, S P Fodor, T R Gingeras, D J Lockhart, 1999, High density synthetic oligonucleotide arrays: Nat.Genet., v. 21, p. 20-24.

Lisitsyn,N, N Lisitsyn, M Wigler, 1993, Cloning the differences between two complex genomes: Science, v. 259, p. 946.

Liu,S, P Liu, A Borras, T Chatila, S H Speck, 1997, Cyclosporin A-sensitive induction of the Epstein-Barr virus lytic switch is mediated via a novel pathway involving a MEF2 family member: EMBO J., v. 16, p. 143-153.

Liu,Y, Z Cseresnyes, W R Randall, M F Schneider, 2001, Activity-dependent nuclear translocation and intra-nuclear distribution of NFATc in adult skeletal muscle fibres: J Cell Biology, v. 155, p. 27-39.

Liu,YF, J M Steinacker, 2001, Changes in skeletal muscle heat shock proteins: pathological significance: Front.Biosci., v. 6, p. d12-d25.

Lockhart,DJ, E A Winzeler, 2000, Genomics, gene expression and DNA arrays: Nature, v. 405, p. 827-836.

Maitra,A, C Iacobuzio-Donahue, A Rahman, T A Sohn, P Argani, R Meyer, C J Yeo, J L Cameron, M Goggins, S E Kern, R Ashfaq, R H Hruban, R E Wilentz, 2002, Immunohistochemical validation of a novel epithelial and a novel stromal marker of pancreatic ductal adenocarcinoma identified by global expression microarrays: sea urchin fascin homolog and heat shock protein 47: Am.J.Clin.Pathol., v. 118, p. 52-59.

Marcotte,ER, L K Srivastava, R Quirion, 2001, DNA microarrays in neuropsychopharmacology: Trends Pharmacol.Sci., v. 22, p. 426-436.

Markuns,JF, J F Wojtaszewski, L J Goodyear, 1999, Insulin and exercise decrease glycogen synthase kinase-3 activity by different mechanisms in rat skeletal muscle: J.Biol.Chem., v. 274, p. 24896-24900.

Masuda,ES, R Imamura, Y Amasaki, K Arai, N Arai, 1998, Signalling into the T-cell nucleus: NFAT regulation: Cell Signal., v. 10, p. 599-611.

Matsui,T, T Nagoshi, A Rosenzweig, 2003, Akt and PI 3-kinase signaling in cardiomyocyte hypertrophy and survival: Cell Cycle, v. 2, p. 220-223.

McGavin,MD, W W Carlton, J F Zachary, 2001, Thomson's Special Veterinary Pathology (edition 3) [Schrefer JA, ed]: Mosby, Inc., chapter 9, p. 461.

McKinsey,TA, C L Zhang, E N Olson, 2002, MEF2: a calcium-dependent regulator of cell division, differentiation and death: Trends Biochem.Sci., v. 27, p. 40-47.

McMahon,JA, S Takada, L B Zimmerman, C M Fan, R M Harland, A P McMahon, 1998, Noggin-mediated antagonism of BMP signaling is required for growth and patterning of the neural tube and somite: Genes Dev., v. 12, p. 1438-1452.

McManus,EJ, D R Alessi, 2002, TSC1-TSC2: a complex tale of PKB-mediated S6K regulation: Nat.Cell Biol., v. 4, p. E214-E216.

Meissner,JD, G Gros, R J Scheibe, M Scholz, H P Kubis, 2001, Calcineurin regulates slow myosin, but not fast myosin or metabolic enzymes, during fast-to-slow transformation in rabbit skeletal muscle cell culture: J.Physiol, v. 533, p. 215-226.

Mitch,WE, A L Goldberg, 1996, Mechanisms of muscle wasting. The role of the ubiquitin-proteasome pathway: N.Engl.J.Med., v. 335, p. 1897-1905.

Mitchell,PO, S T Mills, G K Pavlath, 2002, Calcineurin differentially regulates maintenance and growth of phenotypically distinct muscles: Am.J.Physiol Cell Physiol, v. 282, p. C984-C992.

Molkentin,JD, E N Olson, 1996, Defining the regulatory networks for muscle development: Curr.Opin.Genet.Dev., v. 6, p. 445-453.

Murgia,M, A L Serrano, E Calabria, G Pallafacchina, T Lomo, S Schiaffino, 2000, Ras is involved in nerve-activity-dependent regulation of muscle genes: Nat.Cell Biol., v. 2, p. 142-147.

Musaro,A, K McCullagh, A Paul, L Houghton, G Dobrowolny, M Molinaro, E R Barton, H L Sweeney, N Rosenthal, 2001, Localized IGF-1 transgene expression sustains hypertrophy and regeneration in senescent skeletal muscle: Nat.Genet., v. 27, p. 195-200.

Musaro,A, K J McCullagh, F J Naya, E N Olson, N Rosenthal, 1999, IGF-1 induces skeletal myocyte hypertrophy through calcineurin in association with GATA-2 and NF-ATc1: Nature, v. 400, p. 581-585.

Nabeshima,Y, K Hanaoka, M Hayasaka, E Esumi, S Li, I Nonaka, Y Nabeshima, 1993, Myogenin gene disruption results in perinatal lethality because of severe muscle defect: Nature, v. 364, p. 532-535.

Naidu,PS, D C Ludolph, R Q To, T J Hinterberger, S F Konieczny, 1995, Myogenin and MEF2 function synergistically to activate the MRF4 promoter during myogenesis: Mol.Cell Biol., v. 15, p. 2707-2718.

Nakayama,M, J Stauffer, J Cheng, S Banerjee-Basu, E Wawrousek, A Bounanno, 1996, Common core sequences are found in skeletal muscle slow- and fast-fibre-type-specific regulatory elements: Mol Cell Biol, v. 16, p. 2408-2417.

Nakatani,K, H Sakaue, D A Thompson, R J Weigel, R A Roth, 1999, Identification of a human Akt3 (protein kinase B gamma) which contains the regulatory serine phosphorylation site: Biochem.Biophys.Res.Commun., v. 257, p. 906-910.

Naya,FJ, B Mercer, J Shelton, J A Richardson, R S Williams, E N Olson, 2000, Stimulation of slow skeletal muscle fiber gene expression by calcineurin in vivo: J.Biol.Chem., v. 275, p. 4545-4548.

Naya,FJ, C Wu, J A Richardson, P Overbeek, E N Olson, 1999, Transcriptional activity of MEF2 during mouse embryogenesis monitored with a MEF2-dependent transgene: Development, v. 126, p. 2045-2052.

Noguchi,S, T Tsukahara, M Fujita, R Kurokawa, M Tachikawa, T Toda, A Tsujimoto, K Arahata, I Nishino, 2003, cDNA microarray analysis of individual Duchenne muscular dystrophy patients: Hum.Mol.Genet., v. 12, p. 595-600.

Norton,JD, GT Atherton, 1998, Coupling of cell growth control and apoptosis functions of Id proteins: Mol Cell Biol., v. 18 (4), p. 2371-2381.

Nyholm,B, Z Qu, A Kaal, S B Pedersen, C H Gravholt, J L Andersen, B Saltin, O Schmitz, 1997, Evidence of an increased number of type IIb muscle fibres in insulin-resistant first-degree relatives of patients with NIDDM: Diabetes, v. 46, p. 1822-1828.

Odelberg,SJ, A Kollhoff, M T Keating, 2000, Dedifferentiation of mammalian myotubes induced by msx1: Cell, v. 103, p. 1099-1109.

Olson,EN, R S Williams, 2000a, Calcineurin signaling and muscle remodeling: Cell, v. 101, p. 689-692.

Olson,EN, R S Williams, 2000b, Remodeling muscles with calcineurin: Bioessays, v. 22, p. 510-519.

Orrenius,S, P Nicotera, 1994, The calcium ion and cell death: J Neural Transm Suppl, v. 43, p. 1-11

Pallafacchina,G, E Calabria, A L Serrano, J M Kalhovde, S Schiaffino, 2002, A protein kinase B-dependent and rapamycin-sensitive pathway controls skeletal muscle growth but not fiber type specification: Proc.Natl.Acad.Sci.U.S.A, v. 99, p. 9213-9218.

Parker,MH, P Seale, M A Rudnicki, 2003, Looking back to the embryo: defining transcriptional networks in adult myogenesis: Nat.Rev.Genet., v. 4, p. 497-507.

Parsons,SA, B J Wilkins, O F Bueno, J D Molkentin, 2003, Altered skeletal muscle phenotypes in calcineurin Aalpha and Abeta gene-targeted mice: Mol.Cell Biol., v. 23, p. 4331-4343.

Patanjali,SR, S Parimoo, S M Weissman, 1991, Construction of a uniform-abundance (normalized) cDNA library: Proc.Natl.Acad.Sci.U.S.A, v. 88, p. 1943-1947.

Patapoutian,A, J K Yoon, J H Miner, S Wang, K Stark, B Wold, 1995, Disruption of the mouse MRF4 gene identifies multiple waves of myogenesis in the myotome: Development, v. 121, p. 3347-3358.

Perry,RLS, M A Rudnicki, 2000, Molecular mechanisms regulating myogenic determination and differentiation: Front Biosci., v. 5, p. D750-767.

Pette,D, R S Staron, 1990, Cellular and molecular diversities of mammalian skeletal fibers: Rev.Physiol.Biochem.Pharmacol., v. 116, p. 2-76.

Pierobon,BS, S Sartore, L D Libera, M Vitadello, S Schiaffino, 1981, Fast isomyosins and fibre types in mammalian skeletal muscle: Journal of Histochemistry and Cytochemistry, v. 29, p. 1179-1188.

Pietu,G, E Eveno, B Soury-Segurens, N A Fayein, R Mariage-Samson, C Matingou, E Leroy, C Dechesne, S Krieger, W Ansorge, I Reguigne-Arnould, D Cox, A Dehejia, M H

Pollard,TD, et al., 1999, Guidebook to the Cytoskeletal and Motor Proteins [second edition] (Kreis T and Vale R, ed): A Sambrook & Tooze Publication at Oxford University Press, p. 11-13, p. 159-167, p. 421-425.

Polymeropoulos, M D Devignes, C Auffray, 1999, The genexpress IMAGE knowledge base of the human muscle transcriptome: a resource of structural, functional, and positional candidate genes for muscle physiology and pathologies: Genome Res, v. 9, p. 1313-1320.

Raffray,M, G M Cohen, 1997, Apoptosis and necrosis in toxicology: a continuum or distinct modes of cell death?: Pharmacol Ther, v. 75, p. 153-177.

Rajeevan,MS, D G Ranamukhaarachchi, S D Vernon, E R Unger, 2001a, Use of real-time quantitative PCR to validate the results of cDNA array and differential display PCR technologies: Methods, v. 25, p. 443-451.

Rajeevan,MS, S D Vernon, N Taysavang, E R Unger, 2001b, Validation of array-based gene expression profiles by real-time (kinetic) RT-PCR: J.Mol.Diagn., v. 3, p. 26-31.

Randall,D, W Burggren, K French, 2002, Eckert Animal Physiology - Mechanisms and Adaptations: W. H. Freeman and Company, chapter 10, p. 361-379.

Rao,A, C Luo, P G Hogan, 1997, Transcription factors of the NFAT family: regulation and function: Annu.Rev.Immunol., v. 15, p. 707-747.

Reshef,R, M Maroto, A B Lassar, 1998, Regulation of dorsal somitic cell fates: BMPs and Noggin control the timing and pattern of myogenic regulator expression: Genes Dev., v. 12, p. 290-303.

Ridgeway,AG, S Wilton, I S Skerjanc, 2000, Myocyte enhancer factor 2C and myogenin up-regulate each other's expression and induce the development of skeletal muscle in P19 cells: J.Biol.Chem., v. 275, p. 41-46.

Rink,A, M Santschi, C W Beattie, 2002, Normalized cDNA libraries from a porcine model of orthopedic implant-associated infection: Mammal.Genome, v. 13, p. 198-205.

Rohwer,A, W Kittstein, F Marks, M Gschwendt, 1999, Cloning, expression and characterization of an A6-related protein: Eur.J.Biochem., v. 263, p. 518-525.

Rommel,C, S C Bodine, B A Clarke, R Rossman, L Nunez, T N Stitt, G D Yancopoulos, D J Glass, 2001, Mediation of IGF-1-induced skeletal myotube hypertrophy by PI(3)K/Akt/mTOR and PI(3)K/Akt/GSK3 pathways: Nat.Cell Biol., v. 3, p. 1009-1013.

Rommel,C, B A Clarke, S Zimmermann, L Nunez, R Rossman, K Reid, K Moelling, G D Yancopoulos, D J Glass, 1999, Differentiation stage-specific inhibition of the Raf-MEK-ERK pathway by Akt: Science, v. 286, p. 1738-1741.

Rothermel,BA, R B Vega, R S Williams, 2003, The role of modulatory calcineurin-interacting proteins in calcineurin signalling: Trends Cardiovasc Med, v. 13 (1), p. 15-21.

Rudin,CM, C B Thompson, 1997, Apoptosis and disease: regulation and clinical relevance of programmed cell death: Annu Rev Med, v. 48, p. 267-281.

Rudnicki,MA, P N Schnegelsberg, R H Stead, T Braun, H H Arnold, R Jaenisch, 1993, MyoD or Myf-5 is required for the formation of skeletal muscle: Cell, v. 75, p. 1351-1359.

Russell,B, D Motlagh, W W Ashley, 2000, Form follows function: how muscle shape is regulated by work: J. Appl. Physiol., v. 88, p. 1127-1132.

Ryder,JW, R Bassel-Duby, E N Olson, J R Zierath, 2003, Skeletal muscle reprogramming by activation of calcineurin improves insulin action on metabolic pathways: J.Biol.Chem., v. 278, p. 44298-44304.

Sakamuro,D, K J Elliot, R Wechsler-Reya, G C Prendergast, 1996, Bin1 is a novel Myc-interacting protein with features of a tumour suppressor: Nat.Genet., v. 14, p. 69-77.

Sakuma,K, J Nishikawa, R Nakao, K Watanabe, T Totsuka, H Nakano, M Sano, M Yasuhara, 2003, Calcineurin is a potent regulator for skeletal muscle regeneration by association with NFATc1 and GATA-2: Acta Neuropathol.(Berl), v. 105, p. 271-280.

Sato,T, S Irie, S Kitada, JC Reed, 1995, FAP-1: a protein tyrosine phosphatase that associates with Fas: Science., v. 268(5209), p. 411-5.

Schena,M, D Shalon, R W Davis, P O Brown, 1995, Quantitative monitoring of gene expression patterns with a complementary DNA microarray: Science, v. 270, p. 467-470.

Schiaffino,S, C Reggiani, 1994, Myosin isoforms in mammalian skeletal muscle: J.Appl.Physiol, v. 77, p. 493-501.

Schiaffino,S, C Reggiani, 1996, Molecular diversity of myofibrillar proteins: gene regulation and functional significance: Physiol Rev., v. 76, p. 371-423.

Schiaffino,S, A Serrano, 2002, Calcineurin signaling and neural control of skeletal muscle fiber type and size: Trends Pharmacol.Sci., v. 23, p. 569-575.

Schulze,A, J Downward, 2001, Navigating gene expression using microarrays--a technology review: Nat. Cell Biol., v. 3(8), p. E190-E195.

Sciote,JJ, T J Morris, 2000, Skeletal muscle function and fibre types: the relationship between occlusal function and the phenotype of jaw-closing muscles in human: J.Orthod., v. 27, p. 15-30.

Scott,JE, V A Ruff, K L Leach, 1997, Dynamic equilibrium between calcineurin and kinase activities regulates the phosphorylation state and localisation of the nuclear factor of activated T-cells: Biochem. J., v. 324, p. 597-603.

Scott,PH, G J Brunn, A D Kohn, R A Roth, J C Lawrence, Jr., 1998, Evidence of insulin-stimulated phosphorylation and activation of the mammalian target of rapamycin mediated by a protein kinase B signaling pathway: Proc.Natl.Acad.Sci.U.S.A, v. 95, p. 7772-7777.

Seale,P, M A Rudnicki, 2000, A new look at the origin, function, and "stem-cell" status of muscle satellite cells: Dev.Biol., v. 218, p. 115-124.

Seale,P, A Asakura, MA Rudnicki, 2001, The potential of muscle stem cells: Dev. Cell, v. 1(3), p. 333-342.

Semsarian,C, M J Wu, Y K Ju, T Marciniec, T Yeoh, D G Allen, R P Harvey, R M Graham, 1999, Skeletal muscle hypertrophy is mediated by a Ca2+-dependent calcineurin signalling pathway: Nature, v. 400, p. 576-581.

Serrano,AL, M Murgia, G Pallafacchina, E Calabria, P Coniglio, T Lomo, S Schiaffino, 2001, Calcineurin controls nerve activity-dependent specification of slow skeletal muscle fibers but not muscle growth: Proc.Natl.Acad.Sci.U.S.A, v. 98, p. 13108-13113.

Shioi,T, J R McMullen, P M Kang, P S Douglas, T Obata, T F Franke, L C Cantley, S Izumo, 2002, Akt/protein kinase B promotes organ growth in transgenic mice: Mol.Cell Biol., v. 22, p. 2799-2809.

Smerdu,V, I Karsch-Mizrachi, M Campione, L Leinwand, S Schiaffino, 1994, Type IIx myosin heavy chain transcripts are expressed in type IIb fibers of human skeletal muscle: Am.J.Physiol, v. 267, p. C1723-C1728.

Smyth,GK, Y H Yang, T Speed, 2003, Statistical issues in cDNA microarray data analysis: Methods Mol.Biol., v. 224, p. 111-136.

Soares,MB, M F Bonaldo, P Jelene, L Su, L Lawton, A Efstratiadis, 1994, Construction and characterization of a normalized cDNA library: Proc.Natl.Acad.Sci.U.S.A., v. 91, p. 9228-9232.

Socjima,H, S Kawamoto, J Akai, O Miyoshi, Y Arai, T Morohka, S Matsuo, N Niikawa, A Kimura, K Okubo, T Mukai, 2001, Isolation of novel heart-specific genes using the BodyMap database: Genomics, v. 74, p. 115-120.

Sonenberg,N, A C Gingras, 1998, The mRNA 5' cap-binding protein eIF4E and control of cell growth: Curr.Opin.Cell Biol., v. 10, p. 268-275.

Southern,E, K Mir, M Shchepinov, 1999, Molecular interactions on microarrays: Nat.Genet., v. 21, p. 5-9.

Spangenburg,EE, J H Williams, R R Roy, R J Talmadge, 2001, Skeletal muscle calcineurin: influence of phenotype adaptation and atrophy: Am.J.Physiol Regul.Integr.Comp Physiol, v. 280, p. R1256-R1260.

Squire,JM, E P Morris, 1998, A new look at thin filament regulation in vertebrate skeletal muscle: FASEB J. v. 12, p. 761-771.

Stambolic,V, A Suzuki, J L de la Pompa, G M Brothers, C Mirtsos, T Sasaki, J Ruland, J M Penninger, D P Siderovski, T W Mak, 1998, Negative regulation of PKB/Akt-dependent cell survival by the tumor suppressor PTEN: Cell, v. 95, p. 29-39.

Stewart,S, G R Crabtree, 2000, Transcription. Regulation of the regulators.: Nature, v. 408 (6808), p. 46-47.

Storlien,LH, D A Pan, A D Kriketos, J O'Connor, I D Caterson, G J Cooney, A B Jenkins, L A Baur, 1996, Skeletal muscle membrane lipids and insulin resistance: Lipids, v. 31 Suppl, p. S261-265.

Sun,Y, A C Gore, J L Roberts, 1998, The role of calcium in the transcriptional and posttranscriptional regulation of the Gonadotropin-releasing hormone gene in GT1-7 cells: Endocrinology, v. 139 (6), p. 2685-2691

Sun,YM, N da Costa, R Birrell, A L Archibald, H Alzuherri, K C Chang, 2001, Molecular and quantitative characterisation of the porcine embryonic myosin heavy chain gene: J.Muscle Res.Cell Motil., v. 22, p. 317-327.

Tajbakhsh,S, U Borello, E Vivarelli, R Kelly, J Papkoff, D Duprez, M Buckingham, G Cossu, 1998, Differential activation of Myf5 and MyoD by different Wnts in explants of mouse paraxial mesoderm and the later activation of myogenesis in the absence of Myf5: Development, v. 125, p. 4155-4162.

Takahashi,A, Y Kureishi, J Yang, Z Luo, K Guo, D Mukhopadhyay, Y Ivashchenko, D Branellec, K Walsh, 2002, Myogenic Akt signaling regulates blood vessel recruitment during myofiber growth: Mol.Cell Biol., v. 22, p. 4803-4814.

Talmadge,RJ, 2000, Myosin heavy chain isoform expression following reduced neuromuscular activity: potential regulatory mechanisms: Muscle Nerve, v. 23, p. 661-679.

Taniguchi,M, K Miura, H Iwao, S Yamanaka, 2001, Quantitative assessment of DNA microarrays--comparison with Northern blot analyses: Genomics, v. 71, p. 34-39.

Tawa,NE, Jr., R Odessey, A L Goldberg, 1997, Inhibitors of the proteasome reduce the accelerated proteolysis in atrophying rat skeletal muscles: J.Clin.Invest, v. 100, p. 197-203.

Tawfic,S, S Yu, H Wang, R Faust, A Davis, K Ahmed, 2001, Protein kinase CK2 signal in neoplasia: Histol.Histopathol., v. 16, p. 573-582.

Thirion,C, R Stucka, B Mendel, A Gruhler, M Jaksch, K J Nowak, N Binz, N G Laing, H Lochmuller, 2001, Characterization of human muscle type cofilin (CFL2) in normal and regenerating muscle: Eur.J.Biochem., v. 268, p. 3473-3482.

Tikkanen,HO, M Harkonen, H Naveri, E Hamalainen, R Elovainio, S Sarna, M H Frick, 1991, Relationship of skeletal muscle fibre type to serum high density lipoprotein cholesterol and apolipoprotein A-I levels: Atherosclerosis, v. 90, p. 49-57.

Timmerman,LA, N A Clipstone, S N Ho, J P Northrop, G R Crabtree, 1996, Rapid shuttling of NF-AT in discrimination of $Ca^{2+}$ signals and immunosuppression: Nature, v. 383, p. 837-840.

Toft I, K H Bonaa, S Lindal, T Jenssen, 1998, Insulin kinetics, insulin action, and muscle morphology in lean or slightly over-weight persons with impaired glucose tolerance: Metabolism, v. 47, p. 848-854.

Tomida,T, K Hirose, A Takizawa, F Shibasaki, M Iino, 2003, NFAT functions as a working memory of Ca2+ signals in decoding Ca2+ oscillation: EMBO J., v. 22, p. 3825-3832.

Trump,BF, I K Berezesky, 1996, The role of altered $[Ca^{2+}]_i$ regulation in apoptosis, oncosis, and necrosis: Biochim Biophys Acta, v. 1313, p. 173-178.

Tsutsui,K, Y Maeda, S Seki, A Tokunaga, 1997, cDNA cloning of a novel amphiphysin isoform and tissue-specific expression of its multiple variants: Biochem.Biophy.Res.Com., v. 236, p. 178-183.

Vandenburgh,HH, P Karlisch, J Shansky, R Feldstein, 1991, Insulin and IGF-I induce pronounced hypertrophy of skeletal myofibres in tissue culture: Am.J.Physiol, v. 260, p. C475-C484.

Vander,A, J Sherman, D Luciano, 2001, Human Physiology - The Mechanisms of Body Function (eighth edition): McGraw Hill Press, chapter 11, p. 291-305.

Venter,JC, M D Adams, E W Myers, P W Li, R J Mural, G G Sutton, H O Smith, et al., 2001, The sequence of the human genome: Science, v. 291, p. 1304-1351.

Vivanco,I, C L Sawyers, 2002, The phosphatidylinositol 3-Kinase AKT pathway in human cancer: Nat.Rev.Cancer, v. 2, p. 489-501.

von Stein,OD, 2001, Isolation of differentially expressed genes through subtractive suppression hybridization, in MP Starkey and R Elaswarapu (eds), Genomics protocols: Totowa, Human Press Inc., p. 263-278.

Wada,MR, M Inagawa-Ogashiwa, S Shimizu, S Yasumoto, N Hashimoto, 2002, Generation of different fates from multipotent muscle stem cells: Development, v. 129, p. 2987-2995.

Wechsler-Reya,RJ, K J Elliot, G C Prendergast, 1998, A role for the putative tumor suppressor bin1 in muscle cell differentiation: Mol.Cell.Biol., v. 18, p. 566-575.

Weiss,A, L A Leinwand, 1996, The mammalian myosin heavy chain gene family: Annu.Rev.Cell Dev.Biol., v. 12, p. 417-439.

Welsh,GI, C M Miller, A J Loughlin, N T Price, C G Proud, 1998, Regulation of eukaryotic initiation factor eIF2B: glycogen synthase kinase-3 phosphorylates a conserved serine which undergoes dephosphorylation in response to insulin: FEBS Lett., v. 421, p. 125-130.

Westphal,S, H Kalthoff, 2003, Apoptosis: Targets in Pancreatic: BioMed Central (BMC) Cancer Molecular Cancer 2:6.

Willmann,R, J Kusch, K R Sultan, A G Schneider, D Pette, 2001, Muscle LIM protein is upregulated in fast skeletal muscle during transition toward slower phenotypes: Am.J.Physiol Cell Physiol, v. 280, p. C273-C279.

Winslow,MM, J R Neilson, G R Crabtree, 2003, Calcium signalling in lymphocytes: Curr.Opin.Immunol., v. 15, p. 299-307.

Winter,B, I Kautzner, O G Issinger, H H Arnold, 1997, Two putative protein kinase CK2 phosphorylation sites are important for Myf-5 activity: Biol.Chem., v. 378, p. 1445-1456.

Woloshin,P, K Song, C Degnin, A M Killary, D J Goldhamer, D Sassoon, M J Thayer, 1995, MSX1 inhibits myoD expression in fibroblast x 10T1/2 cell hybrids: Cell, v. 82, p. 611-620.

Wray,CJ, J M Mammen, D D Hershko, P O Hasselgren, 2003, Sepsis upregulates the gene expression of multiple ubiquitin ligases in skeletal muscle: Int.J.Biochem.Cell Biol., v. 35, p. 698-705.

Wu,H, F J Naya, T A McKinsey, B Mercer, J M Shelton, E R Chin, A R Simard, R N Michel, R Bassel-Duby, E N Olson, R S Williams, 2000, MEF2 responds to multiple calcium-regulated signals in the control of skeletal muscle fiber type: EMBO J., v. 19, p. 1963-1973.

Wu,H, B Rothermel, S Kanatous, P Rosenberg, F J Naya, J M Shelton, K A Hutcheson, J M DiMaio, E N Olson, R Bassel-Duby, R S Williams, 2001, Activation of MEF2 by muscle activity is mediated through a calcineurin-dependent pathway: EMBO J., v. 20, p. 6414-6423.

Xu,Z, D Stokoe, L P Kane, A Weiss, 2002, The inducible expression of the tumor suppressor gene PTEN promotes apoptosis and decreases cell size by inhibiting the PI3K/Akt pathway in Jurkat T cells: Cell Growth Differ., v. 13, p. 285-296.

Yanagisawa,J, M Takahashi, H Kanki, H Yano-Yanagisawa, T Tazunoki, E Sawa, T Nishitoba, M Kamishohara, E Kobayashi, S Kataoka, T Sato, 1997, The molecular interaction of Fas and FAP-1: J Biol Chem., v. 272(13), p. 8539-45.

Yang,YH, T Speed, 2002, Design issues for cDNA microarray experiments: Nat.Rev.Genet., v. 3, p. 579-588.

Yeh,K, RW Lim, 2000, Genomic organisation and promoter analysis of the murine Id3 gene: Gene, v. 254(1-2), p. 163-171.

Youn,HD, T A Chatila, J O Liu, 2000, Integration of calcineurin and MEF2 signals by the coactivator p300 during T-cell apoptosis: EMBO J., v. 19, p. 4323-4331.

Zhang,W, R R Behringer, E N Olson, 1995, Inactivation of the myogenic bHLH gene MRF4 results in up-regulation of myogenin and rib anomalies: Genes Dev., v. 9, p. 1388-1399.

Zimmers,TA, M V Davies, L G Koniaris, P Haynes, A F Esquela, K N Tomkinson, A C McPherron, N M Wolfman, S J Lee, 2002, Induction of cachexia in mice by systemically administered myostatin: Science, v. 296, p. 1486-1488.

Zammit,PS, J R Beauchamp, 2001, The skeletal muscle satellite cell: stem cell or son of stem cell?: Differentiation, v. 68, p. 193-204.